



Mwenechanya, Roy (2014) *Use of polyomics approaches to understanding drug resistance in kinetoplastid protozoa*. PhD thesis.

<http://theses.gla.ac.uk/5416/>

Copyright and moral rights for this work are retained by the author

A copy can be downloaded for personal non-commercial research or study, without prior permission or charge

This work cannot be reproduced or quoted extensively from without first obtaining permission in writing from the author

The content must not be changed in any way or sold commercially in any format or medium without the formal permission of the author

When referring to this work, full bibliographic details including the author, title, awarding institution and date of the thesis must be given

Enlighten:Theses  
<http://theses.gla.ac.uk/>  
theses@gla.ac.uk

# **Use of Polyomics Approaches to Understanding Drug Resistance in Kinetoplastid Protozoa**

**Roy Mwenechanya**

Submitted in fulfilment of the requirements for the  
degree of Doctor of Philosophy

School of Life Sciences  
College of Medical, Veterinary and Life Sciences  
University of Glasgow

June 2014

## Abstract

The lack of new drugs coming through to the market, to add to those few available, for use against diseases caused by trypanosomatids, calls for ways of safe-guarding the use of the current drugs to prolong their usefulness. This can be achieved by studying mechanisms of resistance to the drugs currently in use. In this thesis, the complementary use of untargeted metabolomic and whole genome sequence analyses was applied to elucidate the mechanisms of amphotericin B (AmB) resistance in *L. mexicana* promastigotes and isometamidium (ISMM) resistance in bloodstream forms of *T. brucei*.

Resistance to AmB and ISMM was induced by step-wise increase of the drug concentration in the growth medium of *L. mexicana* promastigotes and bloodstream forms of *T. brucei*, respectively.

Untargeted metabolomics results were used to link a single SNP in the lanosterol 14 $\alpha$ -demethylase (CYP51) gene of the sterol (ergosterol) biosynthetic pathway from a multitude of SNPs that were found in generated AmB resistant cells as compared to the parental wild-type cells. The identified SNP was found to be a non-synonymous mutation, causing the change N176I, outside the active sites of CYP51 and was accompanied by accumulation of the enzyme's product, 4, 4-dimethylcholesta-8, 14, 24-trien-3 $\beta$ -ol. These results suggested a break down in a possible protein-protein interaction of CYP51 with the next enzyme in the pathway, sterol C14-reductase, for efficient flow of the metabolite. Although the main subcellular localisation is different for these enzymes, they had a common localisation in the ER. AmB resistance was accompanied by depleted levels of ergosterol in AmB resistant cells. Expression of the wild-type CYP51 in AmB resistant cells restored ergosterol levels to those of the parental wild-type. Associated with restoration of ergosterol synthesis was reversal of resistance to AmB and susceptibility to pentamidine observed in AmB resistant cells. Thus N176I mutation in CYP51 underlies resistance to AmB in *L. mexicana* promastigotes.

*T. brucei* resistance to isometamidium was accompanied by loss of the kinetoplast and maintenance of a much reduced mitochondrial membrane

potential as compared to the parental wild-type cells. Reduction of the mitochondrial membrane potential was not connected to any apparent alteration of the energy metabolism of related metabolites. However, a perturbation in sphingolipid metabolism was observed to lead to depletion of sphingomyelin and accumulation of its precursor ceramide in the resistant cells. The responsible reaction enzyme, choline phosphorylceramide synthase (SLS4), was found to have 4 non-synonymous mutations which were outside the active site. The ISMM resistant cells exhibited a slow growth phenotype which has also been associated with perturbation of the sphingolipid synthesis pathway. ISMM resistant cells also showed cross resistance to diminazene aceturate and ethidium bromide used for control of African animal trypanosomiasis.

# Table of Contents

Abstract .....	ii
List of Tables .....	ix
List of Figures .....	x
Acknowledgement .....	xiii
Dedication .....	xiv
Author's Declaration .....	xv
Definitions/Abbreviations .....	xvi
Chapter One .....	1
1 General Introduction .....	1
1.1 African trypanosomiasis .....	1
1.1.1 Human African Trypanosomiasis .....	1
1.1.2 African Animal Trypanosomiasis .....	3
1.1.3 Burden (Economic) of African Animal trypanosomiasis .....	3
1.1.4 Trypanosomiasis in Zambia .....	3
1.2 Life cycle of <i>Trypanosoma brucei</i> .....	5
1.2.1 Cellular organization - Glycosome, mitochondrion, kinetoplast .....	6
1.2.2 Energy metabolism in <i>T. b. brucei</i> .....	8
1.3 Leishmaniasis .....	15
1.3.1 Distribution of the Leishmaniasis .....	15
1.3.2 Life cycle of Leishmania .....	16
1.4 Biochemistry of <i>Leishmania</i> .....	18
1.4.1 Sterol biosynthesis .....	20
1.5 Control of the African animal trypanosomiasis .....	25
1.5.1 Chemotherapeutic control of the trypanosomiasis .....	26
1.5.2 Chemotherapeutic control of Animal Trypanosomiasis .....	27
1.6 Control of Leishmaniasis .....	32
1.6.1 Chemotherapeutic control of Leishmaniasis .....	33
1.6.2 Amphotericin B .....	34
1.7 Shortcomings of chemotherapy in AAT and leishmaniasis .....	36
1.7.1 Drug resistance .....	37
1.8 Methods of assessing drug resistance mechanisms .....	45
1.9 Next Generation Sequencing .....	46
1.10 Metabolomics .....	48
1.11 Proteomics .....	51
1.11.1 Two-Dimensional electrophoresis .....	52

1.11.2	Difference gel electrophoresis .....	52
1.12	Aims of the project.....	54
Chapter Two	.....	55
2	Methods.....	55
2.1	Culturing BSF and PCF <i>Trypanosoma brucei</i> and <i>Leishmania mexicana</i> promastigotes .....	55
2.2	Alamar Blue Assay .....	56
2.3	Induction of drug resistance .....	57
2.4	Selection of clones .....	57
2.4.1	Making stabilates of clones.....	58
2.5	<i>In vitro</i> transformation of AmB resistant promastigotes into amastigotes .....	58
2.6	Monitoring mitochondrial membrane potential .....	58
2.7	Genomic DNA extraction .....	59
2.7.1	Diagnostic PCR for kinetoplast DNA.....	60
2.7.2	Next-Generation Genomic DNA sequencing.....	61
2.7.3	<i>L. mexicana</i> gene cloning using pNUS expression vectors .....	61
2.7.4	Protein over-expression .....	67
2.8	Fluorescence Microscopy .....	68
2.8.1	Immobilisation of live stained cells for imaging .....	68
2.8.2	DNA staining with DAPI .....	68
2.8.3	Mitochondria staining with Mito-Tracker.....	68
2.8.4	Filipin III staining of parasite sterols.....	69
2.8.5	Endoplasmic reticulum (ER) staining with ER-Tracker Red dye .....	69
2.8.6	Imaging cells expressing GFP-tagged proteins.....	69
2.8.7	Cell length measurement.....	70
2.9	[ <sup>3</sup> H]Pentamidine Uptake Assay .....	70
2.10	Metabolomics analysis .....	71
2.10.1	Sample extraction.....	71
2.10.2	Liquid Chromatography/Mass spectrometry.....	71
2.10.3	Data processing.....	72
2.11	Proteomics analysis .....	73
2.11.1	Protein extraction.....	73
2.11.2	Protein concentration determination .....	73
2.11.3	Protein labeling .....	74
2.11.4	Iso-Electric Focusing .....	74
2.11.5	Second dimension electrophoresis.....	74
2.11.6	Total protein staining .....	75
2.11.7	Protein spot picking .....	75

2.11.8	In-gel trypsin digestion .....	75
2.11.9	Protein separation, detection and identification .....	76
2.12	Statistical Analysis.....	76
Chapter Three	.....	77
3	Amphotericin B resistance in <i>Leishmania mexicana</i> promastigotes .....	77
3.1	Introduction .....	77
3.2	Results .....	78
3.2.1	Selection for Amphotericin B resistant <i>L. mexicana</i> .....	78
3.2.2	Characterisation of the derived amphotericin B resistant <i>L. mexicana</i> promastigotes.....	79
3.3	Genomic DNA sequencing and comparison of Wt and AmB resistant <i>L. mexicana</i> .....	82
3.3.1	Identification of genetic alterations in sterol biosynthetic pathway enzymes .....	83
3.3.2	Status of N176I mutation in AmB resistant clones of lower resistance .....	85
3.4	Proteomics analysis of the wild-type and AmB resistant cells .....	86
3.5	Metabolomic comparison of Wt and AmB resistant <i>L. mexicana</i> .....	88
3.5.1	Alterations in the polyamine and thiol metabolic pathways .....	92
3.5.2	Ergosterol supplementation in growth medium .....	97
3.5.3	<i>In vitro</i> transformation and infectivity of AmB resistant <i>L. mexicana</i> promastigotes.....	99
3.5.4	Filipin III staining .....	100
3.6	Discussion .....	103
3.6.1	Stability of AmB resistance.....	103
3.6.2	AmB resistant <i>L. mexicana</i> cross-resistance to other antileishmanial drugs .....	104
3.6.3	Genetic alterations in sterol biosynthetic pathway enzymes .....	107
3.6.4	Response of <i>L. mexicana</i> to different concentrations of AmB .....	108
3.6.5	Effect of exogenous ergosterol supplementation .....	110
3.6.6	Dependence of filipin staining on presence of ergosterol .....	110
3.6.7	Sensitivity of AmB resistant <i>L. mexicana</i> to oxidative stress .....	112
3.6.8	Reduction in cell length of AmB resistant <i>L. mexicana</i> .....	116
Chapter Four	.....	117
4	Participation of <i>Leishmania mexicana</i> lanosterol 14 $\alpha$ -demethylase in amphotericin B resistance .....	117
4.1	Introduction .....	117
4.2	Results .....	118
4.2.1	Position of N176I in <i>L. mexicana</i> 's lanosterol 14 $\alpha$ -demethylase....	118
4.2.2	Alignment of various trypanosomatid lanosterol 14 $\alpha$ -demethylase	119

4.3	Expression of <i>L. mexicana</i> Wt lanosterol 14 $\alpha$ -demethylase into AmB resistant <i>L. mexicana</i> .....	120
4.3.1	Checking for presence of both Wt and AmBR lanosterol 14 $\alpha$ -demethylases in re-expresser clones.....	120
4.3.2	Restoration of Ergosterol levels in re-expresser cells.....	122
4.3.3	Reversal of resistance to AmB .....	123
4.3.4	AmB resistant cells expressing Wt- lanosterol 14 $\alpha$ -demethylase's sensitivity to other anti-leishmanial drugs .....	124
4.4	Effect of sterol C14-reductase inhibitors on AmB resistant cells.....	126
4.4.1	Effect of exposure of <i>L. mexicana</i> Wt to Sterol C14-reductase inhibitors and fenhexamid on AmB sensitivity .....	127
4.4.2	Ergosterol expression after exposure to Sterol C14-reductase inhibitors and fenhexamid .....	128
4.5	Sub-cellular localisation of lanosterol 14 $\alpha$ -demethylase .....	130
4.6	Sub-cellular localisation of sterol C14-reductase.....	131
4.7	Cloning and over-expression of lanosterol 14 $\alpha$ -demethylase in <i>E. coli</i> .....	133
4.8	Discussion .....	134
4.8.1	N176I mutation affected a conserved amino acid residue.....	134
4.8.2	Restoration of ergosterol synthesis following complementation of AmB-R cells with wild-type lanosterol 14 $\alpha$ -demethylase .....	135
4.8.3	Lanosterol 14 $\alpha$ -demethylase interaction with other sterol biosynthetic pathway enzymes .....	138
4.8.4	Effect of sterol C14-reductors inhibitors on wild-type and AmB resistant <i>L. mexicana</i> .....	140
4.8.5	Subcellular localisation of lanosterol 14 $\alpha$ -demethylase and Sterol C14-reductase .....	142
4.8.6	Over-expression of <i>L. mexicana</i> lanosterol 14 $\alpha$ -demethylase in <i>E. coli</i> . .....	143
	Chapter Five.....	144
5	Isometamidium resistance in BSF <i>T. b. brucei</i> .....	144
5.1	Introduction .....	144
5.2	Results .....	145
5.2.1	Induction of isometamidium resistance in BSF <i>T. b. brucei</i> .....	145
5.2.2	Characterisation of isometamidium resistant strains .....	146
5.2.3	Metabolic changes in isometamidium resistant BSF <i>T. brucei</i> .....	156
5.2.4	Genetic status of sphingolipid pathway enzymes .....	161
5.2.5	Comparison of endocytosis between the wild-type and ISMM resistant <i>T. brucei</i> through uptake of Lucifer yellow CH dye.....	163
5.3	Discussion .....	164
5.3.1	Isometamidium resistance selection.....	164
5.3.2	Isometamidium cross-resistance to diminazene aceturate and ethidium bromide .....	165

5.3.3	Susceptibility of ISMM resistant BSF <i>T. brucei</i> to eflornithine .....	166
5.3.4	Maintenance of a low $\Delta\Psi_m$ by ISMM resistant BSF <i>T. brucei</i> .....	167
5.3.5	Perturbation of the sphingolipid biosynthetic pathway.....	168
Chapter Six	.....	171
6	General Discussion .....	171
6.1	Amphotericin B resistance .....	171
6.2	Isometamidium resistance .....	174
Appendices	.....	179
Appendix A: Reagent recipes	.....	179
Appendix B: Monitoring mitochondrial membrane potential.....		182
Appendix C: Ritseq result of the <i>T. b. brucei</i> 927 exposed to isometamidium..		183
Appendix D: <i>S. cerevisiae</i> sterol biosynthetic pathway enzymes and <i>L. mexicana</i> orthologs.....		184
Appendix E: Ergosterol pathway enzyme wise SNP and CNV annotations for Wt and AmB-R cell lines .....		186
Appendix F: <i>L. mexicana</i> lanosterol 14 $\alpha$ -demethylase gene and enzyme sequences.....		203
Appendix G: Comparison of lanosterol 14 $\alpha$ -demethylase sequences of trypanosomatids, <i>S. cerevisiae</i> and <i>H. sapiens</i> .....		204
Appendix H: Two-Dimensional electrophoresis gels showing differences in proteins from <i>L. mexicana</i> wild-type and AmB resistant cell lines. ....		207
Appendix I: Possible identifications of the gel 2-DE spots from <i>L. mexicana</i> wild-type and the derived AmB resistant cell lines. ....		208
Appendix J: Chromatograms of the sterol metabolites detected in wild-type AmB resistant and re-expressor <i>L. mexicana</i> cell lines. ....		213
References.....		216

## List of Tables

Table 2.1 Oligonucleotides used for amplification of kinetoplast related genes.	60
Table 2.2 Oligonucleotides used in cloning experiments. ....	63
Table 3.1 SNPs distribution in wild-type and AmB resistant with reference to U1103 genome. ....	83
Table 3.2 Ploidy of chromosomes harbouring enzymes of the sterol biosynthetic pathway. ....	84
Table 3.3 Proteins identified in proteomics as expressed differently by the wild-type and AmB resistant cells. ....	87
Table 3.4 Reported altered sterol composition in amphotericin B resistant <i>Leishmania</i> species. ....	90
Table 3.5 Sterol metabolites detected in <i>L. mexicana</i> AmB resistant and wild-type cells. ....	91
Table 3.6 Polyamine precursor/substrates and thiols abundance in Wt and AmB-R cells. ....	94
Table 3.7 Comparison of EC <sub>50</sub> values of anti-leishmanial drugs in the presence and absence of N-acetyl-cysteine. ....	96
Table 3.8 Comparison of cross-resistance to other antileishmanial drugs between reported AmB <i>L. donovani</i> and AmB <i>L. mexicana</i> resistant parasites. ....	106
Table 4.1 Characteristics of detected ergosterol in Wt, AmB-R and re-expressor cell lines. ....	123
Table 4.2 Effect of anti-leishmanial drugs on AmB resistant cells expressing the Wt CYP51. ....	125
Table 4.3 Comparison of sterol C14-reductase specific inhibitors on AmB resistant cells. ....	127
Table 5.1 Cross-resistance of isometamidium resistant trypanosomes to AAT and HAT trypanocides. ....	148
Table 5.2 ATPase gamma subunit protein mutations in Wt and ISMM resistant clones. ....	154
Table 5.3 Sphingolipids identified in isometamidium resistant clone and the wild-type cells. ....	159
Table 5.4 Choline phosphorylceramide synthase point mutations of ISMM resistant clones. ....	162

## List of Figures

Figure 1.1 Distribution of reported cases of Human African Trypanosomiasis. ...	2
Figure 1.2 The distribution of tsetse flies in Eastern Zambia and occurrence of clinical HAT.....	4
Figure 1.3 The life cycle of African trypanosomes. ....	6
Figure 1.4 Schematic representation of the organisation of major organelles of bloodstream form of <i>Trypanosoma brucei</i> .....	7
Figure 1.5 <i>Trypanosoma brucei</i> procyclic form energy metabolism. ....	10
Figure 1.6 Global distribution of leishmaniasis and Leishmania/HIV co-infection, 1990-1998.....	16
Figure 1.7 Life cycle of leishmania in mammals and sandfly. ....	17
Figure 1.8 Simplified <i>Leishmania major</i> sterol biosynthetic pathway.....	23
Figure 1.9 Sterol C14-demethylase catalyzed reaction of the sterol biosynthetic pathway.....	24
Figure 1.10 Molecular structures of diminazene (A) and homidium (B). ....	29
Figure 1.11 Molecular structure of isometamidium. ....	29
Figure 1.12 Molecular structures (a) Quinapyramine, (b) Cymelarsan and (c) Suramin. ....	31
Figure 1.13 Molecular structures of the drugs that are used against Leishmaniasis.....	36
Figure 1.14 Occurrence of trypanocidal resistance in African Animal Trypanosomiasis. ....	38
Figure 2.1 The pNUS-HnN and pNUS-GFPcN expression vector maps. ....	62
Figure 2.2 Schematic representation of the serial dilution of the transfected <i>L. mexicana</i> for cloning.....	67
Figure 3.1 Comparison of AmB EC <sub>50</sub> values for various <i>L. mexicana</i> AmB resistant clones. ....	79
Figure 3.2 Comparison of the cell body length of the wild-type and the AmB resistant cells. ....	80
Figure 3.3 Amphotericin B cross-resistance to other anti-leishmanial drugs. ....	81
Figure 3.4 [ <sup>3</sup> H]Pentamidine up-take in AmB resistant cells compared to the wild-type cells. ....	82
Figure 3.5 Comparison of CNV of parental wild-type and the derived AmB resistant clone. ....	83
Figure 3.6 Point of N176I occurrence in AmB resistant clones at different selection points. ....	85
Figure 3.7 PCA of the metabolomic comparison of Wild-type and AmB resistant cells. ....	89
Figure 3.8 Volcano plot of the identified metabolites in metabolomics analysis.	92

Figure 3.9 Comparison of polyamine and thiol metabolites in Wt and AmB resistant cells. ....	93
Figure 3.10 Susceptibility to AmB and pentamidine in the presence of exogenous ergosterol.....	98
Figure 3.11 Comparison of transformation into amastigotes and infectivity between Wt and AmB resistant <i>L. mexicana</i> promastigotes. ....	100
Figure 3.12 Differential filipin III staining of the wild-type and AmB resistances cells. ....	101
Figure 3.13 Fillin staining of macrophages infected with Wt and AmB resistant <i>L. mexicana</i> .....	102
Figure 3.14 Molecular structure of ergosterol showing the numbering of atoms .....	114
Figure 4.1 <i>L. mexicana</i> wild-type promastigote lanosterol 14 $\alpha$ -demethylase structure. ....	119
Figure 4.2 Primary structure alignment of lanosterol 14 $\alpha$ -demethylase of trypanosomatids. ....	120
Figure 4.3 PCR amplification of chromosomal and extra-chromosomal AmB-R CYP51. ....	121
Figure 4.4 Sequence alignment of the chromosomal and extra-chromosomal CYP51. ....	122
Figure 4.5 Restoration of ergosterol levels in AmB resistant cells expressing Wt CYP51 .....	123
Figure 4.6 Reversal of AmB resistance by complementation of AmB-R with Wt CYP51. ....	124
Figure 4.7 <i>L. mexicana</i> Wt sensitivity to AmB after exposure to sterol biosynthesis inhibitors .....	128
Figure 4.8 Sterol biosynthetic pathway inhibitors' effect on ergosterol expression. ....	130
Figure 4.9 Mito- and ER-Tracker staining of GFP-tagged wild-type and AmB resistant CYP51. ....	131
Figure 4.10 Mito- and ER-Tracker staining of GFP-tagged Wt and AmB-R sterol C14-reductase.....	132
Figure 4.11 Over-expression of Wild-type and AmB resistant lanosterol 14 $\alpha$ -demethylase.....	134
Figure 4.12 4, 4-dimethylcholesta-8, 14, 24-trien-3 $\beta$ -ol to 4 $\alpha$ -zymosterol part of the sterol biosynthetic pathway of yeast. ....	141
Figure 5.1 Isometamidium resistance selection in <i>T. brucei</i> 427 bloodstream forms. ....	145
Figure 5.2 Comparison of growth of <i>T. brucei</i> Wt and derived ISMM resistant cells. ....	146
Figure 5.3 Isometamidium cross-resistance to ethidium bromide and diminazene aceturate. ....	147

Figure 5.4 Monitoring mitochondrial membrane potential of bloodstream forms of <i>T. brucei</i> 427 wild-type and the derived isometamidium resistant clones. ..	150
Figure 5.5 Loss of the kinetoplast by isometamidium resistant BSF <i>T. brucei</i> 427 .....	152
Figure 5.6 PCR amplification of the kinetoplast based maxicircle genes of BSF <i>T. brucei</i> . .....	153
Figure 5.7 BSF <i>T. brucei</i> active mitochondria staining with Mito-Tracker Red CMXRos. ....	155
Figure 5.8 Pie chart representation of all identified metabolites analysed using IDEOM. ....	157
Figure 5.9 Differentiation of the wild-type from the isometamidium resistant clone by PCA. ....	158
Figure 5.10 Most changing <i>T. brucei</i> metabolites of the sphingolipid biosynthetic pathway. ....	160
Figure 5.11 Non-synonymous mutations detected in choline phosphorylceramide synthase. ....	162
Figure 5.12 Comparison of the internalisation of lucifer yellow CH fluorescent dye. ....	163

## Acknowledgement

I shall always remain grateful to Prof. M. P. Barrett for all the support, guidance and indeed for allowing me to work under his supervision.

I extend my special thanks to Mum for everything - you were always at hand when Dad unleashed the words of wisdom, especially his emphasis on the importance of education in one's life.

To Judy my wife, thank you for all your support and understanding. Isaac and Malumbo, our wee ones, you cheered me up after work and for that I commend you. You are a blessing indeed. I acknowledge my brothers and sisters for the patience and support while I pursued my studies.

My acknowledgements would be incomplete without mentioning Uncle Jolly and Auntie Yvonne. I most sincerely thank you for giving me unrestricted space at the time it looked like all hope was lost. To this end, Auntie Mwika and Uncle Robert you also made a contribution in your own way, I sincerely thank you.

I thank everyone in the Mike Barrett Lab group for the period September 2010 - May 2014, for sharing their knowledge and the various interactions I have had with all of them. I particularly express my gratitude to those mentioned in the various parts of the thesis for their contribution. It was a delight to work with you all. I also wish to thank Anthonious and Daniel from Level 5 of GBRC, for all that we shared, and Benjamin Cull from Level 6 of GBRC.

This study was made possible by a scholarship from the Commonwealth Scholarship Commission in the UK and a PhD study fellowship from the University of Zambia.

# Dedication

You shall always be remembered

this one is for you, Dad.

## Author's Declaration

I declare that, unless where explicitly stated of the contributions made by others, this dissertation is the result of my own work and has not been submitted for any other degree or qualification at The University of Glasgow or any other institution.

Roy Mwenechanya

June 2014

## Definitions/Abbreviations

$\Delta\Psi_m$	Mitochondrial membrane potential
°C	Degrees Celsius
$\mu\text{m}$	micr- meter
$\mu\text{M}$	micro-molar
A	Adenine
AAT	African Animal Trypanosomiasis
AmB	Amphotericin B
AOX	Alternative oxidase
AQP	Aquaglyceroporin
ATP	Adenosine triphosphate
BSF	Bloodstream form
CMM	Creek's minimal medium
DA	Diminazene Aceturate
DAPI	4, 6-diamidino-2-phenylindole
DDT	Dichlorodiphenyltrichloroethane
DIGE	Difference gel electrophoresis
DNA	Deoxyribonucleic acid
ER	Endoplasmic reticulum
EtBr	Ethidium Bromide
FACS	Fluorescence Activated Cell Sorting
FAD	Oxidised Flavin adenine dinucleotide
FADH <sub>2</sub>	Reduced flavin adenine dinucleotide
GC/MS	Gas Chromatography/ Mass Spectrometry
GFP	Green fluorescent protein
gRNA	guide Ribonucleic acid
HIV	Human immunodeficiency virus
IEF	Iso-electric focusing

Ig	Immunoglobulin
ISMM	Isometamidium
KCN	Potassium cyanide
kDNA	kinetoplast Deoxyribonucleic acid
LC/MS	Liquid Chromatography/Mass Spectrometry
mM	Milli-molar
mRNA	Messenger ribonucleic acid
NAC	N-Acetyl-L-cysteine
NAD <sup>+</sup>	Oxidised nicotinamide adenine dinucleotide
NADH	Reduced nicotinamide adenine dinucleotide
NGS	Next generation sequencing
PAT	Potassium Antimony tartrate
PBS	Phosphate buffered saline
PCA	Principal Components Analysis
PCF	Procyclic form
PCR	Polymerase chain reaction
RNA	Ribonucleic acid
ROS	Reactive oxygen species
SAT	Sequential aerosol techniques
SEM	Standard Error of the Mean
SHAM	Salicylhydroxamic acid
SIT	Sterile insect technique
SNPs	Single nucleotide polymorphisms
T	Thymine
TAO	Trypanosomal alternative oxidase
VSG	Variant surface glycoproteins
WHO	World Health Organisation

# Chapter One

## 1 General Introduction

Kinetoplastid protozoa are characterised by the presence of a flagellum and a network of circular DNA organized as an organelle called the kinetoplast. They cause some of the most debilitating neglected diseases in humans and animals. The Leishmaniases caused by *Leishmania* species and trypanosomiases caused by *Trypanosoma* species, respectively, are examples of such diseases. These diseases are controlled primarily by chemotherapy although there are few effective drugs and there is no known vaccine. The shortage of drugs for treating these diseases and their well-known shortcomings inspired this study to assess possible ways of prolonging the use of two anti-kinetoplastid drugs by identifying molecular markers of resistance and the possible mechanisms, and how to circumvent resistance should it arise.

### 1.1 African trypanosomiases

African trypanosomiases are infectious diseases that affect both humans and animals and are caused by species of *Trypanosoma*. Two broad types of African trypanosomiasis can be distinguished based on the hosts of the causative agents. The type affecting humans as hosts is referred to as Human African Trypanosomiasis (HAT) also commonly called African sleeping sickness. The second type affects animals as hosts and is called African Animal Trypanosomiasis (AAT).

#### 1.1.1 Human African Trypanosomiasis

HAT affects the populations of poor remote rural parts of Africa more than the urban or peri-urban area populations (Brun *et al.*, 2010). Sleeping sickness occurs in about 36 sub-Saharan African countries (Figure 1.1), putting 60 million people at risk of contracting the disease (Fairlamb, 2003). The distributions of the diseases overlap with the distribution of the vector, the tsetse flies of the genus *Glossina* (Barrett *et al.*, 2003). It was estimated that 300, 000 - 500, 000 people were infected with the disease in the year 1998 while in 2001, 50, 000 deaths were recorded (Barrett *et al.*, 2003; Fairlamb, 2003). The disease

statistics have been thought to be underestimates because the disease occurs in the rural remote areas where not all cases can be diagnosed and hence unreported (Barrett *et al.*, 2003). In recent years, incidence has declined to less than 10, 000 reported in 2011 (Simarro *et al.*, 2011). HAT is caused by two distinct subspecies of *Trypanosoma brucei* or *T. brucei*, occurring in separate geographical foci of the African continent. In West and Central Africa, *T. b. gambiense* causes the chronic form of the disease while in east and southern Africa, the predominant *T. b. rhodesiense* causes the acute form of the disease (Figure 1.1). HAT is zoonotic with the humans acting as the main reservoirs of *T. b. gambiense*, while the major reservoirs of *T. b. rhodesiense* are wild and domestic animals, especially cattle (Brun *et al.*, 2010; Simarro *et al.*, 2008; Wilkinson and Kelly, 2009).

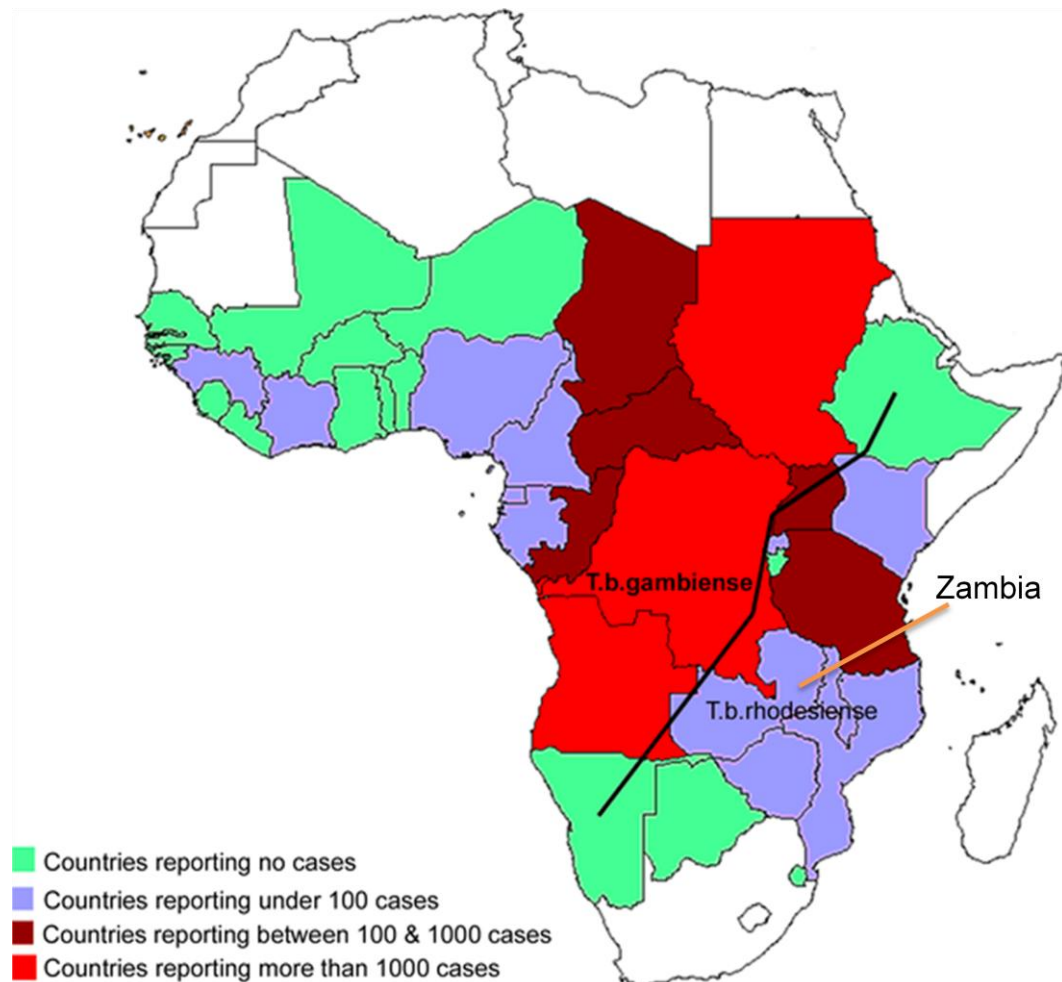


**Figure 1.1** Distribution of reported cases of Human African Trypanosomiasis. The two areas of the continent in which distribution of HAT caused by *T. b. gambiense* and *T. b. rhodesiense* is divided by the black line. Adapted from Simarro *et al.*, 2008 with the Creative Commons Attribution License authorisation.

### 1.1.2 African Animal Trypanosomiasis

African Animal Trypanosomiasis is endemic in 37 African countries where it is estimated that about 50 - 70 million animals are at risk from trypanosomiasis. AAT is common in domesticated animals. *T. congolense*, *T. vivax* and, to a lesser extent, *T. b. brucei* are the causative agents of the disease in domestic animals (Geerts *et al.*, 2001). There have been reports of these three non-human pathogens causing trypanosomiasis in man (Brun *et al.*, 2010).

### 1.1.3 Burden (Economic) of African Animal trypanosomiases

Human African trypanosomiasis and African Animal trypanosomiasis are a major cause of underdevelopment in the sub-Saharan rural areas (Brun *et al.*, 2010; Welburn *et al.*, 2006). AAT results in estimated annual economic losses of USA \$1.340 billion (Kristjanson *et al.*, 1999). Livestock, especially cattle, provide food, transport, manure and draught power, for the rural population. However, AAT has been reported to reduce animal numbers and those that survive are too weak and ill to provide even the basic of benefits (Welburn *et al.*, 2006). This deprives people a way out of poverty by reducing what could have been realised from the sale of animal meat and other products.

### 1.1.4 Trypanosomiases in Zambia

Zambia is located at latitude 15° 0' South and 30° 0' East in the Southern African region (Figure 1.1). It lies in the common (tsetse) fly belt region covering Zambia, Zimbabwe, Mozambique and Malawi. The common fly belt is mostly centred in the eastern part of Zambia that is drained by the Zambezi and the Luangwa rivers (Figure 1.2). Within this belt, the highest tsetse densities are situated around the two river valleys. *Glossina morsitans morsitans* (Westwood) and *Glossina pallidipes* (Austen) are the most common species of tsetse fly in this region (Munang'andu *et al.*, 2012). The proliferation of the tsetse in the river valleys seems to be supported by the conducive climate, the relative abundance and wide range of hosts from which the flies take blood meals. Despite various strategies aimed at tsetse fly control or elimination as well as wild animal conservation being put in place, dating as far back as the pre-colonial era and on into the young Zambian nation, there seem to have been a

sustained infestation and confinement of the vector to the Luangwa and Zambezi valley. Eastern Zambia will continue to harbour trypanosomiasis because of the close interactions between the vectors, the two hosts and the causative parasites (Munang'andu *et al.*, 2012). To reduce these interactions the government of Zambia established national parks, around which are game management areas which act as buffer zones between wild-life and humans. Sustained tsetse fly infestation of parts of eastern Zambia could be the reason why the transmission foci of HAT have remained in this part of the country while it has since been reported to have disappeared from most parts of the country even in the absence of active control strategies (Figure 1.2). The disappearance of HAT has so far been attributed mostly to anthropogenic activities. HAT in Zambia is caused by *T. b. rhodesiense* and is zoonotic (Mwanakasale and Songolo, 2011). The first recorded case of HAT in Zambia was in 1908 when it was diagnosed in a European mineral explorer who travelled in the area prospecting for minerals (Stephens and Fantham, 1910).

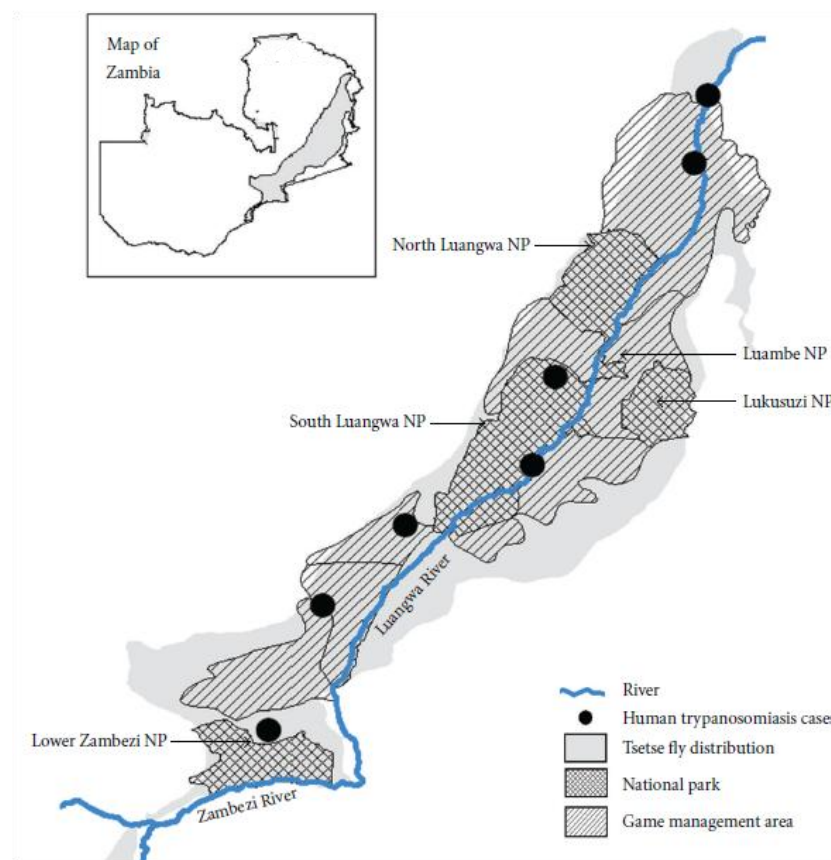


**Figure 1.2** The distribution of tsetse flies in Eastern Zambia and occurrence of clinical HAT. Insert map shows the position of eastern Zambia. Adapted from Munang'andu *et al.*, 2012 with the Creative Commons Attribution License authorisation.

The main causative agent of AAT in Zambia is *T. congolense* while *T. vivax* is responsible for a few infections in cattle. Cattle are the most affected by AAT with a monthly risk of infection at 6% on the plateau area of eastern Zambia (Simukoko *et al.*, 2007; Simukoko *et al.*, 2011). The highest prevalence of AAT affecting cattle was in 1992 but varies from year to year, with 25, 000 animals reportedly affected in the Eastern province of Zambia for the period from 1988 to 2008. The various intervention strategies instituted from then on has precipitated a decline in the prevalence of the disease. These strategies included use of isometamidium chloride every four months for prophylaxis and diminazene aceturate for the treatment of infected animals. This regimen is still in use for controlling the disease. Insecticide based techniques targeting the tsetse flies have also been used to control AAT (Mubamba *et al.*, 2011).

## **1.2 Life cycle of *Trypanosoma brucei***

Trypanosomes undergo differentiation in two different hosts; namely mammals and tsetse flies. The two hosts present distinct environments with different nutrients available to the trypanosomes as a consequence the parasites assume different forms to adapt to the environment and this results in their having a complex life cycle (Figure 1.3). A bite of the mammalian host by an infected tsetse fly during a blood meal leads to delivery of metacyclic forms of trypanosomes. The metacyclic forms transform into the replicative long slender trypomastigotes or bloodstream forms, which multiply by binary fission with a doubling time of about six hours (Vickerman, 1985). The long slender trypomastigotes express variant surface glycoproteins (VSG) on their surface. The VSGs are recognised by the host (mammal) immune system which leads to production of IgM and IgG antibodies that neutralise the trypanosomes. This results in a reduction in parasitaemia. The surviving trypanosomes, however, avoid the host immune response against them by producing different VSGs from the ones that were initially recognised leading to an increase in parasitaemia. The long slender trypomastigotes then transform into non - dividing stumpy trypomastigotes which have altered their biochemical physiology as a pre-adaptation for the tsetse fly (Vickerman, 1985).

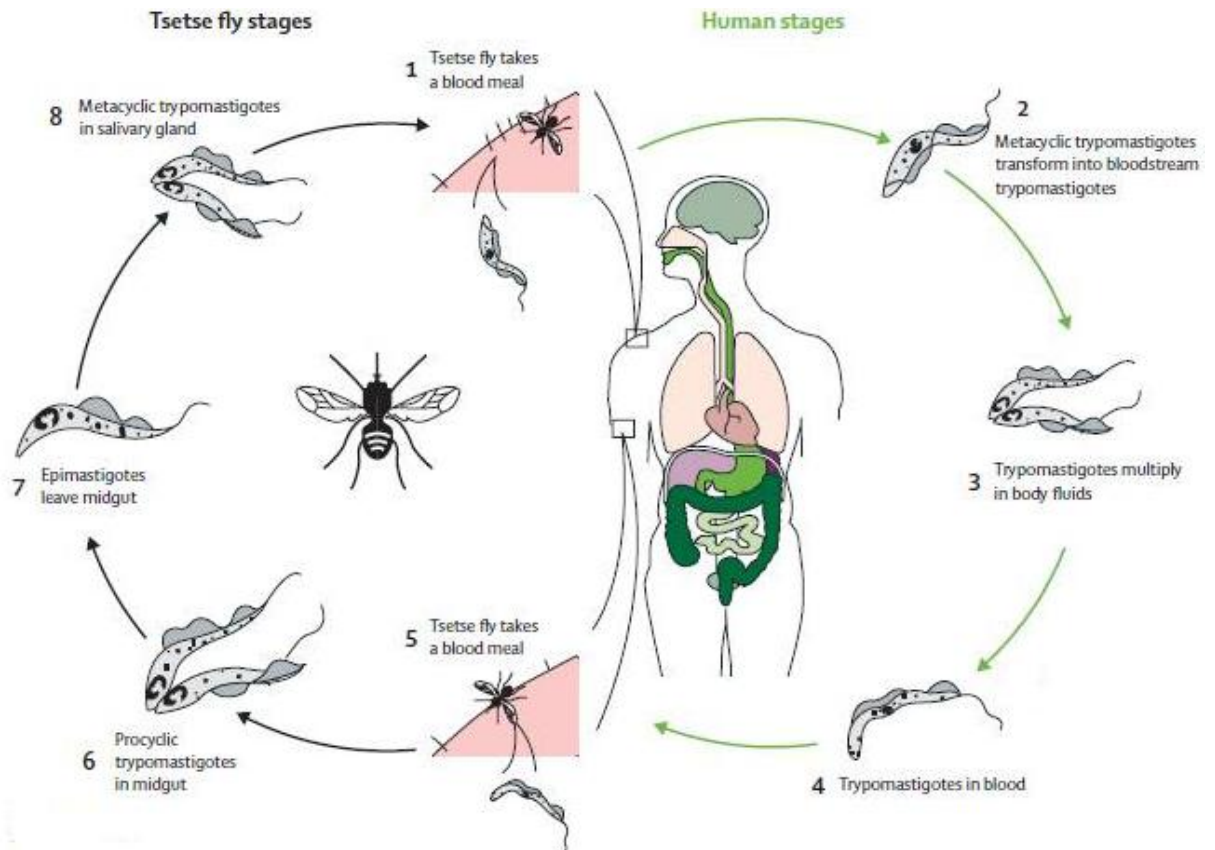


**Figure 1.3 The life cycle of African trypanosomes.**  
(Source; Blum, *et al.*, 2008).

The next bite of an infected mammal by the tsetse fly leads to transmission of the stumpy trypomastigotes, which are able to continue the life cycle in the vector. When the infected blood is ingested by the tsetse fly and upon reaching the lumen of the midgut, the stumpy trypanosomes transform into the procyclic trypanosomes (Vickerman, 1985). The procyclic trypanosomes increase in body length and the mitochondrion becomes more elaborate. The procyclic forms transform into the proliferative epimastigotes in the salivary glands. The epimastigotes transform into the non-proliferative metacyclics that are ready for injection into the mammals at the next infected tsetse fly blood meal (Vickerman, 1985; Wheeler, 2010).

### 1.2.1 Cellular organization - Glycosome, mitochondrion, kinetoplast

Trypanosomes are single celled organisms measuring 15 to 30  $\mu\text{m}$  in length and possess a flagellum (Brun *et al.*, 2010) which is involved in several cell processes including cell motility, cytokinesis, cell morphogenesis, host immune evasion and

host cell attachment in *T. brucei* (Ralston and Hill, 2008). They are obligate parasites with a eukaryotic cellular organization (Figure 1.4). However, some of their organelles possess unique features compared to those of the other eukaryotes (Brun *et al.*, 2010).

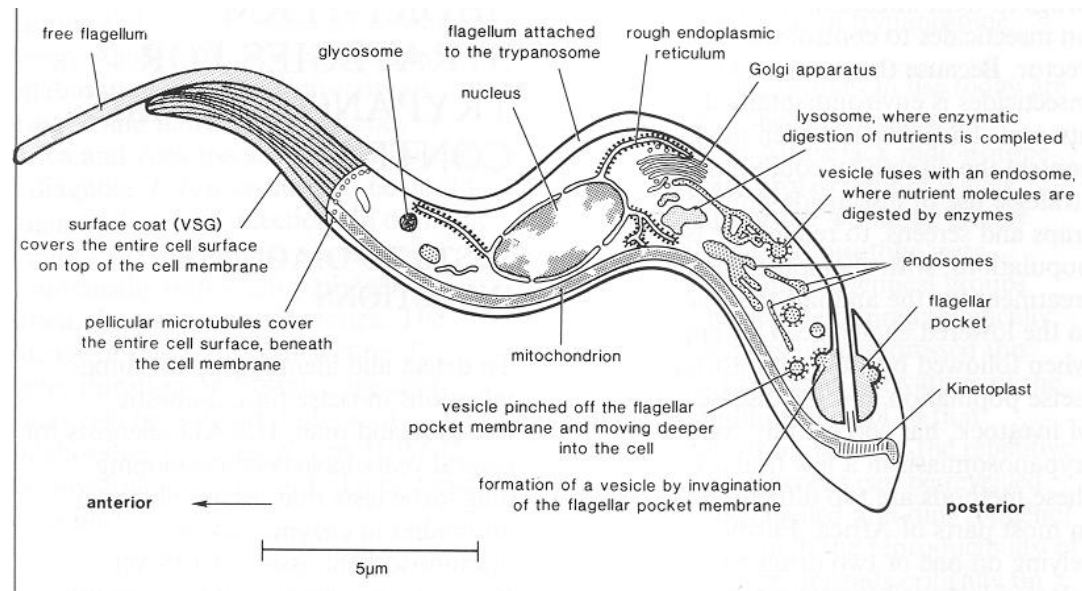


**Figure 1.4 Schematic representation of the organisation of major organelles of bloodstream form of *Trypanosoma brucei*.**

Adapted from <http://www.ilri.org/InfoServ/Webpub/fulldocs/llrad88/Trypanosomiasis.htm>

Trypanosomes possess a single large mitochondrion spanning the entire cell length. The mitochondria assume different forms at different stages of the trypanosomes' life cycle. It changes from the simple tubular form in the bloodstream forms to a branched network having prominent well developed discoid or plate-like cristae in the procyclic forms (Opperdoes, 1987; Vickerman, 1985). The mitochondrion contains DNA called kinetoplast DNA. It forms a disk-like structure in the mitochondrial matrix and is located adjacent to the flagellum basal body (Simpson, 1987). kDNA is a network of DNA circles called minicircles and maxicircles (Shapiro and Englund, 1995). The minicircles encode small guide RNA (gRNA) that are used for editing transcripts of the maxicircles in a process that involves insertion or deletion of uridine residues to form functional mRNAs (Aphasizhev and Aphasizheva, 2011). The maxicircles of *T. brucei* are the equivalents of the mitochondrial genome in other eukaryotic cells and encode the ribosomal RNA namely the 9S and 12S subunit genes and a ribosomal protein called RPS12. The maxicircle genes also encode subunits or protein subunits of the electron transport chain and these include the ATPase A6

subunit, six subunits of complex I, apocytochrome b of complex III and three subunits of complex IV (Schnauffer *et al.*, 2002).

The cytoplasm contains many spherical or ellipsoidal peroxisome-like organelles called glycosomes. There is an average of 230 glycosomes per cell, each of which is bound by a single membrane and they occupy about 4.3% of the total cell volume in *T. brucei* (Opperdoes *et al.*, 1984). They contain most of the glycolytic enzymes which earned peroxisomes in these protozoa the name, glycosomes (Opperdoes and Borst, 1977). Glycosomes change in shape from being spherical to a bacilliform or rod-shaped organelles as the trypanosome transforms from bloodstream forms into procyclic forms (Vickerman, 1985).

### **1.2.2 Energy metabolism in *T. b. brucei***

The complexity of the life cycle of the *T. brucei* parasites makes them adopt different metabolic patterns at different stages of their life cycles as their differentiation alternates between the blood stream forms and the procyclic forms. This is due to the different carbon sources found in the two hosts (Bringaud *et al.*, 2006; van Hellemond *et al.*, 2005a).

The bloodstream form trypanosome has the simplest energy metabolism which is based on glycolysis because of the high concentration of glucose (5 mM) in the vertebrate hosts, as compared to the procyclic form. The procyclic forms depend on amino acid catabolism, in particular L-proline, which is among the prominent constituents of insect's hemolymph and tissue fluids, and L-threonine (Bringaud *et al.*, 2006) which is the main carbon source in the fatty acid and sterol biosynthetic pathways (Millerioux *et al.*, 2013). The prominence of proline in the insect is due to the fact that it is used by tsetse flies as an energy source for flight (Vickerman, 1985). However, procyclic forms of *T. brucei*, preferentially use glucose when both glucose and amino acids are available, but use proline in glucose diminished environments (Lamour *et al.*, 2005).

#### **1.2.2.1 The Glycolytic pathway**

Carbohydrate energy metabolism in trypanosomes is said to be compartmentalised as it occurs in the glycosome, the cytosol and the

mitochondrion (Opperdoes, 1987). In procyclic forms of *T. brucei* the first seven reactions of the glycolytic pathway, converting glucose to 3-phosphoglycerate, occur in the glycosome. The last three of the ten classical glycolytic reactions, involving conversion of 3-phosphoglycerate into pyruvate, take place in the cytosol (van Hellemond *et al.*, 2005a). Part of the phosphoenolpyruvate produced in these last three reactions is imported from the cytosol into the glycosome and subsequently metabolized in four reactions to succinate (Figure 1.4) (Besteiro *et al.*, 2005). The remaining phosphoenolpyruvate, in the cytosol, is converted to the end-product of glycolysis, pyruvate.

In bloodstream forms of *T. brucei*, glucose is classically believed to be catabolised as far as pyruvate which is secreted from the cell (Besteiro *et al.*, 2005; van Hellemond *et al.*, 2005a). However, recently it has become clear that a more extensive metabolism of glucose occurs in bloodstream forms (Kerkhoven, 2013 - In Press). Although the primary flux does end in pyruvate, many of the pathways present in procyclic forms also occur in bloodstream forms (Creek and Barrett, Unpublished). Indeed it has also been shown that glucose is also catabolised to acetate. Acetate derived from glucose catabolism and that from threonine is said to be essential for cell viability and is used for fatty acid synthesis by the bloodstream forms of *T. brucei* (Mazet *et al.*, 2013).

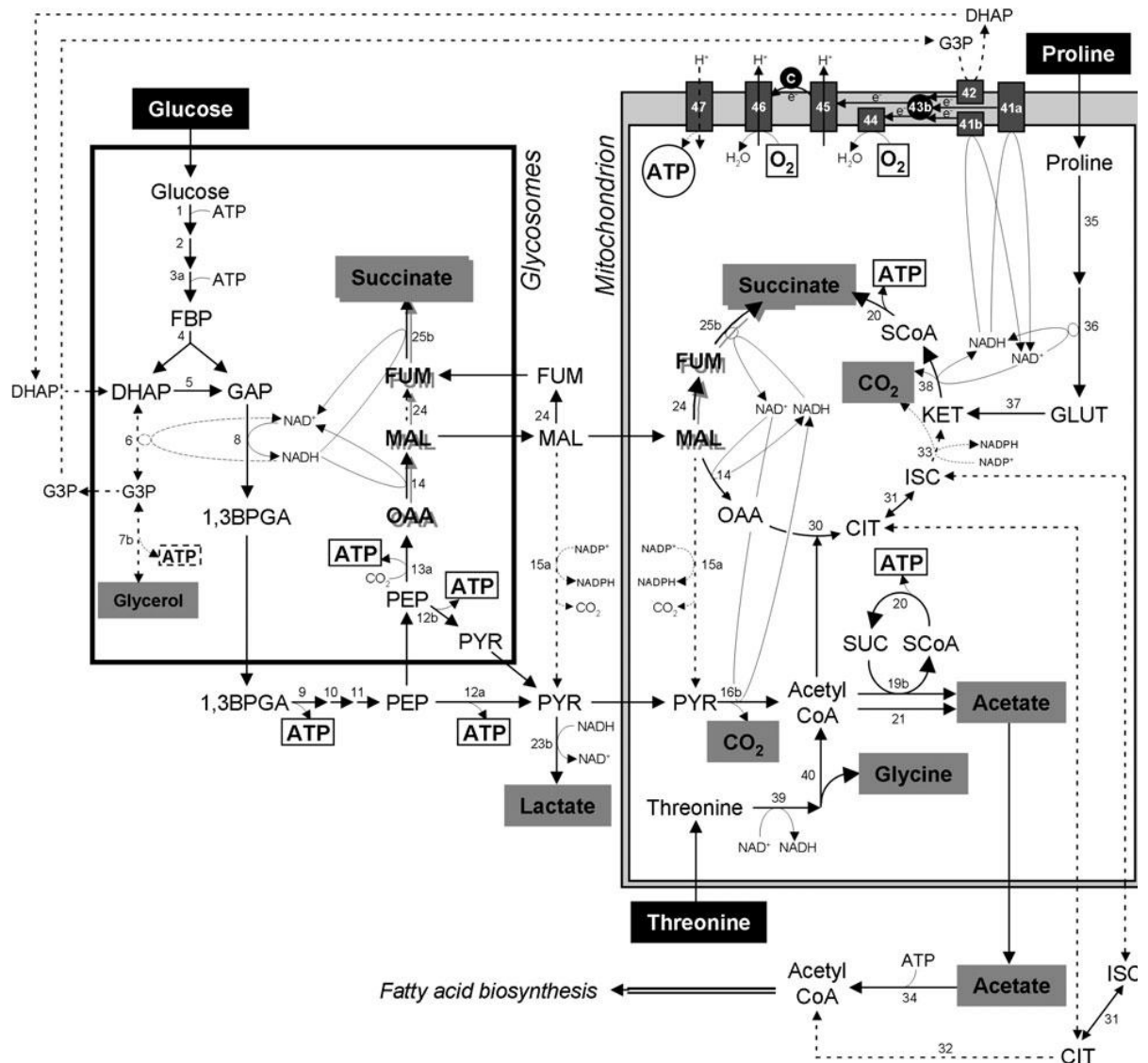


**Figure 1.5 *Trypanosoma brucei* procyclic form energy metabolism.** Representation of parasite grown in an environment with an abundance of glucose. Glucose, proline and threonine catabolism excreted end products are shown with a grey background. Reactions with uncertain occurrence under standard growth conditions are indicated by dashed arrows. Occurrence of succinate fermentation pathways in the glycosome and mitochondria are shadowed. Substrate level phosphorylation and oxidative phosphorylation ATP yield are boxed and circled, respectively. 1,3BPGA = 1,3-bisphosphoglycerate; c = cytochrome c; CIT = citrate ;DHAP = dihydroxyacetone phosphate; e<sup>-</sup> = electrons; FBP = fructose 1,6-bisphosphate; G3P = glycerol-3-phosphate; GAP = glyceraldehyde-3-phosphate; Fd = ferredoxin; FUM = fumarate; GLUT = glutamate; ISC = isocitrate ; KET = 2-ketoglutarate ; MAL = malate; MCoA = methylmalonyl-CoA; OAA = oxaloacetate; PCoA = propionyl-CoA; PEP = phosphoenolpyruvate; PPi = inorganic pyrophosphate; PYR = pyruvate; SCoA = succinyl-CoA; SUC = succinate. Numbered enzymes are: 1 = hexokinase; 2 = glucose-6-phosphate isomerase; 3a = ATP-dependent phosphofructokinase (ATP-PFK); 3b = PPi-dependent phosphofructokinase (PPi-PFK); 4 = aldolase; 5 = triose-phosphate isomerase; 6 = glycerol-3-phosphate dehydrogenase; 7a = glycerol-3-phosphatase; 7b = glycerol kinase; 8 = glyceraldehyde-3-phosphate dehydrogenase; 9 = phosphoglycerate kinase; 10 = phosphoglycerate mutase; 11 = enolase; 12a = pyruvate kinase (PYK); 12b = pyruvate phosphate dikinase (PPDK); 13a = phosphoenolpyruvate carboxykinase (PEPCK); 13b = phosphoenolpyruvate carboxytransphosphorylase; 14 = malate dehydrogenase; 15a = malic enzyme; 15b = malate dehydrogenase (decarboxylating) ; 16a = pyruvate:ferredoxin oxidoreductase; 16b = pyruvate dehydrogenase complex; 17 = ferredoxin:NAD oxidoreductase; 18 = hydrogenase; 19a = Acetyl-CoA synthetase 'ADP forming' ('ADP forming' AceCS); 19b = acetate:succinate CoA-transferase (ASCT); 20 = succinyl-CoA synthetase (SCoAS); 21 = unknown enzyme; 22 = bifunctional acetyl-CoA reductase/alcohol dehydrogenase; 23a = lactate dehydrogenase;

23b = unknown enzyme; 24 = fumarase, 25a, membrane-bound fumarate reductase (FRD); 25b = NADH-dependent fumarate reductase (NADH-FRD); 26 = propionate:succinate CoA-transferase; 27 = methylmalonyl-CoA mutase; 28 = methylmalonyl-CoA racemase; 29 = propionyl-CoA carboxylase; 30 = citrate synthase; 31 = aconitase; 32 = citrate lyase; 33 = isocitrate dehydrogenase; 34 = acetyl-CoA synthetase 'AMP forming' ('AMP forming' AceCS); 35 = L-proline dehydrogenase; 36 = pyrroline-5 carboxylate dehydrogenase; 37 = alanine aminotransferase; 38 = 2-ketoglutarate dehydrogenase complex; 39 = L-threonine dehydrogenase; 40 = acetyl-CoA:glycine C-acetyltransferase; 41a = rotenone-sensitive NADH dehydrogenase (complex I of the respiratory chain); 41b = rotenone-insensitive NADH dehydrogenase; 42 = FAD-dependent glycerol-3-phosphate dehydrogenase (FAD-GPDH); 43a = rhodoquinone, such as menaquinone; 43b = ubiquinone; 44 = SHAM-sensitive alternative oxidase; 45 = complex III of the respiratory chain; 46 = complex IV of the respiratory chain; 47 = F<sub>0</sub>F<sub>1</sub>-ATP synthase. (Source: Bringaud, *et al.*, 2010)

The glycolytic pathway in trypanosomes is regulated by the compartmentation of the glycolytic pathway to the glycosomes instead of by the typical allosteric regulation of enzymes as is in mammals and many other species (Haanstra *et al.*, 2008; Tielens and van Hellemond, 2009).

### 1.2.2.2 The Krebs's Cycle

The fate of pyruvate under certain conditions is different in different species of trypanosomes. It is converted to L-lactate instead of D-lactate anaerobically in *T. b. gambiense* procyclic forms by an unknown enzyme (Darling *et al.*, 1988). The procyclic forms of *T. brucei* do not excrete pyruvate but take it up into the mitochondrion where it is further degraded by pyruvate dehydrogenase to acetyl-CoA. Acetyl-CoA is not degraded in the usual way of the Krebs's cycle but into acetate. The conversion of acetyl-CoA to acetate is catalysed by acetate:succinate transferase which transfers the CoA from acetyl-CoA to succinate to yield succinyl-CoA which is converted back to succinate by succinyl-CoA synthetase to produce ATP (van Hellemond *et al.*, 2005a). The combined action of succinyl-CoA synthetase and acetyl CoA thioesterase results in acetate being produced and excreted to the cytosol (Bringaud *et al.*, 2010; van Hellemond *et al.*, 2005a). As a result procyclics do not use a complete Krebs's cycle to generate energy (van Grinsven *et al.*, 2009; van Hellemond *et al.*, 2005a; van Weelden *et al.*, 2003). This happens despite all the Krebs's cycle enzyme genes being present in the genome and are expressed in the procyclic forms of *T. brucei* (Tielens and van Hellemond, 2009). The acetate formed in the mitochondrion is also exported to the cytosol where the essential cytosolic acetyl-CoA synthetase converts it into acetyl-CoA which is used in the biosynthesis of lipids (Riviere *et al.*, 2009).

A part of the Krebs cycle is used when proline happens to be the main carbon source for the procyclics and is degraded to succinate as the major end product through  $\alpha$  - ketoglutarate (van Weelden *et al.*, 2005). The first two reactions of the cycle have been assumed to be involved in metabolism in the wild-type strains of procyclic *T. brucei* as was shown in the accumulation of citrate in aconitase knockout procyclic *T. brucei* (van Weelden *et al.*, 2003). The presence of the Krebs cycle enzymes in the mitochondrion of these parasites led to the interpretation that the Krebs cycle may have a role to play in energy generation or metabolism of the parasite's life cycle stages in the salivary glands of the tsetse fly (van Weelden *et al.*, 2003). The phosphoenolpyruvate produced from the glycolytic pathway can be re-exported back into the glycosomes where it is converted to malate through oxaloacetate. The malate may also be exported to the mitochondrion where it is converted through fumarate to succinate in a similar reaction to the one which occurs in the glycosome. This conversion is believed to be part of the Krebs cycle that is utilised by the procyclic forms of *T. brucei* (Figure 1.5). In the glycosome and mitochondrion the produced succinate is excreted (Tielens and van Hellemond, 2009). The bloodstream forms of *T. brucei* lack most of the Krebs cycle enzymes (van Hellemond *et al.*, 2005a).

### 1.2.2.3 The Electron Transport Chain

The procyclic forms of *T. brucei* have a fully functional branched electron-transport chain (van Hellemond *et al.*, 2005a; van Hellemond *et al.*, 2005b). The flow of electrons in complex I, complex III and complex IV leads to translocation of protons from the mitochondrial matrix into the mitochondrial intermembrane space thereby producing a proton gradient that leads to generation of a proton motive force (van Hellemond *et al.*, 2005b). The proton motive force is used for generating ATP by ATP synthase or ATPase. Oxygen is the final acceptor of the electrons leading to the formation of water (van Hellemond *et al.*, 2005b). The proton gradient is responsible for the generation of the mitochondrial membrane potential which in turn is also important in the importation of proteins and key metabolites from the cytosol into the mitochondrion (Besteiro *et al.*, 2005; Jensen *et al.*, 2008). Therefore, both substrate-level and oxidative phosphorylation contribute to ATP generation in procyclic trypanosomes. ATP generation by oxidative phosphorylation is essential in the presence of lower concentrations of glucose when metabolism shifts to use of amino acids while

generation of ATP by substrate-level phosphorylation dominates in the presence of high concentrations of glucose (Besteiro *et al.*, 2005; Bringaud *et al.*, 2010). However, ATP generation by oxidative phosphorylation in procyclic *T. brucei* was shown not to be essential while ATP generation through substrate level phosphorylation in the cytosol was indicated to be essential (Coustou *et al.*, 2003).

The branching of the electron transport chain of procyclic *T. brucei* (Figure 1.5) is due to the presence of the plant like alternative oxidase (AOX) (van Hellemond *et al.*, 2005b). The plant like alternative oxidase is sometimes referred to, in bloodstream forms of the African trypanosomes, as trypanosome alternative oxidase (TAO) and its activity is maintained at relatively low levels in procyclic *T. brucei*. The flow of electrons obtained from the oxidation of the reduced ubiquinol pool through the plant-like alternative oxidase does not result in ATP synthesis. The AOX has been assumed to be involved in control of proton gradient generation as a means of regulating oxidative phosphorylation or as a reduction-oxidation dissipating system for trypanosomes (Bringaud *et al.*, 2006). The trypanosomal alternative oxidase in the procyclic form of trypanosomes seems to help the parasites tolerate the non-constant supply of oxygen and nutrients in the insect's alimentary canal and salivary glands (Chaudhuri *et al.*, 2006).

The bloodstream forms of the *T. brucei* family and *T. evansi* have a relatively simple mitochondrion. Among other things they have a glycerol-3-phosphate dehydrogenase, ubiquinol pool and a plant-like alternative oxidase but lack the cytochromes and hence the full complement electron transport chain (van Hellemond *et al.*, 2005a). Electrons from glycosomal NADH are transported to the mitochondria by the glycerol-3-phosphate/dihydroxyacetone phosphate shuttle where the electrons are donated to the ubiquinone/ubiquinol pool through the FAD-linked glycerol-3-phosphate dehydrogenase. The plant-like alternative oxidase is the final acceptor of the electrons from the reduced ubiquinol. This flow of electrons does not result in ATP synthesis as no proton translocation is involved although the mitochondrion contains the  $F_0F_1\text{-H}^+$ -ATPase which is expressed at lower levels than in the procyclic forms (van Hellemond *et al.*, 2005a). The  $F_0F_1\text{-H}^+$ -ATPase is used for the generation of the mitochondrial

membrane potential through its reverse function of ATP breakdown and leads to translocation of protons (Brown *et al.*, 2006). The mitochondria of bloodstream forms of *T. brucei* also contain the subunits of NADH dehydrogenase or complex I which are assembled into  $\alpha$  and  $\beta$  sub-complexes, although the complex has been found not to be important for the bloodstream stages of *T. brucei* (Surve *et al.*, 2012).

The main excretory products of glucose metabolism in procyclic *T. brucei* are acetate and succinate, while those of L-proline and threonine metabolism are succinate/alanine and acetate, respectively (Bringaud *et al.*, 2010). This kind of metabolism where substrates are partially oxidised to fermentation products like acetate and succinate which are excreted with oxygen acting as the final electron acceptor during oxidation of NADH in the electron transport chain is referred to as aerobic fermentation. This process in procyclics of *T. brucei* is accompanied by oxidative phosphorylation (Cazzulo, 1992; Tielens and van Hellemond, 2009).

The procyclic forms of *T. brucei* maintain a redox and ATP balance in their glycosomes through re-oxidation of the generated NADH into  $\text{NAD}^+$  (Bringaud *et al.*, 2006; van Hellemond *et al.*, 2005a). The wild-type procyclic *T. brucei* glycosomal redox balance is adequately maintained by glycosomal succinate fermentation alone. The glycosomal succinate fermentation involves the conversion of phosphoenolpyruvate imported from the cytosol through oxaloacetate, malate and fumarate to succinate. Alternatively, the redox balance can be maintained by either the glycerol-3-phosphate/dihydroxyacetone phosphate shuttle or down-regulation of glucose metabolism or switch the energy metabolism to that of proline as the main substrate (Ebikeme *et al.*, 2010). This ability of procyclic *T. brucei* to easily shift its energy metabolism is assumed to allow for adaptation to rapid environmental changes in nutrient supply (Bringaud *et al.*, 2006; Ebikeme *et al.*, 2010).

The degradation of glucose and/or glycerol, and amino acids like proline leads to generation of large amounts of reducing equivalents namely  $\text{FADH}_2$  and  $\text{NADH} + \text{H}^+$  in procyclic *T. brucei* mitochondria. These reducing equivalents are further metabolized in the electron transport chain, highlighting the importance and

ultimately the essentiality of the electron transport chain to the parasites' energy metabolism (Coustou *et al.*, 2003; Tielens and van Hellemond, 2009; van Weelden *et al.*, 2003; van Weelden *et al.*, 2005). The essentiality of the respiratory chain in procyclic forms of *T. brucei* was demonstrated by the simultaneous inhibition of both complex IV and plant like alternative oxidase with potassium cyanide (KCN) and Salicylhydroxamic acid (SHAM) respectively, which led to the rapid death of the procyclic *T. brucei* cells (Coustou *et al.*, 2003; van Weelden *et al.*, 2003).

## 1.3 Leishmaniasis

The Leishmaniasis are a complex of diseases caused by intracellular trypanosomatid protozoa parasites called *Leishmania*. Over 21 species of *Leishmania* cause the diseases (Ouellette *et al.*, 2004). The diseases occur in various forms depending on the clinical symptom presentations. The three main forms of the diseases are cutaneous, mucocutaneous and visceral leishmaniasis. The cutaneous form is caused by *L. braziliensis*, *L. major*, *L. guyanensis*, *L. tropica*, *L. panamensis*, *L. aethiopica*, *L. mexicana*, *L. amazonensis*, *L. donovani*, *L. aethiopica*, *L. pifanoi* and *L. infantum* in various geographical regions, presents with ulcers on the exposed parts of the body. While the lesions in the mucocutaneous form affect the mucous membranes of the throat, nose and the mouth which may lead to partial or total destruction of the tissues of the affected part of the body. It is caused by *L. braziliensis* and *L. panamensis*. Visceral leishmaniasis affects the organs like the liver and spleen and may lead to their swelling and can be fatal if left untreated (Grevelink and Lerner, 1996). The other characteristics of visceral leishmaniasis are irregular fevers and weight loss. It is caused by *L. donovani*, *L. infantum* and *L. tropica* and each of these causes the disease in different parts of the world ([http://www.who.int/leishmaniasis/disease\\_epidemiology/en/](http://www.who.int/leishmaniasis/disease_epidemiology/en/)).

### 1.3.1 Distribution of the Leishmaniasis

The Leishmaniasis are endemic in 98 countries covering five continents putting 350 million people at risk of contracting the diseases (Figure 1.6). The estimated incidences of new cases of visceral and cutaneous leishmaniasis stand at 0.5 and 1.5 million, respectively, per annum. Visceral leishmaniasis is known to cause an

estimated 50, 000 deaths annually. Leishmaniasis is an opportunistic infection in HIV positive individuals. The severity of the leishmaniasis is enhanced by co-infection with HIV and management of such infections are difficult (WHO, 2010). Visceral leishmaniasis occurs more often in the co-infections with HIV than the other forms of leishmaniasis. Leishmaniasis co-infection with HIV was reported in 35 countries by 2010 (WHO, 2010). The increased infections of HIV and its spread into rural areas has led to increased transmission and spread of leishmaniasis into the urban areas resulting in geographical overlap of the two diseases (WHO, 2010).

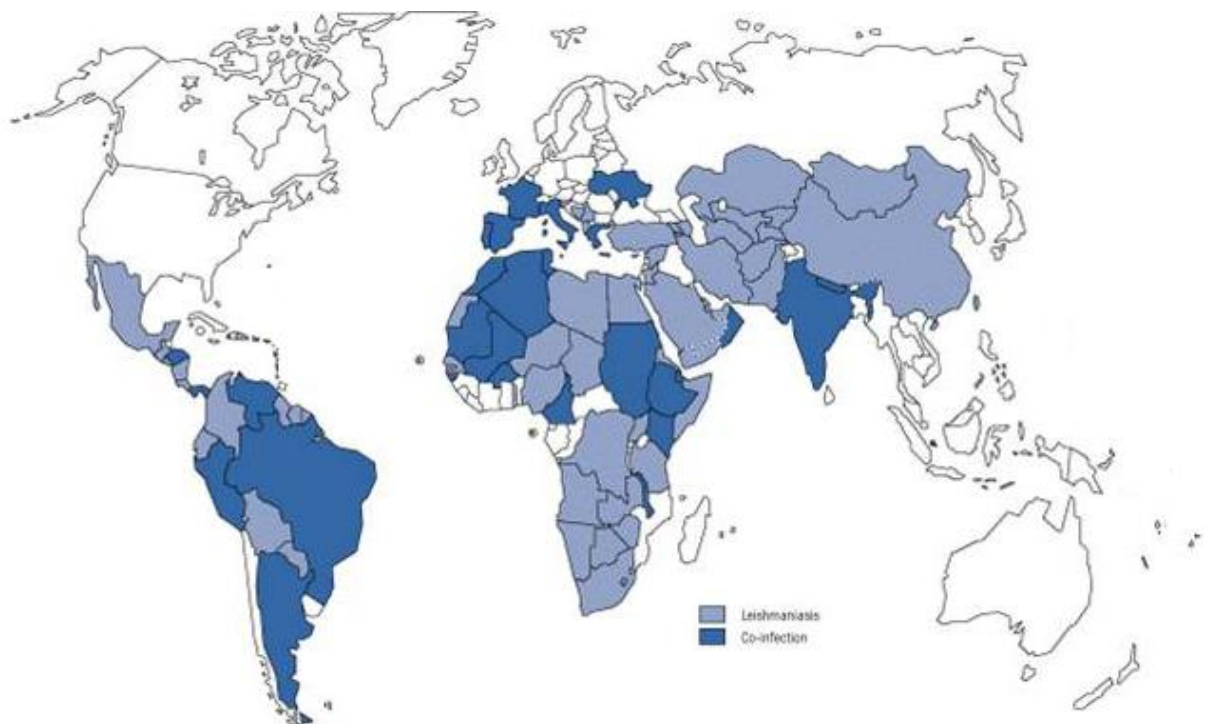


**Figure 1.6** Global distribution of leishmaniasis and Leishmania/HIV co-infection, 1990-1998. ([http://www.who.int/csr/resources/publications/CSR\\_ISR\\_2000\\_1leish/en/](http://www.who.int/csr/resources/publications/CSR_ISR_2000_1leish/en/))

### 1.3.2 Life cycle of Leishmania

The life cycle of *Leishmania* species is complex (Figure 1.7). Like that of the other trypanosomatids, it involves vertebrate and invertebrate hosts. In the vertebrate hosts they exist as intracellular parasites while in the invertebrate they exist as extracellular organisms. The invertebrate hosts are sand flies of two important genera, *Phlebotomus* found in the new world and *Lutzomya* which occur in the old world (Banuls *et al.*, 2007). The cycle starts with the bite of an infected female sand fly that needs the blood meal for egg development. During

feeding the metacyclic promastigotes are deposited into the mammal through the skin. The metacyclic promastigotes have small slender bodies and possess

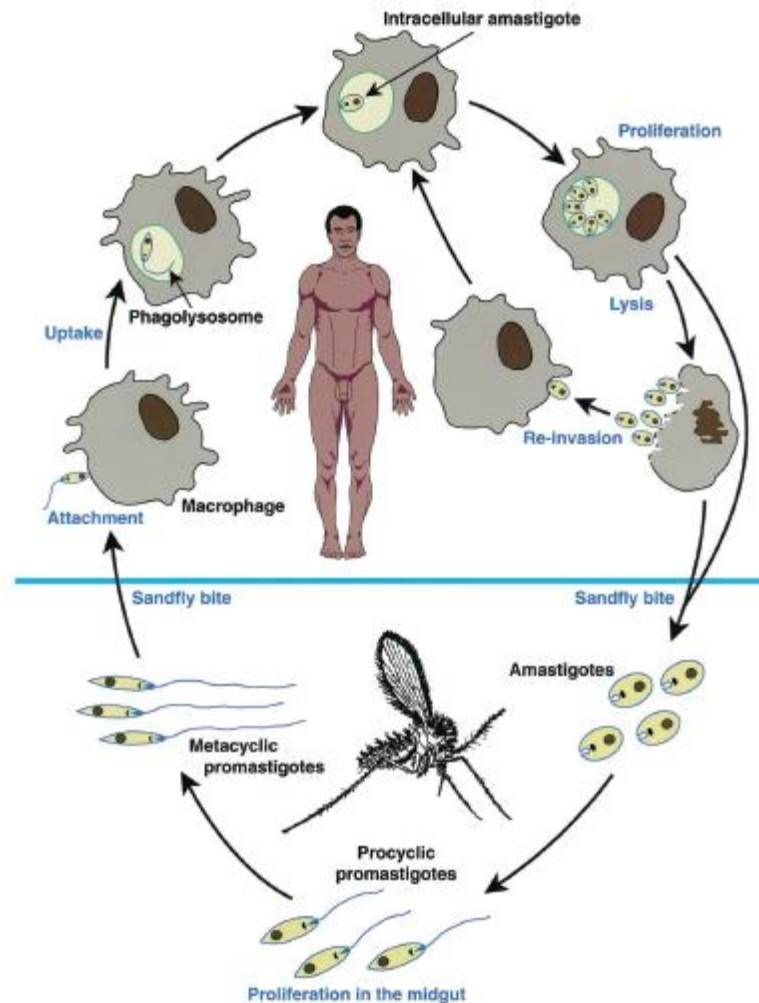


**Figure 1.7 Life cycle of leishmania in mammals and sandfly. (Source: Handman, 2001).**

long free flagella. The presence of the flagella makes these cells very motile. The promastigotes are then taken up by macrophages through phagocytosis and they metamorphose into amastigotes. The amastigotes reside within the parasitophorous vacuole of macrophages of the host. The amastigotes are ovoid in shape with a diameter of about 2.5 - 5  $\mu\text{m}$ . They do not possess free flagella and therefore they are not motile. The amastigotes divide by binary fission and as they increase in number this leads to rupture of the infected macrophage and resulting in release of the amastigotes that infect neighbouring macrophages (Banuls *et al.*, 2007). The amastigotes are transported to the draining lymph nodes from the site of bite by the dendritic cells (Moll *et al.*, 1993). A bite of the infected vertebrate by the sand fly during a blood meal leads to taking up of

macrophages infected with amastigotes. These amastigotes transform into procyclic promastigotes in the sand fly's intestines. Cultured late log phase promastigotes have an average body length of  $15.22 \pm 3.49 \mu\text{m}$  (Bates, 1994). The division of the procyclic promastigotes is rapid resulting in their increased numbers. Procyclic promastigotes mature and differentiate into metacyclic promastigotes (Banuls *et al.*, 2007). The bite of a mammal by an infected sand fly leads to delivery of the metacyclic promastigotes thereby completing and starting the life cycle.

## 1.4 Biochemistry of *Leishmania*

*Leishmania* species are known to have the most extensive metabolic network compared to trypanosomes and enzymes of the major metabolic pathways are known to be encoded by about 400 genes (Opperdoes and Coombs, 2007). The digenetic life cycle involving two different hosts have made the *Leishmania* species develop means and ways of adapting to the two environments. The two hosts provide environment with different nutrients. As a result, the biochemistry of *leishmania* species is influenced by not only how these parasites acquire the nutrients but also how they compete for the nutrients with the host (Burchmore and Barrett, 2001; Landfear, 2000). *Leishmania* use surface membrane protein transporters to take up the nutrients and to compete for these nutrients, usually each transporter is able to transport more than one substrate. Thus, the three glucose transporters of *L. mexicana* have an overlapping transportation of mannose, glucose, galactose, fructose and ribose (Naula *et al.*, 2010; Rodriguez-Contreras *et al.*, 2007).

*Leishmania* energy metabolism is similar to that of *T. brucei* (section 1.2.2). However, there are differences between the two. *Leishmania* promastigotes are able to utilise disaccharides and plant starch found in nectar which is fed on by sand flies, as sources of glucose. Excess glucose, as glucose 6-phosphate, is converted to a potential energy store mannogen although its utilisation is not well understood (Opperdoes and Coombs, 2007; Saunders *et al.*, 2010). All the Krebs's cycle enzymes are present but it is not known whether the cycle proceeds as a cyclic pathway. Generally there is no difference in the expression of central carbon metabolism enzymes at various stages of the life cycle of *Leishmania* (Saunders *et al.*, 2010). The presence of a full-complement electron transport

chain which is functional throughout the life cycle is without the alternative oxidase (Opperdoes and Coombs, 2007; Saunders *et al.*, 2010). While inhibition of the electron transport chain leads to cell death in *T. brucei*, it only leads to reversible effects on metabolism in *Leishmania* (Opperdoes and Coombs, 2007). Gluconeogenesis is operational in *Leishmania* and derives its carbon skeleton mostly from the amino acids. Regulatory mechanisms of gluconeogenesis which are supposed to prevent futile operation of the glycolytic pathway are not known (Saunders *et al.*, 2010).

*Leishmania* parasites do not have a *de novo* purine synthesizing mechanism, therefore they rely on the host for purine substrates for their purine salvage pathway, making the pathway a probable drug target (Carter *et al.*, 2008; Landfear *et al.*, 2004). The pyrimidine biosynthesis of *Leishmania* proceeds as in the mammalian cells and as a result it has always been thought to be a less likely target for drugs (Carter *et al.*, 2008). This view about the pathway is likely to change as it has been shown to be essential to promastigotes and together with the pyrimidine salvage pathway contribute to an effective amastigote infectivity of the mammalian cells (Wilson *et al.*, 2012). *Leishmania* use nucleoside transporters to acquire purine substrates. Although the *L. donovani* nucleoside transporters do not have a broad and overlapping specificity for their substrate, each is able to transport more than one substrate. The high affinity nucleoside transporters, LdNT1 transports adenosine, uridine, thymidine and cytidine, and LdNT2 transports inosine and guanosine (Aronow *et al.*, 1987). Two more nucleobase transporters exist in *L. major* and these are high affinity NT3 and low affinity NT4 whose substrates are xanthine, hypoxanthine, adenine and guanine, and adenine, respectively (Ortiz *et al.*, 2007; Sanchez *et al.*, 2004). These transporters actively transport their substrates into the cells and they are known to be concentrative transporters that help the parasites accumulate substrates in competition with the host cells. The challenge posed by the difference in pH between the parasites' environments in terms of nutrient acquisition is overcome by having transporters which function optimally at given pH points. For example, *L. major* NT4 functions optimally at acidic pH and therefore suited to function in amastigotes that reside in macrophages' acidic parasitophorous vacuoles while NT3 optimal pH is neutral and is thought to be suited for transportation of substrates in the promastigotes (Ortiz *et al.*, 2009).

Polyamine transporters have been reported in *L. donovani*, *L. mexicana* and *L. major*. These are the putrescine and spermidine transporters and are high affinity transporters that function at neutral and acidic optimal pH for promastigotes and amastigotes, respectively (Basselin *et al.*, 2000; Hasne and Ullman, 2005). Spermidine and putrescine transported across the membrane by these transporters serve as the salvage source of these metabolites. However, *Leishmania* parasites have a fully functional polyamine biosynthetic pathway which provides for the cell's polyamine requirements (Colotti and Ilari, 2011). One important function of the polyamine pathway to the parasites is the generation of trypanothione, a molecule which is unique to *Leishmania* and trypanosomes and therefore is regarded as a possible drug target (Fairlamb *et al.*, 1985). Trypanothione functions in the cell are equivalent to those of glutathione in other eukaryotic cells although trypanothione is more reactive hence more efficient than glutathione. Apart from functioning as a reductant in the cells trypanothione is more efficient at nitric oxide neutralisation than glutathione (Bocedi *et al.*, 2010; Krauth-Siegel *et al.*, 2003).

#### 1.4.1 Sterol biosynthesis

Sterols are constituents of the cell membrane where they render a structural function, contribute to membrane fluidity and permeability, and exert an indirect influence on the functionality of integral membrane proteins like enzymes and ion channels. They also play a role in cell cycle regulation (Dufourc, 2008; Lepesheva and Waterman, 2007; Roberts *et al.*, 2003). Sterol synthesis and composition of *Leishmania* species is similar to that of fungi because *Leishmania* sterols are dominated by the ergostane (C<sub>28</sub>) sterols including ergosterol and ergosterol-like sterols that are typical sterols of fungi (Berman, 1988). This has been supported by the sensitivity of *Leishmania* species to antifungal drugs that target the sterol biosynthetic pathway (Roberts *et al.*, 2003). Sterols, sterol esters and triacylglycerols make up about 14 - 55% of the 2 - 5% total lipids of dry weight of *Leishmania* promastigotes (Berman, 1988). The major sterol of *Leishmania* promastigotes and amastigotes is ergosta-5,7,24 (28)-trien-3-ol and makes up about 85% of the total sterols in *L. mexicana* (Al-Mohammed *et al.*, 2005) while ergosta-5,7,22-trien-3-ol or ergosterol the major sterol of fungi, occurs in smaller amounts. *Leishmania* promastigotes contain

about 5% stigmastane (C<sub>29</sub>) related sterols of the total sterols. For example stigmasta-5, 7, 24(28)-trien-3 $\beta$ -ol is present in small amounts in promastigotes. Amastigotes of some species of *Leishmania* can contain as much as 20% of stigmastane-related sterols (Roberts *et al.*, 2003). Cholesterol from the culture medium or of host animal origin is present in variable amounts of not less than 10% of the total sterols in various species of *Leishmania* (Roberts *et al.*, 2003).

The sterols of *Leishmania* are mainly synthesized from L-leucine which provides up to about 80% of the carbon in sterols while the rest of the carbon atoms may be derived from isoleucine, glucose, threonine and acetate (Ginger *et al.*, 1996; Ginger *et al.*, 1999). There are variations in the extent of utilization of leucine for sterol biosynthesis among *Leishmania* species studied so far. *L. mexicana*, *L. major* and *L. amazonensis* seem to utilize more leucine for sterol biosynthesis than *L. donovani*, *L. tropica* and *L. braziliensis* (Ginger *et al.*, 2000). However, it was later shown that the entire leucine carbon skeleton is incorporated into the sterols through the formation of 3-hydroxy-3-methyl-glutaryl-CoA (HMG-CoA), which is subsequently converted to mevalonate by HMG-CoA reductase in *L. mexicana* (Ginger *et al.*, 2001). However, isoleucine, glucose, threonine and acetate are the major contributors of carbon atoms in triacylglycerols and phospholipids while leucine is a minor contributor to synthesis of triacylglycerols and phospholipids (Ginger *et al.*, 1996; Ginger *et al.*, 1999).

The sequence of reactions in the sterol biosynthetic pathway (Figure 1.8) in trypanosomatidae starting from acetyl-CoA up to lanosterol is well known. However, the reaction sequences from lanosterol to ergosterol are yet to be clarified (Lepesheva and Waterman, 2011a). This could partly be the reason why little is known about enzyme localization after the lanosterol synthesis reaction. The sterol biosynthetic pathway occurs in more than one cellular compartment as the enzymes catalyzing the reactions characterised so far have been indicated to localise to various sub-cellular compartments. The reason for the occurrence of the biosynthetic pathway in various sub-cellular compartments is not known although there are speculations of a possible role in regulation of the trypanosomatidae's utilisation of sterols (Lepesheva and Waterman, 2011a).

The enzymes of the mevalonate or isoprenoid part of the sterol biosynthetic pathway have been indicated to be found mainly in the mitochondria and the glycosomes. The synthesis of HMG-CoA from condensation of acetoacetyl-CoA and acetyl-CoA is catalyzed by 3-hydroxy-3-methyl-glutaryl-CoA synthase, which has been shown to localise to the mitochondria (Carrero-Lerida *et al.*, 2009). The subsequent reaction involving conversion of HMG-CoA to mevalonate is catalyzed by 3-hydroxy-3-methyl-glutaryl-CoA reductase which is also localised in the mitochondria in *L. major* (Pena-Diaz *et al.*, 2004). Earlier reports associated 3-hydroxy-3-methyl-glutaryl-CoA reductase with mainly the glycosome and its minor activity with the mitochondria/microsome compartment in *L. mexicana* (Urbina *et al.*, 2002). The next enzyme mevalonate kinase in *L. major*, catalysing the formation of mevalonate phosphate from mevalonate is localised in the glycosome (Carrero-Lerida *et al.*, 2009).

Enzymes of the pathway downstream the mevalonate pathway have also been reported to localise to different subcellular compartments of the cells of leishmania. Farnesyl diphosphate synthase of *L. major* is localised in the cytosol and converts geranyl diphosphate to farnesyl diphosphate (Ortiz-Gomez *et al.*, 2006). Squalene synthase, a membrane bound enzyme of *L. mexicana*, is found in two compartments, the glycosome and the mitochondria/microsomal vesicle (Urbina *et al.*, 2002). Sterol C24 methyl transferase further downstream in the pathway catalysing the introduction of a double bond between carbon atom number 24 and carbon atom number 24<sup>1</sup> on fecosterol from zymosterol, is localised mainly in the endoplasmic reticulum in *L. major* (Jimenez-Jimenez *et al.*, 2008).

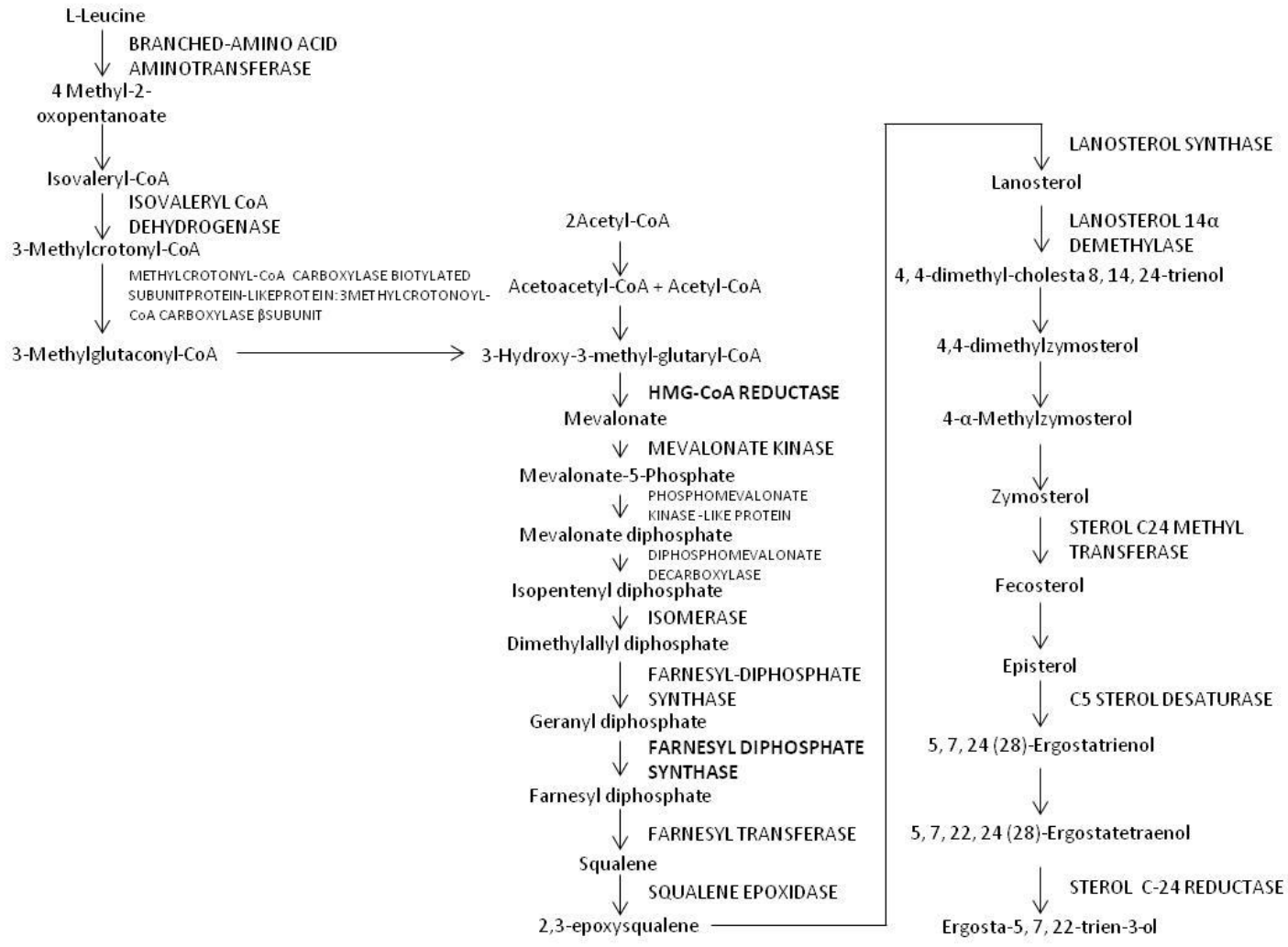
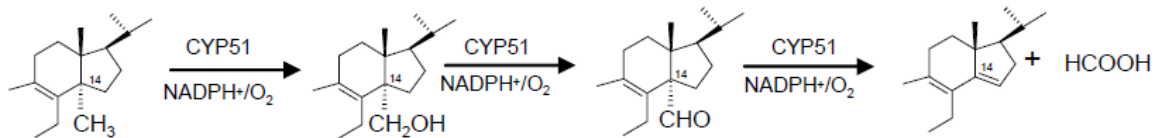


Figure 1.8 Simplified *Leishmania major* sterol biosynthetic pathway (Adapted from biocyc.org).

Lanosterol 14 $\alpha$ -demethylase for *L. donovani* classified as CYP5122A1 is reportedly a novel P450-like protein whose half knock-out led to reduced ergosterol synthesis in the mutant cells compared to the wild-type cells. The protein was found to localise to three sub-cellular compartments, the mitochondria, glycosome and the endoplasmic reticulum (Verma *et al.*, 2011).

Sterol (lanosterol) 14 $\alpha$ -demethylase is a heme containing enzyme and member of the CYP51 gene family belonging to the Cytochrome P450 monooxygenases. In conjunction with NADPH cytochrome P450 reductase, sterol 14 $\alpha$ -demethylase catalyzes a three step removal of methyl groups (Figure 1.9) from position C14 of 2, 3-epoxysqualene of the sterol biosynthetic pathway (Lepesheva and Waterman, 2011a; Waterman and Lepesheva, 2005).



**Figure 1.9 Sterol C14-demethylase catalyzed reaction of the sterol biosynthetic pathway. (Source: Waterman and Lepesheva, 2005)**

Failure to remove the C14 methyl group and the presence of a methyl group at C4 leads to blocking of parasite growth (de Souza and Rodrigues, 2009). Although sterol 14- $\alpha$  demethylases from other organisms have a relatively broad spectrum of substrates, *Leishmania* sterol 14 $\alpha$ -demethylase exhibit a low range of substrate specificity. Cloned *L. infantum* sterol 14 $\alpha$ -demethylase is able to catalyse demethylation of C4-norlanosterol, C4-desmethylated obtusifoliol, and 14-methylzymosterol, although it exhibits high specificity for C4-norlanosterol and obtusifoliol (Hargrove *et al.*, 2011). There are very few sequence similarities in the enzyme primary structure between trypanosomatidae and human enzyme, offering possibilities of development of inhibitors that are selective for the parasite (Lepesheva and Waterman, 2011a). *Leishmania* lanosterol 14 $\alpha$ -demethylase is targeted for inhibition by azoles like ketoconazole (de Souza and Rodrigues, 2009; Lepesheva and Waterman, 2011a). The inhibition of sterol 14 $\alpha$ -demethylase leads to death of unicellular organisms due to blockage of the sterol biosynthetic pathway (Lepesheva and Waterman, 2007). To avoid ketoconazole toxicity, certain leishmania species have been reported to increase the intracellular drug target. Thus, *in vitro* ketoconazole resistance by *L.*

*amazonensis* was associated with up-regulation of expression of sterol 14 $\alpha$ -demethylase (Andrade-Neto *et al.*, 2012). This signifies the importance of the enzyme to the pathway and ultimately the unicellular organisms.

## 1.5 Control of the African animal trypanosomiasis

The control of trypanosomes involves the use of strategies that target the causative agent, the trypanosome or the vector, the tsetse fly.

The control of trypanosomiasis targeting the vector aimed at halting the transmission of the diseases started in the early 20<sup>th</sup> century (Schofield and Maudlin, 2001). A number of strategies have been used since then to try and eradicate the tsetse fly.

The earliest was that of woodland destruction or bush clearing and wild animal killing. This was done to eliminate both the habitat and the animal reservoir/host of the vector. The method was stopped due to its negative effects on the environment and wild-life population. The discovery of insecticides in 1945 led to their application in the control of the disease (Allsopp, 2001). Methods such as ground spraying with insecticides like dichlorodiphenyltrichloroethane (DDT), aerial application of residual insecticides, and sequential aerosol techniques (SAT) at low dosage of insecticides have all been employed. However, concerns over environmental contamination and effects on untargeted organisms have created scepticism over the use of insecticides. Target directed insecticide methods which do not pose serious risk of contaminating the environment are preferred and these include the odour-baited traps and targets (fabric sheets). These methods involve use of traps or targets impregnated with insecticides. A variant of these has been the dipping of animals in insecticides or use of pour-on formulations of insecticides. This method is called “live bait”, due to application of insecticides, mostly pyrethroids, on live animals. In these methods, the insecticides used are less toxic. The sterilization of male tsetse flies by irradiation is another method that has been used to control the disease and it is called the sterile insect technique (SIT). SIT was successfully used in Unguja Zanzibar but at a great cost (Vreysen *et al.*, 2000). SIT can be used as a follow-up for eradication of the flies in conjunction with either dipping or use of targets (Allsopp, 2001; Schofield and Maudlin, 2001).

The technologies aimed at stopping transmission have been able to reduce the distribution of the tsetse flies but failed to eradicate them. In certain instances they reduced the use of anti-trypanosomal drugs (Hargrove *et al.*, 2000). Various reasons have been cited for the failure to eradicate the tsetse fly despite it being susceptible to insecticides. There has been a lack of sustaining the control achievements due to reinvasion of the cleared areas. A large part of the African continent, greater than 40% of the total land area covering the 37 African countries affected by trypanosomiasis (Allsopp, 2001), is infested with the tsetse fly so huge investment would be required to cover this area. Impoverished African nations depend on aid to carry out these projects and often the aid for such comes with conditions dictated by the donor communities. Often the duration of these donor-financed projects is for a limited period of time. Trypanosomiasis affect mostly poor rural communities who cannot afford the simplest or cheapest of these technologies (Hargrove *et al.*, 2000; Schofield and Maudlin, 2001).

### **1.5.1 Chemotherapeutic control of the trypanosomiasis**

Chemotherapy has been the mainstay for the control of diseases caused by trypanosomes for some time (Barrett *et al.*, 2003; Kinabo, 1993). However, there are only a few drugs for this purpose. There are four licensed drugs used for treatment of human African trypanosomiasis and whose choice of use depends on the subspecies of *T. brucei* causing the disease. These drugs are melarsoprol, eflornithine, pentamidine and suramin. Pentamidine and suramin are the first line drugs used in the early stages of the disease before the parasites invade the central nervous system and are used against *T. b. gambiense* and *T. b. rhodesiense*, respectively (Barrett *et al.*, 2003; Brun *et al.*, 2010). Melarsoprol is used as a first-line drug for the treatment of the late-stage of the disease caused by *T. b. rhodesiense*. Eflornithine is only used against the disease caused by *T. b. gambiense*. Eflornithine requires large doses which complicates its use despite the drug having fewer side-effects as compared to other trypanocides. The use of eflornithine in combination with nifurtimox is now recommended as the overall dose and treatment duration are reduced and resistance selection is less likely (Priotto *et al.*, 2009). Nifurtimox monotherapy, which is used against Chagas' disease, has been used against late-stage

melarsoprol-refractory human African trypanosomiasis but with limited efficacy. Another drug that has been used occasionally to treat human African trypanosomiasis without a licence is diminazene (berenil), a drug which is indicated for veterinary use. Suramin is used effectively against the early stage of human African trypanosomiasis caused by *T. b. rhodesiense*. The drug is not effective against the early stage of the disease caused by *T. b. gambiense* and the late stage of human African trypanosomiasis caused by both *T. b. rhodesiense* and *T. b. gambiense* (Wilkinson and Kelly, 2009). Currently all of the drugs in use against human African trypanosomiasis are able to induce adverse side effects (Barrett *et al.*, 2003).

### 1.5.2 Chemotherapeutic control of Animal Trypanosomiasis

Currently, there are only three drugs used for the treatment of African animal trypanosomiasis. These are isometamidium, homidium, and diminazene (Geerts *et al.*, 2001). Isometamidium is not only active against *T. congolense* and *T. vivax* in domestic animals but also in *T. brucei* and *T. evansi* causing the disease in donkeys, horses and camels. Homidium is active against *T. congolense* and *T. vivax* (Kinabo, 1993). Diminazene is used against *T. congolense*, *T. vivax* and *T. b. brucei* in cattle, sheep and goats where they are the primary pathogens of the disease (Peregrine and Mamman, 1993). Isometamidium is mainly used for prophylactic purposes while homidium, which has limited prophylactic properties, and diminazene are both used as therapeutic agents (Delespaux *et al.*, 2008; Geerts *et al.*, 2001).

Diminazene was introduced onto the market in 1955 for the treatment of trypanosomiasis and babesiosis in domestic livestock (Peregrine and Mamman, 1993). It is an aromatic diamidine made up of two amidinophenyl groups that are joined by a triazene group (Figure 1.10A) and is commercially available as a diacetate salt. It is manufactured in combination with phenyldimethyl pyrazolone to increase the stability of the aqueous solution of the drug from a few days to a couple of weeks. It is mostly sold commercially as Berenil. The drug is thought to have a low prophylactic activity because it is easily excreted and as a result is recommended for therapeutic use only. Diminazene is known to bind to kinetoplast DNA of trypanosomes. It has specific non-intercalating

interaction with adenine-thymine (A - T) rich sites in DNA. The binding of diminazene to kDNA leads to the accumulation of replication intermediates due to the inhibition of the RNA primers. Diminazene also inhibits trypanosomal mitochondrial topoisomerase II (Peregrine and Mamman, 1993).

Homidium is a phenanthridinium compound and is commercially available as Novidium, the chloride salt called ethidium chloride, or ethidium, the bromide salt called ethidium bromide (Figure 1.10B). The drug was extensively used in the 1960s and 1970s, however, widespread resistance greatly limited its usefulness (Kinabo, 1993). Despite its being mutagenic, ethidium bromide has continued to be used widely for treatment of animal trypanosomiasis in many countries (Delespaux *et al.*, 2008). The killing of the bloodstream form of *T. brucei* strain 427 by ethidium bromide has been reported to be through inhibition of the initiation of replication of free minicircles (Chowdhury *et al.*, 2010). It also inhibits nuclear DNA replication in dyskinetoplastic cells. The free minicircles were shown to be the primary targets of the drug as they were not shielded by the stabilising bound multiple proteins. It was concluded that the effective targeting of the minicircle replication by ethidium bromide could be due to differences in the intra-mitochondrial and extracellular concentration of ethidium bromide brought about by the requirement of the mitochondrial membrane potential to transport ethidium into the mitochondrial matrix which result in higher concentrations of the drug in the mitochondrial matrix (Chowdhury *et al.*, 2010).

Isometamidium (Figure 1.11) is a phenanthridinium compound which is commercially marketed as samorin or trypanidium. It was initially synthesized by coupling homidium (Figure 1.10B) with para-aminophenyldiazonium chloride (Kinabo, 1993). This synthetic route of isometamidium gives it a structure that differs from homidium by a meta-amidinophenyl-azo-amine moiety, a part of the diminazene drug (Figure 1.10A). Isometamidium is a cationic molecule and has hydrophobic properties due to the presence of a charged nitrogen atom in the phenanthridine nucleus and phenyl groups, respectively. The commercial form of the drug contains 70% isometamidium and 30% is made up of a mixture of its isomers, a bis-compound which occurs in small proportions and homidium (Kinabo, 1993; Kinabo and Bogan, 1988).

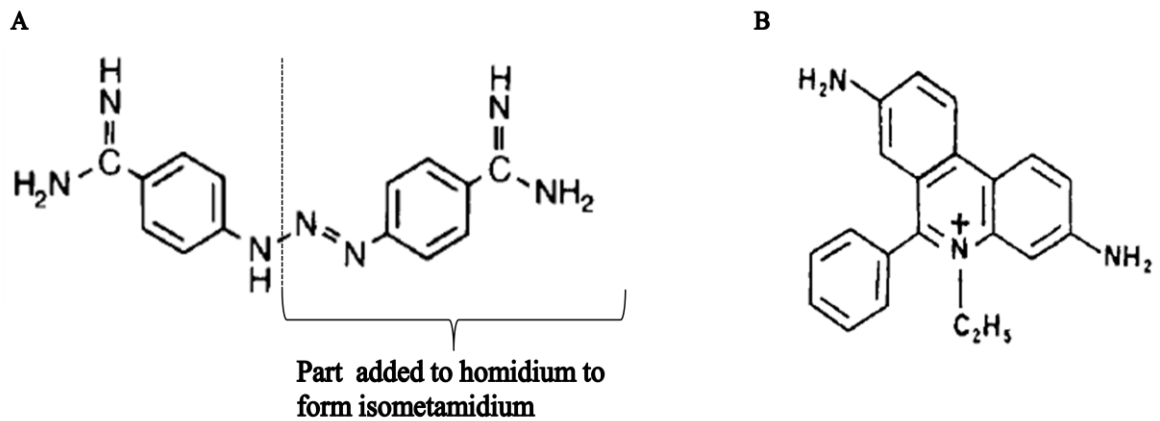


**Figure 1.10** Molecular structures of diminazene (A) and homidium (B). In A, the diminazene part which is added to homidium during synthesis of isometamidium is indicated (Sources/Adapted from: Peregrine and Mamman, 1993 and Kinabo, 1993, respectively).

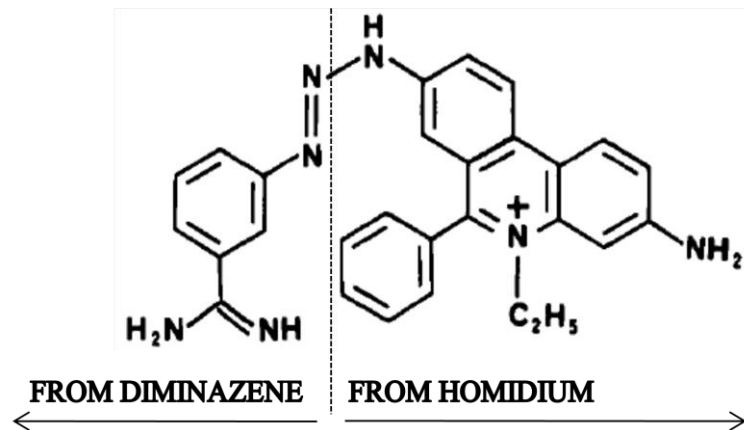


**Figure 1.11** Molecular structure of isometamidium. The dotted line shows the two parts that make up isometamidium and their sources as labelled (Source/Adapted from: Kinabo, 1993).

The prophylactic and therapeutic treatment of ruminants and horses against trypanosome infections with isometamidium chloride is done by intramuscular or subcutaneous injection at 0.5 mg/kg body weight and 1 mg/kg body weight, respectively (Desquesnes *et al.*, 2013). The prophylactic treatment is done every three months as the drug protects the animals for at least four months (Mubamba *et al.*, 2011), a period over which the drug remains detectable in the sera of the animals (Eisler *et al.*, 1996). The use of isometamidium is recommended over the other phenanthridinium compounds which are carcinogenic because it does not have such a property. Isometamidium chloride is used with diminazene aceturate as a sanative pair, where failure of any of the two is replaced by the other (Desquesnes *et al.*, 2013).

A number of targets and processes were indicated to be responsible for the antitrypanosomal activity of isometamidium and homidium. However, cleavage of kinetoplast DNA minicircles was one of the identified biochemical peculiarities of the trypanosomes that could account for selective toxicity action of the drugs (Kinabo, 1993). This was later found to be the action of ethidium bromide, a related phenanthridinium compound, in trypanosomes (Chowdhury *et al.*, 2010).

The other drugs that are used against animal trypanosomiasis are suramin, quinapyramine and cymelarsan.

Quinapyramine a derivative of aminoquinaldine (Figure 1.12A), is both a therapeutic and prophylactic drug for animal trypanosomiasis that was introduced in the 1950s. It can be used in the treatment of cattle, goats and sheep infected with *T. brucei*, *T. vivax*, and *T. congolense*. It was once regarded as a drug of choice for treatment against *T. evansi*, *T. equiperdum* and *T. equinum* infections before its eventual withdrawal from use in the 1970s due to widespread resistance to the drug in most parts of Africa (Kinabo, 1993). The continued use of quinapyramine in the wake of its lost effectiveness due to resistance development could have compromised the effectiveness of the other trypanocides like isometamidium, homidium and diminazene as quinapyramine cross resistance to these drugs was possible. Quinapyramine cross resistance by *T. congolense* to isometamidium, diminazene and homidium was demonstrated in mice and the resistant *T. congolense* were able to infect tsetse flies (Ndoutamia *et al.*, 1993). The ease with which quinapyramine cross resistance to isometamidium, homidium and diminazene developed resulted in quinapyramine not being recommended for use in cattle (Desquesnes *et al.*, 2013). The drug was later re-introduced following a change in its formulation and method of administration in donkeys and camels infected with *T. evansi* (Kinabo, 1993). A therapeutic and prophylactic combination of quinapyramine sulphate and quinapyramine chloride has since been effective in treatment and protection of horses and camels against *T. evansi* infections (Desquesnes *et al.*, 2013).

Suramin was developed around 1916 and only gained widespread use in 1923 (Wainwright, 2010) although its use against HAT began in 1922 (Barrett and

Gilbert, 2006). Suramin is a colourless highly anionic polysulphonated naphthylamine urea compound (Figure 1.12C) which is readily soluble in water. Its ability to cross the blood-brain barrier is limited by its ionic nature (Fairlamb, 2003) and that is why the drug is only used against early stage of HAT (Barrett and Gilbert, 2006; Brun *et al.*, 2011; Fairlamb, 2003). The drug is administered intravenously in both humans and animals (Desquesnes *et al.*, 2013; Fairlamb, 2003), and has a long half life. The drug's mode of action is not known and despite resistance to the drug being easily selected in the laboratory its occurrence in the field is not common, in case of HAT (Brun *et al.*, 2011). However, resistance to the drug in the animal form of trypanosomiasis caused by species of *T. brucei* group is known to exist. There are mixed reports on the stability of suramin resistance with regard to *T. evansi* infections. Suramin resistance in laboratory derived *T. evansi* seems to have a cost on the fitness of the resistant parasites while resistance in field isolates is believed to be stable as it persisted even after withdrawal of the drug for over two decades (Barrett and Gilbert, 2006). Suramin is reportedly no longer in use against *T. evansi* infections in horses and camels (Desquesnes *et al.*, 2013).

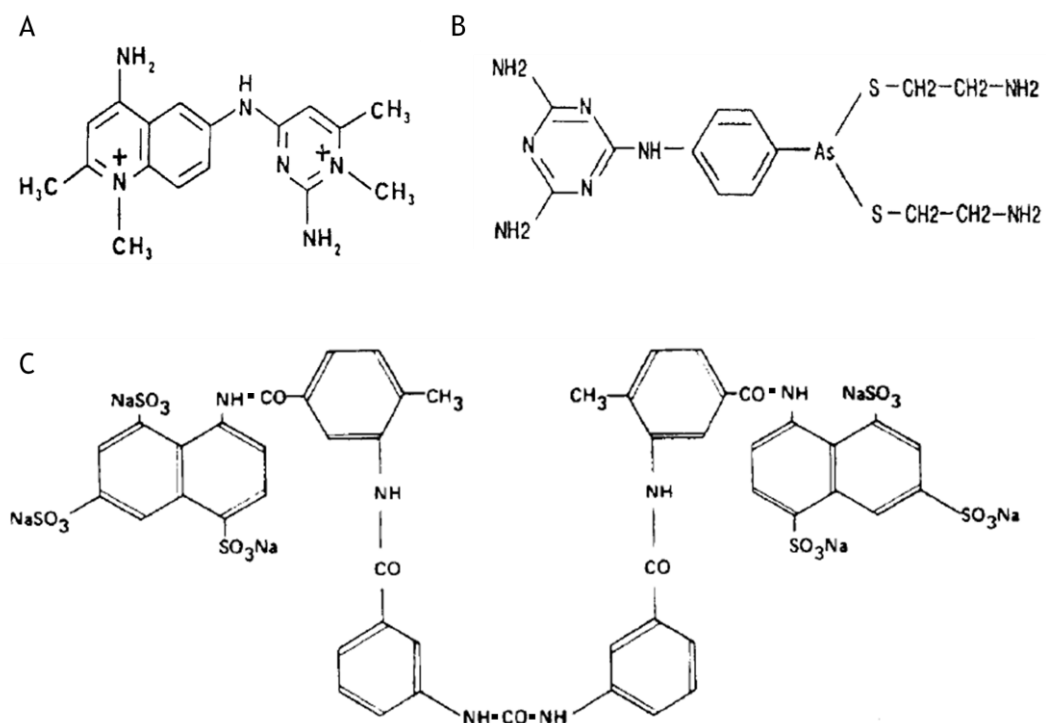


**Figure 1.12** Molecular structures (a) Quinapyramine, (b) Cymelarsan and (c) Suramin. The drugs are used against animal trypanosomiasis (Source/Adapted from: Kinabo, 1993).

Cymelarsan is a water soluble trivalent arsenical compound (Figure 1.12B) which was discovered in 1985 (Kinabo, 1993). It decomposes to between 33% and 42% melarsen oxide in aqueous solution (Berger and Fairlamb, 1994). Therapeutic concentrations of melarsen oxide have been shown to penetrate the blood-brain barrier in mice (Keiser *et al.*, 2000). Cymelarsan is active against *T. evansi* infections in horses, camels, cattle and buffaloes (Kinabo, 1993). Cymelarsan could be effective in treating goats at doses twice the recommended dosage for the treatment of *T. evansi* in horses and camels (Gutierrez *et al.*, 2008). In the absence of an officially recommended drug for the treatment of *T. equiperdum* in horses, cymelarsan has been shown to be effective against both acute and chronic experimental infections with *T. equiperdum* (Hagos *et al.*, 2010).

## 1.6 Control of Leishmaniasis

The choice of control strategies for Leishmaniasis in different geographical parts of the world depends on whether the disease is anthroponotic or zoonotic. Anthroponotic leishmaniasis involves the transmission of the disease by the sandfly as the vector to human hosts who also act as reservoirs of the parasite. The most effective control strategy of anthroponotic leishmaniasis is based on the treatment of the disease with an appropriate drug after its detection and diagnosis (WHO, 2010). Zoonotic leishmaniasis has non-human mammals, for example dogs, acting as reservoirs where the parasites are picked up by the sandfly vector, during a blood meal and transmitted to humans (Alvar *et al.*, 2006). Animal reservoir control is a zoonotic infection control method that involves the culling of dogs that show the presence of parasites in their blood and killing of the rodents or wild animals with poisoned baits and destruction of their habitats around settlement areas. Dipping of dogs in insecticides has also been used to reduce infection of these animals. A variant of dipping involves use of insecticide treated collars tied around the necks of dogs (Davies *et al.*, 2003).

Vector control aims at reducing the transmission of the disease. The control of leishmaniasis based on the vector is achieved through residual spraying of houses and animal shelters with insecticides and use of insecticide treated bednets (WHO, 2010). Residual house spraying, which was firstly done with DDT and later replaced with pyrethroids, is more widely used than bednets impregnated with

insecticide. Residual house spraying is useful against endophilic sand flies, i.e., those that rest indoors after feeding. Insecticide treated nets are best suited for endophagic sand flies, i.e., those that feed indoors. Residual house spraying has had successes in efficiently reducing fly populations. However, the extent to which the risk of infection can be reduced by the reduction in the insect population remains to be fully established. A sustained residual house spraying is required if the sand fly populations are to be diminished to effectively reduce incidence of the disease. There are various reasons for lack of sustained control of the vector. High cost and logistical limitations tend to curtail the application of sustained residual house spraying. It is also expensive and difficult to implement environmental management as a means of controlling the animal reservoir (Desjeux, 2004). Moreover, the insecticides used in residual spraying tend to lose their efficacy in high environmental temperatures, high radiation levels and in places prone to accumulation of dust (Claborn, 2010).

### **1.6.1 Chemotherapeutic control of Leishmaniasis**

The organic antimonials' first use as anti-leishmanial drugs is known to have been about 100 years ago (Ouellette *et al.*, 2004). The trivalent forms of antimonials (SbIII) were initially used and later replaced by the less toxic pentavalent antimonials (SbV). The two pentavalent antimonials in use are sodium stibogluconate and meglumine antimoniate (Figure 1.13), and have been in use for just over 60 years (Croft and Olliaro, 2011). They are used as first line drugs in other parts of the world except in Bihar state of India where resistance to the pentavalent antimonial is wide-spread (Croft and Olliaro, 2011; Croft *et al.*, 2006; Ouellette *et al.*, 2004).

Pentamidine (Figure 1.13) is an aromatic diamidine compound whose salts, pentamidine isethionate or pentamidine methanesulphonate, have been used as the second line drugs for the treatment of cutaneous leishmaniasis, mucocutaneous leishmaniasis and visceral leishmaniasis. It was also used to treat failed pentavalent antimonial treatment of visceral leishmaniasis. The drug's toxicity which can lead to hypotension, hypoglycaemia, diabetes and nephrotoxicity coupled with its increasing treatment failure rates has limited its use (Ouellette *et al.*, 2004).

Miltefosine is a member of the phosphocholine esters of aliphatic long chain alcohols classified generally as alkylphosphocholine compounds (Figure 1.13). Alkylphosphocholine activities against protozoan parasites and ability to kill cancerous cells were discovered in the early 1980s (Dorlo *et al.*, 2012). However, miltefosine was approved for the treatment of visceral leishmaniasis in 2002 in India. It is the only antileishmanial drug that is administered orally, although its course of treatment is relatively long, 28 days. Vomiting, diarrhoea, anorexia, and nausea are the common gastrointestinal side effects which are induced by miltefosine. Among these side effects vomiting and diarrhoea are observed in 38% and 20% of the treated patients, respectively (WHO, 2010). These side effects get resolved and treatment is continued. However, occasional severe side effects that prompt treatment interruption have been reported and these include elevated hepatic transaminase concentrations and skin allergy (WHO, 2010). The drug is contraindicated for use in women of child bearing age due to its teratogenic properties (Dorlo *et al.*, 2012).

Paromomycin (Figure 1.13) is a broad spectrum aminoglycoside antibiotic which was isolated from *Streptomyces krestomuceticus* filtrates in 1950. Paromomycin has activity against many gram-positive and gram-negative bacteria, protozoa and cestodes. It is the only aminoglycoside with activity against *leishmania* species (Davidson *et al.*, 2009). Paromomycin was licensed for use against visceral leishmaniasis in India in 2006. It is known to cause reversible ototoxicity in 2% of patients while renal toxicity is rare. The drug is manufactured in injectable and topical application forms for treatment of visceral and cutaneous leishmaniasis, respectively (Davidson *et al.*, 2009).

### 1.6.2 Amphotericin B

Amphotericin B (Figure 1.13) as a natural product was first isolated from *Streptomyces nodosus* in 1959. It is a non-aromatic antimycotic and antiparasitic polyene antibiotic (Lemke *et al.*, 2005). It has been in use for the treatment of leishmaniasis since the 1960s as a second line drug (Croft *et al.*, 2006). The drug's adverse side effects, nephrotoxic effects and low solubility in aqueous solutions limited its use. Its nephrotoxicity is due to its affinity for cholesterol in the renal membrane where it forms pores upon binding, leading to compromised

renal membrane integrity. The low solubility prevents it being administered orally due to lack of absorption in the gastrointestinal tract. The alternative route of administration is parenteral injection where it is given with a solubilising agent, deoxycholate. The improved solubility did not reduce the toxicity of the drug and therefore other formulations were made with varying improved properties. These formulations included colloids and emulsions, cochleates, nanoparticulate carrier systems and a liposomal formulation (Lemke *et al.*, 2005). The liposomal formulations have increased bioavailability and reduced toxicity properties. This has led to the liposomal form being recommended by the WHO for the treatment of visceral leishmaniasis and AmBisome is now the drug of choice when available. Currently, AmBisome is available free of charge (500, 000 doses per year) to WHO for distribution to endemic countries (WHO/Gilead, 2011). Recently it has been proposed that liposomal AmBisome is given as a single injection as part of a public health campaign to diminish the *Leishmania* burden in India (Mondal *et al.*, 2014; Sundar *et al.*, 2010). This approach could be catastrophic since it implies using a drug dosing close to the limit of efficacy and so risks selecting resistance.

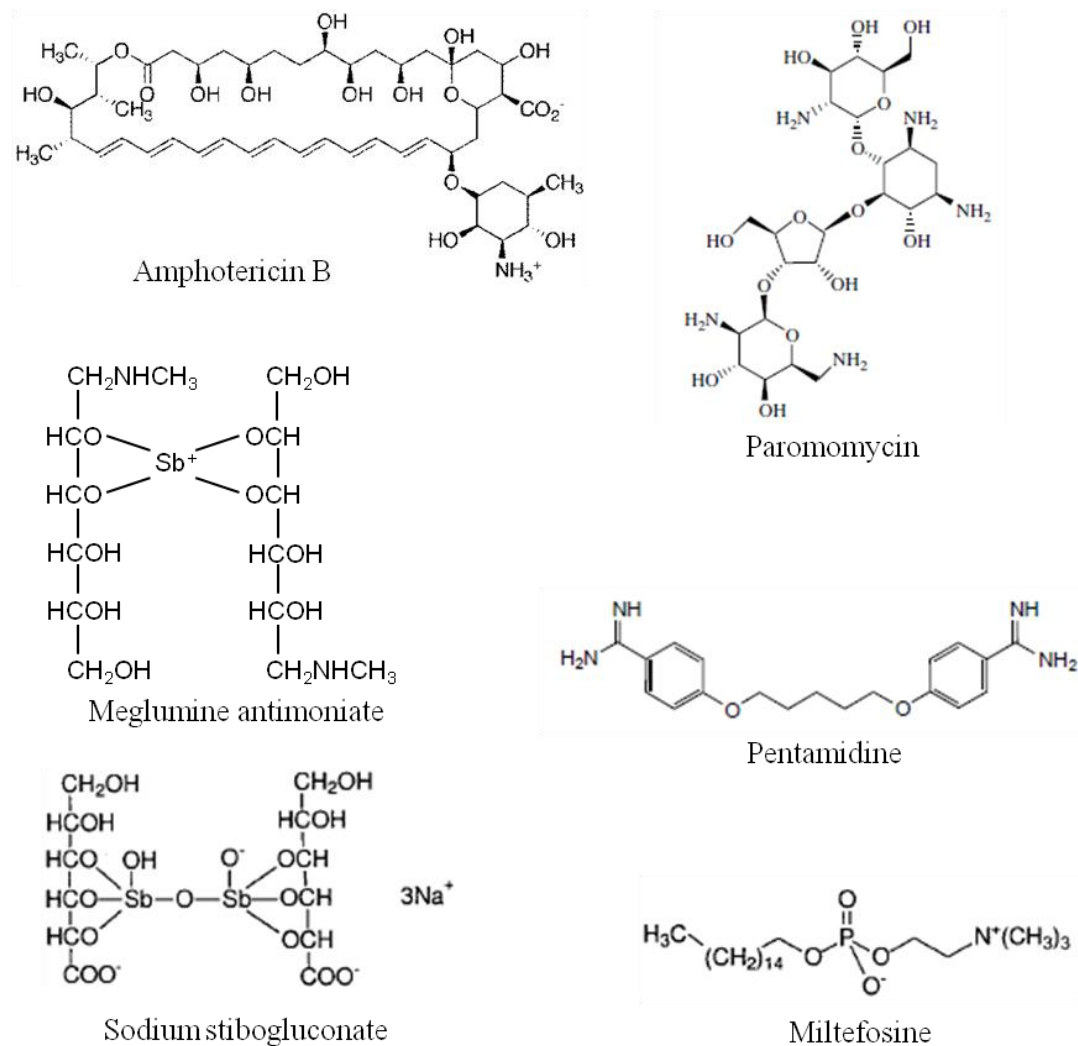


**Figure 1.13 Molecular structures of the drugs that are used against Leishmaniasis. Miltefosine is the only orally administered drug. Amphotericin B, miltefosine, paromomycin and antimonials show varying efficacies against different species of leishmania. Pentamidine is rarely used due to its unpleasant side effects.**

## 1.7 Shortcomings of chemotherapy in AAT and leishmaniasis

The chemotherapeutic control of the trypanosomiasis with the current drugs has been in practise for a long time. However, the usefulness of these drugs has been compromised by several factors including toxicity, poor efficacy and limited supply. There is generally a lack of interest by pharmaceutical companies to invest in trypanocide development for AAT due to the low value market of such drugs for African farmers thereby limiting the choice of drug treatment (Geerts *et al.*, 2001). Moreover, chemotherapy with the available drugs has further been compromised by development of drug resistance and there are no vaccines against these diseases (Barrett *et al.*, 2003; Brun *et al.*, 2011; Handman, 2001).

Amphotericin B, miltefosine, paromomycin and antimonials show varying activities against the different species of *Leishmania* and this has been attributed to differences in the parasites' biochemical and molecular features (Alvar *et al.*, 2006). This implies that no one drug can be used in the different geographical regions with the same success. All the recommended antileishmanials show varying levels of toxicity and severe side effects to the host. They are given intravenously or intra-muscularly and in some cases require to be given in hospital for patient monitoring, except miltefosine which is given orally (WHO, 2010). Newer drugs, namely amphotericin B and miltefosine are also expensive although the gratis provision of 500, 000 annual doses of AmBisome ameliorates this. Leishmaniasis occurs mostly in developing countries and affects mainly the world's poorest people who live in remote areas with limited or no access to health facilities. Therefore, these people have limited or no access to such expensive drugs. Generally, the antileishmanial drugs are not easily accessible in most endemic countries resulting in an estimation of over 50% of the affected people failing to access appropriate treatment (den Boer *et al.*, 2011). Moreover, the infrequent supply of drugs leads to elevated prices on the black market. In such situations lack of compliance to treatment regimens is inevitable. Besides, the long treatment regimens can exacerbate the problem of compliance to treatment regimens of some of these drugs, like miltefosine, and may result in the development of drug resistance (Alvar *et al.*, 2006). The biggest threat to limiting the use of antileishmanials seems to be emerging resistance, which already exists for the antimonials and is reported increasingly for miltefosine. However *in vitro* resistance has been induced to all the drugs and the mechanisms of action for these drugs have not been fully worked out in leishmaniasis (Croft *et al.*, 2006).

### 1.7.1 Drug resistance

Drug resistance to therapeutic compounds in use for treatment of bovine African trypanosomiasis has been reported in at least 17 African countries (Figure 1.14) (Delespaux *et al.*, 2008). Included in this list is Zambia, where resistance to both isometamidium and diminazene was reported to exist in the eastern part of the country (Sinyangwe *et al.*, 2004). In most of these countries information on trypanocidal drug resistance is obtained from reported cases rather than

comprehensive study reports and baseline information on trypanosomal drug resistance prevalence is not available (Delespaux *et al.*, 2008). The problem of drug resistance in African animal trypanosomiasis could have been exacerbated by several factors. For example, the relaxation in control of the importation and marketing of the trypanocides together with many other pharmaceutical products by most African countries through the privatization of veterinary services has led to trypanocides becoming easily accessible from various sources like local pharmacists, agro-veterinary suppliers and the informal sector (Geerts *et al.*, 2001). All these factors coupled with the small number of prophylactic and therapeutic trypanocidal compounds currently in use has contributed to the imprudent use of these drugs, especially by poor rural farmers (Delespaux *et al.*, 2008; Geerts *et al.*, 2001). Multiple drug resistance to trypanocides has been reported. However, trypanosomal resistance to isometamidium chloride is more common than that to diminazene aceturate (Delespaux *et al.*, 2008; Geerts *et al.*, 2001).



**Figure 1.14 Occurrence of trypanocidal resistance in African Animal Trypanosomiasis. Trypanocidal resistance is indicated by a star. (Source: Delespaux, *et al.*, 2008)**

### 1.7.1.1 Resistance to isometamidium

Isometamidium resistance has been recognised to exist for quite some time, although mechanisms of resistance have not been worked out. Isometamidium resistant *T. congolense* accumulate less isometamidium chloride than isometamidium susceptible *T. congolense* (Sutherland *et al.*, 1991). Drug resistant *T. congolense* also show reduced uptake of isometamidium (Sutherland *et al.*, 1992). Samorin (isometamidium) is known to be accumulated in the mitochondrion and has a specific interaction with the kinetoplast of drug sensitive bloodstream forms of *T. congolense* (Wilkes *et al.*, 1997). However, there are no reports of an isometamidium effect on the nuclear DNA in *T. equiperdum* and *T. congolense* so far (Shapiro and Englund, 1990; Wilkes *et al.*, 1997).

The specific interaction of isometamidium with the kinetoplast probably leads to the loss of the kinetoplast in isometamidium resistant *T. congolense* (Wilkes *et al.*, 1997). Loss of the kinetoplast has also been observed to be induced by trypanocides like hydroxystilbamidine, ethidium bromide, acriflavine, berenil and pentamidine, although the kinetoplast can also be lost naturally (Schnauffer *et al.*, 2002; Shapiro and Englund, 1995). However, dyskinetoplastidy does not easily occur in both *in vivo* and *in vitro* drug induction (Timms *et al.*, 2002). The complete or partial loss of the kinetoplast DNA is generally referred to as dyskinetoplastidy while a complete loss is called akinetoplastidy in trypanosomatids (Schnauffer *et al.*, 2002). Isometamidium has been proposed to promote formation of kDNA - protein complexes that are easily cleaved by topoisomerase II leading to linearization of the minicircles and generation of free minicircles in *T. equiperdum* (Shapiro and Englund, 1990). Loss of the kinetoplast would entail loss of maxicircle genes whose products bloodstream form *T. brucei* are dependent upon for the generation of the mitochondrial membrane potential through the reverse function of ATPase or  $F_1F_0$  - ATP synthase (Brown *et al.*, 2006). The subunit 6 of the  $F_0$  is encoded in the kinetoplast DNA and therefore loss of the kinetoplast leads to loss of this subunit. This loss has been suggested to be compensated for by a mutation in the  $\gamma$  subunit of the  $F_1$  and this allows the dyskinetoplastic cells to generate the mitochondrial membrane potential for their viability (Dean *et al.*, 2013; Schnauffer *et al.*, 2005).

The disturbances to the structural integrity of the  $F_0F_1$  ATP synthase is also thought to lead to reduced ATP hydrolysis in trypanosomes (Schnauffer *et al.*, 2005). This would suggest alteration in the generation of the mitochondrial membrane potential as was observed in isometamidium resistant *T. congolense*. Alteration in the maintenance of the spontaneous mitochondrial membrane potential resulted in altered rate of accumulation of isometamidium (Wilkes *et al.*, 1997), as inhibition of the spontaneous mitochondrial membrane potential led to a decrease in the rate of accumulation of isometamidium. It was concluded that parasites expressing lower mitochondrial electrical potential would have decreased rates of accumulation of isometamidium and would be less affected by the drug due to decreased toxicity. Thus the modulation of the mitochondrial membrane potential was thought to possibly have a role in the mechanism for isometamidium resistance by *T. congolense* (Wilkes *et al.*, 1997).

#### 1.7.1.2 Resistance to Antileishmanial drugs

The use of pentavalent antimonials against leishmaniasis has continued despite reports of the development of resistance to these drugs by some species of *Leishmania* in some parts of the world (Croft *et al.*, 2006). The widespread treatment failure rates with antimonials have been attributed largely to drug resistance by the parasite in north Bihar state of India. The easy accessibility of these drugs, lack of compliance to treatment regimen and poor quality of the generic forms of the drugs are some of the factors that have been identified to have contributed to the development of pentavalent antimonial resistance in this part of the world (Sundar, 2001).

The mechanism of resistance to antimony is believed to involve several factors although definitive mechanisms are not fully understood, as what is currently known comes mostly from *in vitro* studies (Ashutosh *et al.*, 2007). There are five aquaglyceroporins (AQP) encoded by the *L. major* genome and one, AQP1, is involved in the transport of trivalent antimonials and other metalloids into the parasite (Mukhopadhyay, 2013). Down-regulation of AQP1 leads to less accumulation of SbIII in *L. major* and field isolates of *L. donovani*, thus leading to antimony resistance by the parasites (Mukherjee *et al.*, 2013; Rai *et al.*, 2013). Down-regulation of expression of AQP1 has been found to be due to reduction in the copy number as a result of deletion of AQP1 gene in the

telomeric region of chromosome 31 (Mukherjee *et al.*, 2013). AQP1 is thought to be an essential channel due to failure of generating knock-out of both of its alleles in *Leishmania* (Mukhopadhyay, 2013). Perhaps this could be one of the reasons why down-regulation of AQP1 is not the only cause of antimony resistance. Other factors are known to contribute to antimony resistance in *Leishmania* (Ashutosh *et al.*, 2007). To further protect itself from the active drug that makes it into the cell, the parasites use P-glycoprotein efflux pumps, to pump out the drug, further reducing drug concentration inside the cell. This mechanism has also been reported in both laboratory and field isolates of *L. donovani* that are resistant to SbIII (Rai *et al.*, 2013).

Another method of antimony resistance involves increased trypanothione levels in the resistant cells. Trypanothione is a reducing cofactor that is present in protozoan parasites where it provides a reducing environment within the cells of the kinetoplasts and hence protects them against oxidative stress (Fairlamb and Cerami, 1992). Besides this main function, trypanothione not only reduces antimony drugs from the pentavalent to the more active trivalent antimony, but also together with other thiols like glutathione forms conjugates with trivalent antimony that is destined for efflux or sequestration. The *Leishmania* multi-drug resistance related protein (MRPA) pump sequesters metal-thiol conjugates as a way of reducing drug effect on the parasite (Haldar *et al.*, 2011). This method of resistance has been found to be present in both laboratory and field isolates of *L. donovani* where higher resistance results from up-regulated expression of the pump (Rai *et al.*, 2013).

Elevated levels of trypanothione have been reported in antimony and arsenite resistant laboratory *Leishmania* species and field isolates of *L. donovani* (Haldar *et al.*, 2011; Rai *et al.*, 2013). The elevated levels of the thiols are believed to increase the conjugation of the drug thereby reducing the drug concentration in the parasites. The increased levels of thiols is said to be due to the up-regulation of  $\gamma$ -glutamylcysteine synthetase and ornithine decarboxylase in various *Leishmania* species (Haldar *et al.*, 2011). The two enzymes are involved in the synthesis of glutathione and spermidine, respectively (Fairlamb and Cerami, 1992). However elevated levels of thiols in both laboratory and field isolates of *L. donovani* showed both up- and down- regulation of  $\gamma$ -

glutamylcysteine synthetase while ornithine decarboxylase was up-regulated in field isolates only (Rai *et al.*, 2013). In maintaining a reduced environment within the cells, trypanothione itself is kept in the reduced state by trypanothione reductase (Fairlamb and Cerami, 1992). The participation of trypanothione reductase in antimony resistance is through its overexpression. The over-expression of trypanothione has been detected through increased levels of its RNA and increased enzyme activity in both field and laboratory isolates of *L. donovani* (Rai *et al.*, 2013).

High relapse rates have been reported with miltefosine within the short time that the drug has been in use. This could suggest that resistance to this new drug could easily develop (Croft *et al.*, 2006).

Miltefosine and other analogues of glycerolphospholipids are transported into *Leishmania* cells by a plasma membrane localized P-type ATPase pump called the miltefosine transporter (Perez-Victoria *et al.*, 2003b). *In vitro*, miltefosine resistant *L. donovani* were shown to have reduced uptake of the drug (Perez-Victoria *et al.*, 2003a). Point mutations in *in vitro* miltefosine resistant *Leishmania* parasites have been identified to be the cause of the inactivation of the miltefosine transporter leading to reduced translocation of the drug into the cells thereby reducing the parasites' susceptibility to the drug. Point mutations affecting conserved amino acid residues lead to the inactivation of the protein and the most resistant parasites carried homozygous mutations in *L. major* (Coelho *et al.*, 2012). In *L. donovani*, different point mutations were detected in both alleles of the miltefosine transporter that were responsible for miltefosine resistance (Perez-Victoria *et al.*, 2003b). Point mutations have also been detected in a miltefosine resistant clinical isolate of *L. infantum* with one of the detected SNPs at L832F being common to both *L. infantum* and *L. donovani* miltefosine resistant parasites (Cojean *et al.*, 2012). Miltefosine resistance in *L. donovani* promastigotes, brought about by inactivation of the miltefosine transporter, is maintained upon transformation into amastigotes both in *in vitro* and *in vivo* macrophages (Seifert *et al.*, 2007). Miltefosine resistant *L. donovani* also show increased activity of enzymes involved in redox reactions when compared to the wild-type. Superoxide dismutase and ascorbate peroxidase, whose function is to detoxify and reduce the levels of reactive oxygen species

(ROS), have been indicated to have increased activity in the miltefosine resistant parasites. However, usually there is a marked increase in accumulation of ROS accompanied by reduction in the mitochondrial membrane potential in the wild-types cells leading to their apoptotic death (Das *et al.*, 2013). Enzymes involved in fatty acid metabolism have been indicated to be upregulated in miltefosine resistant parasites (Das *et al.*, 2013).

Paromomycin is widely used for treatment of cutaneous leishmaniasis which is capable of self curing and this may not influence development of resistance to it. However, there are indications that resistance to this drug is possible although no clinical resistance has been reported so far (Croft *et al.*, 2006). *In vitro*, *L. donovani* paromomycin resistance seems to be a multi-factorial process involving processes like energy metabolism, translation, stress response, virulence and vesicle trafficking. An increased number of vacuolar vesicles was observed in paromomycin resistant cells compared with wild-type cells and there was a corresponding up-regulation of vacuolar ATPase pumps involved in vesicle trafficking, fusion and endocytosis (Chawla *et al.*, 2011).

### 1.7.1.3 Resistance to Amphotericin B

The high success rate of treatment of leishmaniasis with amphotericin B may be short-lived due to the reported emerging resistance (Croft *et al.*, 2006; Purkait *et al.*, 2012) that may be worsened by leishmaniasis co-infection with HIV (WHO, 2010). Amphotericin B acts by binding to ergosterol to form complexes in the cell membrane. At concentrations of amphotericin B that are able to kill the *Leishmania* cells, binding of amphotericin B leads to formation of trans-membrane aqueous pores thereby disturbing the membrane integrity. This makes the cells leaky, leading to their death by osmotic lysis (Ramos *et al.*, 1996). Amphotericin B kills *Saccharomyces cerevisiae* primarily by binding to ergosterol in the membrane and formation of pores in the membrane is reportedly only secondary in killing yeast, thereby enhancing the drug's potency (Gray *et al.*, 2012). The binding of amphotericin B to ergosterol forms the basis of the selectivity of this drug against fungi, *Leishmania* species and *Trypanosoma cruzi* as these organisms have more ergosterol in their membranes than the vertebrate hosts which have cholesterol instead. The varying levels of ergosterol in the different species of *Leishmania* have been thought to be responsible for the

difference in the drug's activity against different species (Croft *et al.*, 2006; Lemke *et al.*, 2005). The varying effect of amphotericin B on the sterol composition in both clinical isolates and laboratory adapted amphotericin B sensitive and resistant *L. mexicana* and *L. donovani* has been demonstrated (Al-Mohammed *et al.*, 2005; Mbongo *et al.*, 1998; Purkait *et al.*, 2012). The perturbation in sterol composition due to amphotericin B resistance was demonstrated in laboratory derived amphotericin B resistant promastigotes and amastigotes although amphotericin B resistant *L. mexicana* promastigotes and not amastigotes were shown to be infective to mice (Al-Mohammed *et al.*, 2005). Amphotericin B resistant *Leishmania* have also been shown to stop synthesising ergosterol as it was not detected (Al-Mohammed *et al.*, 2005; Mbongo *et al.*, 1998; Purkait *et al.*, 2012) thus removing the drug target. Studies on amphotericin B resistant *Leishmania* in comparison to their wild-type progenitors indicate an accumulation of certain intermediates of the sterol biosynthetic pathway (Al-Mohammed *et al.*, 2005; Mbongo *et al.*, 1998; Purkait *et al.*, 2012). Changes in sterol composition were shown to be a stable feature of amphotericin B resistance in *L. mexicana* even after passage of the drug resistant promastigotes in mice (Al-Mohammed *et al.*, 2005). These studies have all used sterol targeting methods for detecting alterations in the sterol composition of the wild-type and amphotericin B resistant *Leishmania* cells.

Induction of amphotericin B resistance has not been confined to its monotherapy use but also to drug combination therapy, although it is generally believed that use of drug combination therapy can delay drug resistance development (Olliaro, 2010). It has been shown that resistance to amphotericin B in combination with other anti-leishmanial drugs like miltefosine, paromomycin and trivalent antimony, can be selected relatively easily *in vitro* in both promastigotes and amastigotes of *L. donovani* (Garcia-Hernandez *et al.*, 2012). Resistance to combinations of amphotericin B with other antileishmanial drugs was not only found to be a stable phenotype but also resulted in significant cross-resistance to other antileishmanial drugs. For instance amphotericin B/trivalent antimony resistant promastigotes were found to be cross-resistant to paromomycin while amphotericin B/miltefosine resistant promastigotes were cross-resistant to paromomycin and trivalent antimony (Garcia-Hernandez *et al.*, 2012).

## 1.8 Methods of assessing drug resistance mechanisms

*In vitro* selection of drug resistance offers a clean method to study drug resistance risk and mechanism before it arises in the field (Berg *et al.*, 2013a; Horn and Duraisingh, 2014). The derived resistant lines' ability to tolerate the drug to which they are resistant, and possible cross resistance to other drugs, is assessed through use of toxicity or susceptibility assays. The *in vitro* susceptibility assays for *Leishmania* suffer from being time-consuming and their lack of being standardised and are performed in an environment that does not mimic the parasite's natural environment (Berg *et al.*, 2013a). Animal trypanosomiasis field isolates can be assessed for susceptibility *in vitro* although they take longer due to their slow adaptation to *in vitro* culture conditions. Standardized *in vivo* susceptibility assays for animal trypanosomiasis are performed in mice or ruminants but they take longer and some species of trypanosome like *T. vivax* and *T. congolense*, do not survive readily in mice (Delespaux *et al.*, 2008).

Laboratory generated and field resistant isolates can be assessed for drug resistance using genetic methods. Genetic assessment ranges from targeted approaches like DNA hybridization, DNA microarrays, PCR based methods, to untargeted approaches like functional cloning, comparative genome hybridisation arrays, full genome microarrays and whole genome sequencing to establish single nucleotide polymorphism, copy number variations and insertion or deletion differences and ploidy that may have arisen due to drug exposure (Berg *et al.*, 2013a; Horn and Duraisingh, 2014). Targeted genetic methods are useful when a sequence or gene(s) is suspected to be involved in the drug resistance mechanism. In the absence of prior knowledge on the possible mechanism of resistance the untargeted approach becomes useful. The presence of post-transcriptional regulation of gene expression in trypanosomatids tends to limit the utilisation of genomes, transcriptomes and proteomes in studying mechanisms of drug resistance. However, proteomics is best suited to study stage specific protein expression levels although it has been used successfully in anti-leishmanial resistance studies (Berg *et al.*, 2013a). The end products of the genome's coding, the metabolites, can be studied in relation to drug resistance mechanism using untargeted metabolomics. The connectivity of various

metabolites through pathways and the global profiling capability of untargeted metabolomics make it a method of choice for studying mechanisms of drug resistance (Vincent *et al.*, 2010). Whichever method is used to study mechanisms of drug resistance, the obtained results have to be confirmed experimentally using techniques like over-expression or transfection of the wild-type or mutated gene to determine whether the altered phenotype can be reversed (Berg *et al.*, 2013a).

Genetic changes to the genome that may have arisen due to adaptation of the parasites to drug pressure in the environment can be assessed by sequencing the whole genome of a drug resistant parasite and its subsequent comparison to its progenitor's and reference genome (Downing *et al.*, 2011). The number of *Leishmania* species that can be assessed in this way has increased because of the availability of the reference genome sequences of *L. mexicana*, *L. donovani* and refined reference genome sequences of *L. major*, *L. infantum* *L. braziliensis* and the non-human pathogen *L. tarentolae* (Downing *et al.*, 2011; Raymond *et al.*, 2012; Rogers *et al.*, 2011). Currently, whole genome sequencing can be achieved by using various Next Generation DNA sequencing (NGS) platforms (Rogers *et al.*, 2011).

## 1.9 Next Generation Sequencing

NGS is a high-throughput method of determining the order or connectivity of bases in a DNA molecule and is relatively cheap compared to the traditional Sanger capillary electrophoresis method. The early next generation sequencing platforms were based on a common general workflow. The workflow involves the fragmentation of target genomic DNA (generally by physical means for example by nebulization or sonication to generate a DNA library), ligation of adaptor primers to the generated target fragments, amplification of the fragments mainly by emulsion PCR for signal amplification, sequencing of the fragment libraries and assembly of sequence reads by aligning them to a reference genome sequence using bioinformatics (Hui, 2014). The first three early and commonly used next generation sequencing platforms were the Roche/454FLX pyrosequencer, Applied Biosystems SOLiD sequencer and Illumina Genome

Analyser (Mardis, 2008). The platforms differ mainly in the method of identifying nucleotides during the sequencing step.

In the pyrosequencer, the incorporation of an added known nucleotide leads to release of pyrophosphate in the presence of pyrosequencing reagents (Ansorge, 2009; Mardis, 2008). The pyrophosphate reacts with adenosine 5' phosphosulphate catalyzed by sulfurylase and produces ATP which in turn reacts with luciferin in the presence of oxygen and luciferase to produce oxyluciferin and light (Nyren and Lundin, 1985). The emission of light confirms incorporation of a nucleotide. The use of pyrophosphate in the sequencing step has thus led the platform being called a pyrosequencer (Ansorge, 2009; Mardis, 2008).

The Applied Biosystems SOLiD sequencer uses octamer oligonucleotides which have a fluorescent group at one end and are ligated to the sequencing primer by a ligase in the presence of ligation reagents. Excitation of one of the four fluorescent groups (four DNA bases) leads to confirmation and identification of two bases due to the light given off. The detected fluorescent group and part of the oligonucleotide are cleaved off to allow ligation of the next oligonucleotide to the growing primer for the next identification, earning this method the name of synthesis by ligation (Ansorge, 2009; Mardis, 2008).

The Illumina Genome Analyser (GAIIx platform) uses four nucleotides with different fluorescent groups and a blocked 3'-hydroxyl group in the sequencing step. The nucleotides with a blocked 3'-hydroxyl group allow the incorporation of a single nucleotide at a time. The incorporated nucleotide is detected by its unique fluorescent property after which the 3'-hydroxyl blocking group is chemically removed to allow the incorporation of the next blocked fluorescent nucleotide. Thus, DNA sequencing using the Illumina Genome Analyser is by synthesis (Ansorge, 2009; Mardis, 2008).

Ion torrent's Ion proton sequencer or Personal Genome Machines use a semiconductor sequencing technology based platform and is mostly designed for research and clinical applications (Liu *et al.*, 2012). It uses the sequencing by synthesis approach and follows the same work flow as the other three sequencing platforms in the preparation of DNA before the sequencing steps but

differs in the signal detection of an incorporated nucleotide (Rothberg *et al.*, 2011). Detection of incorporation of a known nucleotide into the growing chain of DNA after providing all four nucleotides in stepwise form during sequencing is based on the pH change in the solutions in the flow cell caused by the released proton. The change in pH is proportional to the number of nucleotides incorporated and is detected as a voltage signal (Rothberg *et al.*, 2011). Therefore, this platform does not use optics for signal detection resulting in reduced size of the instrument, increased speed of sequencing and is relatively cheap (Liu *et al.*, 2012).

The early next-generation sequencing platforms and their applications have continued to evolve. The most used application of the technique has been the whole genome sequencing with the ultimate aim of identifying insertions or deletions, mutations, single nucleotide polymorphism, both gene and chromosome copy number variation (Hui, 2014).

The downstream phenotypic effects of mutations, gene and/or chromosome copy number variations are not easily identified. Perhaps one way of ascertaining these phenotypic effects would be to assess the changes in the set of the small molecules called metabolites. Metabolites are regarded as the best indicators of the biochemical status of a given cell that are closely and can easily be linked to the observed phenotype (Patti *et al.*, 2012). The relevance of metabolites in the elucidation of phenotypic effects resulting from genetic alterations in drug resistance is that most drug targets have been shown to be metabolites and may result in alteration of their levels (Scheltema *et al.*, 2010). Therefore, an assessment of these metabolites could yield a wealth of information regarding the cell's biochemical and physiological status. Metabolite profile in a given cell or tissue sample can be obtained using metabolomics.

## **1.10 Metabolomics**

Metabolomics is a technology that allows for the identification and quantification of metabolites that are required for the maintenance, growth and normal function of a cell (Dettmer *et al.*, 2007; Lokhov and Archakov, 2008). Metabolomic analysis can be applied using both metabolic profiling (or targeted

metabolomics) and metabolic fingerprinting (or untargeted metabolomics). Targeted metabolomics specifically measures a group of related metabolites that may belong to a particular chemical group or one or more pathways that are related. It is a method that aims at providing a solution to a specific biochemical investigation. Untargeted metabolomics measurements aim at capturing as many metabolites as can possibly be achieved in a given biological sample at a given time. This approach is useful for establishing differences in patterns of metabolites in such samples as urine, plasma, and tissues or cells due to disease, toxin exposure including drug effect, environmental or genetic alterations. It can be performed without need for a specific hypothesis related to a question. Untargeted metabolomics is not only used to assess intracellular metabolites in cell culture systems but also the extracellular metabolites excreted into the culture medium and nutrients levels of spent medium (Dettmer *et al.*, 2007; Patti *et al.*, 2012).

Several analytical separation and mass detecting platforms are used in metabolomics to analyse the metabolites. One such platform is liquid chromatography (LC) interfaced with the mass spectrometer (MS) or simply LC/MS. Liquid chromatography allows separation of compounds of a wide range of polarity with little effort in sample preparation compared to other separation methods that can be interfaced with the mass spectrometer. This property has made liquid chromatography the most versatile separation method among other separation methods as it brings about reduction of ion suppression caused by co-elution of compounds. It is able to separate isomers and isobaric (isotopic) interferences in the case of low resolving mass analyzers (Dettmer *et al.*, 2007; Moco *et al.*, 2007). The chromatographic fractions obtained are fed into the mass spectrometer which is made up of three principal components, the ionisation source, a mass analyser and a detector (Allwood and Goodacre, 2010). Thus, the abundance of the generated ions from chromatographic fractions and their mass-to-charge ( $m/z$ ) ratios are detected by the mass spectrometer. The retention time, relative abundance and mass-to-charge ratio forms the basis of small-molecule metabolite identification.

There are a number of challenges in the analysis of metabolites of small molecular weight that are often encountered in metabolomics. The variability of

widely diverse and chemical complexity of the metabolites which does not permit their detection by a single metabolomic platform has been the biggest challenge to metabolomic analyses. This challenge seems to have lessened due to the development of the mass spectrometers of high resolution and mass accuracy (down to 1 ppm) detection, for example the Fourier transform ion cyclotron resonance mass spectrometry (FTICR-MS). Also good is the Orbitrap mass spectrometer family which are cheaper and easier to maintain than the FTICR-MS. These mass analysers have been thought to be suitable for metabolomics because their mass analysis accuracy increases with decreasing molecular weight of analytes (Breitling *et al.*, 2006). The untargeted metabolomic analysis generates huge data sets that sometimes pose an equally huge challenge in analysing. Moreover, the widely diverse nature of the small-molecule metabolites has led to difficulties in identifying most of the detected analytes in untargeted metabolomic analysis due to insufficient entries of standards in existing metabolite databases (Creek *et al.*, 2012a; Patti *et al.*, 2012). However, despite all these challenges a lot of success has been attained in studying metabolism in trypanosomes and leishmania using metabolomics (Creek *et al.*, 2012a). The determination of the differences in global metabolite levels between sodium stibogluconate sensitive and sodium stibogluconate resistant clinical *L. donovani* isolates was achieved using untargeted metabolomic analysis. The noted major difference was the increased abundance of phospholipids and sphingolipids in the resistant cell lines compared to the susceptible cell lines suggesting membrane lipid alterations (t'Kindt *et al.*, 2010). Metabolic differences during differentiation from procyclic promastigotes to metacyclic promastigotes and the response to sodium stibogluconate exposure of both sodium stibogluconate susceptible and resistant *L. donovani* was compared using LC/MS untargeted metabolomics. Higher level of resistance in the parasites showed a corresponding increase in the levels of indole acrylate, capryloylglycine, valerylglycine, butyrylglycine, and homocysteine detected. Moreover indole acrylate, capryloylglycine and homocysteine levels were observed to increase further upon exposure of the parasites to sodium stibogluconate leading to a proposition of these metabolites being possible resistance markers of sodium stibogluconate in *L. donovani* (Berg *et al.*, 2013b). The other notable success of LC/MS untargeted metabolomics was the elucidation of the mode of action of eflornithine and nifurtimox in *T. brucei*

(Vincent *et al.*, 2012). Also eflornithine resistance related to loss of a transporter causing loss of drug uptake, as seen by LC/MS (Vincent *et al.*, 2010).

## 1.11 Proteomics

Proteomics can also be used to study drug resistance. Proteomics aims at characterising as many proteins as possible from a full complement of proteins referred to as the proteome of a given cell or tissue. It is a comparative study technique that determines alterations in the expression of proteins that may be due to changes in the environmental conditions at a given time (Prenni *et al.*, 2007). Mass spectrometry-based proteomics is divided into two experimental approaches based on the sample treatment before analysis, these are the top-down and bottom-up proteomics. In top-down proteomics the intact protein samples, without any pre-analysis protein modification, are analyzed while in bottom-up proteomics the protein samples are first proteolytically digested before analysis. The bottom-up proteomics is the most commonly used approach (Messana *et al.*, 2013).

Proteomics experiments are broadly divided into proteomics discovery experiments and proteomics assay experiments depending on what is to be realized from the sample analysis (Mallick and Kuster, 2010). Proteomics assay experiments also called targeted or restrictive or directed proteomics is used to determine the quantity of a few predefined groups of peptides or proteins. The analysis of proteins which are not pre-selected for study from the onset of the study constitutes what is called discovery proteomics experiments (Mallick and Kuster, 2010).

The proteomics workflow is generally the same and variations arise from the approach used in sample preparation. The workflow involves separation of proteins or peptides by either electrophoresis or chromatography or both, with or without fragmentation of the proteins/peptides and their subsequent detection in the mass spectrometer (Mallick and Kuster, 2010).

### 1.11.1 Two-Dimensional electrophoresis

The extracted protein samples are separated by two-dimensional electrophoresis (2-DE) in which the proteins are first separated based on their isoelectric points in what is called isoelectric focusing (IEF) and then separated based on their mass in the second dimension. The resolved protein spots are visualised by either autoradiography of radio-labelled samples prior to separation or coomassie or silver staining (Ofarrell, 1975).

### 1.11.2 Difference gel electrophoresis

Difference gel electrophoresis (DIGE) is a modification of the 2-DE technique that uses mass and charge matched fluorescent dyes to pre-label protein mixtures before two-dimensional electrophoresis. There are three types of fluorescent dyes called CyDye DIGE fluors, namely Cy2, Cy3 and Cy5. Based on the protein residues that are labelled two types of CyDye fluors can be distinguished. The first type being the minimal Cy2, Cy3 and Cy5 dyes and allow for the labelling of up to three protein samples. The minimal CyDyes are covalently bonded to proteins through the lysine residues. The second type is called the saturation CyDyes comprising of the saturation Cy3 and Cy5 dyes which allow for labelling of up to two protein samples. The neutrally charged saturation CyDyes label proteins through the cysteine residues (Marouga *et al.*, 2005). The pre-labelled protein samples are mixed and simultaneously separated on a single gel compared to 2-DE in which no more than one protein sample can be separated on a single gel. The resolved protein spots are visualised by fluorescent imaging using fluorescent properties of the dyes (Marouga *et al.*, 2005; Unlu *et al.*, 1997).

The resolved proteins are extracted from excised gel pieces and proteolytically digested normally with trypsin or chemically cleaved into peptides. The peptide mixtures are separated by liquid chromatography. The eluates are ionised by either electrospray ionisation (IES) or matrix-assisted desorption/ionisation (MALDI) to facilitate their detection by the mass spectrometer (Prenni *et al.*, 2007). The electrospray ionisation and matrix-assisted desorption/ionisation are used in proteomics because of their soft ionisation of protein/peptide species which does not lead to sample degradation (Yates *et al.*, 2009). The ion trap,

quadrupole, time-of-flight (TOF) and FTICR-MS are the four basic mass analyzers used in proteomics (Aebersold and Mann, 2003). Mass detection can also be done using tandem mass spectrometry (MS/MS), in which two mass spectrometers are coupled to each other. Tandem MS not only detects the mass with an accuracy of parts per million (ppm) by the first mass spectrometer but also provides a means of getting information on the amino acid sequence in the peptides in the second mass spectrometer (Prenni *et al.*, 2007).

Proteins are identified by comparing the mass spectrum for a particular peptide or protein generated by the mass spectrometer with the in-silico trypsin digestion spectrum of proteins in the database. The fragmented peptide ion patterns in tandem MS are compared to the theoretical fragmentation patterns of peptide ions in the database to get the identification of the proteins in the sample (Prenni *et al.*, 2007).

The proteomes have turned out to be complex and quite dynamic in nature resulting in huge datasets being generated in proteomics studies that possess the challenge of analysis (Aebersold and Mann, 2003; Mallick and Kuster, 2010). The achievements that can be realized from use of proteomics in studying phenotypic effects are thought to be limited and in drug resistance studies putative protein identifications are somewhat common (Scheltema *et al.*, 2010). However, proteomic comparison of drug resistant and drug susceptible cell lines have resulted in identification of several, some unrelated, proteins leading to the conclusion of several factors being at play. Hence, antimony resistance was found to implicate several unrelated protein alterations involved in different cell functions (Matrangolo *et al.*, 2013). This seems to confirm earlier observations of several factors being involved in antimony mode of action and resistance (Croft *et al.*, 2006). MS based proteomics revealed the overexpression of pteridine reductase in *in vitro* methotrexate resistant *L. major* (Drummelsmith *et al.*, 2004). Pteridine reductase is an enzyme that performs some of the functions of dihydrofolate reductase-thymidylate synthetase (Bello *et al.*, 1994) and is known to be the main target of methotrexate (Papadopoulou *et al.*, 1992).

## 1.12 Aims of the project

In a quest to look for molecular markers of drug resistance, it is important to characterise drug resistant parasites as a way of understanding how they tolerate such drugs. This can then help provide possible ways of circumventing resistance to the drugs as well as providing diagnostic tools.

Several techniques have been used to elucidate drug resistance with limited success. The emergence of untargeted metabolomics, with its wide coverage of metabolites, holds promises of elucidating more mechanisms of drug resistance by revealing changes in metabolite profiles. Therefore a combination of whole genome sequencing and metabolomics complemented with proteomics can provide a wealth of information due to the global metabolite and protein coverage which would aid understanding mechanisms of resistance.

It is against this background that the aims of the project were

1. To use metabolomics and Next Generation Sequencing to gain some insight or an understanding how isometamidium resistance occurs by comparing the wild-type and derived isometamidium resistant laboratory adapted *T. brucei*.
2. To use whole genome sequencing and metabolomics in complement with proteomics to identify the relevant changes in the genome of the amphotericin B resistant *L. mexicana* that could subsequently lead to alteration in protein or metabolite profiles.
3. To identify possible molecular markers of resistance to isometamidium and amphotericin B.

## Chapter Two

### 2 Methods

Study of drug resistance mechanisms has lately incorporated the use of the various "omics" in what has been termed as polyomics. Polyomics provides a wealth of information that can help identify the possible mechanisms of drug resistance. This has been made possible by the fact that detected genetic alterations can be correlated to changes in metabolite levels and other related changes in other metabolites of various pathways because of their connectedness in pathway networks. This can then be followed up at the protein and RNA levels to further confirm observed phenotypes in drug resistance. Therefore, polyomics allows the use of "omics" methodologies in complement to each other to confirm the observed phenotypic alterations.

#### 2.1 Culturing BSF and PCF *Trypanosoma brucei* and *Leishmania mexicana* promastigotes

The procyclic form of *T. brucei* strain TREU927 were cultured in vitro in semi-defined medium - 79 (SDM79) (GIBCO) (Brun and Schonemberger, 1979) containing 2 - 2.5 mg/ml hemin and supplemented with 10% foetal bovine serum - Gold (FBS) (PAA Laboratories GmbH) while the bloodstream forms of *T. brucei* strain 427 were grown in commercial HMI-9 (GIBCO) supplemented with 10% FBS - Gold (Hirumi and Hirumi, 1994). The procyclic forms of *T. brucei* 927 were maintained with a starting density of  $1 \times 10^5$  cells/ml in 5 ml cultures in 50 ml Corning non-vented culture flasks incubated at 27°C and passaged every 72 hours. Bloodstream forms of *T. brucei* 427 were incubated at 37°C in the presence of 5% CO<sub>2</sub> in 5 ml cultures using 50 ml Corning vented culture flasks at a starting density of  $2 \times 10^4$  cells/ml and passaged every 48 hours.

*L. mexicana* promastigotes MNYC/BZ/62/M379 were cultured in Homem (GIBCO) medium (Berens *et al.*, 1976), supplemented with 10% FBS-Gold. The cultures were maintained as the procyclic forms of *T. brucei*.

The bloodstream forms of *T. brucei* 427 for metabolomics analysis were grown in 50 - 60 ml cultures in 250 ml Corning vented culture flasks while cultures for *L.*

*mexicana* for metabolomics analysis were grown in 20 ml cultures in 250 ml Corning non-vented culture flasks. The bloodstream forms of *T. brucei* 427 and *L. mexicana* promastigotes were grown to  $2 \times 10^6$  cells/ml in 200 ml and  $0.5 - 1 \times 10^7$  cells/ml in 50 ml cultures for genomic DNA extraction in vented 500 ml and non-vented 250 ml Corning culture flasks, respectively.

## 2.2 Alamar Blue Assay

The toxic effect of compounds on cells was assessed using an adaptation of the Alamar Blue assay (Raz *et al.*, 1997). The cells were counted using the improved Neubauer hemocytometer under the light microscope and cell density adjusted to twice the starting cell density. Two drugs were assessed on one 96-well plate. The first drug was added to each of the first and third wells of the first column of a 96-well plate at twice the required starting concentration in 200  $\mu$ l growth medium. Similarly, the second drug was added to each of the fifth and seventh wells of the first column of the same 96-well plate. One hundred micro-litres of culture medium was added to each of the remaining 92 wells of the plate. A serial dilution of the two drugs was performed across the plate into 22 wells for each of the four wells to which the drugs were added, leaving the last (the 24<sup>th</sup>, 48<sup>th</sup>, 72<sup>nd</sup>, and 96<sup>th</sup>) wells drug-free as negative controls. A 100  $\mu$ l inoculum of bloodstream forms of *T. brucei* was added to each well to a final cell density of  $1 \times 10^5$  cells/ml. The plates were incubated at 37°C with 5% CO<sub>2</sub> for 48 hours. The plates were incubated for a further 24 hours after addition of 20  $\mu$ l of 0.49 mM resazurin (Sigma) in 1 $\times$  phosphate-buffered saline (PBS) (Sigma) pH 7.4 solution. All drugs used for sensitivity assays were bought from Sigma unless stated otherwise.

The procyclic forms of *T. brucei* and *L. mexicana* promastigotes response to compound exposure was assessed as the bloodstreams forms of *T. brucei* but with an initial incubation of 72 hours and a further incubation of 48 hours after addition of 0.49 mM resazurin. Starting cell densities used for the assays were  $5 \times 10^5$  cells/ml and  $1 \times 10^6$  cells/ml for procyclic *T. brucei* and *L. mexicana* promastigotes, respectively.

Fluorescence was measured using the FLUOstar OPTIMA (BMG LabTech, Germany) fluorescence spectrometer set at excitation wavelength of 530 nm and emission wavelength of 590 nm. The EC<sub>50</sub> values were determined using GraphPad Prism 5 software. At least three replicates were done for each compound or set of compounds assayed.

## 2.3 Induction of drug resistance

Selection for drug resistance was done by stepwise increase in concentration of the drug exposure of the cells. The wild-type cells of *T. brucei* bloodstream and procyclic forms were exposed to a starting 0.01 nM isometamidium (Merial, France). The starting concentration of 0.01 nM isometamidium was chosen after the cells were unable to grow at the concentration equal to the EC<sub>50</sub> value determined for the wild type cells or at 10 fold less than the EC<sub>50</sub> value. At these drug concentrations the cells could not grow beyond the third passage. Cultures of wild-type cells of the two cell lines were set up in another set of flasks without the drug and these were passaged in parallel with the cells exposed to the drug. The cells were passaged for at least five times at the same concentration once they were assessed to survive at that drug concentration by checking for an increase in cell density.

Amphotericin B resistance in *L. mexicana* promastigotes was selected by exposing the wild type cells to 0.0135 µM amphotericin B in the growth medium. A sterile-filtered 250 µg/ml Amphotericin B solution in deionised water, ( product number A2942 from Sigma) was used. A culture of the wild type cells without the drug was grown in parallel to the resistance selection culture. The drug concentration was doubled when the cells exposed to the drug were growing to similar densities over a similar length of time with the wild types cells growing in the absence of amphotericin B.

## 2.4 Selection of clones

The derived cells growing in the presence of the drug during drug resistance selection were cloned by estimating the cell density using the improved Neubauer hemocytometer and diluting them to 1 cell/ml in 20 ml growth medium. The diluted cells were added at 200 µl per well to a transparent 96-

well plate and incubated at growth conditions for the particular cell type. Clones were only obtained from plates having less than 30% of the 96 wells with growing cells by checking under the light microscope as calculated using the poisson distribution for a 96 well plate.

### **2.4.1 Making stabilates of clones**

Stabilates of *T. brucei* clones growing at different concentrations of the drug were made in 10% glycerol at various stages of drug resistance selection. The stabilates were made by mixing equal volumes of cells in log phase and pre-chilled growth medium containing sterile 20% glycerol and transferring 1 ml of the mixture into 1.5 or 2 ml cryovials. The cryovials were wrapped in cotton wool and stored at - 80°C overnight. The stabilates were kept in liquid nitrogen for long term storage. Stabilates of *L. mexicana* in log phase were similarly made but in 5% dimethyl sulphoxide (Sigma).

## **2.5 *In vitro* transformation of AmB resistant promastigotes into amastigotes**

Transformation of the promastigotes to amastigotes was carried out in Schneider's Drosophila Medium (SDM) supplemented with 10% heated inactivated calf serum, 2.5 mg/ml hemin in 50 mM NaOH with the complete medium at pH5.0 (Bates *et al.*, 1992). Promastigotes in late log phase stage were washed in PBS. The washed promastigotes at  $1 \times 10^6$  cell/ml were suspended in complete SDM medium in vented culture flasks and incubated at 32.5°C supplemented with 5% CO<sub>2</sub>.

## **2.6 Monitoring mitochondrial membrane potential**

Bloodstream *T. brucei* 427 wild-type cells and derived isometamidium resistant cells were grown to approximately  $2 \times 10^6$  cells/ml. The cells were harvested by centrifugation at 1,000g for 10 min and cell densities adjusted to  $1 \times 10^6$  cells/ml in fresh medium. Four aliquots of 1 ml for each cell line were set up in pre-labeled 1.5 ml eppendorf tubes, for drug free, isometamidium, valinomycin (Sigma), and troglitazone (Sigma). Isometamidium was added to a final concentration of 500 nM to a set of two tubes, one from each cell line, and all

the tubes were incubated at 37°C supplemented with 5% CO<sub>2</sub> for a set time. Valinomycin and troglitazone were added to a second set of four tubes, two for each cell line, to final concentrations of 1 μM and 10 μM, respectively. Troglitazone and valinomycin were used as controls for increasing and abolishing the mitochondrial membrane potential, respectively (Denninger *et al.*, 2007; Figarella *et al.*, 2005). The tubes were incubated as above. The samples were centrifuged at 2,500g for 10 minutes at room temperature and re-suspended in PBS containing 25 nM Tetramethylrhodamine ethyl ester perchlorate (TMRE) (Sigma) dye (Perry *et al.*, 2011) and incubated as above. The cells were transferred to appropriately labeled FACS tubes and kept on ice for at least 30 minutes. The treated cells were analyzed using the CellQuest Pro software on BD FACSCalibur cell sorter.

## 2.7 Genomic DNA extraction

Genomic DNA for whole genome sequencing was extracted using the phenol/chloroform/isoamyl alcohol method. The cells were harvested by centrifuging at 2,500 rpm for 5 minutes. The pellets were washed once in 1× PBS and re-suspended in 500 μl NTE buffer (Appendix A) to which 25 μl of 10% SDS and 50 μl of 10 mg/ml RNase A (Sigma) were added. The mixture was warmed to 37°C, mixed by inverting and incubated for 30 minutes at 37°C. The cell lysates were incubated at 37°C for overnight after addition of 25 μl of 20 mg/ml pronase (sigma). The samples were extracted twice with Phenol: chloroform: isoamyl alcohol (25:24:1) (Sigma) and then twice with chloroform. Before each extraction the samples were mixed on a rotary mixer for 5 minutes. The samples were centrifuged at 16,000g for 5 minutes and the aqueous phase was transferred to 15 ml Falcon tubes to which absolute ethanol 2.5 times the volume of the aqueous phase was added. The mixture was gently mixed by inverting the tubes. The precipitated DNA was transferred to new 1.5 ml eppendorff tubes and washed with 70% ethanol. The DNA samples were centrifuged at 16,000g for 10 minutes and air-dried in the fume hood before re-suspending in 50 μl of TE buffer at 4°C overnight. The concentration of the DNA was measured using the NANODROP 1000 spectrophotometer (Thermo Scientific).

Genomic DNA for routine PCR work was extracted using the NucleoSpin Tissue kit following the manufacturer's standard protocol for human or animal and cultured cells (Macherey-Nagel, Germany).

### 2.7.1 Diagnostic PCR for kinetoplast DNA

The presence of the maxicircle encoded NADH dehydrogenase (ND) subunit genes, ND4, ND5, ND7 and A6 subunit of ATP synthase of bloodstream forms of *T. brucei* 427 was determined by use of PCR (Domingo *et al.*, 2003; Lai *et al.*, 2008). The cell nucleus encoded actin gene was used as the control. The primers used to amplify the genes are given in Table 2.1.

Primer	Primer sequence	PCR product size in bp
Actin Forward	5' CCGAGTCACACAACGT 3'	456
Actin Reverse	5' CCACCTGCATAACATTG 3'	
ND5 Forward	5' TGGGTTTATATCAGGTTTCATTTATG 3'	395
ND5 Reverse	5' CCCTAATAATCTCATCCGCAGTACG 3'	
ND4 Forward	5' TGTGTGACTACCAGAGAT 3'	256
ND4 Reverse	5' ATCCTATACCCGTGTGTA 3'	
ND7 Forward	5' ATGACTACATGATAAGTA 3'	161
ND7 Reverse	5' CGGAAGACATTGTTCTACAC 3'	
A6 Forward	5' AAAAATAAGTATTTTGATATTATTAAG 3'	381
A6 Reverse	5' TATTATTAACCTTATTTGATC 3'	

**Table 2.1 Oligonucleotides used for amplification of kinetoplast related genes.**

The gene fragments were amplified using 2.5 U Go-Taq DNA polymerase (Promega) in a 25 µl reaction by polymerase chain reactions (PCR) on a G-Storm thermal cycler. The final concentration of the reaction mixture constituents was made up of 300 µM dNTPs, 300 µM primers in 1× Go-Taq DNA polymerase buffer. Template DNA was used at 10 ng to 60 ng. The thermal cycler program used was; heated lid 112°C; initial denaturation 95°C, 5 minutes; 35 cycles of denaturation at 95°C for 1 minute, annealing at 54°C for 1 minute, elongation 72°C for 30 seconds and final elongation at 72°C for 8 minutes.

## 2.7.2 Next-Generation Genomic DNA sequencing

The genomic DNA for *L. mexicana* M379 wild type, derived *L. mexicana* M379 amphotericin B resistant (AmB-R) at 0.27  $\mu\text{M}$  of amphotericin B, bloodstream form of *T. brucei* 427 wild-type, isometamidium (ISMM) resistant clones growing in the presence of 4 nM, 40 nM and 1  $\mu\text{M}$  ISMM were sequenced at Glasgow Polyomics, University of Glasgow. Paired-end samples of the cell lines' genomic DNA were sequenced using Illumina GAIIX next generation DNA sequencing platform. The sequencing data were analyzed by Dr. Nicholas Dickens (Wellcome Trust Center for Molecular Parasitology, University of Glasgow) and Dr. Manikhandan Mudaliar (Glasgow Polyomics, University of Glasgow).

## 2.7.3 *L. mexicana* gene cloning using pNUS expression vectors

### 2.7.3.1 Expression vectors and primer design

The pNUS-HnN and pNUS-GFPcN (Figure 2.1) expression vectors for *Crithidia fasciculata* and *Leishmania* (Tetaud *et al.*, 2002) were used to clone and express the wild-type lanosterol 14 $\alpha$ -demethylase gene fused to the His-Tag at the N-terminus in *L. mexicana* AmB-R and the GFP-Tag at the C-terminus of both wild type and AmB-R lanosterol 14 $\alpha$ -demethylase genes in wild type *L. mexicana*, respectively, using neomycin for selection in both cases. Lanosterol C14-reductase with a GFP tag at the C-terminal was similarly cloned but was expressed both in the wild-type and AmB resistant cell lines. CLC genomics workbench 6 was used to design primers for PCR amplification of gene fragments. Restriction sites were incorporated into the designed primers (Table 2.2), where this was required to facilitate the ligation of the gene fragment into the linearized expression vector backbone. The pNUS expression vector-specific primers were designed using the vector sequences downloaded from <http://www.ibgc.u-bordeaux2.fr/pNUS/index.html>. All the primers were bought from Eurofins MWG Operon, Germany. All the primer pair optimal annealing temperatures were determined by gradient PCR.

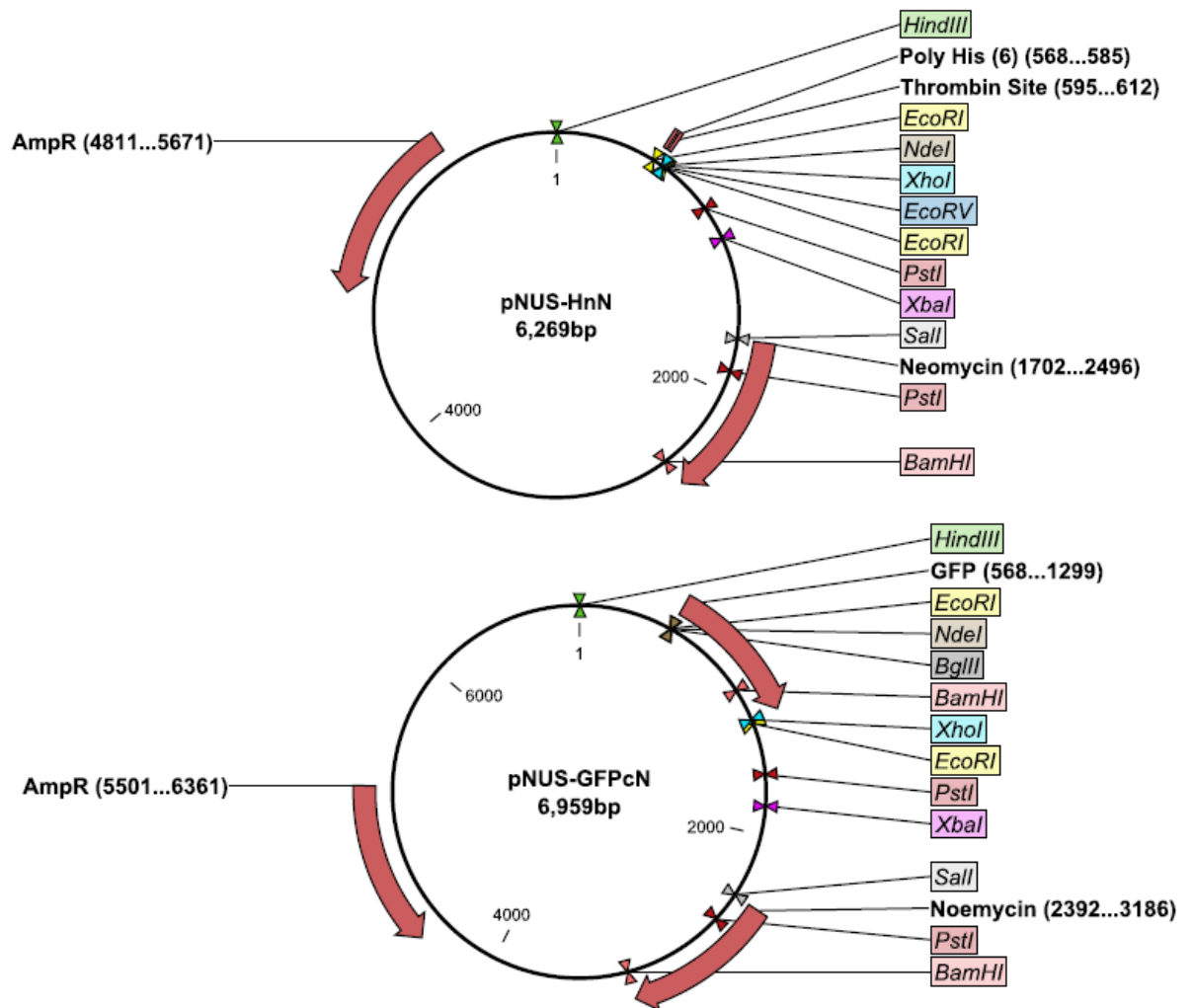


Figure 2.1 The pNUS-HnN and pNUS-GFPcN expression vector maps. Adapted from <http://www.ibgc.u-bordeaux2.fr/pNUS/index.html> and annotated using CLC Genomics Workbench 6 software.

### 2.7.3.2 PCR amplification of gene fragments

The gene fragments for cloning were amplified by PCR using concentrations of primers and dNTPs as in section 2.7.1. Phusion High-Fidelity DNA polymerase (New England Biolabs) was used at 1 U in 1× Phusion GC HF buffer for a 50 µl reaction. The Phusion High-Fidelity DNA polymerase was used because it is less likely to introduce PCR mutations to the fragment being amplified. The gene fragments were amplified from a template DNA concentration of approximately 150 ng using the primers indicated in table 2.2. The PCR program was; heated lid at 112°C, initial denaturation 95°C, 5 minutes, 30 cycles of denaturation at 95°C for 1 minute, annealing at 69.7°C for 30 seconds, elongation 72°C for 1 minute 30 seconds and final elongation 72°C for 5 minutes.

Primer Designation	Primer sequence	Primer specificity	Restriction sites	Expected band size
MB769	<u>GCATATGATGATCGGCGAGCTTCTCC</u>	lanosterol 14 $\alpha$ -demethylase (CYP51)	<i>NdeI</i>	1452 bp
MB770	<u>CTCGAGCTAAGCCGCCGCTTCT</u>		<i>XhoI</i>	
MB0243	GTAAAACGACGGCCAG	pGEM-T easy vector		*233 bp
MB0424	CAGGAAACAGCTATGAC			
MB0781	CATCATCATCACAGCAGC	pNUSHnN		*103 bp
MB0782	GTCGAAGGAGCTCTTAAAACG			
MB0037	ATGATTGAACAAGATGGATTGC	Neomycin cassette		795 bp
MB0038	TCAGAAGAAGCTCGTCAAGAAG			
MB0787	CGCGAAATAGATATAAAGCACACG	43 bp from CYP51 ATG		788 bp
MB0788	TCGCGAGCGATGATAATCTCG	CYP51 internal		
MB0755	GGTATTGAGGGTTCGCATGATCGGCGAGCTTCTCCT	pET30 Xa/LIC/CYP51		1473 bp
MB0756	AGAGGAGAGTTAGAGCCCTAAGCCGCCGCTTCTTCT			
MB791	5' <u>CATATGATGATCGGCGAGCTTCTCCT</u> 3'	CYP51	<i>NdeI</i>	1452 bp
MB792	5' <u>AGATCTAGCCGCCGCTTCTTC</u> 3'		<i>BglII</i>	
MB0793	5' TATCTTCCACTTGTCAAGCGAAT 3'	pNUS-GFPcN		*115 bp
MB0794	5' CCCATTACATCGCCATCCAGTTC 3'			
MB0795	5' ATGAGCAAGGGCGAGGAACTGTTC 3'	GFP cassette		717 bp
MB0796	5' TCACTTGTACAGCTCGTCCATGCC 3'			

**Table 2.2 Oligonucleotides used in cloning experiments.**

**Underlined sequences show the named restriction enzymes' restriction sequences used. \*Depending on the restriction sites used, the expected PCR product size would be the gene insert added to the indicated size in the table less the fragment removed by restriction digestion.**

The PCR products were A-tailed with 300  $\mu$ M dATP in the presence of 1 U Go-Tag DNA polymerase in 1 $\times$  Go-Taq polymerase buffer at 72 °C for 15 minutes and gel purified using the NucleoSpin Gel and PCR clean up kit (Macherey-Nagel, Germany). The PCR products were A-tailed to facilitate their ligation into the linear sub-cloning vector pGEM-T Easy vector (Promega) which has 3'-terminal thymidine overhang at both ends. The ligation was done by mixing 3.5  $\mu$ l of purified A-tailed PCR product with 50 ng pGEM-T Easy vector and 1 U T4 DNA ligase (Promega) in 1 $\times$  Rapid ligation buffer (Promega) in 10  $\mu$ l total reaction volume and incubation at 4 °C overnight.

### **2.7.3.3 Transformation of bacteria**

The gene insert/pGEM-T easy vector constructs were transformed into XL1 Blue *E. coli* competent cells (Promega) to obtain large quantities of the gene insert. The transformation was done by mixing thawed 50  $\mu$ l XL1 Blue *E. coli* competent cells on ice with 5  $\mu$ l of the ligation product and incubated on ice for 30 minutes. The cells were heat-shocked for 45 seconds in a water bath set at 42 °C. The cells were immediately incubated on ice for 2 minutes and 100  $\mu$ l SOC medium was added before incubating at 37 °C with shaking at 250 rpm for 1 hour. A further 200  $\mu$ l of SOC medium was added and 100  $\mu$ l of the solution was plated out on LB agar (Sigma) plates containing 100  $\mu$ g/ml ampicillin (Sigma). The plates were incubated at 37 °C overnight.

### **2.7.3.4 PCR colony screening**

The colonies were screened for the gene insert using PCR. The PCR reactions were carried out in a 20  $\mu$ l total reaction volume with pGEM-T easy vector specific primers, MB0243 and MB0424 (Table 2.2), and dNTPs at 500  $\mu$ M final concentrations, using Go-Taq DNA polymerase at 2.5 U in 1 $\times$  Go-Taq DNA polymerase buffer. The following PCR program was used:- heated lid 112 °C; initial denaturation 95 °C for 3 minutes; 35 cycles of denaturation at 95 °C, 40 seconds; annealing at 55 °C, 40 seconds; elongation 72 °C, 1 minute 30 seconds and final elongation at 72 °C for 5 minutes.

The identified positive single colonies were picked, streaked on new LB agar plates containing 100  $\mu$ g/ml ampicillin and incubated at 37 °C overnight. The

positive colonies were grown in 5 ml LB broth (Sigma) containing 100 µg/ml ampicillin by incubating the cultures at 37° C overnight with shaking at 250 rpm. The cells were harvested by centrifuging at 4 500 rpm for 10 minutes.

#### **2.7.3.5 Restriction digestion**

The plasmids were extracted from the harvested cells using the NucleoSpin Plasmid/Plasmid (NoLid kit) (Macherey-Nagel, Germany). Three microgram of extracted plasmids were double digested with 30 U of each of the two restriction enzymes of interest in 1× of an appropriate buffer (Promega) supplemented with 1× BSA (Promega) in a 70 µl total reaction volume. The pNUS-HnN and pNUS-GFPcN expression vectors, a gift from Dr. E. Myburgh, MVLS-III University of Glasgow, were similarly digested. The restriction digests were resolved on a 1% agarose gel and the bands of interest were excised. The DNA was extracted from the gel pieces using the NucleoSpin Gel and PCR clean up kit (Macherey-Nagel, Germany).

The gene fragments and the linear expression vectors, with complementary sticky ends, were ligated in 1× T4 ligase buffer with 1 U T4 DNA ligase (Promega). This was done by mixing 2 µl of the linear vector and 6 µl of the enzyme insert in a total reaction volume of 10 µl. The reaction mixture was incubated at 4° C overnight.

The gene/expression vector constructs were transformed into XL1 Blue *E. coli* competent cells as in section 2.7.3.3. The single colonies carrying the gene inserts were identified by PCR colony screening using pNUS expression vector-specific primers (Table 2.2). The PCR reaction conditions and program were carried out as in section 2.7.3.2 but with 2.5 U Go-Taq DNA polymerase in 1× Go-Taq DNA polymerase buffer and 56.4° C annealing temperature. The identified positive single colonies were grown in 5 ml LB broth as described earlier to obtain large quantities of the plasmid. The plasmids or constructs were extracted as described earlier and were sequenced at Eurofin MWG Operon, Germany. The obtained sequences were aligned with the enzyme gene sequence downloaded from TriTryp DB website using CLC genomics workbench 6. This was done to check for any alterations in the sequence that could have resulted from various treatments that the gene was subjected to.

### 2.7.3.6 Transfection of *L. mexicana* promastigotes

The pNUS-HnN plasmid with the correct sequence of the wild-type lanosterol 14 $\alpha$ -demethylase gene sequence with the added His-Tag was transfected into derived amphotericin B resistant *L. mexicana* promastigotes. This was done to determine whether the wild-type enzyme would have an influence on the resistance to amphotericin B status of these cells. To determine whether there was any difference in cell localization of the enzymes from the two cell lines, the plasmids with the correct sequences of the wild-type and derived amphotericin B resistant lanosterol 14 $\alpha$ -demethylase gene sequences with the GFP tag at the C-termini were transfected into the wild type *L. mexicana* promastigotes. *L. mexicana* to be transfected with the expression plasmids were grown to log phase cell density and  $1 \times 10^7$  cells/ml were harvested and washed once by resuspending in fresh 5 ml Homem supplemented with 10% FBS-Gold. The cells were centrifuged at  $1000 \times g$  for 10 minutes and resuspend in 100  $\mu$ l Tb BSF buffer (Appendix A) and added to 10  $\mu$ g of plasmid DNA in a cuvette. Using program U-033 the cells were zapped in an Amaxa biosystems Nucleofector<sup>®</sup>II (Lonza). The cells were incubated on ice for 10 minutes and then transferred into pre-warmed 10 ml of Homem supplemented with 10% FBS-Gold and left to recover for 18 hours at the usual incubation temperature for leishmania (section 2.1). The selection drug G418 disulfate salt (Sigma) at 50  $\mu$ g/ml was added to the growth culture medium and the Homem used for diluting cells during making of clones. A serial dilution of 1/24 was done, from which a 1/288 dilution was made and 1/576 dilution was made from the 1/288 dilution (Figure 2.2). The diluted cells were transferred to 3 transparent 96 well plates at 200  $\mu$ l per well. After 14 days the clones were obtained from the third dilution plate and transferred to 10 ml Homem supplemented with 10% FBS-Gold containing 50  $\mu$ g/ml G418 disulfate salt. The clones were maintained in Homen containing 50  $\mu$ g/ml G418 disulfate salt and stabilates were made as in section 2.1.

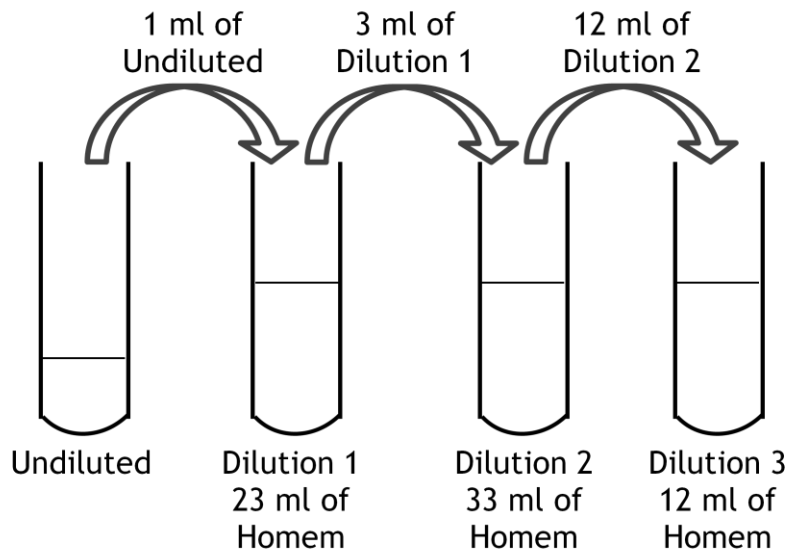


**Figure 2.2** Schematic representation of the serial dilution of the transfected *L. mexicana* for cloning.

### 2.7.4 Protein over-expression

The wild-type and derived AmB-R lanosterol 14 $\alpha$ -demethylase were amplified by PCR using primers MB0755 and MB0756 (Table 2.2). The PCR products were cloned into the ligation independent vector pET-30 Xa/LIC following the manufacturer's protocol (Novagen, Merk).

Small scale over-expression using the pET-30 Xa/LIC- lanosterol 14 $\alpha$ -demethylase constructs were carried out by growing transformed BL21 *E. Coli* and the derivative Rosetta strains (Novagen) in 50 ml LB broth containing 30  $\mu$ g/ml kanamycin and 30  $\mu$ g/ml chloramphenicol, respectively. Kanamycin and chloramphenicol were used for selection of BL21 and Rosetta competent cells, respectively. The cultures were incubated at 37 $^{\circ}$ C until the OD<sub>600</sub> was 0.6 when protein over-expression was induced by addition of isopropylthio- $\beta$ -galactoside (IPTG) (Melford) to a final concentration of 1 mM. The protein over-expression was done at 37 $^{\circ}$ C for 3 hours. The cells were harvested by centrifugation at 4,500 rpm for 20 minutes at room temperature.

The presence of over-expressed protein was checked by performing small scale purification on Ni-NTA spin columns (Qiagen) using the Protein Purification under Native Conditions from *E. coli* Lysates protocol supplied together with the spin columns. The proteins were resolved on NuPAGE Bis-Tris Mini Gels following the

manufacturer's protocol (NOVEX). The protein bands were stained with Coomassie blue stain (Appendix A) overnight and destained with several washes with destaining solution (Appendix A).

## **2.8 Fluorescence Microscopy**

### **2.8.1 Immobilisation of live stained cells for imaging**

Live stained cells were immobilised using 1% agarose, low-gelling temperature (Sigma). This was done to limit the movements of the stained cells so that they could easily be viewed under the microscope (Lanteri *et al.*, 2008). An equal volume of cells in PBS and 1% to 2% agarose in PBS was mixed and 50  $\mu$ l of the mixture was added to the glass slide. Agarose at 27°C and 37°C was used for *Leishmania* and trypanosome cells, respectively. Cover-slips were applied to the slides and slides were left at room temperature for 10 to 15 minutes or in the fridge for 5 minutes before viewing on the fluorescent microscope.

### **2.8.2 DNA staining with DAPI**

Fifty micro-litres of cells grown to mid-log phase were spread onto a microscope glass slide using a cover-slip and air dried in the fume-hood. The cells were fixed in absolute methanol for overnight at -20°C. The methanol was evaporated in the fume-hood and the fixed cells were rehydrated with 1 ml PBS for 10 minutes. The excess PBS was removed by tilting the glass slide on a folded tissue paper. Fifty micro-litres of PBS containing 1  $\mu$ g/ml 4, 6-diamidino-2-phenylindole (DAPI) (Sigma) and 1% 1, 4-Diazobicyclo-(2, 2, 2) octane (DABCO) (Sigma) was applied to the glass slides and observed under UV light using the DAPI filter with excitation wavelength of 365 nm and emission wavelength of 445 nm on a ZEISS Axioplan 2 Imaging fluorescent microscope under oil immersion after applying the cover slips.

### **2.8.3 Mitochondria staining with Mito-Tracker**

The mitochondria were stained with the mitochondrion selective probe CMXRos Mito-Tracker (Invitrogen) in PBS to a final concentration of 1 nM using  $2 \times 10^7$  cells/ml in 1 ml growth medium. The cells were washed once in PBS and re-suspended in PBS. The cells were further stained with DAPI as in section 2.7.2.

The cells were immobilized with agarose as in section 2.7.1 and observed using the Cy3 or DSRed filter set with an excitation wavelength of 550 nm and emission wavelength of 605 nm.

#### **2.8.4 Filipin III staining of parasite sterols**

The presence of sterols in live cells was visualized by staining with filipin III (F4767, Sigma). Cells at  $1 \times 10^7$  per ml were washed with fresh growth medium and re-suspend in pre-warmed fresh medium containing 1  $\mu$ M filipin III. Stock solution of filipin III was initially dissolved in DMSO at 5 mM and then diluted to 200  $\mu$ M in PBS before further dilution or addition to the growth medium. The cells were incubated at 26°C protected from light for 3 hours and every 15 minutes an aliquot of 25  $\mu$ l cells was immobilized as in section 2.7.1 and viewed under the fluorescent microscope using DAPI filters.

#### **2.8.5 Endoplasmic reticulum (ER) staining with ER-Tracker Red dye**

The endoplasmic reticulum (ER) was labeled with the ER-Tracker Red dye for live cells (Invitrogen). The cells in log phase were harvested and adjusted to  $1 \times 10^7$  cells/ml and washed in PBS by centrifuging at 1,000g for 10 minutes. The cells were re-suspended in 100  $\mu$ l complete Homem medium containing 100 nM ER-Tracker Red dye and incubated at 27°C for 30 minutes. The cells were centrifuged at 1,000g for 10 minutes and re-suspended in fresh complete Homem without the staining dye. The cells were fixed with paraformaldehyde to a final concentration of 2% at 27°C for 2 minutes and subjected to 5 minutes wash in PBS twice. The cells were mounted onto glass slides and covered with cover slips. The treated cells were observed under oil immersion using the DSRed filters as in section 2.7.2 on a ZEISS Axioplan 2 Imaging fluorescent microscope.

#### **2.8.6 Imaging cells expressing GFP-tagged proteins**

The cells expressing GFP-tagged proteins were fixed in methanol (section 2.8.2). They were observed on a ZEISS Axioplan 2 Imaging fluorescent microscope under oil immersion using the GFP filter set with excitation wavelength of 470 nm and emission wavelength of 525 nm.

### 2.8.7 Cell length measurement

The cell length of *L. mexicana* promastigotes was estimated using the SoftWoRx 5.5 software on the DeltaVision microscope. The cells in the late log phase were fixed in methanol and stained with DAPI (section 2.8.2). The cell length was measured from the anterior end to the posterior end of the cell body.

## 2.9 [<sup>3</sup>H]Pentamidine Uptake Assay

The uptake of 0.1  $\mu\text{M}$  tritiated pentamidine was done using approximately  $1 \times 10^8$  cells/ml in assay buffer (Appendix A) (DeKoning and Jarvis, 1997) at room temperature. The cells were harvested, washed once and re-suspended in assay buffer. The cells were mixed with pentamidine on 300  $\mu\text{l}$  oil [7/1; v/v; dibutylphalate/light mineral oil; Density 1.018 g/ml] (sigma) in 1.5 ml Eppendorf tubes. At the set end time of incubation the reactions were stopped by centrifuging the tubes at 16, 100g for 1 minute. The tubes were frozen in liquid nitrogen and the bottoms of the tubes containing the cells were cut off into scintillation tubes. Three replicates were set up for each time point. To each of the tubes for the various time points and three tubes with no tritiated pentamidine for negative radiation controls were set up and 300  $\mu\text{l}$  of 2% SDS was added to the tubes. A further three tubes containing 10  $\mu\text{l}$  of 0.4  $\mu\text{M}$  tritiated pentamidine were set up for radiation level controls. All the samples were mixed on the rocker for at least 30 minutes. To each of the tubes, 3 ml Optiphase 'Hisafe' 2 scintillation liquid (PerkinElmer) was added for the determination of radiolabel count per minute. The samples were incubated at room temperature for overnight. Three replicates of the experiment were done. The radioactivity was read on 1450 Microbeta Wallac trilux Liquid scintillation and luminescence counter (PerkinElmer). The counts were converted to pmole uptake of pentamidine per  $1 \times 10^7$  cells over time in minutes and plotted using the GraphPad Prism 5 software.

## 2.10 Metabolomics analysis

### 2.10.1 Sample extraction

The samples were extracted using the chloroform:methanol:water (1:3:1) solvent mixture containing 1  $\mu$ M each of Theophylline, 5-Fluorouridine, Cl-phenyl-cAMP, N-methyl glucamine, Canavanine and Piperazine as internal standards. The internal standards used are not expected to be present in biological systems and are used to monitor the instrument response during separation and detection of masses. Cell culture volumes containing  $1 \times 10^8$  cells for each sample were calculated using the culture cell density. Calculated volumes of cells cultures of less than 10 ml were transferred to 15 ml Corning tubes while calculated volumes of cells of more than 20 ml were transferred to 50 ml Corning tubes. Cells were quenched rapidly by cooling them to 4°C by submerging Falcon tubes in a dry ice/ethanol bath while mixing vigorously during cooling to avoid freezing and possible cell lysis. The cells were centrifuged at 1, 250g for 10 minutes at 4°C in a refrigerated bench top centrifuge and 5  $\mu$ l of supernatant was removed for spent medium analysis while the rest of the supernatant was discarded leaving about 1 ml in which the pellet was re-suspended. The re-suspended cells were centrifuged at 2, 500g for 5 minutes at 4°C and the supernatant was removed completely. The pellet was re-suspend in 200  $\mu$ l of chloroform:methanol:water (1:3:1) at 4°C. The same amount of extraction solvent was added to the 5  $\mu$ l supernatant and 5  $\mu$ l of growth medium. The samples were broken up and re-suspended in extraction solvent by pipetting up and down vigorously. The samples were incubated at 4°C for 1 hour with vigorous shaking. The mixtures were centrifuged at 13, 000g for 5 minutes at 4°C. An equal amount of extraction solvent as the samples was set aside and treated as the other samples for use as a blank. The supernatant (180  $\mu$ l) was removed and stored under argon gas at -80°C until analysis using LC/MS.

### 2.10.2 Liquid Chromatography/Mass spectrometry

The Dionex UltiMate 2000 Liquid chromatography system coupled to the Orbitrap Exactive mass spectrometer was used for the separation and mass detection of the metabolites at the Scottish Metabolomics Facility (ScotMet), University of Glasgow (by either Dr. Karl Burgess or Dr Darren Creek or Miss Suzanne Eadie or

Dr. Stefan Weidt or Dr Hyun Dong Kim) all of whom use the same procedure. The samples were run on the LC/MS alongside 179 authentic standards at 10  $\mu$ M each because they provide a means of recalculating the retention times that may result from varying performances of the column. Moreover, the authentic standards are useful in ruling out false identification by comparing their retention times and mass-to-charge ratios with those of the putative identifications during data analysis (Creek *et al.*, 2011). The auto sampler was set at 4 °C with an injection volume of 10  $\mu$ l. The ZIC-HILIC (Hydrophilic Interaction chromatography) column with the diameter of 4.6 mm, column length of 150 mm and pore size of 5  $\mu$ m were used. A ZIC pHILIC column was used which provides a better resolution of both sugar phosphates and carboxylic acids, two classes of molecules integral to energy metabolism and is best suited for metabolites such as nucleotides. The column temperature was 24 °C and the flow rate was set at 300  $\mu$ l/min. A 0.1% solution of formic acid in water and 0.08% formic acid in acetonitrile as solvents A and B and 20 mM ammonium carbonate in water and acetonitrile as solvents A and B for the ZIC-HILIC and ZIC-pHILIC columns respectively, were used. The gradient for liquid chromatography was 0 min 80% B; 30 min 20% B; 32 min 5% B; 40 min 5% B; 42 min 80% B; 47 min 8% B. The mass detection of the eluates was performed with the mass spectrometer set at a resolution of 50, 000 and switching mode between positive and negative mode. The mass spectrometer was operated with spray voltages of +4.5 and -3.5 kV; Capillary voltage +40 V and -30 V; Tube voltage +70 V and -70 V; Skimmer voltage +20 V and -18 V; HEIS and Capillary temperatures 150 °C and 250 °C respectively; Sheath, Auxiliary, and Sweeping gases 40 units, 20 units and 1 unit, respectively.

### **2.10.3 Data processing**

The raw data was processed and analyzed using Identification and evaluation of metabolomics data from LC/MS (IDEOM). IDEOM is an excel spreadsheet automated to process untargeted metabolomics data. It utilizes the features of XCMS and mzmatch.R tools to process raw data from LC/MS for identification of metabolites and automatically generates scripts that are executed in R software to provide a statistical presentation of results (Creek *et al.*, 2012b). Data was obtained from Glasgow Polyomics as an IDEOM file.

## 2.11 Proteomics analysis

### 2.11.1 Protein extraction

All protocols from section 2.11.1 to 2.11.6 were performed by Mr. Alan Scott. The protein samples were extracted from  $1 \times 10^8$  cells of each of wild type and AmB resistant *L. mexicana* promastigotes. The cells were harvested and washed twice in  $1 \times$  PBS by centrifugation at 1, 000g for 10 minutes. The cell pellets were re-suspended in lysis buffer (Appendix A) by vigorous pipetting up and down in 1.5 ml eppendorf tubes. The cells were immediately lysed by ten 1 - 2 second's probe sonication cycles with 1 minute of cooling on ice between sonications. The lysates were incubated at room temperature for 10 minutes with gentle mixing. The insoluble materials were removed by centrifuging at  $13\ 000 \times g$  for 10 minutes and the supernatants were transferred to new 1.5 ml eppendorf tubes. The soluble proteins were precipitated using 4 times the volume of the supernatant of cold acetone at  $-20^\circ\text{C}$ . The samples were mixed and incubated at  $-20^\circ\text{C}$  for least 1 hour. The samples were centrifuged at  $13\ 000 \times g$  for 10 minutes and the pellets were washed twice with cold 80% acetone. The protein samples were re-suspended in small volumes of the lysis buffer to get protein concentration of more than 5 mg/ml. The re-suspended protein samples were centrifuged at  $13\ 000 \times g$  for 10 minutes to remove the insoluble material. The supernatants were transferred to new eppendorf tubes.

### 2.11.2 Protein concentration determination

The protein concentrations of the samples were determined by the Bradford assay using bovine serum albumin (BSA) (Promega) as the standard. A series of BSA standards from 0 to 0.5 mg/ml were prepared for a standard curve of absorbance against protein standard concentration. Water was used as a blank. A 1 in 10 dilution of protein samples was done using distilled water. Ten microlitres of the standards and the protein samples were transferred to a 96 well plate in duplicates. Two hundred microlitres of the Bradford reagent diluted five times with distilled water was added to the samples. The solutions were mixed for 5 minutes to fully develop the color of the reacted Bradford reagent. The absorbances of all samples were read at 595 nm. The protein sample concentrations were determined by interpolating their absorbance values

on the standard curve. The concentration of the samples was adjusted to 5 mg/ml using the lysis buffer.

### **2.11.3 Protein labeling**

The wild-type line protein samples were labeled with Cy3 while the amphotericin B resistant line protein samples were labeled with Cy5. The protein samples at 5 µg in lysis buffer were labeled with the two cyanine dyes. The protein samples were mixed with the cyanine dyes at 400 pmol and incubated at 4 °C for 30 minutes in the dark. The reactions were stopped by addition of 10 mM lysine and incubated for 10 minutes on ice and in the dark. The labeled samples were otherwise stored at -80 °C until use. Otherwise, the labeled samples were mixed together and the volume made up to a total of 450 µl with DiGE rehydration buffer (Appendix A).

A 100 µl of unlabeled protein samples at 5 mg/ml were mixed with 350 µl DiGE rehydration buffer for running preparative gels for the two protein samples.

### **2.11.4 Iso-Electric Focusing**

The protein sample solutions were added to the IEF ceramic IPG strip holders and covered with the IPG (pH 3 - 10) strips with the gel surface facing downwards. The protein sample solutions and IPG strips were then overlaid with mineral oil without trapping any air bubbles. The IEF was run on the Ettan IPG phor Iso-Electric Focusing System (Pharmacia Biotech) with the following parameters; 50 µA per strip, step 1 was done at 30 volts (V) for 10 hours (hr), step 2 at 300 V for 1 hr, the gradient steps 3, 4, and 5 at 600 V for 1 hr, 1000 V for 1 hr, 8000V for 3 hrs respectively, and step 6 (step and hold) at 8000 V for 8 hrs and 30 minutes.

### **2.11.5 Second dimension electrophoresis**

The run IPG strips were equilibrated in DiGE Equilibration buffer I (Appendix A) and DiGE Equilibration buffer II (Appendix A) for 15 minutes in each buffer. The equilibrated strips were washed by dipping in 1× SDS running buffer (Appendix A) and were then applied to the top of the SDS gels. The IPG strips were sealed in

place with 0.5% agarose sealing solution, containing 0.5% bromophenol blue. The gels were run at 120 V overnight on Ettan DALT II System (Pharmacia Biotech) with a 1× SDS running buffer in the bottom chamber and the 2× SDS running buffer in the top chamber. Electrophoresis was stopped immediately after bromophenol blue had run through the bottom of the gel.

The gels were scanned on the Typhoon 9400 variable mode imager. Cy3 labeled proteins were scanned at an excitation wavelength of 532 nm (green) and emission wavelength of 580 nm with a band pass (BP) filter 30. While the Cy5 labelled protein were scanned at 633 nm (red) excitation wavelength and emission wavelength 670 nm (BP 30).

### **2.11.6 Total protein staining**

Preparative gels were stained with Coomassie blue (Appendix A) for total protein visualization. The run gels were stained with Coomassie blue stain solution and destained with the destaining solution as in section 2.6.4. The destained gels were scanned at 633 nm (red laser) on the Typhoon 9400 variable mode imager.

### **2.11.7 Protein spot picking**

The scanned DiGE gel images were analyzed by Dr. Richard J. S. Burchmore and were processed using the DeCyder 2-D Differential In-gel Analysis (DIA) Software (GE Healthcare) to compare the protein (spots sizes) expression levels and generate the picking list. Using the picking list from the DiGE gel analysis, corresponding protein spots of interest on the preparative Coomassie blue stained gels were manually cut out.

### **2.11.8 In-gel trypsin digestion**

The protein spots were subjected to in-gel trypsin digestion to obtain peptides fragments. The excised gel pieces were washed for one hour with 100 mM ammonium bicarbonate with shaking at room temperature. The gel pieces were then washed twice with 50% acetonitrile in 100 mM ammonium bicarbonate for one hour and the second wash was done with shaking. The gel pieces were dehydrated with acetonitrile for 10 minutes and dried in the speed vac

(Eppendorf concentrator 5301) after removal of the solvent. Trypsin at 0.2 µg/µl in 25 mM ammonium bicarbonate was added to rehydrate the gel pieces for 15 minutes thereafter excess trypsin solution was added to completely cover the fully rehydrated gel pieces. The digestion was done at 37°C incubation for overnight. The digestion reactions were stopped with 1% Trifluoroacetic acid. The digested protein samples were desalted using the ZipTips (Merck Millipore) using the manufacturer's protocol.

### **2.11.9 Protein separation, detection and identification**

The proteins were separated and protein spectra generated using the Nanoflow HPLC Electrospray Tandem Mass Spectrometry (nLC-ESI-MS/MS) by Dr. Stefan Weidt. Peptides were solubilized in 0.5% formic acid and separated on a nanoflow uHPLC system (Thermo RSLCnano) prior to online analysis involving ionisation by electrospray ionisation (ESI) and mass detection on an Amazon ion trap MS/MS mass spectrometer (Bruker Daltonics). The peptides were separated on a Pepmap C18 reversed phase column (LC Packings), using a 5 - 85% v/v acetonitrile, in 0.5% v/v formic acid gradient, run over 45 minutes with a flow rate of 0.2 µl/min. The continuous duty cycle of survey MS scan followed by up to ten MS/MS analyses of the most abundant peptides was used to perform mass spectrometric analysis, opting for the most intense multiply charged ions with dynamic exclusion for 120s.

Bruker Data Analysis Software and the automated Matrix Science Mascot Daemon server (v2.1.06) were used to process MS data. The Mascot search engine was used for protein identification assignment following interrogation of protein sequences in the NCBI Genbank database with an allowance mass tolerance of 0.4 Da for both MS and MS/MS analyses. Data was obtained from Glasgow polyomics as a Microsoft spread sheet with web links for the identified proteins.

## **2.12 Statistical Analysis**

Statistical analysis was done using GraphPad Prism 5, Microsoft Excel and IDEOM. Comparison of means was done using Unpaired Student's t-test and ANOVA. A P-value cut-off of 0.05 was used, with  $P < 0.05$  being considered significant.

## Chapter Three

### 3 Amphotericin B resistance in *Leishmania mexicana* promastigotes

#### 3.1 Introduction

Chemotherapy has remained the main control method for infections with *Leishmania* species, although there are many known challenges to this method. Amphotericin B has emerged as the drug of choice for visceral leishmaniasis, when used in its liposomal form. There have been concerns expressed over the preservation of the efficacy of Amphotericin B due to the ease with which resistance to the drug can be induced *in vitro*. Although resistance to amphotericin B in the field is rare in fungi, for which the drug was initially used and it is not known to exist in leishmaniasis (Olliario, 2010) there is a clear risk that resistance is possible. The introduction of a liposomal formulation has reduced toxic effects (Lemke *et al.*, 2005) making it the drug of choice in many regions. It is also convenient and effective to use as a single dose therapy (Mondal *et al.*, 2014). The single dose use of liposomal amphotericin B has been associated with reduced cost of treatment, ease of administration, increased safety due to the reduced side effects and an ability to be administered in rural remote areas (Mondal *et al.*, 2014; Sundar *et al.*, 2010). Further, even when compared to miltefosine which has a more convenient oral route of administration, liposomal amphotericin B single dose infusion (10 mg/kg of body weight) therapy can be used in children and women of child bearing age (Mondal *et al.*, 2014). The drug has also undergone tests to be used in combination therapy to combat the lethal form of leishmaniasis, visceral leishmaniasis, in India with promising results (Olliario, 2010). The drug may enter into mass use due to these favourable attributes. However, use of a drug singly and its mass use tends to predispose the drug to development of resistance by the parasites (Sinha and Bhattacharya, 2014). The situation may be exacerbated for Amphotericin B because the single dose use pushes the drug towards its maximum usable concentration. Amphotericin B no doubt holds an important place in the control of leishmaniasis. Therefore to safeguard its continued use, *Leishmania* parasites resistant to amphotericin B need to be characterised to learn about the mechanisms of resistance. This in turn can lead to development

of ways to assess resistance and also to inform on ways to use the drug that might minimise the risk of resistance.

We undertook to characterise *in vitro* amphotericin B resistance in *L. mexicana* promastigotes with the aim of highlighting the characteristics of the resistant parasites that can help to mitigate the effects of amphotericin B resistance should it arise in future. To achieve our aims we have utilised a complementary use of metabolomics and genomic DNA sequencing to identify characteristics that differentiate generated Amphotericin B resistant cells from wild-type cells.

## 3.2 Results

### 3.2.1 Selection for Amphotericin B resistant *L. mexicana*

Resistance to amphotericin B (AmB) was induced by stepwise increases in drug concentration over 18 passages stretching over six months. During this period, a 13-fold increase in the EC<sub>50</sub> value was recorded, indicating a significant difference ( $P = 0.0007$ ) in EC<sub>50</sub> value between the wild-type and a clone of highest level AmB resistance. While there was a gradual increase in AmB EC<sub>50</sub>, for the two intervening resistant clones closer to the wild-type, there was a jump in the EC<sub>50</sub> value to reach the highest level (Figure 3.1 and Figure 3.6). There was no significant difference ( $P = 0.9647$ ) in the EC<sub>50</sub> value for the clones growing in the presence of 0.027  $\mu\text{M}$  of AmB and the wild-type. However, there was a significant difference in AmB EC<sub>50</sub> values for the clones growing in the presence of 0.054  $\mu\text{M}$  ( $P = 0.0001$ ), 0.081  $\mu\text{M}$  ( $P < 0.0001$ ) and 0.27  $\mu\text{M}$  ( $P < 0.0001$ ) AmB as compared to that of the wild-type *L. mexicana*. There was a significant difference (ANOVA,  $P < 0.0001$ ) in the AmB EC<sub>50</sub> mean values between all of the clones. We did not observe appreciable differences in the growth phenotype between the resistant clones and the wild-type cells, although during the process of drug resistance induction, there were prolonged periods during which the cells needed to adapt to a given drug concentration before they could grow at similar rates as the wild-type cells before raising the drug concentration in growth medium.

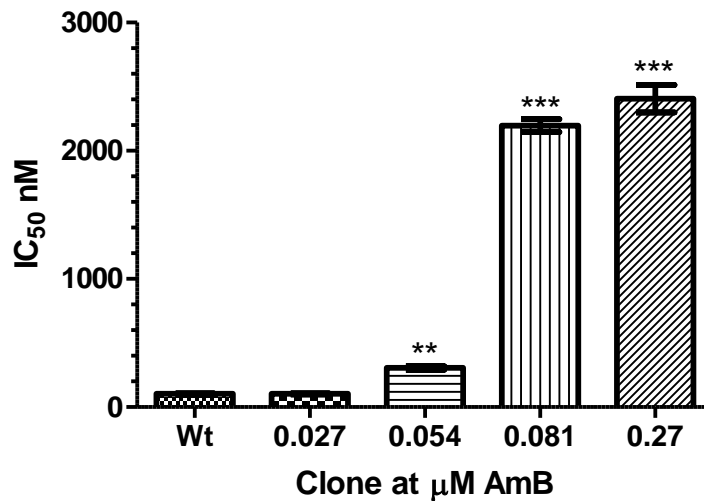
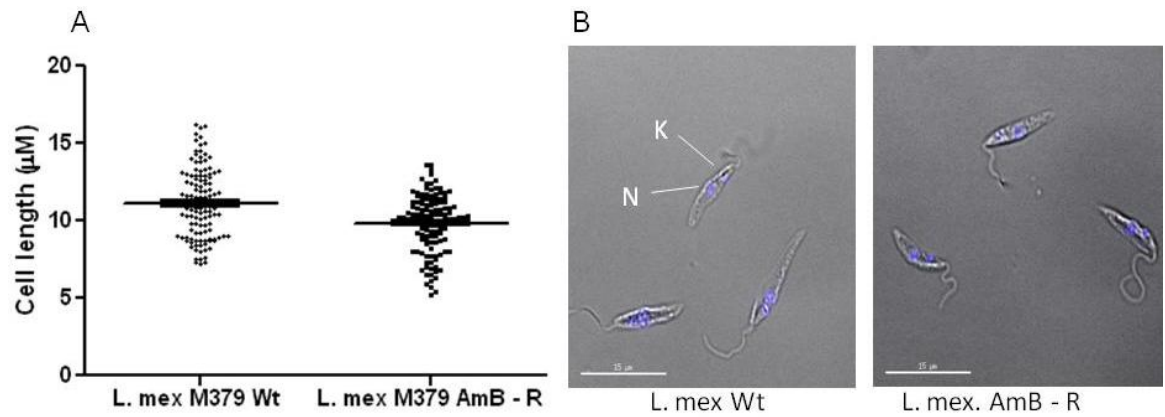


Figure 3.1 Comparison of AmB EC<sub>50</sub> values for various *L. mexicana* AmB resistant clones. The EC<sub>50</sub> values were determined using the modified alamar blue assay of 72 hours drug exposure of cells with the starting cell density of  $1 \times 10^6$  cells/ml and colour development over 48 hours of incubation following addition of 0.49 mM resazurin in PBS. Absorbance results were analysed in GraphPad Prism 5.0. (\*\* P = 0.0001, \*\*\* p < 0.0001). Results are presented as Mean  $\pm$  SEM for at least three independent experimental replicates.

### 3.2.2 Characterisation of the derived amphotericin B resistant *L. mexicana* promastigotes

#### 3.2.2.1 Comparison of cell body length of wild-type and AmB resistant clones

Differences in cell size were noticed between the wild-type and the derived AmB resistant cells when viewed under the light microscope. We investigated this by fixing the late log-phase cells with methanol at  $-20^\circ\text{C}$  and measured the cell body length of 126 individual cells for each of the two cell lines using the software SoftWoRX 5.5 on the delta-vision microscope. There was a significant difference (t-test; P < 0.0001) in cell body length between the wild-type and the AmB resistant clones exhibiting the highest resistance trait i.e., growing in the presence of  $0.27 \mu\text{M}$  AmB (Figure 3.2). The wild-type cells had an average cell body length of  $11.16 \pm 0.19 \mu\text{m}$  while that of the resistant clone was  $9.86 \pm 0.16 \mu\text{m}$ .



**Figure 3.2 Comparison of the cell body length of the wild-type and the AmB resistant cells. (A) Scatter dot plot of the comparison of the cell body length of *L. mexicana* wild-type and AmB resistant clone growing in the presence of 0.27 µM. (B) Cells were fixed in methanol at -20°C overnight and stained with 1 µg/ml DAPI/1%DABCO in PBS before applying to slides and viewing under the fluorescent microscope. The slides were observed under oil immersion. N = nucleus; K = kinetoplast; Bar = 15 µm.**

### 3.2.2.2 Stability of AmB resistance

To check the stability of the induced AmB resistance, the clones of highest resistance were grown in the absence of AmB for 15 passages. The resistant clone growing in the presence of 0.27 µM AmB exhibited no change in the AmB EC<sub>50</sub> value as determined by the modified alamar blue assay. A significant difference ( $P < 0.0001$ ) in AmB EC<sub>50</sub> between the wild-type and the resistant clone was maintained.

### 3.2.2.3 Amphotericin B cross-resistance to other drugs

The stability of the induced AmB resistance led us to investigate any possible AmB cross-resistance to other anti-leishmanial drugs. AmB cross-resistance to other drugs was assessed using the modified alamar blue assay and then comparing the EC<sub>50</sub> values between those of the wild-type and the resistant clone growing in the presence of 0.27 µM AmB. There was a significant difference in the determined EC<sub>50</sub> values between the wild-type and the AmB resistant clone for (R)-N-(1-(2, 4-dichlorophenyl)-2-(1H-imidazol-1-yl) ethyl)-4-(5-phenyl-1, 3, 4-oxadiazol-2-yl) benzamide (VNI), a compound that is specific for Sterol 14α-demethylase and shows potency against *T. cruzi* (Villalta *et al.*, 2013), ( $P = 0.0005$ ) and ketoconazole ( $P = 0.0007$ ) with fold-increase in the EC<sub>50</sub> values of 1.5 and 1.7, respectively (Figure 3.3). These compounds were tested subsequently to finding a role for Sterol 14α-demethylase mutation in resistance (see section 4.3.4) Cross-resistance to potassium antimony tartrate (PAT),

representing the trivalent active form of antimony drugs, and miltefosine involved fold change in  $EC_{50}$  values of 2.9 and 3.9 representing significant differences ( $P = 0.0005$  and  $P < 0.0001$ ) in  $EC_{50}$  values as compared to the wild-type, respectively.

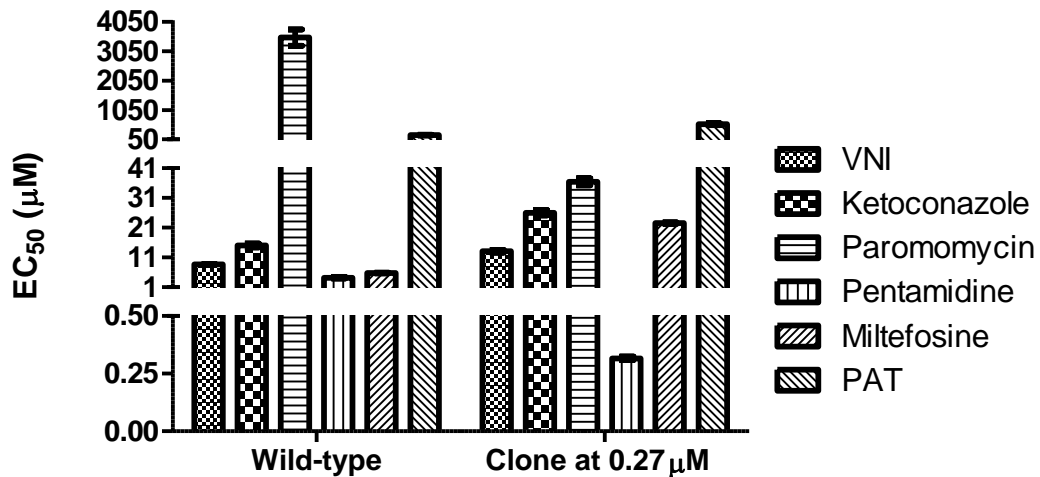


**Figure 3.3 Amphotericin B cross-resistance to other anti-leishmanial drugs.** AmB cross-resistance to other anti-leishmanial drugs in a derived AmB resistant clone growing in the presence of 0.27 µM AmB. Cross-resistance and susceptibility to other anti-leishmanial drugs was determined using the modified alamar blue assay and the  $EC_{50}$  values were computed using the Graph Pad Prism software. VNI = (R)-N-(1-(2, 4-dichlorophenyl)-2-(1H-imidazol-1-yl) ethyl)-4-(5-phenyl-1, 3, 4-oxadiazol-2-yl) benzamide; PAT = Potassium Antimony Tartrate. Results are for at least three independent experiments and plotted as Mean  $\pm$  SEM.

Interestingly, the AmB resistant cells were found to be very significantly more susceptible to paromomycin ( $P = 0.0002$ ) and pentamidine ( $P = 0.0001$ ) with fold-decreases in determined  $EC_{50}$  values of 96.5 and 13.3, respectively.

#### 3.2.2.4 [ $^3$ H]Pentamidine up-take by AmB resistant cells

The susceptibility of the resistant cells to pentamidine was further investigated by comparing the uptake of radiolabel pentamidine by the AmB resistant cells and the parental wild-type *L. mexicana* promastigotes. The AmB resistant clone showed significant ( $P < 0.0001$ ) increase in the uptake of pentamidine at a rate of  $0.258 \pm 0.031$  pmol/ $10^7$  cells/min than the wild-type cells which took up the drug at a rate of  $0.062 \pm 0.009$  pmol/ $10^7$  cells/min (Figure 3.4).

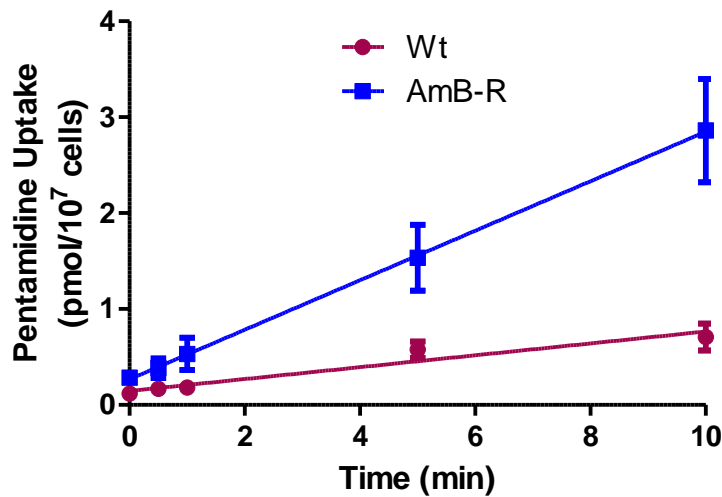
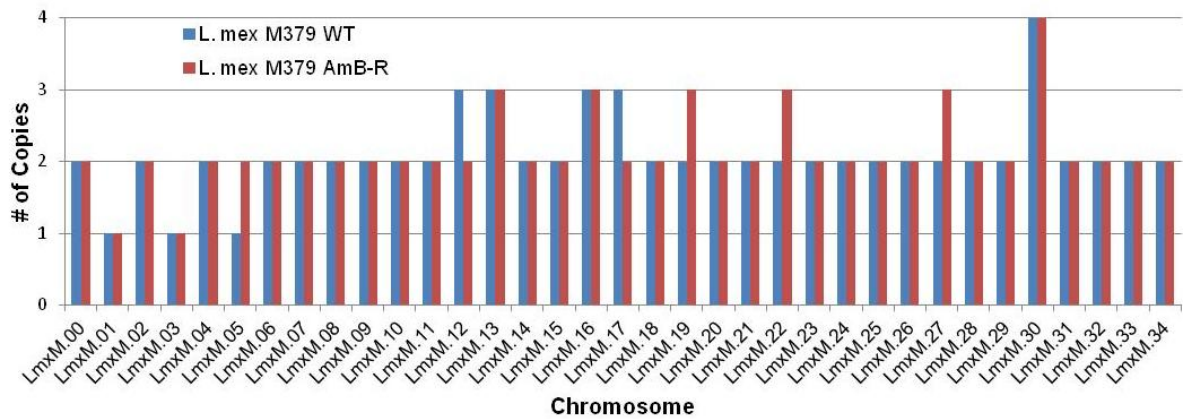


Figure 3.4 [<sup>3</sup>H]Pentamidine up-take in AmB resistant cells compared to the wild-type cells. The uptake was performed with  $1 \times 10^8$  cells/ml in triplicates for each time-point at 0 sec, 30 sec, 1 min, 5 min and 10 min for each experiment. The data was analysed using GraphPad Prism. The data is for four independent replicates. Results are presented as Mean  $\pm$  SEM.

### 3.3 Genomic DNA sequencing and comparison of Wt and AmB resistant *L. mexicana*

The gDNA of derived AmB resistant clone of highest resistance and the wild-type that were passaged in parallel during the induction of resistance was sequenced at University of Glasgow - Glasgow Polyomics. Data was analysed by Dr. Nicholas Dickens and Dr. Manikhandan Mudaliar. A total of 32,238,036 and 27,514,220 reads were obtained and of these 17,138,430 and 15,392,124 reads were aligned for the wild-type and the AmB resistant clone, respectively.

An alignment of the derived AmB resistant to the wild-type and both to reference *L. mexicana* MHOM/GT/2001/U1103 genome, revealed differences in chromosome numbers between the resistant clone and the wild-type cells (Figure 3.5). The AmB resistant cells had gained an extra chromosome for chromosome 05, 19, 22, and 27 and lost a chromosome for chromosome 12 and 17 as compared to the parental wild type cells. There were 22, 692 single nucleotide polymorphisms (SNPs) detected in the wild-type and 23, 641 SNPs in the AmB resistant cells' gDNA as compared to the reference *L. mexicana* MHOM/GT/2001/U1103 genome. Of these SNPs differences, 2, 049 and 2, 998 were found to be unique to the wild-type and the resistant cell line, respectively (Table 3.1). Because of the large numbers of SNPs, we used metabolomics analysis (as presented in section 3.5) to gain more insight into the two cell lines.



**Figure 3.5 Comparison of CNV of parental wild-type and the derived AmB resistant clone. Data was analysed and provided by Dr. Nicholas Dickens and Dr. Manikhandan Mudaliar.**

	Wild-type	AmB resistant
Total SNPs	22, 692	23, 641
Exonic SNPs	9, 530	9, 722
Coding changes	5, 313	5, 458
Unique SNPs	2, 049	2, 998

**Table 3.1 SNPs distribution in wild-type and AmB resistant with reference to U1103 genome. The NGS gDNA sequences of AmB resistant parasites and their parental wild-type passaged in parallel during AmB resistance selection were aligned to MHOM/GT/2001/U1103 reference genome. Data was analysed and provided by Dr. Nicholas Dickens and Dr. Manikhandan Mudaliar.**

### 3.3.1 Identification of genetic alterations in sterol biosynthetic pathway enzymes

Metabolomics revealed perturbations in the ergosterol biosynthetic pathway. *S. cerevisiae*'s 24 enzymes of the sterol biosynthetic pathway were used to identify 21 ortholog enzymes of *L. mexicana* (Table 3.2 and Appendix D) which were used for gDNA sequence analysis. As a result a total of 13 and 10 SNPs were detected in the coding sequences of AmB resistant cells and the wild-type, respectively, with regard to the ergosterol biosynthetic pathway enzymes (Table 3.2). Most of these SNPs were concluded to be SNP calling inconsistencies and only one of them represented a non-synonymous mutation in the AmB resistant cells (Appendix E). The SNP was located on gene ID LmxM.11.1100 positioned at 11.443299, involving a change from A to T within the coding sequence of lanosterol 14 $\alpha$ -demethylase replacing an asparagine residue with isoleucine at position 176 (N176I) of the primary structure of the enzyme. The mutation was found on both alleles of the gene and hence a homozygous mutation.

<i>S cerevisiae</i> Enzyme name	Enzyme gene ID Ortholog <i>L. mex</i>	Chromosome number	Ploidy	
			Wt	AmB-R
Thiolase protein-like (most likely trifunctional protein Beta subunit)	LmxM.30.1640	30	4	4
Hydroxy-3-methylglutaryl coenzyme a reductase	LmxM.29.3190	29	2	2
Mevalonate kinase	LmxM.30.0560	30	4	4
Phosphomevalonate kinase	LmxM.15.1460	15	2	2
Diphosphomevalonate decarboxylase	LmxM.18.0020	18	2	2
Isopentenyl-diphosphate delta-isomerase	LmxM.34.5330	34	2	2
<b>Farnesyl pyrophosphate synthase FPPS</b>	<b>LmxM.22.1360</b>	<b>22</b>	<b>2</b>	<b>3</b>
prenyltransferase, putative	LmxM.28.1320	28	2	2
Farnesyl diphosphate synthetase/solaneyl diphosphate synthase	LmxM.15.1020	15	2	2
Geranylgeranyl transferase type II beta subunit, putative	LmxM.33.4030	33	2	2
Squalene synthase/farnesyl transferase	LmxM.30.2940	30	4	4
Squalene monooxygenase	LmxM.13.1620	13	3	3
Lanosterol synthase	LmxM.06.0650	06	2	2
Sterol 14-alpha (lanosterol) demethylase (CYP51)	LmxM.11.1100	11	2	2
C-14 sterol reductase, putative	LmxM.31.2320	31	2	2
NAD(p)-dependent steroid dehydrogenase-like protein	LmxM.06.0350	06	2	2
Sterol 24-c-methyltransferase	LmxM.36.2380 / LmxM.36.2390	36	2	2
C8-sterol isomerase	LmxM.08_29.2140	29	2	2
Lathosterol oxidase-like protein   C5 sterol desaturase	LmxM.23.1300	23	2	2
C-22 sterol desaturase/cytochrome p450-like protein	LmxM.29.3550	29	2	2
C-24 sterol desaturase	LmxM.32.0680	32	2	2

**Table 3.2 Ploidy of chromosomes harbouring enzymes of the sterol biosynthetic pathway. *S. cerevisiae* sterol biosynthetic enzyme sequences were used to search for their *Leishmania mexicana* orthologs in TriTryp DB and used in gDNA sequence analysis. Comparison of the ploidy for involved chromosomes is made in the last two columns of the table labelled wild-type (Wt) and amphotericin B resistant (AmB-R) promastigotes of *L. mexicana*. Farnesyl pyrophosphate synthase (bold) is the only enzyme of the sterol biosynthetic pathway which was potentially affected by chromosome number change.**

### 3.3.2 Status of N176I mutation in AmB resistant clones of lower resistance

To ascertain the point at which the N176I mutation arose during the resistance induction, we sequenced lanosterol 14 $\alpha$ -demethylase for three intervening resistant clones between the wild-type and the resistant clone growing in the presence of 0.27  $\mu$ M AmB. Sequencing of the PCR products of at least 10 samples of clones growing in the presence of 0.027  $\mu$ M and 0.054  $\mu$ M inserted into the pGEMT easy vector revealed the absence of the N176I mutation. However, the resistant clone growing in the presence of 0.081  $\mu$ M showed the presence of the mutation (Figure 3.6) as in the clone of higher resistance which was sequenced by NGS.

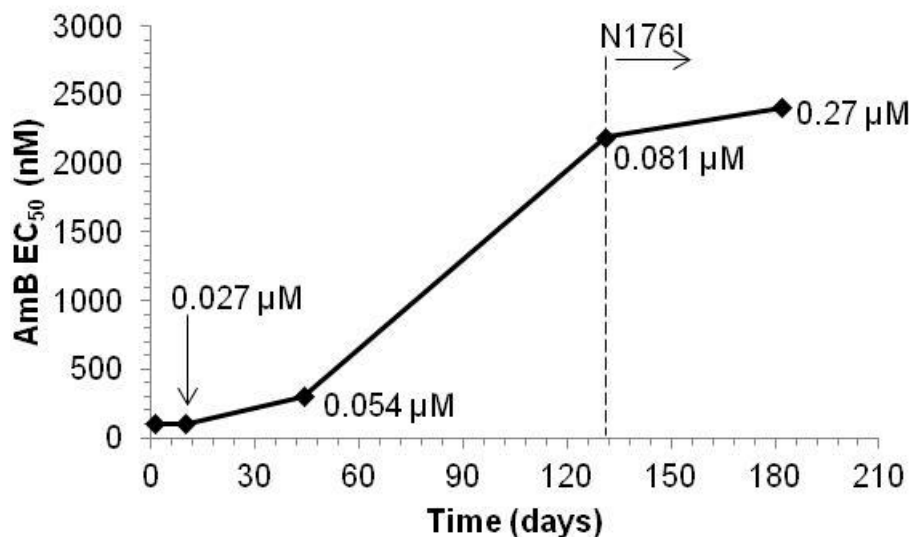


**Figure 3.6** Point of N176I occurrence in AmB resistant clones at different selection points. The occurrence of N176I mutation in various AmB resistant clones was determined by sequencing PCR amplified Sterol 14 $\alpha$ -demethylase of the clones growing in the presence of the shown AmB concentration in the graph. The point at which the mutation was detected is shown by the vertical dashed line starting from the clone growing in the presence of 0.081  $\mu$ M AmB. The EC<sub>50</sub> values plotted are an average of three replicates.

The other enzyme of the sterol biosynthetic pathway which might have been affected by AmB resistance induction was farnesyl diphosphate synthase. The enzyme is located on chromosome 22 with the gene ID LmxM.22.1360. The AmB resistant clone was found to have gained an extra chromosome 22 (Figure 3.5) when compared to the parental wild-type cells as a result an extra gene copy of farnesyl diphosphate synthase was thought to have arisen (Table 3.2).

Having noticed alterations in putrescine and trypanothione levels (section 4.5), we looked at the possibility of the enzymes linked to these metabolites being affected by CNV. A copy number for trypanothione reductase (Gene ID LmxM.05.0350) was found to increase from 2 to 3 due to the extra chromosome 05 gained by the resistant cells. However, ornithine decarboxylase (Gene ID LmxM.12.0280) was thought to have lost a gene copy due to loss of chromosome 12 (Figure 3.5) when compared to the wild-type at the end of resistance induction.

### **3.4 Proteomics analysis of the wild-type and AmB resistant cells**

Following the differences in chromosome number and metabolome (presented in section 3.5) between the wild type and the AmB resistant cells, we investigated possible differences in protein expression between the two cell lines. Proteomics analysis was hoped to provide explanations of the differences in metabolomic analysis and also confirm whether differences in protein expression could be attributed to genetic changes observed in gDNA NGS analysis. We used DiGE by labelling the wild-type and the resistant line with Cy3 and Cy5, respectively, to facilitate comparison of the protein spots from the two cell lines run on one gel using the DeCyder 2-D Differential In-gel Analysis (DIA) Software and generate a protein picking list. The selected protein spots for identification were manually cut from two preparative gels, one for each cell line, and subjected to nLC-ESI-MS/MS.

Protein ID	Gene Accession number	Mascot score	Nominal mass (Da)	Spot Fold increase	pI	Enzyme EC number	Chromosome number
Farnesyl diphosphate synthase	LmxM.22.1360	32	41, 460	2.36	5.42	2.5.1.10	22
Cis-prenyltransferase-like protein	LmxM.13.0020	25	44, 180	2.32	8.47	2.5.1.1	13
S-adenosylmethionine synthetase	LmxM.29.3500	38	34, 286	4.08	5.42	2.5.1.6	29

**Table 3.3 Proteins identified in proteomics as expressed differently by the wild-type and AmB resistant cells. Protein samples were extracted from the wild-type and AmB resistant cells and subjected to two-dimensional gel electrophoresis and Nanoflow HPLC Electropray Tandem Mass Spectrometry (nLC-ESI-MS/MS). MS data was analysed using Data Analysis Software (Bruker) and the automated Matrix Science Mascot Daemon server (v2.1.06). Protein identification was done by interrogation of protein sequences in the NCBI Genebank database**

Out of a total of 37 spots picked from the wild-type and the AmB resistant sample preparative electrophoretic plates that were processed for identification, three proteins (Table 3.3) with links to the sterol biosynthetic pathway were noted, although with low mascot scores. Most of the other identifications were hypothetical proteins (Appendices H and I), a Blast search of which in other organisms like yeast (*S. cerevisiae*) in NCBI yielded no orthologous proteins of known function. It is worth noting that among the identified proteins was farnesyl diphosphate synthase which was noted to be potentially affected by CNV of chromosome 22 in gDNA NGS data analysis. The proteomics data indicated an up-regulation of the protein in the derived AmB resistant cell line with a spot increase of 2.36 which is consistent with the additional copy of chromosome 22. Up-regulation of the enzyme has been indicated to be responsible for resistance to risendronate in *L. major* (Ortiz-Gomez *et al.*, 2006).

### **3.5 Metabolomic comparison of Wt and AmB resistant *L. mexicana***

The comparison of the derived AmB resistant cells to the parental wild-type *L. mexicana* promastigotes was extended to untargeted metabolomics to capture as many differences as possible in terms of metabolites. PCA analysis indicated a clear separation of the wild-type from AmB resistant cell samples (Figure 3.7). All medium related samples clustered together while the quality control (QCs) samples were grouped separately.

The clear separation of the two cell lines derived samples in PCA analysis indicated that there were differences between the two cell lines. To explore these differences, we looked for differences in the sterol biosynthetic pathway metabolites that have been reported (Al-Mohammed *et al.*, 2005; Mbongo *et al.*, 1998; Purkait *et al.*, 2012) in *Leishmania* AmB resistance studies with regard to alterations in the sterol biosynthetic pathway (Table 3.4). These studies used a targeted approach of GC/MS to identify altered sterols.

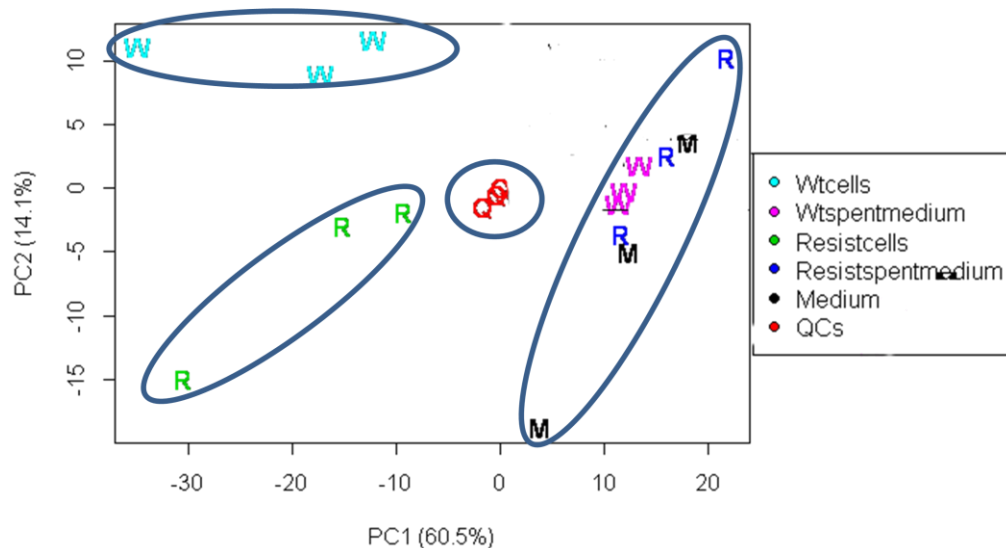


**Figure 3.7** PCA of the metabolomic comparison of Wild-type and AmB resistant cells. The first principal depicts the differentiation of samples using the main variable feature while the second component shows other variations among the samples. PCA analysis was done using IDEOM. The analysis was done using three independent experimental replicates.

The sterols detected in our study (Table 3.5 and Appendix J) were not those that have been reported by other studies (Table 3.4), except ergosterol. The difference could be due to the differences in the platforms used for the analysis of the sterols. We used untargeted metabolomics utilising LC/MS while all earlier studies used GC/MS targeted at sterol metabolite analysis. Our use of untargeted metabolomics was to capture other metabolite changes that could also result from AmB resistance(attached CD). Further, the metabolites were extracted from leishmania samples using different solvent systems to suit the separation and detection methods. Earlier studies reported detection of ergosterol in the wild-type cells and not in the amphotericin B resistant cells but we were able to detect ergosterol in the wild-type cells and diminished levels in amphotericin B resistant cells. This may have been due to difference in sample extraction and platforms of analysis as well as the level of resistance of the cells used in the studies.

Sterol	Monoisotopic mass	Formula	% of total sterol/Reference		Species/Reference
			Wt	AmB-R	
Ergosta-5, 7, 24 (28)-trien-3 $\beta$ -ol	396.34	C <sub>28</sub> H <sub>44</sub> O	85.1A; 32M; 34P	-	<i>L. mex</i> /A; <i>L. don</i> /M; P
Ergosta-7,24,(28)-dienol	398.35	C <sub>28</sub> H <sub>46</sub> O	4.2A	-	<i>L. mex</i> /A
Stigmasta-5,7,24(28)-trienol	410.36	C <sub>29</sub> H <sub>46</sub> O	10.6A	-	<i>L. mex</i> /A
4,14,Dimethyl-cholesta-8,24-dienol	414.40	C <sub>29</sub> H <sub>44</sub> O	-	62.4A; 5M	<i>L. mex</i> /A
4,14,Dimethyl-cholesta-7,24-dienol	414.40	C <sub>29</sub> H <sub>44</sub> O	-	6.5A	<i>L. mex</i> /A
Lanosta-8,24-dienol	426.72	C <sub>30</sub> H <sub>50</sub> O	-	31.1A	<i>L. mex</i> /A
Cholesta-5,7,24-trien-3 $\beta$ -ol	382.32	C <sub>27</sub> H <sub>42</sub> O	-	62P; 58M	<i>L. don</i> /M; P
14 $\alpha$ -Methylergosta-5,7,24(28)-trien- 3 $\beta$ -ol	393.31	C <sub>28</sub> H <sub>41</sub> O	8M	-	<i>L. don</i> /M
Ergosterol (Ergosta-5,7,22E-trien-3 $\beta$ -ol)	396.34	C <sub>28</sub> H <sub>44</sub> O	28P; 30M	-	<i>L. don</i> /M; P
Cholesterol	386.36	C <sub>27</sub> H <sub>46</sub> O	11P; 13M	24P; 27M	<i>L. don</i> /M; P

**Table 3.4** Reported altered sterol composition in amphotericin B resistant *Leishmania* species.

The shown sterol composition and alterations in wild-type and amphotericin B resistant (AMB-R) *L. mexicana* (*L. mex*) and *L. donovani* (*L. don*) promastigotes were determined by targeted GC/MS method. Monoisotopic masses and formulae were obtained from chemspider.com. The letters after the percentage values under % of total sterol/reference column and leishmania species/reference column represent the source of the data, thus A= Al Mohammed *et al.*, 2005; M = Mbongo *et al.*, 1998; P = Purkait *et al.*, 2012.

Mass (m/z)	RT (min)	Formula	Identified metabolite	Fold change
410.35	5.013	C <sub>29</sub> H <sub>46</sub> O	4,4-dimethylcholesta-8, 11,24-trien-3 $\beta$ -ol	111.53
426.35	4.939	C <sub>29</sub> H <sub>46</sub> O <sub>2</sub>	4 $\alpha$ -formyl-4 $\beta$ -methyl-5 $\alpha$ -cholesta-8-24-dien-3 $\beta$ -ol	20.93
396.34	5.026	C <sub>28</sub> H <sub>44</sub> O	Ergosta-5, 7, 22E-trien-3 $\beta$ -ol	0.84
394.32	4.983	C <sub>28</sub> H <sub>42</sub> O	Ergosta-5, 7, 22, 24(28)-tetraen-3 $\beta$ -ol	0.07

**Table 3.5 Sterol metabolites detected in *L. mexicana* AmB resistant and wild-type cells. The wild-type and AmB resistant samples were extracted using the methanol: chloroform: water mixture at 4°C. The sterol biosynthetic pathway metabolites were identified following LC/MS and IDEOM analysis. The fold change is the ratio of the detected sterol metabolite between the wild-type as the control and the derived amphotericin B resistant cells. Rt = Retention time; m/z = mass to charge ratio.**

The accumulation of 4, 4-dimethyl-cholesta 8, 11, 24-trienol in AmB resistant cells was accompanied by depleted relative abundance levels of ergosta-5, 7, 22, 24(28)-tetraen-3 $\beta$ -ol (Table 3.5). Ergosta-5, 7, 22, 24(28)-tetraen-3 $\beta$ -ol a sterol biosynthetic pathway intermediate which occurs in traces in *Leishmania* and is derived from ergosta-5, 7, 24 (28)-trienol the reportedly major sterol of *L. mexicana*, *L. tropica*, and *L. donovani* (Goard *et al.*, 1984). The minor sterol of *Leishmania*, ergosta-5, 7, 22E-trien-3 $\beta$ -ol or ergosterol (Roberts *et al.*, 2003) showed reduced levels in the resistant cells (Table 3.5). Use of the volcano plot (Figure 3.8) revealed 4, 4-dimethyl-cholesta 8, 11, 24-trienol an isomer of 4, 4-dimethyl-cholesta 8, 14, 24-trienol as the metabolite that significantly changed with high intensity ratio. 4, 4-dimethyl-cholesta 8, 14, 24-trienol is a product of lanosterol 14 $\alpha$ -demethylase (Figure 1.8), an enzyme that was found to have a non-synonymous mutation in NGS analysis. 4, 4-dimethyl-cholesta 8, 14, 24-trienol was identified based on IDEOM identification of the metabolite through use of the retention time and the m/z ratio (Attached CD). It is interesting to note that 4, 4-dimethyl-cholesta 8, 14, 24-trienol has been reported in yeast treated with ketoconazole (Baloch *et al.*, 1984) and it is listed in the predicted *Leishmania* sterol biosynthetic pathway in the Biocyc.org website (Figure 1.8).

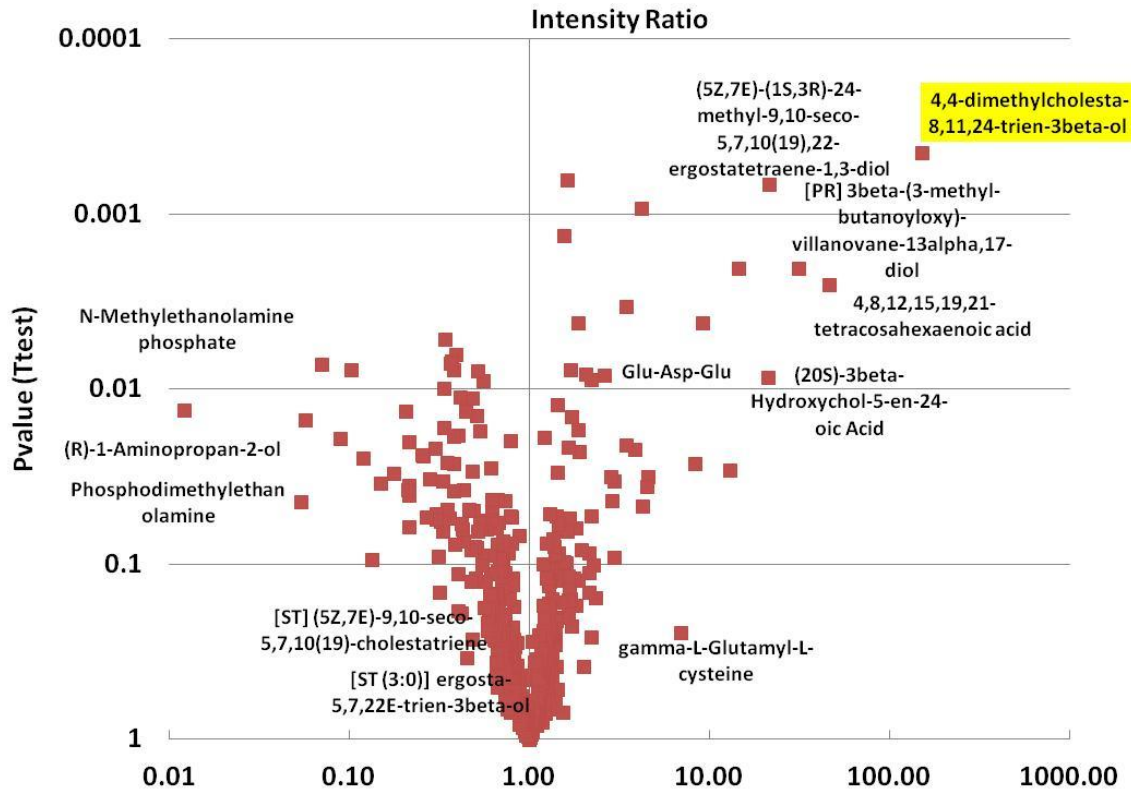


**Figure 3.8** Volcano plot of the identified metabolites in metabolomics analysis. Identification of the significantly changing metabolites identified from the comparison of the AmB resistant cells and the parental cells. 4, 4-dimethyl-cholesta 8, 14, 24-trienol a product of lanosterol 14 $\alpha$ -demethylase highlighted in yellow, was identified to be significantly changing. The volcano plot was generated in IDEOM. The analysis was done using three independent experimental replicates. Graphs were plotted using Mean  $\pm$  SD.

### 3.5.1 Alterations in the polyamine and thiol metabolic pathways

We also noted alterations in the precursors and metabolites of the polyamine pathway (Figure 3.9 and Table 3.6) that were detected during the metabolomic comparison of the parental wild-type and the derived AmB resistant cell lines. The polyamine pathway provides the parasites with molecules that protect them against oxidative stress because spermidine links with two molecules of glutathione creating trypanothione (Fairlamb *et al.*, 1985). The polyamines also play key roles in cell proliferation and are involved in binding to various cellular anions including DNA, RNA and membrane phospholipids (Bacchi, 1981).

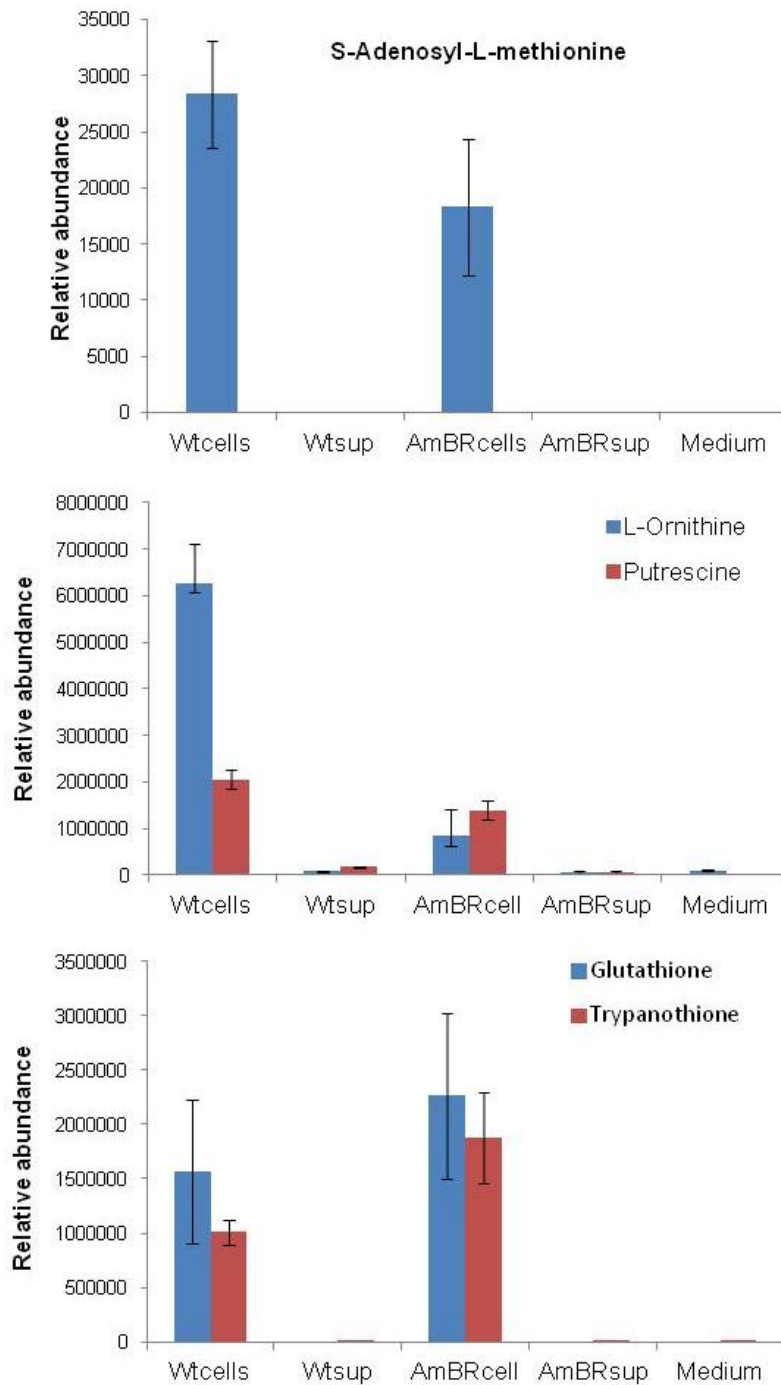


**Figure 3.9 Comparison of polyamine and thiol metabolites in Wt and AmB resistant cells. The wild-type (Wt) and amphotericin B (AmB) resistant samples were extracted using chloroform; methanol; water at 4°C. The extracted samples were analysed using LC/MS and IDEOM. The analysis was done using three independent experimental replicates. Wtcells = samples derived from cells; Wtsup = medium in which wild-type cells were grown; AmBRcell = metabolites extracted from AmB resistant cell samples; AmBRsup = medium in which the cells were grown; Medium = fresh growth medium. Graphs were plotted using Mean  $\pm$  SD.**

Metabolite	Fold-difference	P value
S-Adenosyl-L-methionine	0.65	0.09007
L-ornithine	0.14	0.11771
Putrescine	0.68	0.015073
Glutathione	1.44	0.584761
Trypanothione	1.87	0.271301

**Table 3.6 Polyamine precursor/substrates and thiols abundance in Wt and AmB-R cells. Relative abundance of polyamines substrates and thiols were compared using IDEOM following analysis of samples extracted using the chloroform:methanol:water protocol by LC/MS.**

The relative abundances of trypanothione and glutathione were elevated with fold differences of 1.87 and 1.44 in the resistant cells although this was not statistically significant ( $P = 0.271301$  and  $P = 0.584761$ , respectively) (Figure 3.9 and Table 3.6). Ornithine, putrescine and S-adenosyl-L-methionine showed depleted levels. Although there were differences in the levels of the polyamine precursors and metabolites detected between the two cell lines only the change in putrescine levels was statistically significant (Table 3.6). The difference in the polyamine precursors, polyamine and thiols could be part of the attainment of AmB resistance by the cells as AmB has been shown to induce accumulation of ROS that cause oxidative stress in *L. infantum* (Moreira *et al.*, 2011).

### 3.5.1.1 Comparison of response to oxidative stress

Because of the possible difference in oxidative stress response, we exposed the wild-type and AmB resistant cells ( $2 \times 10^6$  cells/ml) to varying concentrations (20  $\mu\text{M}$ , 200  $\mu\text{M}$ , 500  $\mu\text{M}$  and 1 mM) (Das *et al.*, 2001) of  $\text{H}_2\text{O}_2$  in growth medium in 6-well plates to compare the response by the two cell lines through observation under a light microscope at different time points for 72 hours. Generally, both cell lines were unaffected by 20  $\mu\text{M}$   $\text{H}_2\text{O}_2$ . The resistant cells were more affected by  $\text{H}_2\text{O}_2$  than the wild-type cells at concentrations of  $\text{H}_2\text{O}_2$  starting from 200  $\mu\text{M}$ . The resistant cells looked swelled and rounded in shape and were settling to the bottom of the plate within 90 minutes, while the wild-type maintained their shape and looked like the wild-type control cells grown in  $\text{H}_2\text{O}_2$  free medium. After 4 hours of incubation a few wild-type cells seemed affected by settling to the bottom of the plate with reduced movement while resistant cells continued

to swell and settle at the bottom of the plate. However, both cell lines did recover after 24 hours of incubation.

Exposure of the two cell line to 500  $\mu\text{M}$  and 1 mM  $\text{H}_2\text{O}_2$ , had no apparent immediate effect on the cells. However swelled and round-shaped cells at both concentrations of  $\text{H}_2\text{O}_2$  were observed after 5 minutes of incubation. The cells exhibited sluggish to no movement with the effect being pronounced in the AmB resistant cells in the presence of 500  $\mu\text{M}$   $\text{H}_2\text{O}_2$  in growth medium after 30 minutes. While the cells in 1 mM  $\text{H}_2\text{O}_2$  showed no movement after 30 minutes, leading to cell clumping after 90 minutes, although the cells were of normal shape. These effects were observed up to 24 hours of exposure after which cells were noticed to have started to recover in growth medium containing 500  $\mu\text{M}$   $\text{H}_2\text{O}_2$ . The cells in growth medium containing 1 mM  $\text{H}_2\text{O}_2$  died within 24 hours. After 72 hrs, more of the wild type cells than the AmB resistant cells had recovered in growth medium containing 500  $\mu\text{M}$   $\text{H}_2\text{O}_2$  to about  $9 \times 10^6$  cells/ml and  $4 \times 10^6$  cell/ml, respectively.

We also used methylene blue to further explore the susceptibility of the AmB resistant cells to oxidative stress. Methylene blue is known to induce oxidative stress by depleting the levels of  $\text{NADPH} + \text{H}^+$  resulting in the activation of the pentose phosphate pathway to provide fresh  $\text{NADPH} + \text{H}^+$  for anti-oxidant use and hence has been used to observe or test both phenomena (Maugeri *et al.*, 2003). The AmB resistant cells were found to be significantly ( $P < 0.0001$ ) more susceptible to methylene blue than the wild-type cells ( $\text{EC}_{50}$  values:  $0.117 \pm 0.001$   $\mu\text{M}$  and  $4.20 \pm 0.22$   $\mu\text{M}$ , respectively).

### **3.5.1.2 Use of NAC to alleviate oxidative stress**

The observation that the AmB resistant cells seemed to be affected more by oxidative stress than the wild-type led us to carrying out susceptibility assays through the modified alamar blue assay in the presence of an antioxidant N-Acetyl-L-cysteine (NAC). Twenty millimolar NAC has been used to scavenge for reactive oxygen species that cause oxidative stress in *Leishmania*, as well as serving as a precursor to glutathione synthesis (Verma *et al.*, 2011). We first

Drug	Wt			AmB-R		
	- NAC	+ NAC	Fold Change	- NAC	+ NAC	Fold Change
AmB	0.071 ± 0.0007	0.033 ± 0.0011	0.47	1.311 ± 0.17	0.43 ± 0.0149	0.33
PAT	197.6 ± 11.79	448.6 ± 8.59	2.27	564.6 ± 32.65	282.8 ± 3.45	0.50
Miltefosine	5.824 ± 0.11	5.362 ± 0.41	0.92	22.58 ± 0.20	12.88 ± 0.49	0.57
Pentamidine	4.19 ± 0.27	2.99 ± 0.05	0.71	0.316 ± 0.0077	0.307 ± 0.0017	0.97
Paromomycin	3019 ± 773.40	1255 ± 180.4	0.42	36.68 ± 1.05	79.60 ± 1.89	2.17
M. blue	4.20 ± 0.22	0.658 ± 0.040	0.16	0.1173 ± 0.001	0.0557 ± 0.006	0.47

**Table 3.7 Comparison of EC<sub>50</sub> values of anti-leishmanial drugs in the presence and absence of N-acetyl-cysteine.**

The EC<sub>50</sub> values were determined both in the presence and absence of 200 µM NAC by the modified alamar blue assay and analysed using Prism GraphPad. The analysis was done using three independent replicates. The wild-type were less sensitive to PAT while the AmB resistant cells were less sensitive to Paromomycin in the presence of NAC. EC<sub>50</sub> values expressed as Mean ± SEM, NAC = N- acetyl-L-cysteine; PAT = Potassium Antiomny Tartrate; M. Blue = Methylene blue; Wt = wild-type cells; AmB-R = Amphotericin B resistant cells; Fold change = AmB-R EC<sub>50</sub>/ Wt EC<sub>50</sub>. All values are in µM.

determined the toxicity of NAC on both the wild-type and the AmB resistant cell lines. There was a significant difference ( $P = 0.03$ ) in NAC  $EC_{50}$  values of  $44.5 \pm 10.1$  mM and  $12.1 \pm 1.1$  mM for the wild-type and the resistant cells, respectively. We therefore used 200  $\mu$ M as the concentration that would not kill both cell lines. The AmB resistant cells were less sensitive to paromomycin in the presence of 200  $\mu$ M NAC with a fold-change in  $EC_{50}$  value of 2.17. There was no change in the  $EC_{50}$  value for pentamidine but the AmB resistant cells showed increased susceptibility to the rest of the drugs tested (Table 3.7). The wild-type cells were protected from PAT with a fold-increase in  $EC_{50}$  value of 2.27. NAC had no effect on the  $EC_{50}$  value for miltefosine in the wild-type cells. Interesting NAC was found to sensitive both the wild-type and the AmB resistant cells to methylene blue with fold-changes in  $EC_{50}$  values of 0.16 and 0.47, respectively.

### 3.5.2 Ergosterol supplementation in growth medium

Bloodstream forms of *T brucei* are known to take up host cholesterol for their use (Green *et al.*, 2003). *In vitro* ergosterol supplementation of *L. donovani* with a single knock-out of lanosterol 14 $\alpha$ -demethylase gene were reported to have had their growth enhanced than those without ergosterol supplementation (Verma *et al.*, 2011). The reduced abundance of ergosterol in the AmB resistant cells as compared to the wild-type therefore led us to assess whether exogenous supply of ergosterol to the resistant cells would restore their susceptibility to AmB. This was investigated by supplementation of growth medium with 7.6  $\mu$ M ergosterol (Verma *et al.*, 2011) for more than five passages of AmB resistant cells and the wild-type. The susceptibility assays were performed both in the presence and absence of ergosterol in growth medium. We also assessed the susceptibility of both cell lines to pentamidine, to which the AmB resistant cell lines, as stated earlier, were found to be significantly sensitive.

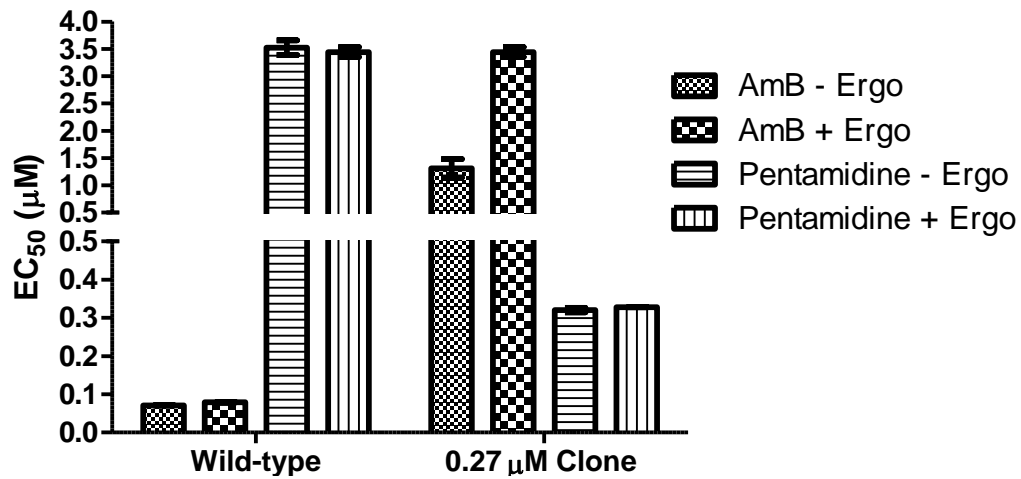


**Figure 3.10 Susceptibility to AmB and pentamidine in the presence of exogenous ergosterol**  
 The wild-type and the AmB resistant were grown in the presence of 7.6 µM ergosterol in the growth medium for five passages before the modified alamar blue assay was done both in the presence and absence of 7.6 µM ergosterol. The data was analysed in Graph Pad Prism software. A significant ( $P = 0.0004$ ) increase in AmB EC<sub>50</sub> value for the AmB resistant cells was observed while there was no change in AmB and pentamidine EC<sub>50</sub> values for the wild-type cells and pentamidine for AmB resistant cells. The results are for three independent experimental replicates. Ergo = ergosterol.

The EC<sub>50</sub> values for AmB for the wild-type cells changed from  $0.072 \pm 0.0008 \mu\text{M}$  in the absence of ergosterol supplementation to  $0.079 \pm 0.0009 \mu\text{M}$  in the presence of ergosterol supplementation representing a fold-change of 1.11 (Figure 3.10). This modest change in EC<sub>50</sub> value for AmB was found to be statistically significant ( $P = 0.0023$ ). However, there was a significant ( $P = 0.0004$ ) increase in EC<sub>50</sub> values for AmB with a fold-change of 2.84 for the AmB resistant cells (Figure 3.10). This result suggested a possible binding of the AmB to the ergosterol supplemented in the medium. This being the case, the resistant cell line having less ergosterol compared to the wild-type had a pronounced increase (nearly threefold) in AmB EC<sub>50</sub> value. Since the wild-type cells express more ergosterol (which would render them more susceptible to AmB), than the resistant cells, exogenous ergosterol would be expected to have little effect on their AmB EC<sub>50</sub> value at the concentration of exogenous ergosterol concentration used in the experiment. The sensitivity of the resistant cells to pentamidine after supplementation of growth medium with exogenous ergosterol remained unchanged.

The lack of reduction in AmB EC<sub>50</sub> value for the resistant cells suggests a lack of taking up exogenous ergosterol by these cells. This is further confirmed by lack of change in AmB EC<sub>50</sub> value for pentamidine for the resistant cell line.

### 3.5.3 *In vitro* transformation and infectivity of AmB resistant *L. mexicana* promastigotes

AmB resistant *L. mexicana* promastigotes have been shown to transform into amastigotes and were able to infect mice and the cells were found to maintain their resistance trait (Al-Mohammed *et al.*, 2005). Therefore we determined whether AmB resistance in the presence of an N176I mutated lanosterol 14 $\alpha$ -demethylase had the capacity to transform into axenic amastigotes, the clinically relevant life cycle form in leishmaniasis. Our AmB resistant cells were able to transform axenically into amastigotes. However, the transformed resistant cells were not able to grow beyond a second passage while the wild-type could not grow beyond a third passage. It was also noticed that the transformed AmB resistant amastigotes grew slower than the wild-type with the wild-type cells growing to a three-, four-fold higher density than the AmB resistant cells over a period of one week (Figure 3.11A). The failure to continuously cultivate these cells in culture was attributed to the fact that the ability of *Leishmania* to transform from promastigotes to amastigotes diminishes with the number of previous passages (Pimenta and Desouza, 1987). We used cells that have been continuously passaged and were not passaged *in vivo*, prior to start of resistance selection. We observed an increase in the number of passages for the transformed wild-type cells with different batches of serum in growth medium. Infection of macrophages, a natural environment for amastigotes, with AmB resistant promastigotes for three hours and incubation for three days was achieved. Andrew Pountain (M.Res. Student I supervised for his M.Res. project) showed that AmB resistant promastigotes were able to infect the murine RAW 246.7 macrophages in 72 hours incubation. Both cell lines showed low infectivity rates with that by wild-type promastigotes being the lowest (Figure 3.11B and C). However, the AmB resistant cells with an N176I mutated lanosterol 14 $\alpha$ -demethylase were able to infect and survive within macrophages, their habitat in natural infections.

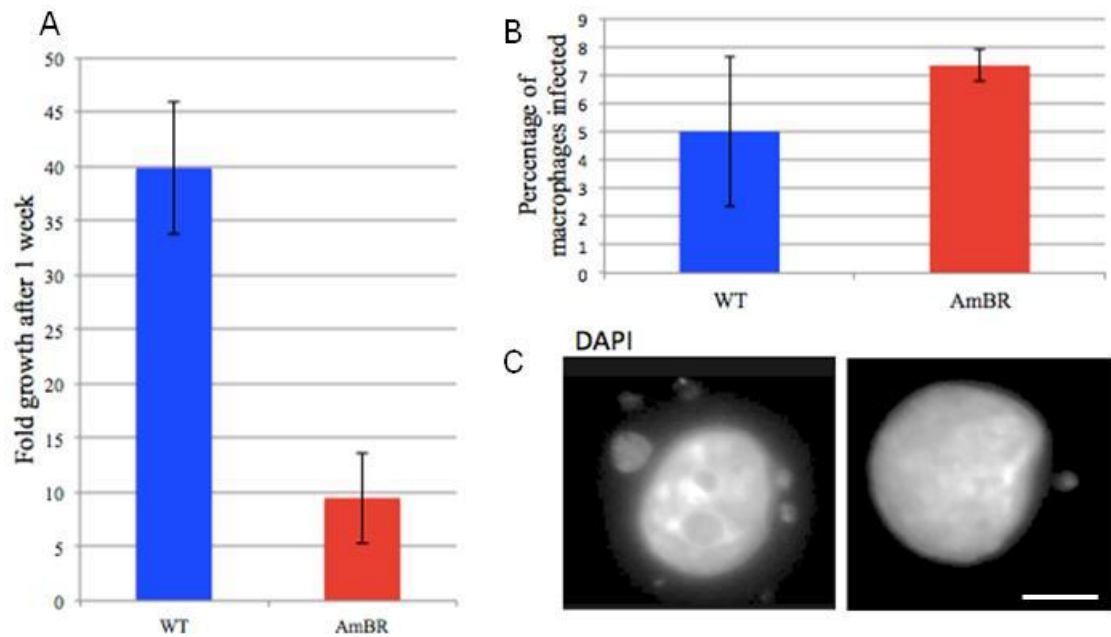


**Figure 3.11** Comparison of transformation into amastigotes and infectivity between Wt and AmB resistant *L. mexicana* promastigotes.

(A) Transformation of promastigotes into amastigote was done in complete Schneider's Drosophila medium for one week prior to counting transformed cells. (B) Percentage of macrophages infected. The percentage of macrophages infected was counted 72 hours post infection, by counting 100 macrophages in three separate wells for each cell line. (C) DAPI staining of macrophages infected with AmB resistant parasites. DAPI staining was done with 0.5  $\mu\text{g/ml}$  DAPI/1% DABCO in PBS. Large stained nuclei are those of the macrophage and smaller stained nuclei are those of infecting AmB resistant parasites. Graphs were constructed using Mean  $\pm$  SD between wells within a single experiment. Results are for three independent replicates. Bar = 10  $\mu\text{m}$ . (Data generated by Andrew Pountain)

### 3.5.4 Filipin III staining

Having established that there were differences in the ergosterol levels between the wild-type and the AmB resistant cell lines in metabolomics analysis, we aimed at finding a simple test that could be used to distinguish the two cell lines. It was hoped the test could be adopted for field use as a marker for AmB resistance. For this purpose filipin III was used to determine staining differences between the wild-type and the AmB resistant cells. Filipin is known to specifically bind to sterols in the plasma membrane of yeast cells (Van Leeuwen *et al.*, 2008). An increasing fluorescent signal (Figure 3.12) with increasing time of exposure of the cells to 1  $\mu\text{M}$  filipin was observed in the wild type cells and not the AmB resistant cells of *L. mexicana* promastigotes. The observed fluorescent signal with the wild-type cells started at about 30 minutes and became more intense after 3 hours of cell exposure to filipin. Wild-type cells were observed to assume a round shape after about 90 minutes of exposure to filipin III and the number of deformed cells increased with time of incubation.

Unfortunately, Photo-bleaching of the stain was observed within five seconds of exposure to UV light. The photo-bleaching was observed for all samples that were taken out at various time points to be viewed under UV illumination during the four hours of incubation of cells in the stain.

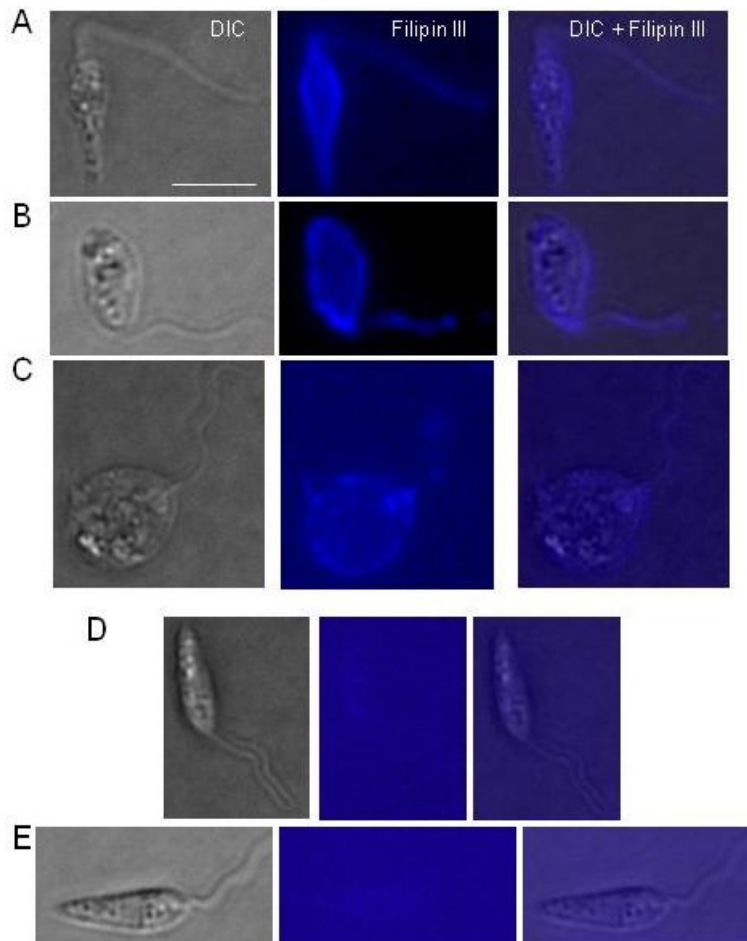


**Figure 3.12** Differential filipin III staining of the wild-type and AmB resistant cells. Live cells were stained with 1  $\mu\text{M}$  filipin III in growth medium and immobilised in 1% low gelling temperature agarose before observation under UV on a ZEISS Axioplan 2 Imaging fluorescent microscope under oil immersion. A, B and C represent images for the wild-type cells observed after 30 min, 1 hr and 3 hrs, respectively, of incubation in filipin, while D and E are for the AmB resistant cells with no fluorescent signal. B and C show the deformation of the cell shape observed after the stated time of exposure to filipin III. Bar = 10  $\mu\text{m}$ .

#### 3.5.4.1 Filipin staining of transformed infecting amastigotes

Having managed to successfully differentiate the wild-type cells from the AmB resistant cells using filipin III due to differences in sterol contents and following transformation of the AmB resistant promastigotes into amastigotes and subsequent infection of macrophages, we set out to determine whether filipin staining could be used to distinguish wild-type and AmB resistant amastigotes within macrophages. This assay was carried out as use of amastigotes within

macrophages was more clinically relevant because this would then indicate whether fluorescent microscopy could be adopted for field use in identifying AmB resistant parasites. Andrew Pountain infected murine RAW 246.7 macrophages with the two cell lines and stained them with filipin. No stained amastigotes were observed in the macrophages (Figure 3.13).

This could have been due to background staining by the macrophages. Even individual amastigotes within the vicinity of macrophages could not be seen to be stained when exposed to UV light (Figure 3.13 B and D). The macrophages have been shown to stain with filipin due to presence of cholesterol (Leventhal *et al.*, 2001). The background staining of macrophages coupled with low infectivity alluded to in section 3.5.3 and photo-bleaching of filipin upon exposure to UV light may have led to lack of observation of amastigotes in the macrophages.

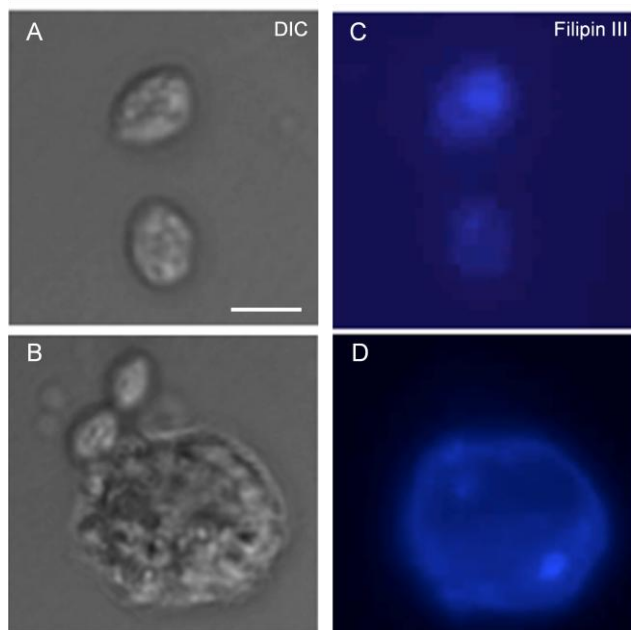


**Figure 3.13** Fillin staining of macrophages infected with Wt and AmB resistant *L. mexicana*. Live infected cells were stained with 1  $\mu\text{M}$  filipin III and observation under UV on a ZEISS Axioplan 2 Imaging fluorescent microscope under oil immersion. Individual amastigotes are seen in A and C while B and D show amastigote within the vicinity of the macrophages. B and D illustrate the overshadowing of filipin staining of amastigotes by the macrophages. Bar  $\approx$  10  $\mu\text{M}$ . (Data generated by Andrew Pountain).

We conclude, therefore, that in spite of selective binding of filipin to wild-type over AMB resistant cells, a test based on this reagent would be too difficult to

adapt to field use. However, other tests e.g. spectroscopic methods that detect ergosterol (Naewbanij *et al.*, 1984; Sokol-Anderson *et al.*, 1988) might be used.

### 3.6 Discussion

The reduction in the cost of the liposomal amphotericin B for monotherapy and possibly combination therapy use (Olliaro *et al.* 2009) could go a long way in alleviating the problems associated with leishmaniasis treatment. However, the drug should be used judiciously, to avoid development of resistance. We have studied the characteristics of *in vitro* AmB resistant *L. mexicana* promastigotes to bring to light characteristics that may assist in monitoring for and countering resistance development.

#### 3.6.1 Stability of AmB resistance

The 23 fold-increase in AmB EC<sub>50</sub> for the derived AmB resistant cell line is comparable to the 16 fold increase reported by Al Mohammed *et al.* (2005) although our resistant lines were able to grow at a much lower concentration of AmB in the growth medium. It is worth noting that the EC<sub>50</sub> values for AmB of  $0.103 \pm 0.004 \mu\text{M}$  for our wild-type and  $2.407 \pm 0.11 \mu\text{M}$  for the AmB resistant lines are also comparable to  $0.10 \pm 0.01 \mu\text{M}$  and  $1.89 \pm 0.12 \mu\text{M}$  reported for the wild-type and AmB resistant *L. donovani* promastigotes, respectively (Mbongo *et al.*, 1998). *In vitro* resistance to AmB, as a single drug and in combination with other anti-leishmanial drugs, is stable once acquired (Al-Mohammed *et al.*, 2005; Garcia-Hernandez *et al.*, 2012; Mbongo *et al.*, 1998). Our resistant cell lines had also acquired a stable resistance trait to AmB as they were able to grow in drug free medium for 15 passages without any change in the drug's EC<sub>50</sub> value. Our AmB resistant clones had not only acquired a stable resistance trait but were also able to infect macrophages in line with the result by Al Mohammed and co-workers (Al-Mohammed *et al.*, 2005). However, our inability to continuously propagate both the wild-type and AmB resistant amastigotes axenically and low infectivity rates achieved could be due to the increased number of passages they have been through as this has been reported to compromise the transformation and infectivity ability of these parasites (Pimenta and Desouza, 1987). It may, therefore, not be the altered sterol composition or the genetic changes in the AmB resistant cells that were responsible for lack of continuous cultivation of

transformed amastigotes of the resistant lines, as AmB resistant promastigotes were reported to be infective to mice and were transformed back into promastigotes again though with altered morphologies (Al-Mohammed *et al.*, 2005).

### **3.6.2 AmB resistant *L. mexicana* cross-resistance to other antileishmanial drugs**

The stability of AmB resistance may pose a serious threat to management of leishmaniasis especially where the disease is anthroponotic as the resistant parasites can spread into the population. The spread of such parasites could be catastrophic as there is a possibility of cross-resistance to other anti-leishmanial drugs. Our AmB resistant cell lines show cross-resistance to trivalent antimony (PAT), the active form of antimony drugs, and miltefosine with fold-increases in  $EC_{50}$  values of 2.9 and 3.9, respectively (Table 3.8). Further, *in vitro* resistance to combinations of AmB and miltefosine, AmB and paromomycin, and AmB and antimony have been reported. These drug combination resistant parasites were also found to be cross-resistant to paromomycin and antimony (Garcia-Hernandez *et al.*, 2012). Therefore, single-dose liposomal AmB and miltefosine combination use (Sinha and Bhattacharya, 2014) should be carefully considered as our study shows a significant AmB cross-resistance to miltefosine. Moreover, use of amphotericin B as a single dose seems to be pushing the drug towards the highest concentration that can be tolerated by the host and thus exposing the parasites to higher drug concentrations. In a study on the safety and use of single dose of amphotericin B, the few participants that failed the single dose therapy were rescued by treatment with 3 mg/kg body weight over 5 days (Sundar *et al.*, 2010). This practise needs to be revisited as the same parasites that were exposed to a higher drug concentration were later exposed to reduced concentrations of the drug over a period of 5 days. A full understanding of the drug's pharmacokinetics and pharmacodynamics, with different *Leishmania* strains is needed to fully assess this risk. Although a high cure rate was recorded, even with the few that failed treatment should parasites infecting them become resistant the possibility of their spreading into the general population are quite high because of the anthroponotic nature of the disease in this part of the world. We are concerned that the WHO policy of single dose liposomal AmB maybe ill-advised and linking it to subsequent higher dose

treatment a potential disaster. A case in point was the continued use of increasing doses of antimonials for treatment of leishmaniasis which never prevented the emergent of antimony resistant parasites in India (Sundar *et al.*, 2000). In fact the strategy might well contribute to the problem.

Our resistant cells showed significantly increased sensitivity to paromomycin and pentamidine. A similar situation was shown in *L. donovani* promastigotes (Mbongo *et al.*, 1998) though with less sensitivity compared to our AmB resistant cells (Table 3.8). We found that the AmB resistant cells were able to accumulate more pentamidine than the wild-type cells, rendering them more susceptible to the drug. This is in contrast to pentamidine resistant *L. mexicana* that accumulate less pentamidine in the mitochondrion (Basselin *et al.*, 2002).

Pentamidine accumulates in the mitochondrion where it is able to induce ROS production in *Leishmania* (Basselin *et al.*, 2002; Moreira *et al.*, 2011). Indeed, pentamidine's action against *L. donovani* promastigotes was suggested to be potentiated by the ROS generated by the inhibition of complex II of the electron transport chain (Mehta and Shaha, 2004). Further, pentamidine was reported to interact with the kinetoplast by binding to the A-T rich regions of the minicircles whose sequences were altered in pentamidine resistant *L. donovani* and *L. amazonensis* although the significance of this kDNA alteration is not known. Amphotericin B and paromomycin resistant *Leishmania* do not have alterations to their kDNA sequences (Basselin *et al.*, 1998) hence are like wild-type cells in this respect. Therefore, the kDNA in this case can be viewed as contributing to the retention of pentamidine in the mitochondrion of our AmB resistant cells and their enhanced accumulation of pentamidine makes them more vulnerable to the toxic effects of the drug. Therefore, our results suggest the use of pentamidine and paromomycin as possible options for use as rescue drugs in the event of AmB treatment failure due to resistance. However, since other studies did not reveal the same degree of hypersensitivity this approach might be highly strain specific.

Drug	Wt	AmB-R	Fold	Wt	AmB-R	Fold	Wt	AmB-R	Fold
	EC <sub>50</sub> (µM)			EC <sub>50</sub> (µM)			EC <sub>50</sub> (µM)		
			change						change
AmB	0.10 ± 0.01	1.89 ± 0.12	18.9	0.70 ± 0.01	0.14 ± 0.04	2	0.10 ± 0.004	2.41 ± 0.11	23
Pentamidine	2.7 ± 0.8	1.4 ± 0.2	0.52	-	-	-	4.19 ± 0.27	0.3164 ± 0.008	0.08
Paromomycin	47.5 ± 3.5	41.0 ± 11.7	0.86	12.09 ± 1.76	19.67 ± 1.30	1.63	3515 ± 278.0	36.42 ± 1.219	0.01
Ketoconazole	>1.9	0.13 ± 0.01	< 0.07	-	-	-	15.06 ± 0.66	26.05 ± 0.942	1.73
Miltefosine	-	-	-	5.84 ± 0.43	5.28 ± 0.58	0.90	5.82 ± 0.11	22.58 ± 0.20	3.88
Sb <sup>III</sup> (PAT)	-	-	-	87.33 ± 5.72	74.38 ± 4.98	0.85	197.6 ± 11.79	564.6 ± 32.65	2.86
Reference	Mbongo <i>et al.</i> , 1998			Garcia-Hernandez <i>et al.</i> , 2012			This study		

**Table 3.8 Comparison of cross-resistance to other antileishmanial drugs between reported AmB *L. donovani* and AmB *L. mexicana* resistant parasites. The reported AmB resistance quoted in the table are for *L. donovani* promastigotes while we used *L. mexicana*. Wt – Wild-type; AmB-R – Amphotericin B resistant parasites; Fold change is the ratio of the EC<sub>50</sub> value for a given drug of the resistant parasite to that of the wild-type parasites. The columns relating to particular study are shown by the reference label in the bottom row of the table. (Data adapted from Mbongo *et al.*, 1998; Garcia-Hernandez *et al.*, 2012).**

Ketoconazole is an antifungal drug belonging to a group of compounds called azoles which target lanosterol 14 $\alpha$ -demethylase (de Souza and Rodrigues, 2009). VNI, a gift from Prof. G. I. Lipesheva of Vanderbilt University, Nashville TN., is a compound that has been found to be potent against experimental acute and chronic forms of Chagas' disease in mice and has also been shown to be highly selective for protozoan lanosterol 14 $\alpha$ -demethylase (Villalta *et al.*, 2013). There was slight cross-resistance to both ketoconazole and VNI exhibited by our AmB resistant *L. mexicana* with EC<sub>50</sub> fold-changes of 1.73 and 1.52, respectively, that significantly ( $p = 0.0005$  and  $P = 0.0007$ , respectively) differed from that of the wild-type. This suggested a possible difference in the target, lanosterol 14 $\alpha$ -demethylase or sterol metabolism more generally, between the wild-type and the AmB resistant cells, although the very marginal difference might relate to other things too.

### 3.6.3 Genetic alterations in sterol biosynthetic pathway enzymes

Chromosome number variation leading to aneuploidy is a frequent event in *Leishmania* species and does not seem to have an effect on the viability of these cells (Rogers *et al.*, 2011). Aneuploidy is part of the plasticity of the *Leishmania* genome that allows them to survive in various environments. For example, aneuploidy contributed to the genetic changes that were observed in antimony resistant *L. infantum* (Leprohon *et al.*, 2009). Our AmB resistant cells were found to have altered chromosome number, but only one enzyme found in the sterol biosynthetic pathway was likely to be affected by the chromosome number change. The enzyme was farnesyl diphosphate synthase which was observed to be possibly affected by CNV of chromosome 22 (Table 3.2). Our proteomics results also showed over-expression of this enzyme in the AmB resistant cells albeit with low mascot score. Moreover, no associated metabolite change was detected in the metabolomics analysis. However, we tested the sensitivity of our AmB resistant cells to alendronate. Alendronate (Sigma - A4978) is a biphosphonate drug that targets farnesyl diphosphate synthase thereby inhibiting the isoprenoid portion of the sterol biosynthetic pathway (de Souza and Rodrigues, 2009). The drug had no effect on either wild-type or the resistant cells even when assayed at the possible maximum concentration of 30 mM. Moreover, neither the substrate nor the product of the enzyme was

detected during metabolomic analysis. However, over-expression of this enzyme in *L. major* promastigotes was shown to result in 10-fold increase in resistance to another bisphosphonate, risedronate (Ortiz-Gomez *et al.*, 2006).

*Cis*-prenyltransferase belongs to a group of ubiquitous enzymes called prenyltransferases that catalyze the attachment of an isopentenyl diphosphate to a growing allyl diphosphate chain in the isoprenoid pathway. There are two types of prenyltransferases depending on the proton that is eliminated from isopentenyl diphosphate. The *cis*-prenyltransferase action result in a *cis* configuration at the end of the growing allyl diphosphate chain while *trans*-prenyltransferase result in a *trans*-configuration at the growing end of the allyl diphosphophate (Takahashi and Koyama, 2006). These reactions occur before the cyclization reactions of the sterol biosynthetic pathway. Although we found a 2.32 spot fold-increase for *cis*-prenyltransferase-like protein (LmxM.13.0020) in our proteomics analysis, the number of copies for the responsible chromosome, chromosome 13, was the same in both cell lines and we were unable to detect metabolites that could be attributed to this enzyme in our metabolomics analysis.

### **3.6.4 Response of *L. mexicana* to different concentrations of AmB**

The formation of the aqueous pores by amphotericin B that are responsible for cell death have been reported to occur at concentrations equal to or greater than 0.1  $\mu\text{M}$  AmB in the growth medium for *L. mexicana* promastigotes (Ramos *et al.*, 1996). The N176I mutation detected in our clone of highest AmB resistance was also detected in the resistant clones growing in the presence of 0.081  $\mu\text{M}$  AmB in the growth medium. This value agrees with the required concentration of 0.1  $\mu\text{M}$  of AmB for the formation of aqueous pores reported by Ramos *et al.* (1996). This would suggest that the parasites respond to exposure to such a concentration of AmB by effecting changes at the genetic level involving lanosterol 14 $\alpha$ -demethylase that leads to perturbation of the sterol biosynthetic pathway. Our AmB resistant clones show homozygosity for the mutation starting from 0.081  $\mu\text{M}$  AmB in growth medium while the resistant clones surviving at concentrations of AmB less than 0.081  $\mu\text{M}$  do not have this mutation. A heterozygous mutation in the gene for lanosterol 14 $\alpha$ -demethylase would still

render the parasites susceptible to AmB which is likely to allow the formation of amphotericin B aqueous pores making them susceptible to the drug. Therefore, to avoid formation of pores and hence the lytic effects of AmB, the mutation has to be homozygous. Indeed this line of thought is supported by an earlier report in which a single knock-out of the gene for CYP5122A1, a *L. donovani* lanosterol 14 $\alpha$ -demethylase sharing 98% amino acid sequence with *L. mexicana*'s lanosterol 14 $\alpha$ -demethylase, resulted in reduced ergosterol in such cells and that they showed about 84% viability in the presence of 1  $\mu$ M AmB compared to 62% for the wild-type cells. Moreover, a double knock-out for the gene was not achieved suggesting a possible essentiality of the gene (Verma *et al.*, 2011).

Amphotericin B at concentrations lower than 0.1  $\mu$ M was reported to arrest the growth of the parasites (Ramos *et al.*, 1996). Further, AmB was shown to kill yeast by merely binding to ergosterol in the membranes before formation of the membrane pores (Gray *et al.*, 2012). The AmB resistant clones growing in the presence of AmB concentrations of less than 0.081  $\mu$ M AmB did not show the presence of the N176I mutation. The absence of N176I mutation in the resistant clones of lower resistance does not rule out a role played by other genetic changes that were observed and these could relate to resistance at lower levels. This would suggest, therefore, that the resistant clones surviving in the presence of lower (< 0.081  $\mu$ M) AmB concentrations may do so by withdrawal of ergosterol from their membrane to some extent as a way of tolerating lower AmB concentrations resulting in a similar mechanism that underlies differences in toxicity of the drug to different species of *leishmania* due to differences in ergosterol concentration in their membranes (Croft *et al.*, 2006). Moreover, membrane fluidity of the AmB resistant *Leishmania* has been reported to be increased compared to wild-type cells resulting in a disordered membrane. The disordered membrane has been suggested to reduce the binding specificity of AmB for ergosterol (Purkait *et al.*, 2012). This suggests that our resistant clones of lower AmB resistance could have been surviving at the stated drug concentration based on the disordered membrane due to different levels of ergosterol withdrawal from their membranes. Indeed a gradual decrease in ergosterol level was observed as resistance to the drug increased.

### 3.6.5 Effect of exogenous ergosterol supplementation

*In vitro* AmB resistant *L. donovani* were shown to stop synthesis of ergosterol as it was not detected in cell extracts (Al-Mohammed *et al.*, 2005; Mbongo *et al.*, 1998; Purkait *et al.*, 2012). However, we detected ergosterol in AmB resistant cells of *L. mexicana*, albeit at much reduced levels when compared to the parental wild-type cells. Supplementation of ergosterol in the growth medium was shown to improve the diminished growth phenotype of half knock-out of lanosterol 14 $\alpha$ -demethylase in *L. donovani* (Verma *et al.*, 2011). Therefore, we investigated whether supplementation of ergosterol in growth medium would restore the sensitivity of resistant cells to AmB and pentamidine following taking up of exogenous ergosterol. The wild-type cells showed a modest but statistically significant ( $P = 0.0023$ ) 1.11 fold-change of AmB EC<sub>50</sub> value while pentamidine EC<sub>50</sub> values remained unchanged following supplementation with ergosterol in the growth medium. Our AmB resistant clones exhibited a significant ( $P = 0.0004$ ) increase in the EC<sub>50</sub> for AmB with a fold-change of 2.84. This indicates that the cells probably do not accumulate and target to the membrane exogenous ergosterol contrary to what was reported in *L. donovani* (Verma *et al.*, 2011). The related trypanosomatid, bloodstream forms of *T. brucei*, is capable of accumulating exogenous cholesterol for their viability (Coppens *et al.*, 1988; Green *et al.*, 2003).

### 3.6.6 Dependence of filipin staining on presence of ergosterol

The difference in the expression of ergosterol between the wild type and the *in vitro* generated AmB resistant parasites can be appreciated by staining both cells lines with the sterol-specific stain, filipin III. Filipin III is an antifungal antibiotic that belongs to the same family as amphotericin B called polyene antibiotics. It is a neutral yellow compound and easily decomposes when exposed to oxygen (air) and light. It is almost insoluble in water and chloroform but soluble in most organic solvents (Whitfield *et al.*, 1955). It has been used to stain sterols in fungi, plants (Boutte *et al.*, 2011; Van Leeuwen *et al.*, 2008) and leishmania (Ignacio *et al.*, 2011; Pimenta and Desouza, 1987) at varying concentrations. In fungi it has been shown to specifically bind to ergosterol *in situ* and the florescence intensity increases with increasing concentration of ergosterol (Van Leeuwen *et al.*, 2008). Our AmB resistant cells showed no

fluorescence with filipin at 1  $\mu\text{M}$  but the wild-type cells did. This clearly showed and confirmed the difference in sterol content as was observed in metabolomics analysis between the two cell lines. While there was a fluorescent signal after filipin staining of the wild-type cells, longer times of staining resulted in the cells assuming rounded shapes of the wild type cells. However, the shape of the resistant cells remained the same for the same duration of staining. It seems swelling of the cells is a common effect at a given concentration of filipin and AmB. Amphotericin B has been reported to cause swelling of the cells giving them a round shape (Ramos *et al.*, 1996). We observed the same effect on the wild-type and not the AmB resistant cells upon incubation in 1  $\mu\text{M}$  AmB resulting in cells dying within 15 minutes of incubation while the AmB resistant cells remained unaffected. The ability to stain the wild-type and not the AmB resistant cells suggests a possible use of filipin to distinguish AmB resistant cells from wild-type cells, at least in *L. mexicana* promastigotes.

To adopt the filipin assay as a field test to distinguish AmB resistant parasites from drug sensitive ones, the assay has to be as simple as possible. Therefore, we attempted to stain cells fixed in methanol. We could not achieve staining of fixed cells at various concentrations of filipin, both higher and lower than that used for staining live cells, a result that is consistent with the requirement for live cells to stain with filipin as reported for *L. m. amazonensis* (Pimenta and Desouza, 1987). While it is not possible to stain fixed *Leishmania* cells with filipin, it is possible to do so with fixed macrophages and fibroblasts based on their cholesterol content (Rabhi *et al.*, 2012; Takamura *et al.*, 2013). Indeed, accumulation of cholesterol in amastigotes has been shown to increase following infection with *Leishmania* parasites (Rabhi *et al.*, 2012). The accumulation of cholesterol by infected amastigotes would therefore cause such high background staining with filipin that it would be difficult to differentiate cholesterol staining from that with infecting *Leishmania* parasites as was observed in our attempt to stain infected amastigotes. Therefore use of filipin to distinguish AmB resistant and AmB susceptible would require use of live parasites that have been transformed from isolated amastigotes into promastigotes, since AmB resistance is a stable trait as shown in this study and other studies (Al-Mohammed *et al.*, 2005). The promastigotes transformed from AmB resistant amastigotes would not be expected to show fluorescence with the stain.

Photo-bleaching of filipin was observed within five seconds of exposure of stained cells. Filipin photo-bleaching has been attributed to use of low concentration of stain in plant root tissues and quick acquisition of images and use of low laser power is suggested to reduce photo-bleaching (Boutte *et al.*, 2011). It is also possible to raise the concentration of filipin with reduced time of incubation although the exposure time is still restricted to less than ten seconds to avoid photo-bleaching (Van Leeuwen *et al.*, 2008). We could not raise the concentrations of filipin to specifically stain ergosterol, because of possible competition for specificity of the stain between ergosterol and phospholipids (Milhaud *et al.*, 1996). Moreover, we noted cell lysis, as observed by others (Pimenta and Desouza, 1987), at higher concentrations of the stain and this may not be ideal for differentiating cells expressing different levels of ergosterol. However, the rounding up phenotype of the AmB sensitive cells could be used as an assay to differentiate the AmB sensitive from the AmB resistant cells following exposure of the cells to the drug for 15 minutes. Filipin's ability to cause rounding up of the AmB sensitive cells can also be used to differentiate the wild type cells from the resistant cells based on the round up phenotype rather than its fluorescence property which is disadvantaged by photo-bleaching.

### **3.6.7 Sensitivity of AmB resistant *L. mexicana* to oxidative stress**

Amphotericin B is accumulated more by wild-type than AmB resistant *L. donovani* and this has been shown to be accompanied by an accumulation of ROS in wild-type cells only in response to exposure to AmB (Mbongo *et al.*, 1998; Purkait *et al.*, 2012). It was also shown that AmB resistant cells had an up-regulation of mRNA for the enzymes involved in the thiol metabolic pathway which is involved in generation and maintenance of trypanothione in the reduced state. This was suggested to be part of AmB resistance mechanism that results in protection of AmB resistance cells from ROS that result from the auto-oxidation of amphotericin B (Purkait *et al.*, 2012). We observed depleted levels of S-adenosyl-L-methionine, ornithine and putrescine with fold-differences of 0.65, 0.14 and 0.68, respectively, in AmB resistant cells as compared to the parental wild-type cells in metabolomics analysis. However, a comparison of these changes with the chromosome number variation from the genomic DNA sequencing data, only ornithine decarboxylase (Gene ID LmxM.12.0280) found on

chromosome 12 was found to have one chromosome 12 less in AmB resistant cells as compared to the wild-type cells. This would imply reduction in copy number of the enzyme and may explain the 0.68 fold-difference of putrescine detected in AmB resistant cell lines as compared to the wild-type. There was no change in chromosome number for the other enzymes namely, Spermidine synthase (LmxM.04.0580), Trypanothione synthetase (LmxM.36.4300), S-adenosylmethionine synthetase (LmxM.29.3500) whose product, S-adenosylmethionine, which is a substrate for S-adenosylmethionine decarboxylase's (LmxM.29.3110 ) was found to be depleted in the AmB resistant cell lines. This is in contrast to the mRNA up-regulation for all enzymes except S-adenosylmethionine synthetase, found in AmB resistant *L. donovani* (Purkait *et al.*, 2012). Our proteomics data indicated an up-regulation of S-adenosylmethionine synthetase in the resistant cells although its reaction product, S-adenosylmethionine, was found to be statistically not significantly ( $P = 0.09007$ ) depleted in resistant cells by a 0.65 fold-difference as compared to the wild-type cells. An up-regulation would suggest an effort to keep up with the demand for its product.

Methylene blue's use as an oxidant is due to its ability to deplete cells of their reducing power, NADPH, resulting in accumulation of  $\text{NADP}^+$ . The depletion of NADPH mimics that observed with detoxification of  $\text{H}_2\text{O}_2$  (Atamna *et al.*, 1994; Baquer *et al.*, 1977). We therefore used methylene blue to investigate the susceptibility of the generated AmB resistant cells growing in the presence of  $0.27 \mu\text{M}$  AmB and the parental wild-type *L. mexicana* promastigotes to oxidative stress. The generated AmB resistant cells were much more susceptible than the wild-type cells to methylene blue and hence oxidative stress. This was further confirmed by the response of the two cell lines to exposure to  $\text{H}_2\text{O}_2$  in growth medium with the resistant cells being more affected than the wild-type cells. We observed a dose dependent effect of  $\text{H}_2\text{O}_2$  on both wild-type as reported elsewhere (Das *et al.*, 2001) and our AmB resistant cells, with the resistant cells being more affected than the wild type cells indicating hypersensitivity to oxidative stress. Oxidative stress brought about by exposure to  $\text{H}_2\text{O}_2$  concentrations lower than 4 mM was shown to kill *L. donovani* through an apoptotic-like death (Das *et al.*, 2001).

Ergosterol plays the role of an antioxidant among other functions in *S. cerevisiae* (Dupont *et al.*, 2012; Landolfo *et al.*, 2010). Yeast is able to take up exogenous ergosterol for their cellular use under anaerobic conditions (Lorenz and Parks, 1991). Ergosterol supplementation in growth medium has been shown to protect yeast from both internal and external oxidative stress challenge (Landolfo *et al.*, 2010). Susceptibility of yeast to oxidative stress is enhanced with inhibition of either Sterol C24-methyltransferase (*erg6*) or sterol C7, 8-isomerase (*erg3*) or both but less so with the enzymes downstream sterol C7, 8-isomerase (Dupont *et al.*, 2012). The susceptibility to oxidative stress by ROS has been attributed to the absence of the conjugated double bonds in fecosterol and episterol. The conjugated double bonds (in ring B) which are close to the hydroxyl group (on ring A) in ergosterol (Figure 3.14) are said to provide delocalisation of a lone pair of electrons during an attack on ergosterol by ROS (Dupont *et al.*, 2012). This property of ergosterol is said to protect the phospholipids in membranes against oxidative stress (Dupont *et al.*, 2012). Therefore, our AmB resistant clones were made more susceptible to oxidative stress challenge than the wild-type cells due to the reduced levels of ergosterol in their membranes which could not protect them against oxidative stress.

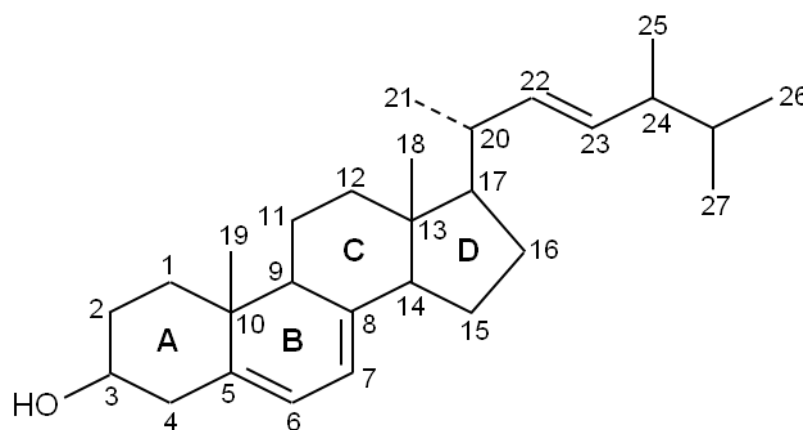


**Figure 3.14** Molecular structure of ergosterol showing the numbering of atoms

Amphotericin B, miltefosine and trivalent antimony have all been shown to induce production of ROS in the mitochondrion, reduction in mitochondrial membrane potential and degradation of gDNA leading to an apoptotic-like death of *L. infantum* (Moreira *et al.*, 2011). The ROS are known to cause oxidative stress in cells. We therefore investigated whether the use of N-acetyl cysteine (NAC), an antioxidant, would protect the resistant cells from miltefosine,

potassium antimony tartrate (PAT) and other antileishmanial drugs. We observed a sensitisation of the resistant cells with fold-changes in  $EC_{50}$  values of 0.57 for miltefosine, 0.33 for AmB and 0.50 for PAT. Our AmB resistant lines could have reacted to exposure to AmB, miltefosine and PAT in the same way as *in vitro* *L. infantum* cell lines resistant to these drugs, i.e. *L. infantum* resistant to either AmB or miltefosine or PAT could not be induced to produce ROS by the drug to which they were resistant (Moreira *et al.*, 2011). Therefore, the reduction in  $EC_{50}$  values for the three drugs suggests that NAC may have exerted toxic effect on the cells. Our results show a different role of NAC other than that of an antioxidant in cells and this is indicative of something complex happening when cells are exposed to drugs in the presence of NAC.

Pentamidine was shown to induce ROS production in wild-type cells while paromomycin was unable in both the wild-type and paromomycin resistant *L. infantum* and the two drugs were suggested to kill *Leishmania* through a different unknown mechanism (Moreira *et al.*, 2011). However, our *L. mexicana* promastigotes resistant to AmB got some protection from paromomycin in the presence of NAC with a 2 fold-increase in  $EC_{50}$  value from  $36.68 \pm 1.05 \mu\text{M}$  in the absence of NAC to  $79.60 \pm 1.89 \mu\text{M}$  in the presence of NAC and this is in stark contrast with the fact that paromomycin was reportedly unable to induce ROS production (Moreira *et al.*, 2011) which would be scavenged by NAC. The  $EC_{50}$  value for Pentamidine in AmB resistant cells remained the same despite an indication that it was able to induce ROS production in *L. infantum* (Moreira *et al.*, 2011). The wild-type used in this set of experiments only showed an increase in  $EC_{50}$  value for PAT with a fold-change of 2.27, a result that agrees with the expected role of NAC, that of scavenging ROS (Verma *et al.*, 2011) whose generation may have been induced by PAT (Moreira *et al.*, 2011). However, our results indicate that NAC, at the concentration used, seems to potentiate, to some extent, the action of paromomycin, pentamidine, AmB and methylene blue on wild-type controls while the action of miltefosine essentially remained unaltered in these cells.

### 3.6.8 Reduction in cell length of AmB resistant *L. mexicana*

Cell size reduction was noticed in AmB resistant cells when compared to the wild-type cells under the light microscope. Shorter and more rounded cells, following exposure of *L. donovani* promastigote wild-type cells to pentamidine and in pentamidine resistant *L. mexicana* promastigotes, have been reported (Basselin *et al.*, 2002; Mehta and Shaha, 2004). However, our AmB resistant cells were predominantly of comparable shape to the wild type, except they were smaller and shorter. To investigate this further we measured the cell body length of individual cells from the two cell lines. We used cell body length to compare the cell sizes of the two cell lines because it does not change significantly at different cell densities although it is represented by a relatively broad range of cell sizes. While cell width as opposed to cell body length is inversely proportional to cell density (Wheeler *et al.*, 2011) and therefore may not be a good comparison parameter. Cultures of the two cell lines were grown to similar cell densities and used the same cell density for both cell lines to fix the cells for measurement. The cell body length range for the wild-type was 7.19 - 16.24  $\mu\text{m}$ , a range that is comparable to that by Wheeler *et al.*, (2011). Compared to the wild-type, the AmB resistant cells had a reduced cell body length (section 3.2.2.1). Sterols are known to perform among other functions that of structural integrity of membranes (Lepesheva and Waterman, 2007; Roberts *et al.*, 2003). It is therefore possible that the reduction in cell body length may have been due to the reduced ergosterol level and the general perturbation of sterol level that was observed in the AmB resistance cells. In fact, reduction in body size is in agreement with what was observed in *L. donovani* with a single knock-out of lanosterol 14 $\alpha$ -demethylase that showed reduced levels of ergosterol as compared to the wild-type cells (Verma *et al.*, 2011).

## Chapter Four

### 4 Participation of *Leishmania mexicana* lanosterol 14 $\alpha$ -demethylase in amphotericin B resistance

#### 4.1 Introduction

One of the biggest threats to use of chemotherapy for control of leishmaniasis is development of drug resistance. Antimonial drugs have thus been stopped from use in Bihar state of India due to development of resistance (Sundar *et al.*, 2000). Moreover, no single drug has had its mechanism of resistance fully worked out although *in vitro* drug resistance has been demonstrated to almost all anti-leishmanial drugs (Croft *et al.*, 2006). Furthermore, only a handful of drugs for use against leishmaniasis are available with limited knowledge of their cellular targets.

The membrane sterols of mammals are different from those of *Leishmania* species and this includes differences in their sterol biosynthetic pathways. Mammals have cholesterol, the end product of their sterol biosynthetic pathway, as the major sterol of their cell membranes. *Leishmania* have ergosterol, the end product of their sterol biosynthetic pathway in these organisms, in their membranes instead of cholesterol when compared to mammals (de Souza and Rodrigues, 2009). *Leishmania* species together with other trypanosomatids are also known to synthesise 24-alkyl sterols which are not found in mammals (Chawla and Madhubala, 2010). These differences in the sterol biosynthetic pathway between mammals and *Leishmania* provide opportunities for drug selectivity and hence unique drug targets (Chawla and Madhubala, 2010; de Souza and Rodrigues, 2009).

The sterol biosynthetic pathway and sterol composition of fungi and *Leishmania* species are similar (Berman, 1988). As a result many antifungals that target sterol biosynthetic pathway enzymes have subsequently been indicated to be active against *Leishmania* species (de Souza and Rodrigues, 2009; Roberts *et al.*, 2003). Thus, the antifungal azole compounds, exemplified by ketoconazole, posaconazole, itraconazole, fluconazole and voriconazol, which target the lanosterol 14 $\alpha$ -demethylase, have been indicated to be active against

*Leishmania* species (Beach *et al.*, 1988; de Macedo-Silva *et al.*, 2013). AmB is an antifungal drug which has increasingly been used for treatment of leishmaniasis and its use against leishmaniasis stems from the similarities in sterol metabolism of fungi and *Leishmania* species. Various studies have established the effect of AmB on the sterol biosynthetic pathway in *Leishmania*. It has been shown that AmB resistance selection perturbs the sterol biosynthetic pathway leading to accumulation of various intermediates of the pathway and inhibition of ergosterol synthesis (Al-Mohammed *et al.*, 2005; Mbongo *et al.*, 1998; Purkait *et al.*, 2012). The perturbation of the sterol biosynthetic pathway in response to selecting resistance to AmB has been attributed to the need by the parasites to reduce the drug's target, ergosterol, thereby reducing its toxicity on the parasites.

It has not been demonstrated how this perturbation of the pathway comes about. However, our study has identified a non-synonymous mutation in the lanosterol 14 $\alpha$ -demethylase gene of AmB resistant *L. mexicana* promastigotes. We also observed an accumulation of 4, 4-dimethyl-cholesta 8, 14, 24-trienol, which is a reaction product of lanosterol 14 $\alpha$ -demethylase. We therefore aimed to determine the role of the mutated lanosterol 14 $\alpha$ -demethylase gene in the induced *in vitro* AmB resistance.

## 4.2 Results

### 4.2.1 Position of N176I in *L. mexicana*'s lanosterol 14 $\alpha$ -demethylase

Use of gDNA sequencing and metabolomics in tandem to compare the wild-type and the AmB resistant cells revealed a non-synonymous point mutation in the lanosterol 14 $\alpha$ -demethylase gene (Chapter 3). The discovery of a definite non-synonymous point mutation in this gene led us to establish, by secondary structure prediction, whether the mutation was in the catalytic site of the enzyme. The non-synonymous mutation (Appendix F) found in the lanosterol 14 $\alpha$ -demethylase (Gene ID LmxM.11.1100) was found to be outside the catalytic site of the enzyme (courtesy of Prof. G. I. Lepesheva (Figure 4.1)). However, the mutation involved a substitution of an amino acid which has a hydrophilic side chain with an aliphatic amino acid whose side chain is hydrophobic at pH7.0

(Monera *et al.*, 1995). The mutated residue was found to be in one of the peripheral helices of the predicted secondary structure of the enzyme as deduced from the amino acid secondary structure prediction in CLC workbench 6.

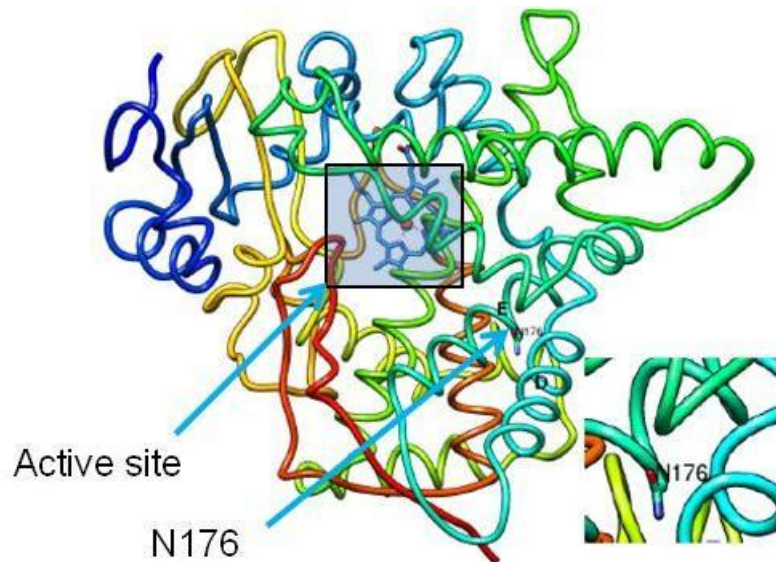


**Figure 4.1** *L. mexicana* wild-type promastigote lanosterol 14 $\alpha$ -demethylase structure. The enzyme structure shows the position of the mutated amino acid residue from the active site. (Enzyme structure was provided by Prof. G. I. Lepesheva, Vanderbilt University, Nashville TN; Hargrove *et al.*, 2011)

#### 4.2.2 Alignment of various trypanosomatid lanosterol 14 $\alpha$ -demethylase

Certain amino acid residues of lanosterol 14 $\alpha$ -demethylase are known to be conserved across the CYP51 family, and the conserved residues which fulfil the structural role have been thought to be involved in the folding and overall shape of the proteins (Lepesheva and Waterman, 2011b). Mutations of residues that are conserved have been shown to affect the enzyme function (Lepesheva *et al.*, 2006). We investigated whether the mutated residue was conserved in various trypanosomatids. An alignment of the primary structures of lanosterol 14 $\alpha$ -demethylase from different trypanosomatids, yeast and humans as downloaded from tritrypDB, GeneDB and nextprot.org websites revealed that the mutated asparagine residue affected by the mutation was conserved among trypanosomatid species analysed but not in yeast (*S. cerevisiae*) or humans (*H. sapiens*) (Figure 4.2 and Appendix G). The conservation could be important as we consider its conservation in other trypanosomatids, for instance it could be important for protein-protein interaction.

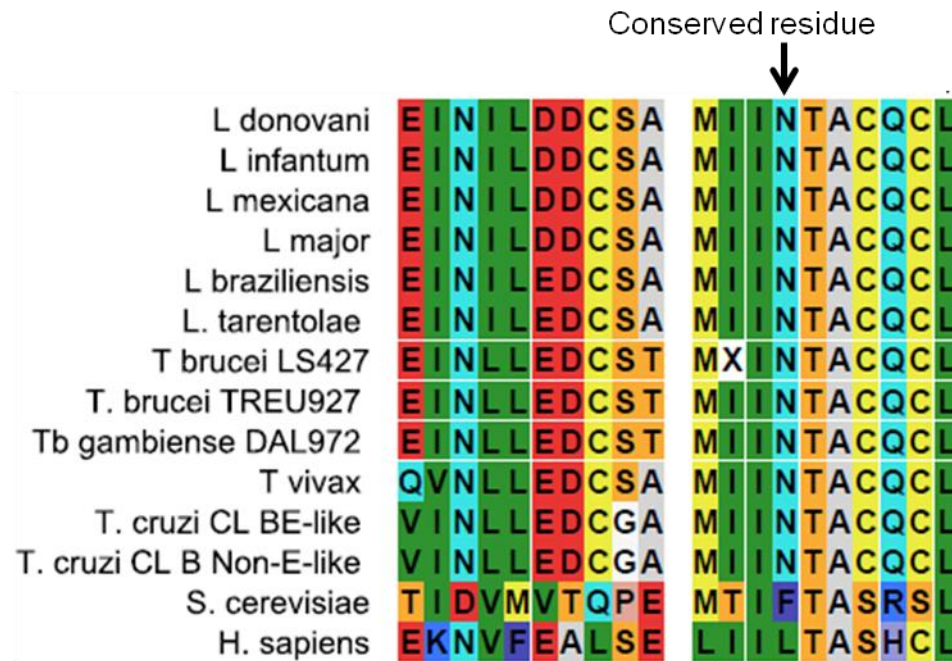


**Figure 4.2 Primary structure alignment of lanosterol 14 $\alpha$ -demethylase of trypanosomatids.** The conserved residue in *leishmania* species and trypanosomes is indicated, but it is not conserved in *S. cerevisiae* and *H. sapiens*. The sequences were downloaded from the TritypDB, GeneDB and nextprot.org, and aligned using CLC Genomics Workbench 6

### 4.3 Expression of *L. mexicana* Wt lanosterol 14 $\alpha$ -demethylase into AmB resistant *L. mexicana*

To confirm a role of the identified mutation in drug resistance, confirmatory experimental assays were carried out (Berg *et al.*, 2013a). We cloned the wild-type enzyme for expression in the AmB resistant cells, using an expression vector for *Crithidia fasciculata* and *Leishmania*, pNUS-HnN plasmid (Tetaud *et al.*, 2002).

#### 4.3.1 Checking for presence of both Wt and AmBR lanosterol 14 $\alpha$ -demethylases in re-expresser clones

The presence of both the chromosomal and extra-chromosomal copies of lanosterol 14 $\alpha$ -demethylase in the *L. mexicana* re-expresser cells was determined using the pNUS-HnN plasmid specific primers (MB0781 and MB0782) (Table 2.2) and the gene specific primers (MB0769 and MB0770) (Table 2.2) whose PCR products sizes were 1, 650 bp and 1, 452 bp, respectively. We used the parental wild-type and the derived AmB resistant cells' DNA as controls. The re-expresser cells yielded two bands for both sets of primers indicating the presence of both the chromosomal and extra-chromosomal copies of lanosterol

14 $\alpha$ -demethylase, while the wild-type and the AmB resistant cells yielded a single PCR product with the gene-specific primers (Figure 4.3).

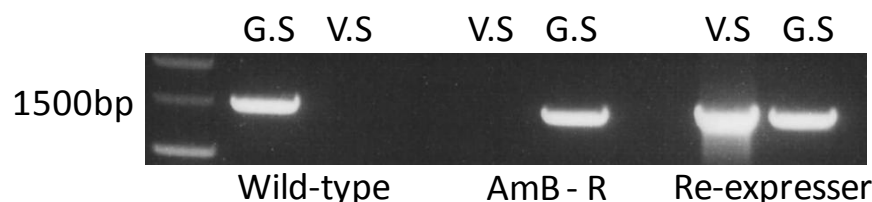


**Figure 4.3 PCR amplification of chromosomal and extra-chromosomal AmB-R CYP51.** The PCR products were amplified from DNA extracted from parental wild-type, AmB resistant cells (AmB-R) and AmB resistant cells expressing the wild-type CYP51 (lanosterol 14 $\alpha$ -demethylase) (Re-expresser). The PCR products were separated on a 1% agarose gel with SYBR safe staining. The PCR products were separated along a 1kb DNA ladder. G.S = Gene specific primer and V.S = Vector specific primer. G.S bands = 1452 bp; V.S band = 1650 bp.

The presence of both the chromosomal (mutated) and extra-chromosomal (wild-type) copies of lanosterol 14 $\alpha$ -demethylase were determined/confirmed by sequencing the PCR products. We used a 24 bp forward primer (MBO787) (Table 2.2) starting from 43 bp from the start codon of the gene and a 21 bp reverse primer (MBO788) (Table 2.2) starting from 231 bp from the point mutation within the gene to amplify the chromosomal copy of lanosterol 14 $\alpha$ -demethylase portion of AmB resistant cells to give a 788 bp PCR product. To amplify the extra-chromosomal copy we used a pNUS-HnN plasmid specific 21 bp forward primer (MBO781) and MBO788 resulting in a 790 bp PCR product. Sequenced PCR products revealed presence of the wild-type copy of lanosterol 14 $\alpha$ -demethylase as an extra-chromosomal copy and the mutated lanosterol 14 $\alpha$ -demethylase as a chromosomal copy (Figure 4.4).

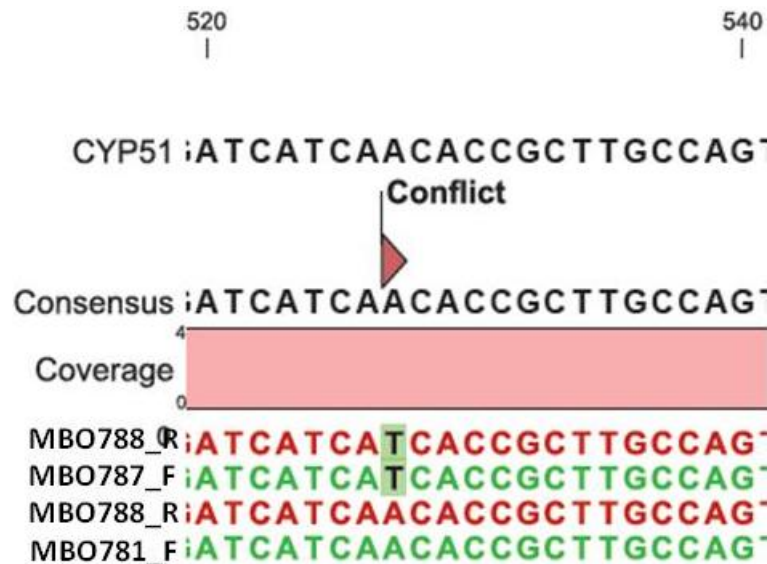


**Figure 4.4** Sequence alignment of the chromosomal and extra-chromosomal CYP51. The PCR amplified products were sequenced after insertion into the pGEMT easy vector. The sequences were aligned to the CYP51 (lanosterol 14 $\alpha$ -demethylase) sequence using CLC genomics Workbench 6. The conflict indicated shows the mutated base in the AmB resistant cells. The sequencing was done at Eurofins MWG Operon, Germany.

### 4.3.2 Restoration of Ergosterol levels in re-expresser cells

AmB resistance has been reported to be accompanied by inhibition of ergosterol synthesis in resistant cells as a way of protecting themselves against AmB. This follows lack of detection of ergosterol in samples derived from *in vitro* generated AmB resistant cells (Al-Mohammed *et al.*, 2005; Mbongo *et al.*, 1998; Purkait *et al.*, 2012). Therefore, following the observation that ergosterol was depleted in the AmB resistant cells as compared to the parental wild-type cells (chapter 3), we investigated whether AmB resistant cells expressing an extra-chromosomal copy of wild-type lanosterol 14 $\alpha$ -demethylase had started synthesising ergosterol using metabolomics. We observed restoration of the ergosterol levels in AmB resistant cells expressing an extra-chromosomal copy of wild-type lanosterol 14 $\alpha$ -demethylase as compared to the wild-type cells and the AmB resistant cells (Figure 4.5 Table 4.1 and Appendix J). Ergosterol was restored in AmB resistant cells with wild-type lanosterol 14 $\alpha$ -demethylase complementation to similar levels as in the parental wild-type cells.

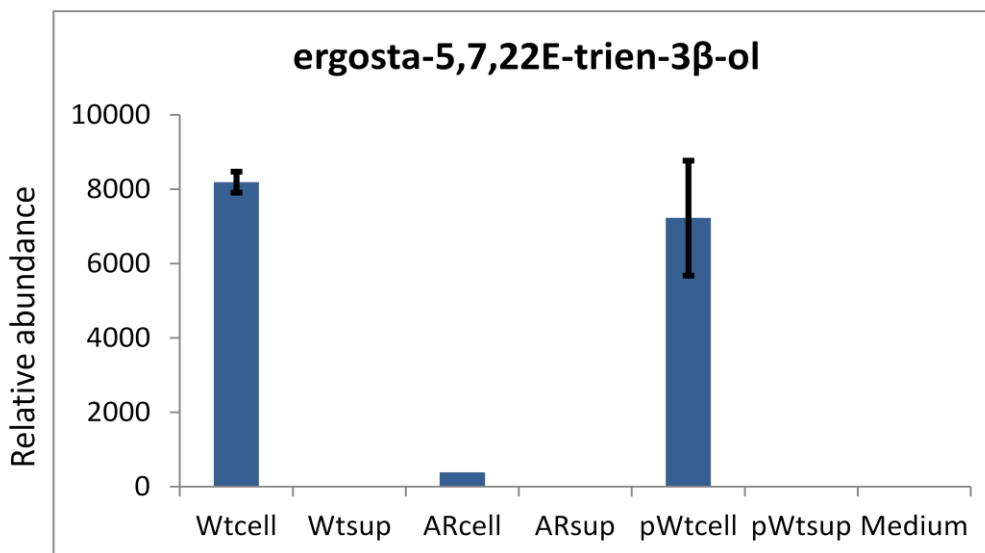


**Figure 4.5 Restoration of ergosterol levels in AmB resistant cells expressing Wt CYP51**  
The samples were extracted from the parental wild-type (Wt), derived AmB resistant and Wt-lanosterol 14 $\alpha$ -demethylase (CYP51) expressing AmB resistant *L. mexicana* using cold (-4C°) chloroform: methanol: water (1:3:1;v/v). The samples were analysed using LC/MS and IDEOM. The data are for three independent experimental replicates. Wtcell = samples derived from wild-type cells; Wtsup = samples from supernatant from the growth medium in which the cells were grown; ARcell = AmB resistant cell samples; ARsup = AmB resistant supernatant; pWtcell = re-expresser cells; ARsup = re-expresser supernatant.

The characteristics described in table 4.1 whose chromatogram is given in Appendix J are consistent with those of ergosterol (ergosta-5, 7, 22E-trien-3 $\beta$ -ol).

Attribute	Determined	
Mass (m/z)	396.34	
Retention Time (min)	5.261	
Formula	C <sub>28</sub> H <sub>44</sub> O	
Identified metabolite	Ergosta-5,7,22E-trien-3 $\beta$ -ol	
Fold change	AmBR	0.05
	Re-expressor	0.88

**Table 4.1 Characteristics of detected ergosterol in Wt, AmB-R and re-expressor cell lines.**  
The identification of ergosterol was done by analysis of wild-type (Wt), amphotericin B resistant (AmB-R) and amphotericin B resistant cells expressing Wt copy of lanosterol 14 $\alpha$ -demethylase (re-expressor) by LC/MS and analysis using IDEOM. The fold change is the comparison of the relative abundance of ergosterol in AmB-R and Re-expressor cells to that in the Wt as the control.

### 4.3.3 Reversal of resistance to AmB

The presence of both copies of the wild-type and the mutated AmB resistant lanosterol 14 $\alpha$ -demethylase in the re-expressers cells and following restoration

of ergosterol led us to check the effect of AmB on these cells. Single knock-out of lanosterol 14 $\alpha$ -demethylase resulted in having reduced ergosterol levels and reduced susceptibility to AmB (Verma *et al.*, 2011). Resistance to AmB was reversed in the re-expresser cells with a significant difference (t-test;  $P < 0.0001$ ) in  $EC_{50}$  value for AmB between the AmB resistant cells and the re-expresser cells (Figure 4.6) with a fold-change in  $EC_{50}$  value of 0.03. The re-expresser cells were found to be significantly ( $P = 0.0009$ ) more sensitive to AmB than the parental wild-type cells with a fold-change in  $EC_{50}$  value of 0.77. This confirmed the requirement of the presence of ergosterol for the drug to exert its toxic effect on the cells.

Expression of wild-type lanosterol 14 $\alpha$ -demethylase in AmB resistant leishmania caused a reversion to wild-type levels of susceptibility to AmB in transformants. Ergosterol expression was also restored to levels of those of the wild-type indicating that ergosterol levels are directly responsible for resistance to AmB.

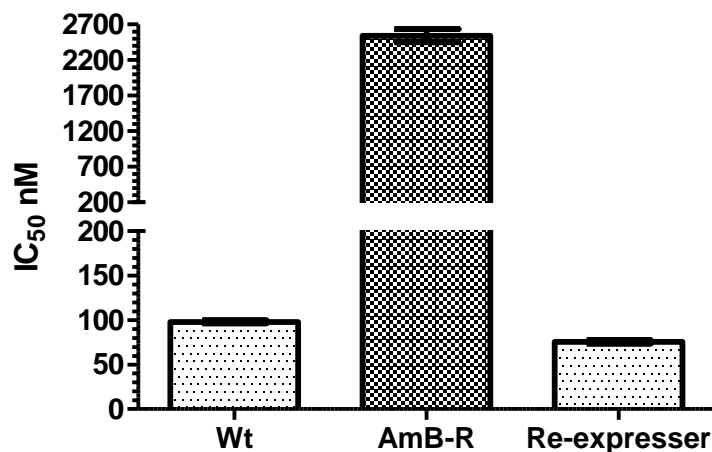


**Figure 4.6** Reversal of AmB resistance by complementation of AmB-R with Wt CYP51. The effect of AmB on the wild-type (Wt), AmB resistant (AmB-R) and AmB resistant cells expressing wild-type lanosterol 14 $\alpha$ -demethylase (Wt CYP51) (Re-expresser) was done using the modified alamar blue assay of 72 hrs cell incubation with the inhibitor. The cells were further incubated for another 48 hrs following addition of 12.5 mM resazurin in PBS. The absorbance data was analysed using GraphPad Prism software.  $EC_{50}$  values; Wt = There was a significant difference (ANOVA;  $P < 0.0001$ ) in the  $EC_{50}$  values. The data analysed was for three independent experiments.

#### 4.3.4 AmB resistant cells expressing Wt- lanosterol 14 $\alpha$ -demethylase's sensitivity to other anti-leishmanial drugs

AmB resistant *Leishmania* showed cross-resistance to ketoconazole, PAT and miltefosine, and increased susceptibility to pentamidine and paromomycin

(Chapter 3). These derived cells were characterised by depleted levels of ergosterol as compared to the parental wild-type cells.

The restoration of the wild-type character in terms of susceptibility to AmB and ergosterol levels by AmB resistant cells expressing the wild-type lanosterol 14 $\alpha$ -demethylase led us, therefore, to also check whether the response of these cells to other anti-leishmanial drugs would be comparable to that of the wild-type cells. We determined the sensitivity of the AmB resistant *L. mexicana* expressing the wild-type copy of lanosterol 14 $\alpha$ -demethylase to other antileishmanial compounds using the modified alamar blue assay. The cells were found to be more resistant to ketoconazole with a fold change in EC<sub>50</sub> value of 2.60 representing a significant difference (P = 0.0072) in EC<sub>50</sub> value as compared to wild type cells (Table 4.2). The AmB resistant cells expressing the wild-type gene for lanosterol 14 $\alpha$ -demethylase were found to have lost sensitivity to pentamidine by reverting back to the wild-type EC<sub>50</sub> value for pentamidine with a fold-change of 0.997. The re-expresser cells were also found to be more sensitive to miltefosine than the parental wild-type cells with a significant difference (P < 0.0001) in EC<sub>50</sub> value. There was a 0.62 fold-change in EC<sub>50</sub> value for miltefosine in comparison to the parental wild-type cells while a fold change in EC<sub>50</sub> value for miltefosine between the wild-type and the AmB resistant cells was 3.88 (Table 4.2).

Drug	EC <sub>50</sub> ( $\mu$ M)		Fold change <sup>1</sup>	EC <sub>50</sub> ( $\mu$ M)		Fold change <sup>2</sup>
	Wt	AmB-R		Re-expresser		
Pentamidine	4.19 $\pm$ 0.27	0.32 $\pm$ 0.01	0.08	4.18 $\pm$ 0.10	0.997	
Miltefosine	5.82 $\pm$ 0.11	22.58 $\pm$ 0.20	3.88	3.591 $\pm$ 0.06	0.62	
Ketoconazole	15.46 $\pm$ 0.84	24.73 $\pm$ 0.57	1.60	40.23 $\pm$ 4.82	2.60	

**Table 4.2 Effect of anti-leishmanial drugs on AmB resistant cells expressing the Wt CYP51.** The effect of pentamidine on the wild-type (Wt), AmB resistant (AmB-R) and re-expresser (AmB resistant cells expressing wild-type lanosterol 14 $\alpha$ -demethylase (Wt CYP51)) was determined using the modified alamar blue assay. A density of  $1 \times 10^6$  cells/ml incubated for 72 hrs in the presence of the drug and a further 48 hrs following addition of 12.5 mM resazurin in PBS. The absorbance data was analysed using GraphPad Prism software. The data are for three independent experimental replicates. All values are expressed as Mean  $\pm$  SEM. Fold-change<sup>1</sup> = Ratio of AmB-REC<sub>50</sub> to Wt EC<sub>50</sub>; Fold-change<sup>2</sup> = Ratio of WtEC<sub>50</sub> to Re-expresser EC<sub>50</sub>.

However, the AmB resistant cells complemented with the wild-type lanosterol 14 $\alpha$ -demethylase showed no sensitivity to either paromomycin or potassium

antimony tartrate, although the wild-type showed EC<sub>50</sub> values of  $2,959 \pm 883.4$   $\mu\text{M}$  and  $198.4 \pm 14.80$   $\mu\text{M}$  for paromomycin and PAT, respectively.

#### 4.4 Effect of sterol C14-reductase inhibitors on AmB resistant cells

Experiments where Wt lanosterol 14 $\alpha$ -demethylase (EC#: 1.14.13.70) expression in AmB resistant cells caused a reversion to sensitivity to the drug demonstrate that the mutation to lanosterol 14 $\alpha$ -demethylase is indeed responsible for the resistance phenotype. However, the mutation to lanosterol 14 $\alpha$ -demethylase in the resistant line is not within the enzyme's catalytic site. Moreover, the product of lanosterol 14 $\alpha$ -demethylase (4, 4-dimethyl-cholesta 8, 14, 24-trienol) continues to be produced, which indicates that this enzyme is still active. However, accumulation of the product could indicate that it is a failure of this metabolite to be further metabolised that causes its accumulation. The next enzyme in the ergosterol biosynthetic pathway is sterol 14 $\alpha$ -reductase (EC#: 1.3.1.71). We therefore investigated whether a defect in the ability of lanosterol 14 $\alpha$ -demethylase enzyme product to reach sterol C14-reductase might underlie resistance. We tested the sensitivity of the AmB resistant cells to reported sterol C14-reductase specific inhibitors: amorolfine, spiroxamine and fenpropidin (Debieu *et al.*, 2000; Katz, 2000; Marcireau *et al.*, 1992; Polak-Wyss, 1995).

We found a mixed response by the AmB resistant cells to the three sterol C14-reductase specific inhibitors. The AmB resistant cells were found to tolerate spiroxamine in a similar way to the parental wild-type cells (Table 4.3). There was no significant difference ( $P = 0.07$ ) in spiroxamine EC<sub>50</sub> for the two cell lines.

The AmB resistant cells were found to be more sensitive to amorolfine, with a fold-change in EC<sub>50</sub> value for the drug of 0.65, than the wild-type with a significant difference ( $P = 0.03$ ) in EC<sub>50</sub> value. However, there was no significant ( $P = 0.08$ ) difference in EC<sub>50</sub> value for fenpropidin with a fold-change of 1.42 between the wild-type and the resistant cell lines (Table 4.3). Generally, the EC<sub>50</sub> value for amorolfine of the wild-type and the AmB resistant cells was found to be minimal albeit statistically different.

Drug	EC <sub>50</sub> (μM)		Fold-change	P
	Wild-type	AmB-R		
Amorolfine	46.15 ± 2.41	29.76 ± 4.35	0.65	0.03
Spiroxamine	36.43 ± 2.51	30.16 ± 0.35	0.83	0.07
Fenpropidin	90.14 ± 4.80	128.50 ± 15.39	1.42	0.08

**Table 4.3 Comparison of sterol C14-reductase specific inhibitors on AmB resistant cells. The effect of sterol C14-reductase specific inhibitors was determined using the modified alamar blue assay of 72 hrs incubation of cells in the presence of the drug followed by another 48 hrs for reaction of 12.5 mM resazurin. The absorbance data for three independent experiments were used for the analysis. The data was analysed using the GraphPad Prism software. Results are presented as Mean ± SEM. Fold-change is the ratio of AmB-REC<sub>50</sub> to that of WtEC<sub>50</sub>.**

#### **4.4.1 Effect of exposure of *L. mexicana* Wt to Sterol C14-reductase inhibitors and fenhexamid on AmB sensitivity**

The observed minimal difference in the response to sterol C14-reductase inhibitors between the wild-type and the resistant cell lines was in line with the absence of alteration to the enzyme gene sequence in both cells (chapter 3). We determined whether exposure of the wild-type cells to the sterol C14-reductase inhibitors, spiroxamine and fenpropidin, and fenhexamid would result in increased tolerance to AmB. Fenhexamid is an antifungal inhibitor of sterol C3-keto reductase of the sterol biosynthetic pathway (Debieu *et al.*, 2001) and it was included in the assay to find out whether inhibition of the sterol biosynthetic pathway at various points would cause an increase in tolerance to AmB by the wild-type *L. mexicana*. Andrew Pountain (a placement student under my supervision) showed that exposure of wild-type cells to concentrations of spiroxamine and fenpropidin equivalent to EC<sub>50</sub> value and 10-fold less the EC<sub>50</sub> value and fenhexamid at 100 μM for 24 hrs (as exposure for longer resulted in cell death) a 5.5-fold significant (P = 0.008) reduction in sensitivity to AmB for cells treated with fenpropidin at a concentration equivalent to EC<sub>50</sub> value and a significant (P = 0.014) 1.8-fold decrease for cells exposed to a concentration of the drug equivalent to 10-fold less the EC<sub>50</sub> value (Figure 4.7). Spiroxamine resulted in a marginal decrease in sensitivity to AmB while fenhexamid showed no effect on AmB sensitivity (Figure 4.7).

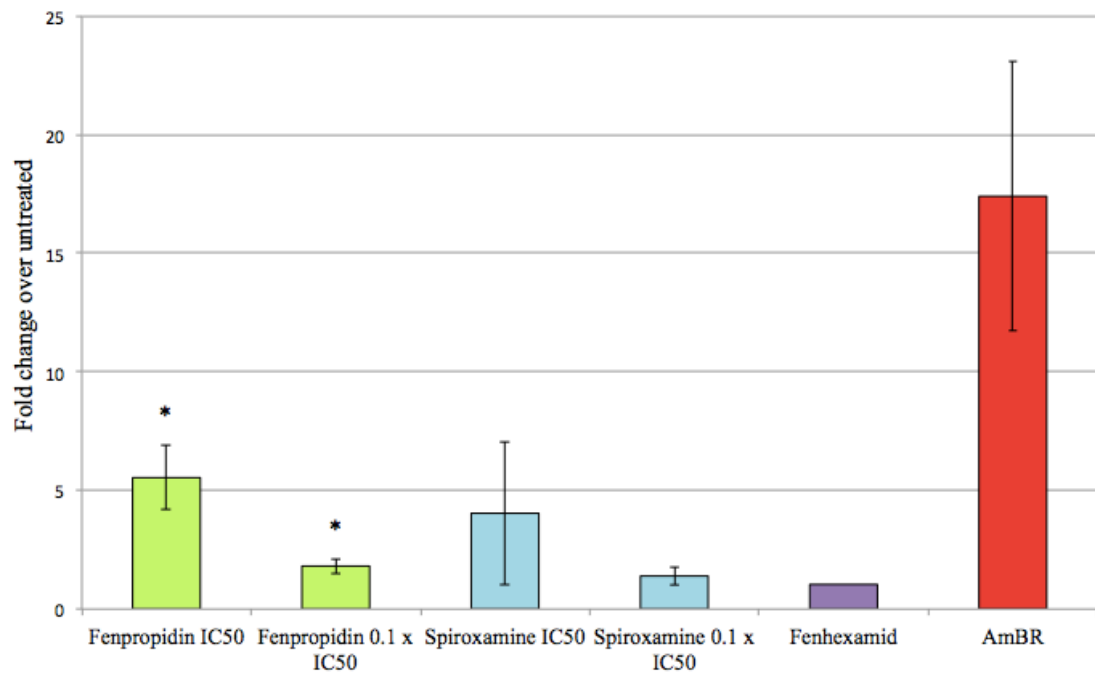


**Figure 4.7** *L. mexicana* Wt sensitivity to AmB after exposure to sterol biosynthesis inhibitors. *L. mexicana* parasites were exposed to fenpropidin and spiroxamine for 24 hours at concentrations shown and to 100  $\mu$ M fenhexamid before withdrawal of the drug and performing AmB sensitivity assays. Fold change equal to EC<sub>50</sub> obtained after drug treatment to EC<sub>50</sub> obtained of untreated wild type parasites, both of the same replicate. AmB resistant cells sensitivity to AmB was used as a control. Error bars represent standard deviation. Asterisk represents significant differences ( $P < 0.05$ ) between untreated and drug treated.  $n = 4$  for fenpropidin and spiroxamine treatment,  $n = 5$  for AmBR cells and  $n = 1$  for fenhexamid treatment. (Data generated by Andrew Pountain)

#### 4.4.2 Ergosterol expression after exposure to Sterol C14-reductase inhibitors and fenhexamid

AmB resistance is accompanied by depleted levels of ergosterol. We have used depletion of ergosterol to differentiate wild-type and the AmB resistant cells using filipin staining (chapter 3). This made us believe that ergosterol could be used as a marker of AmB resistance. The observed reduction in sensitivity to AmB by sterol C14-reductase inhibitors of the wild-type cells led us to test out whether exposure to Sterol C14-reductase inhibitors and fenhexamid would lead to depletion of ergosterol as observed in AmB resistance. We used LC/MS while other studies used GC/MS (Al-Mohammed *et al.*, 2005; Mbongo *et al.*, 1998; Purkait *et al.*, 2012) to assess levels of sterols in AmB resistant cells. Because of the requirement for a simple assay for field use, we adopted the use of UV spectroscopy utilising the presence of conjugated double bonds in ergosterol. Ergosterol is known to absorb UV light at about 282 nm (Naewbanij *et al.*, 1984; Sokol-Anderson *et al.*, 1988). The work was carried out with Andrew Pountain, a student under my supervision.

Following exposure of the wild type cells to the sterol C14-reductase inhibitors and fenhexamid as in section 4.4.1, we showed a clear difference in detected ergosterol between the wild type and AmB resistant parasite samples that were used as controls (Figure 4.8), as monitored at  $\lambda = 281$  nm, consistent with the observation using metabolomics analysis of the two cell lines. Treatment of AmB resistant cells with fenhexamid showed no effect on ergosterol synthesis as compared to the resistant cells not exposed to the drug. Interestingly, spiroxamine- and 100  $\mu$ M fenhexamid-treated wild-type cells showed marked reductions in the absorbance compared to the wild-type cells, indicating a quick adjustment to ergosterol expression by the cells following a 24 hr exposure to the drugs. A surprising result was obtained for fenpropidin which showed more potency in reducing AmB sensitivity (section 4.4.1) by the wild-type cells and yet had a minimal effect on ergosterol expression compared to the wild-type cells which were not exposed to the drug prior to measurement of absorbance.

At this stage we have not validated the spectrophotometric test for ergosterol detection. It would be of interest to use the metabolomics platform to assess the role of fenpropidin and spiroxamine on cells.

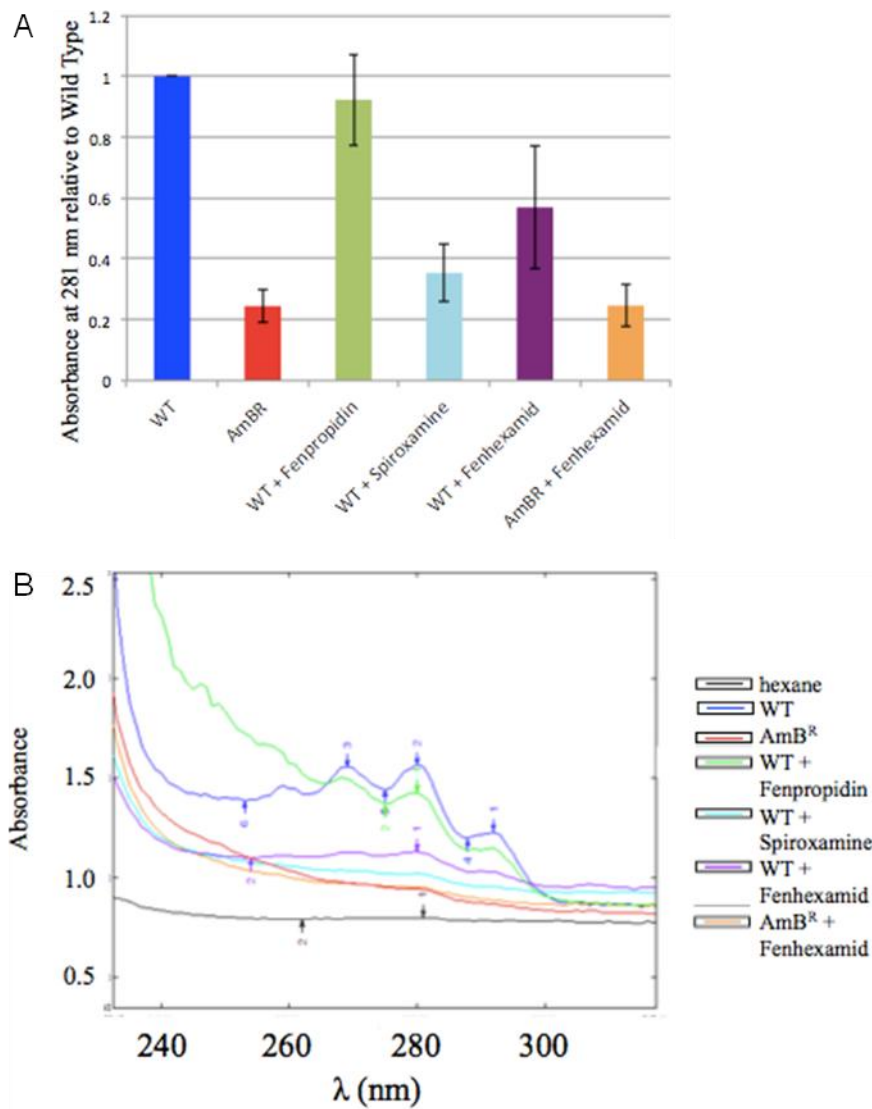


**Figure 4.8 Sterol biosynthetic pathway inhibitors' effect on ergosterol expression.** The UV spectra for ergosterol of wild type and AmB resistant cells exposed to sterol C14-reductase and sterol C3-keto reductase inhibitors was compared to the UV spectra of the two cell line not exposed to the drugs.  $2 \times 10^6$  cells/ml cells were treated with the drugs for 24 hrs prior to sterol extraction with hexane. (A) Measurement of absorbance at 281 nm following exposure to the inhibitors shown.  $n = 2$  for all drug-exposed samples and  $n = 3$  for AmB resistant cells. (B) The UV spectra was recorded from 190 nm to 320 nm on a Shimadzu UV-2550 UV-vis spectrophotometer and analysed using UVProbe software (Shimadzu), ergosterol peak is around 281 nm. Hexane was used as a blank. Data is for two independent experimental replicates. Error bars represent standard deviation. (Data generated by Andrew Pountain)

## 4.5 Sub-cellular localisation of lanosterol 14 $\alpha$ -demethylase

We investigated whether the identified non-synonymous mutation affected the localisation of the lanosterol 14 $\alpha$ -demethylase in the cells by tagging both the wild-type enzyme and the AmB resistant enzyme with green fluorescent protein (GFP) at the C-terminus. The tagged enzymes were expressed in wild-type and AmB resistant cells. The C-terminus was chosen because it is known that

*Leishmania* lanosterol 14 $\alpha$ -demethylase possesses a trans-membrane domain at the N-terminus that might be important to localisation (Hargrove *et al.*, 2011; Verma *et al.*, 2011). A staining of the GFP-tagged lanosterol 14 $\alpha$ -demethylase expressing cells with Mito-Tracker and ER-Tracker for co-localisation of the enzymes revealed co-localisation mainly in the mitochondria with indications of some, albeit minimal, co-localisation in the ER (Figure 4.9). *L. donovani* lanosterol 14 $\alpha$ -demethylase has been shown to localise to the ER, mitochondria and glycosomes (Verma *et al.*, 2011). There were no apparent indications that the mutated enzyme localises differently from the wild-type enzyme in the two cell compartments between the two cell lines. Therefore, the mutation did not seem to affect the localisation of the enzyme in the cell compartments.

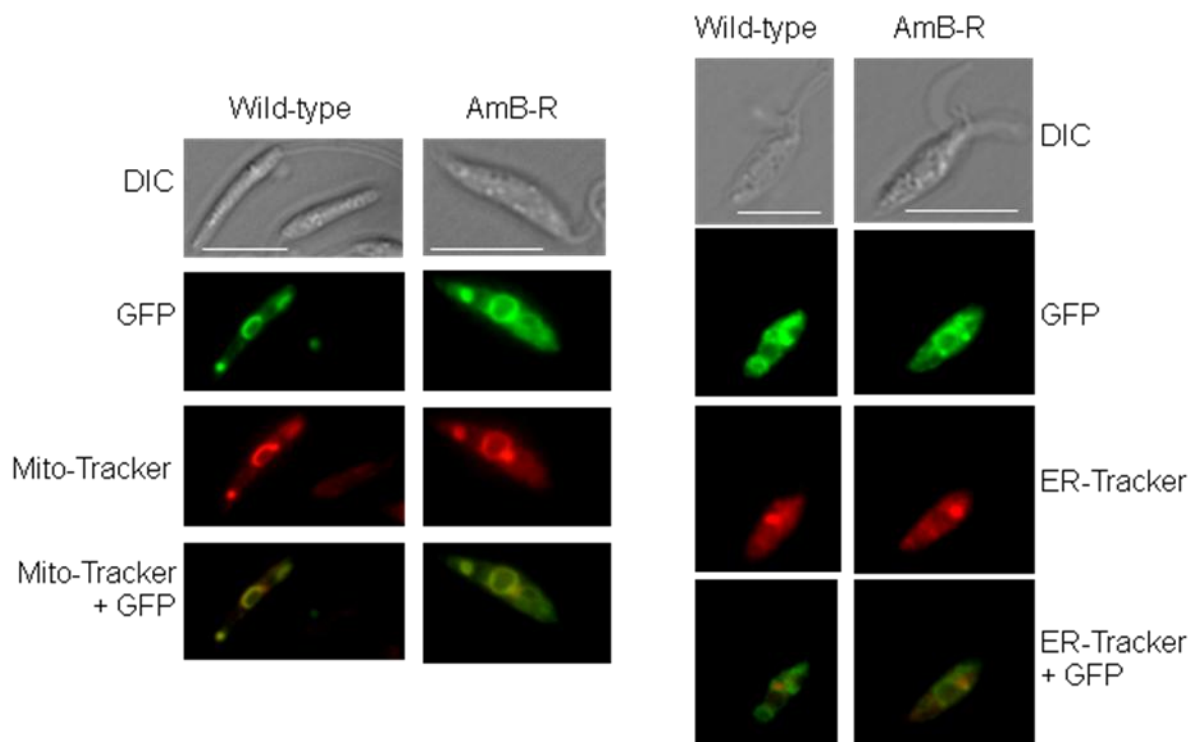


**Figure 4.9** Mito- and ER-Tracker staining of GFP-tagged wild-type and AmB resistant CYP51. Live GFP-tagged CYP51 (lanosterol 14 $\alpha$ -demethylase) expressing wild-type and AmB resistant cells were stained by incubation for 20 – 30 minutes with 1 nM Mito-Tracker or 100 nM ER-Tracker. ER-Tracker stained cells were fixed in 4% formaldehyde for 2 minutes and washed twice in 1 $\times$  PBS. Stained cells were immobilised in 1% low gelling temperature agarose before viewing under oil immersion on a ZEISS Axioplan 2 Imaging fluorescent microscope. GIMP free software was used to merge the images; Bar = 10  $\mu$ m.

## 4.6 Sub-cellular localisation of sterol C14-reductase

Following up on the possibility of lanosterol 14 $\alpha$ -demethylase functioning as a complex with sterol C14-reductase, we investigated whether sterol C14-

reductase would localise in the same compartment of the cell as lanosterol 14 $\alpha$ -demethylase. Staining with Mito-Tracker and ER-Tracker of wild-type and the AmB resistant cells expressing C-terminus GFP-tagged sterol C14-reductase did show minimal co-localisation in the mitochondria but showed strong indications of co-localisation to the endoplasmic reticulum (Figure 4.10). However, there were no apparent indications of alteration in localisation of the sterol C14-reductase in either the endoplasmic reticulum or the mitochondria of the wild-type and AmB resistant cells.

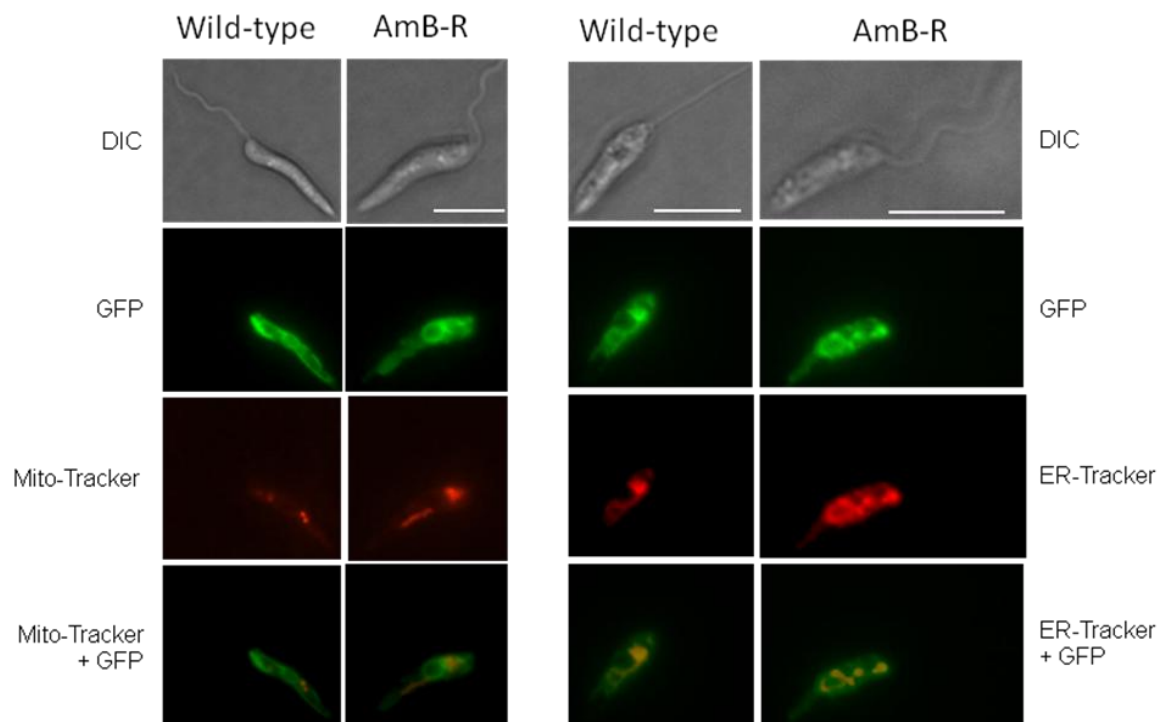


**Figure 4.10** Mito- and ER-Tracker staining of GFP-tagged Wt and AmB-R sterol C14-reductase.

Live GFP-tagged lanosterol 14 $\alpha$ -demethylase expressing wild-type and AmB resistant cells were stained by incubation between 20 to 30 minutes with 1 nM Mito-Tracker or 100 nM ER-Tracker. ER-Tracker stained cells were washed twice in 1 $\times$  PBS following fixing in by incubating in the presence of 4% formaldehyde in growth medium for 2 minutes. Stained cells were immobilised in 1% low gelling temperature agarose before viewing under oil immersion on a ZEISS Axioplan 2 Imaging fluorescent microscope. Images were merged using GIMP; Bar = 10  $\mu$ m.

GFP tagged lanosterol 14 $\alpha$ -demethylase and sterol C14-reductase localises differently and therefore the lanosterol 14 $\alpha$ -demethylase mutation is not likely to cause a lanosterol 14 $\alpha$ -demethylase and sterol C14-reductase decoupling. Moreover, Julie Kovarova and Andrew Pountain showed no pull-down partners (lanosterol 14 $\alpha$ -demethylase and sterol C14-reductase) by immunoprecipitation using anti-GFP antibodies. However, yeast has been shown to have sterol

biosynthetic enzymes function as a complex called an "ergosome" that allows for protein-protein interaction among them. Lanosterol 14 $\alpha$ -demethylase is found at the core of the ergosome with Sterol C4-methyloxidase and sterol C3-keto reductase and share more interactions with the other enzymes of the pathway. Apparently, sterol C14-reductase has been shown to have a moderate interaction with lanosterol 14 $\alpha$ -demethylase in yeast (Mo and Bard, 2005). It must be mentioned that these enzymes are both localised to ER while lanosterol 14 $\alpha$ -demethylase also localises in the cytoplasm in yeast (Natter *et al.*, 2005).

#### **4.7 Cloning and over-expression of lanosterol 14 $\alpha$ -demethylase in *E. coli***

The restoration of susceptibility to AmB of AmB resistant cells expressing an extra-chromosomal copy of lanosterol14 $\alpha$ -demethylase gene, led us to clone whole genes of both the wild-type and mutated enzymes in *E. coli* for over-expression and eventual comparison of their activity. The enzymes cloned into BL21 *E. coli* did not show over-expression of the enzymes. However, the two enzymes were over-expressed in the Rosetta and Rosetta pLysS competent cells (Figure 4.11 A). Rosetta *E. coli* is suitable for over-expression of the proteins whose genes contain codons that are rare in *E. coli*. However, we were unable to purify the enzyme using the Ni-NTA spin columns (Qiagen). The inability to purify the protein was attributed to the protein being expressed as inclusion bodies. Inclusion bodies in *E. coli* are known to be a major impediment to isolation of overexpressed proteins that are not *E. coli* endogenous proteins (Ventura and Villaverde, 2006).

We initially used the whole gene sequence to clone lanosterol 14 $\alpha$ -demethylase, other studies have used truncated gene sequences to clone the enzyme (Hargrove *et al.*, 2011). With the removal of the trans-membrane domain comprising of 23 residues at the N-terminus, Dr. Jean-Christophe Le Bayon got the soluble protein (Figure 5.11 B) from inclusion bodies using Rosetta *E. coli*. Therefore determination and comparison of activity of the wild-type and mutated enzymes will form part of future work.

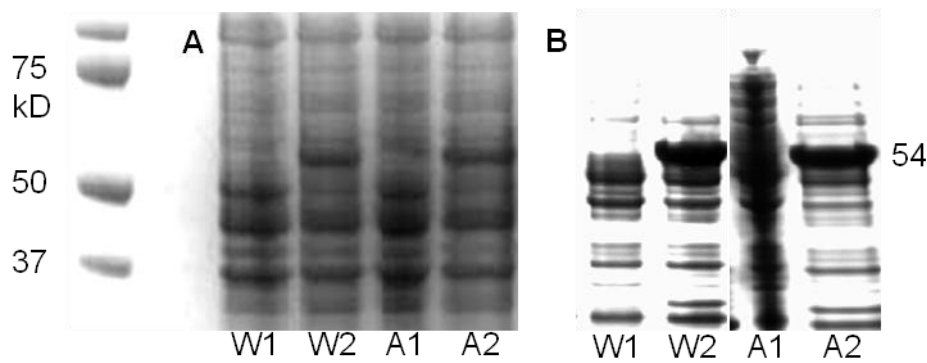


**Figure 4.11 Over-expression of Wild-type and AmB resistant lanosterol 14 $\alpha$ -demethylase.** Wild-type and AmB resistant lanosterol 14 $\alpha$ -demethylase (CYP51s) were inserted into pET30 over-expression vector and cloned into Rosetta *E. coli* competent cells. *E. coli* were grown at 37°C and induced with 1 mM IPTG when O.D reached 0.6 for three hours. Bacteria was boiled in loading dye at 95°C to obtain a crude extract of the proteins which were resolved on NuPAGE Bis-Tris Mini Gels 200 volts. W1 = un-induced wild-type *E.coli* with the wild-type CYP51; W2 = Induced wild-type *E.coli* with the wild-type CYP51; A1 = un-induced wild-type *E.coli* with the AmB resistant CYP51; A2 = Induced wild-type *E.coli* with the wild-type CYP51. In (A) Over-expression of full length gene sequence of lanosterol 14 $\alpha$ -demethylase and (B) over-expression of a truncated sequence of lanosterol 14 $\alpha$ -demethylase. Bacteria was lysed in 10mM Imidazole containing 300mM NaCl, 50mM sodium phosphate (pH8.0) in the presence of Lysozyme and Benzonase nuclease. The pellet was re-suspended in 5M Urea/ 5mM EDTA in PBS and incubated for 30 min at 4°C prior to Freezing at -20°C for 20 min and defrosting. The supernatant was run on a gel as above following centrifugation at 13.000 x g for 30 min at 4°C

## 4.8 Discussion

Lanosterol 14 $\alpha$ -demethylase is an enzyme found in most eukaryotic organisms including plants, fungi, animals and protozoa. It belongs to the cytochrome P450 group of enzymes. Lanosterol 14 $\alpha$ -demethylase is an important enzyme involved in synthesis of ergosterol in fungi and *leishmania* species and cholesterol in mammals. These molecules are important for the formation and function of cell membranes (Lepesheva and Waterman, 2011b). *L. mexicana* shares 97% of its amino acid sequence with *L. infantum*. Both *L. mexicana* and *L. infantum* have 480 amino acid in their structure with a mass of approximately 54 kD (Hargrove *et al.*, 2011).

### 4.8.1 N176I mutation affected a conserved amino acid residue

Mutations of conserved residues of lanosterol 14 $\alpha$ -demethylase can elicit dramatic changes to the functionality of the enzyme. For instance mutation of phyla specific I105F in *T. cruzi* shifts its substrate to that of plants (Lepesheva *et al.*, 2006). Point mutations, including those of conserved amino acid residues, have also been implicated in resistance to miltefosine (Coelho *et al.*, 2012; Perez-Victoria *et al.*, 2003a; Perez-Victoria *et al.*, 2003b). T420N in *L. donovani*

and, P782T, G852D, and G565R in *L. infantum* are some of the point mutations that have been shown to inactivate the miltefosine transporter and are located in conserved sequences of the miltefosine transporter protein (Coelho *et al.*, 2012; Perez-Victoria *et al.*, 2003b). The point mutation in lanosterol 14 $\alpha$ -demethylase in our study was found to affect a conserved residue among trypanosomatids whose sequences were assessed. The conservation of the mutated residue suggests some importance of the residue to these species. The mutation involved a substitution of asparagine with isoleucine in one of the  $\alpha$ -helices of the predicted secondary structure of the enzyme. The occurrence of the helix in this part of the enzyme corresponds to an  $\alpha$ E-helix in the secondary structure of *L. infantum* (Hargrove *et al.*, 2011). Asparagine has a polar uncharged side chain while isoleucine has a bulky and more hydrophobic side chain. Isoleucine has the capability to form more stabilised  $\alpha$ -helices than asparagine (Monera *et al.*, 1995). The introduction of a bulky side chain that has the capability to destabilize the protein may have been compensated for by the isoleucine's ability to form stabilised  $\alpha$ -helices. Therefore, replacement of a small polar side chain with a more hydrophobic bulky side chain suggests a change in the overall conformation of the protein. Moreover, asparagine is able to form hydrogen bonds and therefore its replacement with isoleucine, which is able to form hydrophobic bonds and not hydrogen bonds, is likely to alter the native protein structure. Despite the mutation being outside the active site this may possibly have had an effect on the enzyme function. The alteration in the enzyme function may have led to perturbation of the sterol biosynthetic pathway that aims at protecting the parasites against the effects of AmB.

#### **4.8.2 Restoration of ergosterol synthesis following complementation of AmB-R cells with wild-type lanosterol 14 $\alpha$ -demethylase**

The role of the non-synonymous mutation in the lanosterol 14 $\alpha$ -demethylase gene in Amphotericin B resistance was assessed by use of complementation of the AmB resistant cells with an episomal vector carrying the wild-type copy of the enzyme. This strategy has been used successfully in other studies to restore an altered phenotype in leishmania (Roberts, 2011; Verma *et al.*, 2011). The complementation of the AmB resistant cells with wild-type gene of lanosterol 14 $\alpha$ -demethylase restored ergosterol levels in these cells. The restoration of

ergosterol levels in AmB resistant cells expressing episomal wild-type lanosterol 14 $\alpha$ -demethylase is in agreement with the restoration of ergosterol levels in lanosterol 14 $\alpha$ -demethylase single knock-out *L. donovani*. Ergosterol level restoration in the *L. donovani* lanosterol 14 $\alpha$ -demethylase single knock-out complemented with wild-type lanosterol 14 $\alpha$ -demethylase was twice that in the single knock-out lanosterol 14 $\alpha$ -demethylase cells but half that in the wild-type cells (Verma *et al.*, 2011). However, in our study we witnessed a full restoration of ergosterol in AmB resistant cells complemented with wild-type lanosterol 14 $\alpha$ -demethylase.

#### **4.8.2.1 Restoration of wild-type-like tolerancy of antileishmanial drugs by AmB-R**

Associated with complementation of AmB resistant cells with wild-type lanosterol 14 $\alpha$ -demethylase resulting in restoration of ergosterol levels was restoration of susceptibility to AmB. This implies that the restored levels of ergosterol resulted in restoration of the drug's target in these cells resulting in their losing the tolerance level of AmB they had acquired when they became resistant to the drug. This result further confirms earlier reports of the dependence of AmB's action on the presence of ergosterol in cells in leishmania. Thus, *in vitro* AmB resistance in leishmania has been associated with inhibition of synthesis of ergosterol (Al-Mohammed *et al.*, 2005; Mbongo *et al.*, 1998; Purkait *et al.*, 2012). We also observed the restoration of tolerance of pentamidine by the re-expressers cells to the same level as the wild-type cells. In view of the increased uptake of pentamidine by AmB resistant cells with depleted ergosterol levels than the wild-type, the restoration of ergosterol in the re-expressor would suggest reduced uptake of pentamidine. This reduces accumulation of the drug in the cells leading to reduced toxicity. The restoration of tolerance to pentamidine amid restoration of ergosterol would also suggest the restored ergosterol was able to protect the cells through its antioxidant properties as has been reported in yeast (Dupont *et al.*, 2012; Landolfo *et al.*, 2010) against ROS since pentamidine has been shown to induce accumulation of ROS in wild-type *L. infantum* (Moreira *et al.*, 2011).

Restoration of sensitivity to miltefosine was observed after complementation of AmB resistance cells with the wild-type lanosterol 14 $\alpha$ -demethylase. In fact, the

re-expressor cells were more sensitive to miltefosine than the wild-type cells with a fold-change in  $EC_{50}$  of 0.62. Resistance to miltefosine has been attributed to point mutation in the gene for the membrane bound miltefosine transporter which result in reduced translocation of the drug into the cells (Coelho *et al.*, 2012; Cojean *et al.*, 2012; Perez-Victoria *et al.*, 2003a; Perez-Victoria *et al.*, 2003b). Indeed chemical depletion of sterols from the membranes of wild-type and miltefosine resistant *L. donovani* resulted in increased tolerance of miltefosine by both wild-type and miltefosine resistant cells (Saint-Pierre-Chazalet *et al.*, 2009). Therefore, reversing of tolerance to miltefosine following restoration of ergosterol in the re-expressor cells in this case would suggest the removal of ergosterol from the membrane may have affected the function of the miltefosine transporter possibly due to changes to the conformation structure of the transporter. Indeed it has been shown in nematodes (*Haemonchus cortortus*) that the number of active, albeit with the correct conformation, membrane pumps (the *P*-glycoproteins) increased, to an optimum, as the concentration of free cholesterol (a sterol) increased. It was suggested that the correct conformation of these proteins required a given concentration and distribution of cholesterol in the membranes (Riou *et al.*, 2007). Treatment of *S. cerevisiae* with AmB prior to DNA microarray analysis revealed up-regulation and down-regulation of various membrane proteins involved in nutrient and ion transport across the membrane to counter the loss of these through AmB pore formation (Zhang *et al.*, 2002). A related polyene antibiotic, natamycin, was shown to inhibit membrane transport proteins, including amino acid transporters and the glucose transporter proteins in fungi (*Aspergillus niger*) and yeast (*S. cerevisiae*) (te Welscher *et al.*, 2012). Although natamycin does not form membrane pores like AmB, it is believed to bind ergosterol like AmB. Because different types of proteins were inhibited it was thought that natamycin was able to inhibit the membrane transport proteins by altering ergosterol-protein interaction (te Welscher *et al.*, 2012) and probably resulting in altered conformations of these proteins and hence their inhibition.

Interestingly the complementation of AmB resistance with wild-type lanosterol 14 $\alpha$ -demethylase resulting in restoration of ergosterol levels was accompanied by increased resistance to ketoconazole with a fold-change in  $EC_{50}$  values from 1.60 for the AmB resistant cells compared to the wild-type cells to 2.60 for the

AmB resistant cells complemented with the wild-type lanosterol 14 $\alpha$ -demethylase as compared to the wild-type cells. Ketoconazole belongs to azole compounds that are known to target lanosterol 14 $\alpha$ -demethylase and have been shown to be potent against leishmaniasis (Beach *et al.*, 1988; de Macedo-Silva *et al.*, 2013). Therefore this result suggests an increased drug target resulted in the mildly increased resistance to the drug in line with one of the known strategies of increased drug target employed by parasites to become resistant to a drug. Indeed our result is in agreement with *in vitro* ketoconazole resistance by *L. amazonensis*, where up-regulation of lanosterol 14 $\alpha$ -demethylase resulted in resistance to the drug with a five-fold increase in IC<sub>50</sub> value (Andrade-Neto *et al.*, 2012).

#### **4.8.3 Lanosterol 14 $\alpha$ -demethylase interaction with other sterol biosynthetic pathway enzymes**

Our lack of detection of lanosterol, the substrate of lanosterol 14 $\alpha$ -demethylase, but its product 4,4-dimethylcholesta-8, 14, 24-trien-3 $\beta$ -ol, despite a lack of indication of any changes to the gene sequence of the enzyme that comes after lanosterol 14 $\alpha$ -demethylase, sterol C14-reductase, in the sterol biosynthetic pathway (Figure 1.8), led us to believe that lanosterol 14 $\alpha$ -demethylase may have specific interactions with sterol C14-reductase. Unique protein-protein interactions to form functional enzyme complexes called “ergosomes” in sterol biosynthetic pathway have been reported in yeast. The complexes have been reported to function in association with other enzymes of the pathway (Mo and Bard, 2005). These interactions can be assumed to provide an efficient way of channelling metabolites from one enzyme to the next in the pathway. The centre of the ergosome is occupied by lanosterol 14 $\alpha$ -demethylase, sterol C4-methyloxidase, sterol C3-keto reductase and a protein designated as erg28p (Mo and Bard, 2005). Erg28p provides a means of bringing sterol C4-methyloxidase, sterol C3-keto reductase and sterol C3 dehydrogenase together to enhance their interactions (Gachotte *et al.*, 2001). If an “ergosome” exists in *Leishmania*, it may be different from that in yeast based on the localisation to different cellular compartments of the sterol biosynthetic enzymes. This would mean that lanosterol 14 $\alpha$ -demethylase cannot bind sterol C14-reductase and therefore may need to bind a membrane protein, like the role of a tether played by erg28p in yeast (Gachotte *et al.*, 2001), to efficiently pass on or carry its product to

another cell compartment. Lanosterol 14 $\alpha$ -demethylase has been shown to show specificity to more than one substrate in *L. infantum* (Hargrove *et al.*, 2011). Therefore, existence of an ergosome may also serve the purpose of making sure that the correct substrates are channelled to the next enzyme in the pathway. The fact that the N176I mutation in lanosterol 14 $\alpha$ -demethylase does not seem to affect the activity of the enzyme leading to the accumulation of its product, 4,4 dimethylcholesta-8, 14, 24-trien-3 $\beta$ -ol, it suggests instead an altered transfer of the metabolite to the next enzyme in the pathway. This could happen by a disrupted protein-protein interaction of the enzymes. Indeed, lanosterol 14 $\alpha$ -demethylase has been shown to have a weak interaction with sterol C14-reductase in yeast (Mo and Bard, 2005). In leishmania, however, the demethylase and reductase seem to have different localisations. Therefore, failure to bind to a different element involved in the pathway appears to be responsible.

It is interesting to note that inhibition of yeast's sterol C14-reductase with fenpropidin results in accumulation of 4, 4-dimethylcholesta-8, 14, 24-trienol (Baloch *et al.*, 1984). It would be interesting to investigate if a similar increase occurs in fenpropidin treated leishmania. However, ketoconazole's specific inhibition of lanosterol 14 $\alpha$ -demethylase in leishmania does not appear to lead to accumulation of lanosterol in such cells (Beach *et al.*, 1988). It was suggested lanosterol is metabolised by non P450 lanosterol 4 $\alpha$ -demethylase and isomerised to 4 $\alpha$ , 14 $\alpha$ -dimethylzymosterol, the major sterol detected in the ketoconazole inhibited leishmania cells (Beach *et al.*, 1988). As lanosterol 14 $\alpha$ -demethylase appears to remain active, producing 4,4 dimethylcholesta-8, 14, 24-trien-3 $\beta$ -ol, it is not surprising sensitivity close to wild-type, presumably as ketoconazole prevents production of 4,4 dimethylcholesta-8, 14, 24-trien-3 $\beta$ -ol and thus cannot produce what we presume to be a replacement sterol for ergosterol. The fact that other studies show a rise in 4,4 dimethylcholesta-8, 14, 24-trien-3 $\beta$ -ol indicate that this sterol and not the subsequent intermediates in the pathway might be able to replace ergosterol, thus it might be that lanosterol 14 $\alpha$ -demethylase mutations, similar to our N176I, underlie AmB resistance in other studies.

Apparently sterol C4-demethylase, (ERG25 or EC 1.14.13.72; C4-Sterol methyl oxidase), of *S. cerevisiae* catalyses the conversion of 4, 4-dimethylzymosterol to 4 $\alpha$ -methylzymosterol through four intermediates (Figure 4.12), 4 $\alpha$ -Hydroxymethyl-4 $\beta$ -methyl-5 $\alpha$ -cholesta-8-24-dien-3 $\beta$ -ol, 4 $\alpha$ -formyl-4 $\beta$ -methyl-5 $\alpha$ -cholesta-8-24-dien-3 $\beta$ -ol, 4-methylzymosterol-4-carboxylic acid, 3-keto, 4-methylzymosterol (Bard *et al.*, 1996).

We were able to detect elevated levels of, 4 $\alpha$ -formyl-4 $\beta$ -methyl-5 $\alpha$ -cholesta-8-24-dien-3 $\beta$ -ol (Table 3.5) an intermediate product of sterol C4-methyl oxidase and a substrate of sterol C3-dehydrogense (sterol C4-decarboxylase) (Figure 4.12), both of these enzymes have been shown to have moderate interactions with lanosterol 14 $\alpha$ -demethylase in yeast (Mo and Bard, 2005). Sterol C4-methyloxidase is not listed in the sterol biosynthetic pathway of leishmania. However, a blast search using *S. cerevisiae*'s C4-Sterol methyloxidase protein sequence gave a hypothetical protein with unknown function (LmxM.36.2540.1) in GeneDB for *L. mexicana*. Therefore a disturbance to the sterol biosynthesis enzyme complex, as maybe the case in this study due to the mutated lanosterol 14 $\alpha$ -demethylase, assuming sterol C4-methyl oxidase exist in leishmania, may help explain the elevated levels of 4 $\alpha$ -formyl-4 $\beta$ -methyl-5 $\alpha$ -cholesta-8-24-dien-3 $\beta$ -ol that we observed. It seems likely that leishmania lanosterol C14 $\alpha$ -demethylase functions in complex with other enzymes.

#### **4.8.4 Effect of sterol C14-reductors inhibitors on wild-type and AmB resistant *L. mexicana***

An assessment of the effect of sterol C14-reductase specific inhibitors showed varying potency to both the wild-type and AmB resistant cells. The interpretation of the opposing effect of amorolfine and fenpropidin towards the AmB resistant cells was quite challenging although the results did not seem to indicate whether the altered sequence of lanosterol 14 $\alpha$ -demethylase had affected sterol C14-reductase in any way. However, the sterol C14-reductase inhibitors did show varying potency towards the wild-type and AmB resistant cells. It is unknown how well these compounds enter these cells, nor if they are

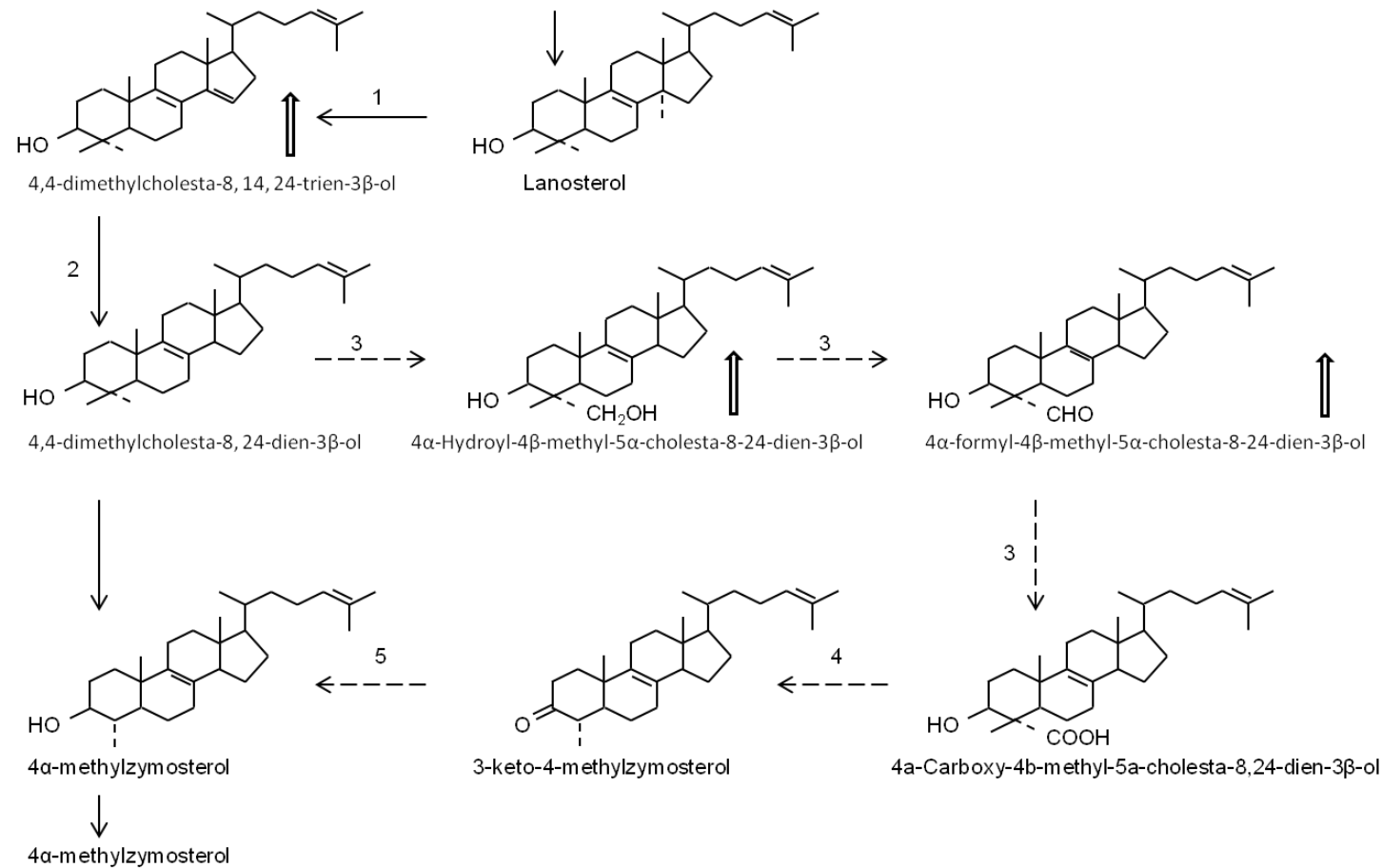


**Figure 4.12** 4, 4-dimethylcholesta-8, 14, 24-trien-3 $\beta$ -ol to 4 $\alpha$ -zymosterol part of the sterol biosynthetic pathway of yeast. The reactions shown with dashed arrows represent reactions as they occur in yeast and yet to be reported in *Leishmania*. The metabolites that were elevated in the metabolomic analysis of our AmB resistant *Leishmania mexicana* promastigote are indicated by an upward pointed arrow. 1 – lanosterol 14 $\alpha$ -demethylase; 2 – sterol C14-reductase; 3 – sterol C4-methyl oxidase; 4 – sterol C3-decarboxylase (-dehydrogenase). (Reaction scheme adapted from Mo and Bard, 2005).

metabolised or necessary potent inhibitors of the enzyme. Indeed, it is possible they affect different enzymes in leishmania and we did not assess these here. Sterol C14-reductase inhibitors have indicated the possibility of inducing resistance to AmB to varying degrees. Despite Fenpropidin inducing a marked increase of tolerance, 5.5-fold increase in EC<sub>50</sub> value, by wild-type to AmB it showed the least reduction in ergosterol synthesis at least judged by the adaption of a spectroscopic method. This result may suggest a mechanism of action that is not directly connected to ergosterol synthesis while fenhexamid and spiroxamine show a link to ergosterol synthesis. Based on these results, the use of a UV spectroscopy based assay to identify AmB resistant parasites in the field would pose a challenge of determining the level of ergosterol which would constitute that synthesised by a resistant parasite.

Indeed, the results with this assay would be misleading in a situation where the parasites have been exposed to other drugs that are able to induce reduction of ergosterol content of cells. This is due to the fact that cells treated with sterol C14-reductase inhibitors for 24 hours also showed reduced ergosterol content. It would be interesting in future work to treat the wild-type parasites with the sterol C14-reductase inhibitors and AmB, and carry out the filipin staining assay to observe whether the treated cells would stain with filipin.

#### **4.8.5 Subcellular localisation of lanosterol 14 $\alpha$ -demethylase and Sterol C14-reductase**

We observed strong indications of lanosterol 14 $\alpha$ -demethylase localising to the mitochondria and sterol C14-reductase to the endoplasmic reticulum. The two enzymes may have possible interaction in the endoplasmic reticulum where lanosterol 14 $\alpha$ -demethylase showed a possible low level co-localisation. Localisation of lanosterol 14 $\alpha$ -demethylase in the mitochondria and endoplasmic reticulum is in agreement with that of lanosterol 14 $\alpha$ -demethylase (*L. donovani* lanosterol 14 $\alpha$ -demethylase shares 98% of its amino acid residue sequence with *L. mexicana* lanosterol 14 $\alpha$ -demethylase) in *L. donovani* (Verma *et al.*, 2011), although our results show much more localisation to the mitochondrion than to the endoplasmic reticulum in contrast to what was reported in *L. donovani* (Verma *et al.*, 2011). An interaction of the two enzymes may also be possible in the endoplasmic reticulum because sterol C14-reductase also showed

localisation to the endoplasmic reticulum. Overall, co-localisation experiments of lanosterol 14 $\alpha$ -demethylase did not indicate any apparent alteration in the localisation of the enzyme associated with the N176I mutation.

#### **4.8.6 Over-expression of *L. mexicana* lanosterol 14 $\alpha$ -demethylase in *E. coli*.**

Our inability to express active lanosterol 14 $\alpha$ -demethylase in *E. coli* may have been due to its being expressed as inclusion bodies. We were able to detect overexpression when we run crude whole cell extracts on the gel but could not purify the protein. Inclusion bodies result from the expression of the protein at rates that are over the concentration that can be protected by chaperones, that protect against misfolding (Wang, 2009). Many leishmania proteins are reportedly insoluble such that their overexpression in *E. coli* results in formation of inclusion bodies (Bhargava *et al.*, 2010; Hargrove *et al.*, 2011). The overexpression of *L. donovani* squalene synthase resulted in 70% of the enzyme being expressed as inclusion bodies at optimised conditions of bacterial culture growth temperature and concentration of IPTG (Bhargava *et al.*, 2010). We used the His-tag for purification purposes. However, the use of the His-tag for purification purposes can also pose a problem of purifying proteins due a possibility of the His tag being masked due to misfolding of the proteins as they emerge from the ribosomes (Bhargava *et al.*, 2010). Therefore, inclusion body formation and masking of the His-tag were possible reasons for our inability to purify the protein. *L. infantum* C lanosterol 14 $\alpha$ -demethylase was overexpressed following 23 amino acid residue truncation of the N-terminus of the protein (Hargrove *et al.*, 2011). We initially tried to overexpress the entire full protein sequence with no success. With the removal of the 23 amino acid residues forming part of the trans-membrane domain, the protein was overexpressed by Jean-Christophe. Determination and comparison of the activities of the wild-type and mutated enzymes has been planned for our future work.

## Chapter Five

### 5 Isometamidium resistance in BSF *T. b. brucei*

#### 5.1 Introduction

Resistance to trypanocidal drugs is of major concern in veterinary productivity in Africa (Geerts *et al.*, 2001). Isometamidium is used as a prophylactic drug because it stays in circulation after administration for up-to 4 months (Eisler *et al.*, 1996). However, concentration of the drug in circulation decreases over the 4 months period such that infections that may occur by the end of the period, and means that parasites are exposed to waning concentrations of the drug. The declining concentration of the drug in circulation may promote the development of resistance to the drug (Matovu *et al.*, 2001). Drug resistance to isometamidium has been reported in most parts of Africa for a long time, although the mode of action and mechanism of resistance is not fully known. However, possible targets and mechanisms of resistance to isometamidium were recognised as early as 1993 (Kinabo, 1993). Strides have been made to understand some of these processes and possible mechanisms of resistance in *Trypanosoma* species. The kinetoplast has been proposed as the target and reduction in mitochondrial membrane potential has been implicated in both isometamidium and ethidium bromide resistance (Chowdhury *et al.*, 2010; Wilkes *et al.*, 1997). Understanding modes of action and resistance mechanism may help delay selection and spread of resistance.

We have initiated a characterization of isometamidium resistance. Our approach has been to elucidate differences between the wild type and selected isometamidium-resistant lines, with the purpose of identifying characteristics, or markers, that are associated with resistance development. To achieve our goal, we characterised isometamidium resistant *T. brucei* bloodstream forms in terms of alterations in growth phenotype, internal morphology of mitochondria, mitochondrial membrane potential, metabolite alterations and cross-resistance to other trypanocidal drugs.

## 5.2 Results

### 5.2.1 Induction of isometamidium resistance in BSF *T. b. brucei*

Isometamidium resistant *T. brucei* were selected *in vitro* in order to characterise the drug resistant parasites. The selection for isometamidium resistance in bloodstream forms over 134 days achieved a ten-fold increase in the EC<sub>50</sub> value relative to that of the wild type. Thereafter, the selection for higher resistance occurred more quickly (Figure 5.1). The fold increase in isometamidium EC<sub>50</sub> values, over the period of isometamidium resistance induction was 2.99, 10.57 and 94.17 for clones growing in the presence of 4 nM, 40 nM and 1 µM, respectively. These fold-increases in EC<sub>50</sub> represented significant differences (Unpaired student t-test; P = 0.0004, P < 0.0001, P < 0.0001, respectively) between isometamidium resistant clones and the wild-type cells.

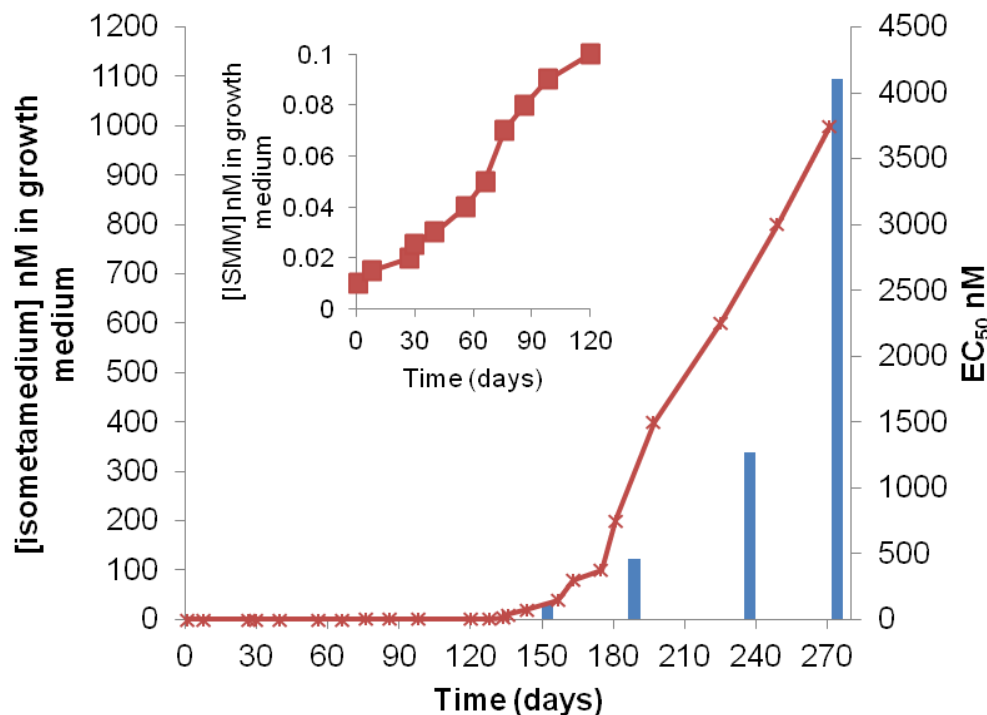


**Figure 5.1** Isometamidium resistance selection in *T. brucei* 427 bloodstream forms. Crosses and left y-axis show concentration of isometamidium in which the cells grew while the bars and the right y-axis show the EC<sub>50</sub> values for the clones growing in the presence of 4, 40 400 and 1, 000 nM isometamidium at various stages of the isometamidium resistance induction. The insert shows the induction of resistance at lower concentrations of the drug, from 0.01 nM of the drug on day 1 and 0.1 nM after 120 days. Resistance was selected for by stepwise increase of drug concentration in the growth medium.

Interestingly we were unable to induce isometamidium resistance in *T. brucei* 927 procyclic forms. Cells exposed to low concentrations of isometamidium could not survive beyond a third passage. Twenty nanomolar isometamidium was

the maximum dose in which procyclic *T. brucei* survived but these cells could not be grown beyond a fourth passage. Attempts were made to grow the cells beyond 20 nM isometamidium for the whole duration of the resistance induction in the bloodstream forms.

## 5.2.2 Characterisation of isometamidium resistant strains

### 5.2.2.1 Growth phenotype

To assess whether there was an effect on the growth phenotype of the derived isometamidium (ISMM) resistant bloodstream *T. brucei*, the growth of the resistant lines were compared to that of the wild-type (Figure 5.2). There was a gradual slowing in growth of the resistant cells as the level of resistance increased.

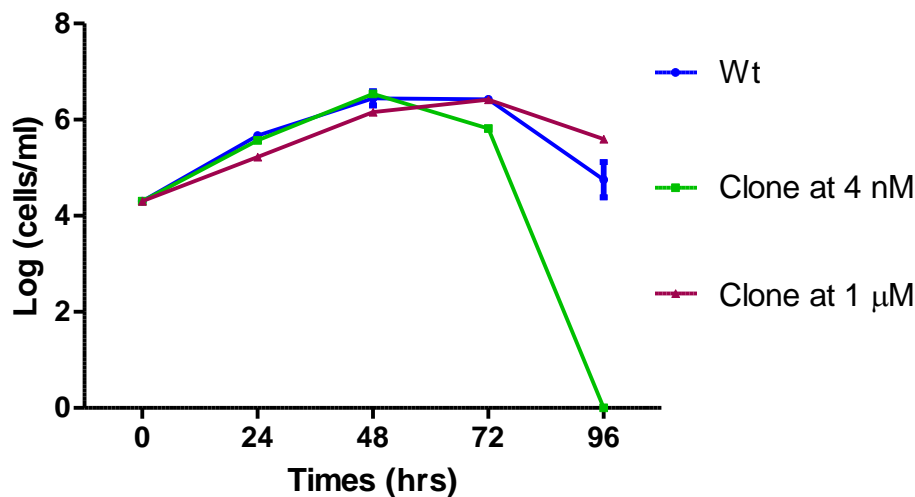


**Figure 5.2 Comparison of growth of *T. brucei* Wt and derived ISMM resistant cells.** The growth curves were made by growing cloned cells in HMI-9 at a starting density of  $2 \times 10^4$  cells/ml and counting the cells every 24 hours using the improved Haemocytometer under the light microscope. The growth curve plots are of three replicates.

The growth phenotype was also assessed in minimal medium (CMM) (Creek *et al.*, 2013). Interestingly, CMM allowed normal growth of wild-type cells but not of the derived resistant cells, (especially for the clones growing in the presence of the higher isometamidium concentration). Clones growing in the presence of isometamidium in HMI-9 starting from 400 nM to 1 µM isometamidium, failed to grow in CMM in the absence of isometamidium. The growth phenotypes of these clones were even more affected when grown in CMM in the presence of ISMM. An attempt to replace the omitted nutrients one by one and in various

combinations was made but no success was achieved in identifying the missing ingredients that could allow the derived resistant lines to proliferate in this medium. The derived isometamidium resistant *T. brucei* showed reduced growth phenotype and hence reached the late log-phase after 72 hours compared to 48 hours for the wild-type in commercial HMI-9 (Figure 5.2). It is worth noting that the derived resistant cells died more quickly than the wild-type cells once they reached the maximum density of growth.

### 5.2.2.2 Cross-resistance of isometamidium resistant trypanosomes to other anti-trypanocides

Derived isometamidium resistant clones were assessed for isometamidium cross-resistance to other trypanocidal drugs using the modified alamar blue assay. This was achieved by comparing the  $EC_{50}$  values of various drugs tested for the wild-type and the derived isometamidium resistant clones. Isometamidium cross-resistance to the widely used trypanocides in AAT are shown in figure 5.3 and HAT trypanocidal drugs (Table 5.1).

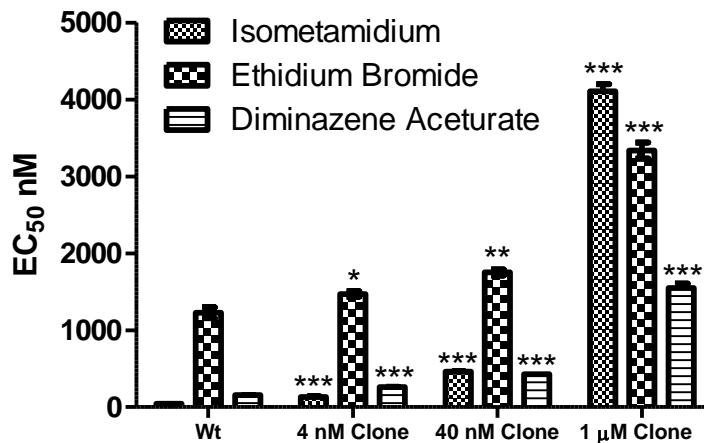


Figure 5.3 Isometamidium cross-resistance to ethidium bromide and diminazene acetate. The  $EC_{50}$  values were determined using the modified Alamar blue assay. An analysis of at least three independent replicates was done and the significance of the difference in  $EC_{50}$  expressed as Mean  $\pm$  SEM between the Wt and each derived ISMM clone was determined using the unpaired t-test in GraphPad Prism software. \*  $P = 0.04$ ; \*\*  $P = 0.003$ ; \*\*\*  $P < 0.0004$ .

	Wt	4 nM Clone		40 nM Clone		1 $\mu$ M Clone	
	EC <sub>50</sub> ( $\mu$ M)	EC <sub>50</sub> ( $\mu$ M)	Fold-change	EC <sub>50</sub> ( $\mu$ M)	Fold-change	EC <sub>50</sub> ( $\mu$ M)	Fold-change
ISMM	0.044 $\pm$ 0.001	0.131 $\pm$ 0.008	3.0	0.461 $\pm$ 0.006	10.47	4.106 $\pm$ 0.092	93.31
DA	0.156 $\pm$ 0.002	0.261 $\pm$ 0.0046	1.67	0.427 $\pm$ 0.0016	2.74	1.548 $\pm$ 0.057	9.92
EtBr	1.23 $\pm$ 0.07	1.469 $\pm$ 0.04	1.19	1.75 $\pm$ 0.04	1.42	3.336 $\pm$ 0.11	2.71
Pentamidine	0.007 $\pm$ 0.0001	0.014 $\pm$ 0.0004	2	0.037 $\pm$ 0.0009	5.3	0.160 $\pm$ 0.008	22.9
Melarsoprol	0.023 $\pm$ 0.0003	0.022 $\pm$ 0.0002	0.96	0.023 $\pm$ 0.0004	1.0	0.023 $\pm$ 0.0005	1.0
Eflornithine	109.3 $\pm$ 2.8	76.6 $\pm$ 1.7	0.7	70.4 $\pm$ 2.3	0.6	40.5 $\pm$ 0.9	0.4

**Table 5.1 Cross-resistance of isometamidium resistant trypanosomes to AAT and HAT trypanocides.**

Cross-resistance of isometamidium (ISMM) resistant trypanosomes to diminazene aceturate (DA) ethidium bromide (EtBr), pentamidine, melarsoprol and eflornithine was determined using the alamar blue assay over 48 hrs incubation with the drug with an additional 24 hrs incubation at 37°C after addition of 12.5 mM resazurin in 96-well plates. Absorbance values were analysed using GraphPad Prism software. Data were collected from three independent experimental replicates. Results are presented as Mean  $\pm$  SEM. Fold-change is the ratio of Isometamidium resistant clone EC<sub>50</sub> value for a drug to Wild-type EC<sub>50</sub> value of the same drug.

Fold-increase of isometamidium cross-resistance to diminazene aceturate was 1.68, 2.74 and 9.93 for the clones growing in the presence 4 nM, 40 nM and 1  $\mu$ M isometamidium, respectively, and for ethidium bromide was 1.20, 1.42 and 2.72 for the clones growing in the presence of 4 nM, 40 nM and 1  $\mu$ M isometamidium, respectively.

Isometamidium cross-resistance to trypanocides used in HAT were also assessed (Table 5.1). Cross-resistance to pentamidine increased as the level of resistance to isometamidium in clones increased. However, increasing sensitivity ( $P = 0.0006$ ,  $P = 0.0004$  and  $P < 0.0001$  for clones at 4 nM, 40 nM and 1  $\mu$ M, respectively) to eflornithine by the clones was observed as the level of resistance to isometamidium increased. There was no isometamidium cross-resistance to melarsoprol in any of the clones, with an average  $EC_{50}$  value being determined as 0.023  $\mu$ M.

### 5.2.2.3 Monitoring mitochondrial membrane potential

Accumulation of isometamidium and ethidium bromide in the mitochondria of bloodstream forms of *T. congolense* and *T. brucei*, respectively, has been associated with maintenance of mitochondrial membrane potential (Wilkes et al., 1998; Chowdhury et al., 2010). It was indicated that a reduction of the mitochondrial membrane potential resulted in reduced accumulation of these drugs. Therefore, the mitochondrial membrane potential of the selected isometamidium resistant *T. brucei* was monitored in comparison to the parental wild-type cells to determine whether the reported modulation of mitochondrial membrane potential in *T. congolense* was operational in our isometamidium resistant clones.

The status of the mitochondrial membrane potential ( $\Delta\Psi_m$ ) in the derived isometamidium resistant bloodstream forms and that of the *T. brucei* 427 wild-type was monitored and compared using the fluorescent signal of the accumulated active-mitochondrial-specific dye TMRE and analyzed by FACS analysis. TMRE is a lipophilic cationic fluorescent dye that accumulates in polarized mitochondria. Its accumulation in mitochondria depends on the level

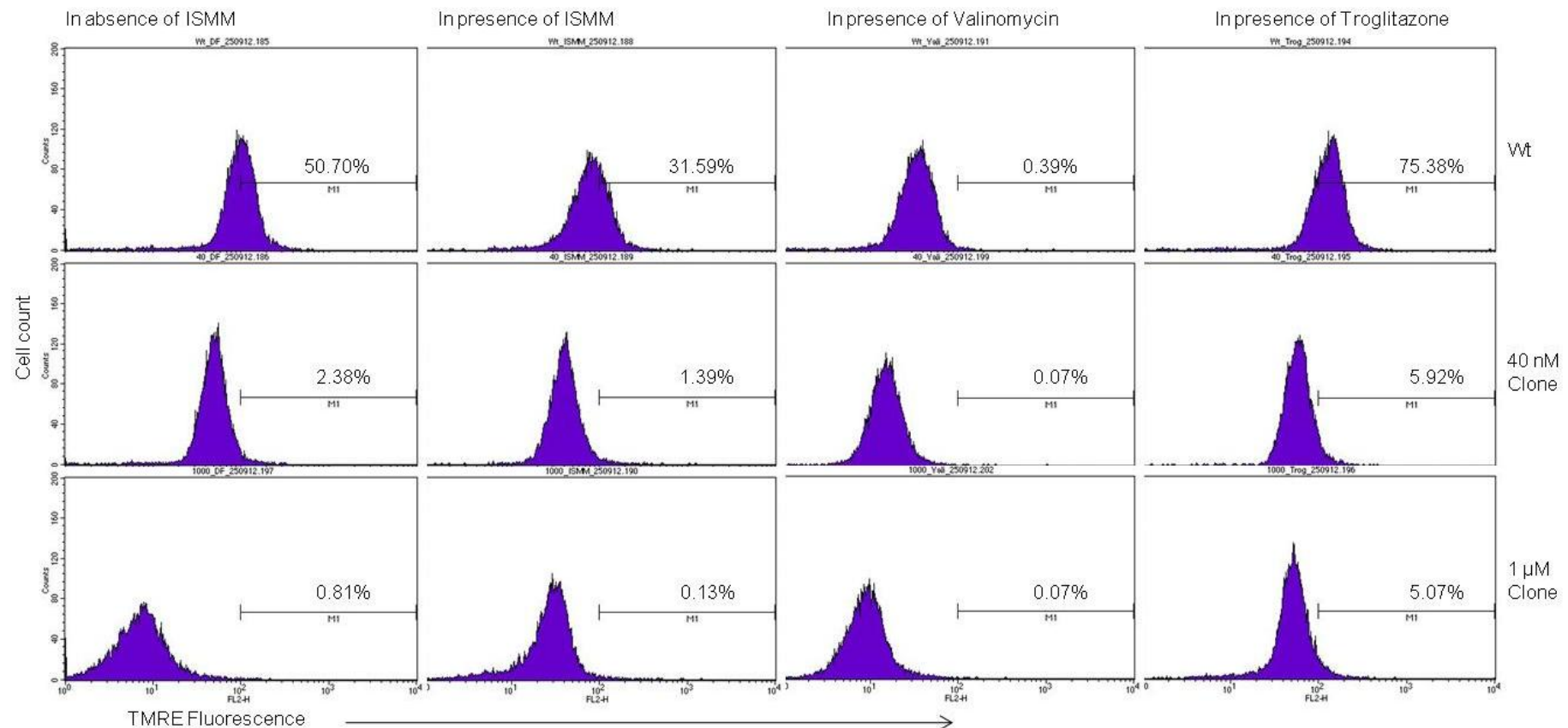


**Figure 5.4 Monitoring mitochondrial membrane potential of bloodstream forms of *T. brucei* 427 wild-type and the derived isometamidium resistant clones.**

Mitochondrial membrane potential was monitored by fluorescence signal of the accumulated active-mitochondrial-specific dye (25 nM) TMRE by  $1 \times 10^6$  cells/ml following incubation for 30 minutes and analyzed by FACS analysis. Troglitazone and valinomycin were used as controls to polarise and depolarise the inner mitochondrial membrane, respectively. The top row represents Wt controls for all conditions tested while the second and third rows are for the isometamidium resistant lines. The columns represent comparison of the three cell lines for each condition tested. At least three replicates were done.

of polarisation of the mitochondria i.e., the less polarised (less negatively charged) the mitochondrial matrix, the less the dye accumulates, and the more polarised (more negatively charged) a mitochondrial matrix the more the dye accumulates (Perry *et al.*, 2011). The  $\Delta\Psi_m$  was monitored and compared for the wild-type and the derived isometamidium resistant clones growing in the presence of 40 nM and 1  $\mu$ M isometamidium (Figure 5.4; Appendix B). The  $\Delta\Psi_m$  was monitored both in the presence and absence of isometamidium and it was observed to be reduced in both cases. There was a progressive reduction of the  $\Delta\Psi_m$  from the 40 nM isometamidium resistant clone to the 1  $\mu$ M isometamidium resistant clone. The monitored  $\Delta\Psi_m$  both in the absence and presence of isometamidium for the two isometamidium resistant clones was significantly ( $P < 0.0001$  and  $P = 0.0001$ ) different from that of the wild-type. The wild type *T. brucei* showed a significant decrease in the  $\Delta\Psi_m$  when monitored in the absence of the drug and then monitored after exposure to 500 nM isometamidium for 30 minutes. However, a comparison of the monitored  $\Delta\Psi_m$  in the absence of, and after exposure to, the drug for each of the clones growing in the presence of 4 nM and 1  $\mu$ M isometamidium showed decreases in  $\Delta\Psi_m$  that were not significant ( $P = 0.0786$  and  $P = 0.2002$ , respectively). This indicates maintenance of a low  $\Delta\Psi_m$  that cannot be reduced significantly after exposure to the drug. Troglitazone which polarizes the inner mitochondrial membrane and valinomycin an ionophore abolishes  $\Delta\Psi_m$  by depolarising the inner mitochondrial membrane, were used as controls to indicate higher and lower levels of  $\Delta\Psi_m$  (Denninger *et al.*, 2007; Figarella *et al.*, 2005). The use of these controls indicated the presence of a functional  $\Delta\Psi_m$  as they were able to increase and abolish it in the resistant cells as was the case with the parental wild-type cells (Figure 5.4).

The selected isometamidium resistant bloodstream forms of *T. brucei* showed maintenance of a low mitochondrial membrane potential as monitored by active mitochondrion labelling dye TMRE. Exposure of the resistant cells to isometamidium results in further reduced mitochondrial membrane potential as compared to that monitored in the absence of the drug. The higher the resistance level the lower the mitochondrial membrane potential.

#### 5.2.2.4 Status of the kinetoplast and kDNA genes

Loss of kinetoplast due to various trypanocides, including isometamidium, has been known for some time (Shapiro and Englund, 1990). We, therefore, set out to determine whether induced isometamidium resistance led to loss of the kinetoplast. To achieve this objective we used the DNA selective staining and fluorescent properties of DAPI. DAPI binds to the A-T rich regions of the minor groove of DNA and is known to show increased fluorescent properties when bound to kinetoplast DNA due to increased abundance of the A-T sequences (Kapuscinski, 1995). The isometamidium resistant clones growing in the presence of as low as 0.1 nM isometamidium were observed to have lost their kinetoplast DNA (Figure 5.5).

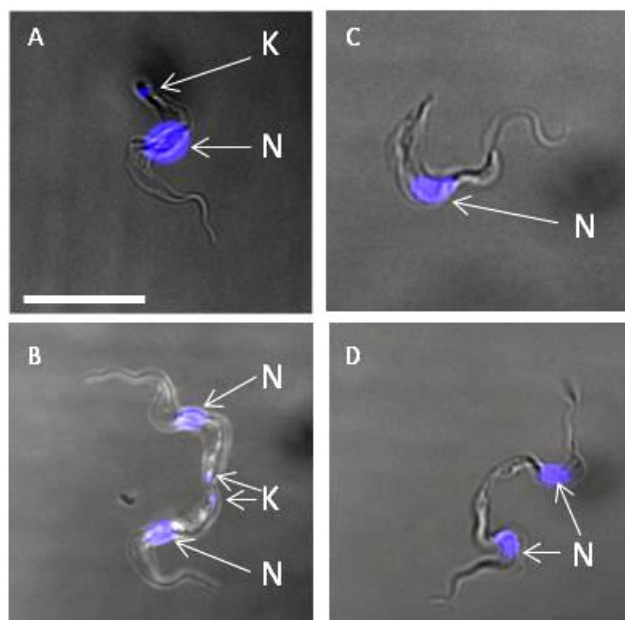


**Figure 5.5 Loss of the kinetoplast by isometamidium resistant BSF *T. brucei* 427**  
 The wild-type (A and B) and isometamidium resistant (C and D) bloodstream forms of *T. brucei* 427 were fixed in methanol at -20°C overnight and stained with 1 µg/ml DAPI/1%DABCO in PBS before applying to slides and viewing under the fluorescent microscope. The slides were observed under oil immersion. B and D show cells in cytokinesis. K = kinetoplast; N = Nucleus; Bar = 10 µm.

The kinetoplast is known to harbour maxicircle genes that code for several genes including ATPase A6 subunit and six subunits of complex I or NADH dehydrogenase or NADH: ubiquinone oxidoreductase of the electron transport chain among other proteins (Schnauffer *et al.*, 2002; Surve *et al.*, 2012). Loss of the kinetoplast would then be confirmed by lack of amplification of these genes by PCR. The loss of the kinetoplast was confirmed by a PCR amplification of the genes encoded by maxicircle genes of the kinetoplast. Amplification of the actin

gene which is encoded by the nucleus was used as a control for the presence of nuclear DNA. The NADH dehydrogenase or NADH: ubiquinone oxidoreductase subunits ND4, ND5, and ND7 and the ATPase A6 subunit (Domingo *et al.*, 2003; Lai *et al.*, 2008) were found to be absent in our isometamidium resistant strains (Figure 5.6). Therefore, lack of staining of the kinetoplast and amplification of the kinetoplast encoded genes by PCR confirmed the loss of the kinetoplast in our isometamidium resistant clones. Loss of the kinetoplast seems to be associated with isometamidium resistance development as it was also observed in bloodstream forms of *T. congolense* (Wilkes *et al.*, 1997).

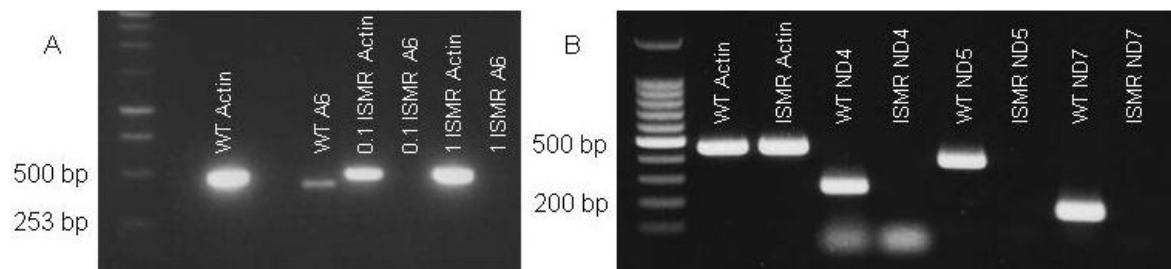


**Figure 5.6** PCR amplification of the kinetoplast based maxicircle genes of BSF *T. brucei*. Presence of kinetoplast based maxicircle genes of wild-type and various isometamidium (ISMM) resistant bloodstream forms of *T. brucei* was compared by PCR amplification of the genes. The amplified DNA was separated on 1% agarose and stained with SYBR safe. Nucleus encoded actin gene was used as the control for the presence of nuclear DNA. In (A) absence of ATPase A6 subunit PCR band in clones growing in the presence of 0.1 nM ISMM (0.1 ISMR) and clone growing in the presence of 1  $\mu$ M ISMM (1 ISMR). In (B) Absence of PCR bands for ND4, ND5 and ND7 genes in the resistant clone, indicated as ISMR, growing in the presence of 1  $\mu$ M ISMM. Expected PCR bands sizes Actin = 456 bp; ND4 = 256 bp; ND5 = 395; ND7 = 161 bp.

### 5.2.2.5 ATPase F<sub>1</sub> gamma subunit compensatory mutations

The F<sub>1</sub>F<sub>0</sub> ATPase is made up of the F<sub>1</sub> and the F<sub>2</sub> components. The F<sub>1</sub> component, which projects into the mitochondrial matrix, is hydrophilic and contains the catalytic sites. It is attached to the hydrophobic F<sub>0</sub> which is a membrane bound component through the stalk made up of the gamma, epsilon and delta subunits (Williams, 1994). The F<sub>0</sub> conducts protons across the inner mitochondrial membrane following the hydrolysis of ATP by the F<sub>1</sub> component during generation of the mitochondrial membrane potential (Dean *et al.*, 2013; Williams, 1994). The loss of the kinetoplast induced by acriflavine exposure of trypanosomes has been reported to be compensated by mutations in the gamma subunit of the ATPase F<sub>1</sub> component. This is to allow the continued generation of the mitochondrial membrane potential by akinetoplastic trypanosomes (Dean *et al.*, 2013; Schnauffer *et al.*, 2005). We checked for the mutations in the gamma

subunit of ATPase through whole genome sequence analysis data. There were no SNPs detected in the ATP synthase F1 subunit gamma protein (Tb427.10.180) which were unique to the isometamidium resistant cells.

However, there were three mutations in both the isometamidium resistant clones and the parental wild-type cells as compared to the reference genome of *T. brucei* 427 Lister strain. Two of the three mutations were synonymous mutations (Table 5.2). The non-synonymous mutation was different from those reported in literature for *T. evansi* and *T. equiperdum* (Dean *et al.*, 2013). Therefore, the occurrence of the mutations in both the parental wild-type cells and the derived isometamidium resistant cell lines indicated these mutations may have arisen due to adaptation to laboratory culture conditions.

SNP Position	Mutation		Amino acid substitution
	Non-synonymous	Synonymous	
Tb427_10_v5			
72460		gcA/gcG	A31
72561	gCc/gTc		A65V
72688		gtC/gtT	V107

Table 5.2 ATPase gamma subunit protein mutations in Wt and ISMM resistant clones.

#### 5.2.2.6 Alteration of the internal morphology of the mitochondrion

Internal mitochondrial structure of the derived isometamidium resistant clones was compared to that of the wild-type BSF *T. brucei* 427 by using the active-mitochondria stain Mito-Tracker Red CMXRos. Mito-Tracker dyes are not only used to determine alterations to the internal morphology of mitochondria but also localisation of dyes (TMRE) used for monitoring the mitochondrial membrane potential. Thus Mito-Tracker dyes are employed to determine the influence of alteration to internal mitochondrial morphology as determined by localisation dyes and how this may influence the monitored  $\Delta\Psi_m$  (Perry *et al.*, 2011). Therefore, our use of the Mito-Tracker Red CMXRos was not only to compare the internal mitochondrial morphology between the wild-type 427 and derived isometamidium resistant cells but also as controls for the monitored  $\Delta\Psi_m$  in Section 5.2.2.3.

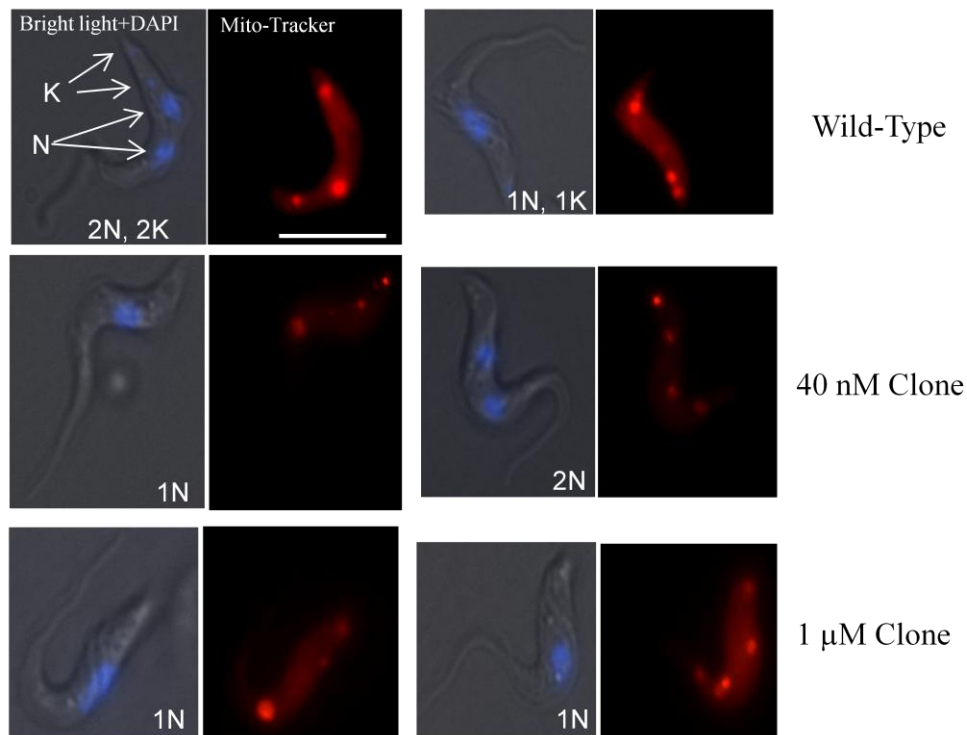


**Figure 5.7** BSF *T. brucei* active mitochondria staining with Mito-Tracker Red CMXRos. The mitochondria of  $2 \times 10^7$  cells/ml in 1 ml growth medium was stained with 1 nM Mito-Tracker Red CMXRos and 0.5  $\mu\text{g/ml}$  DAPI/1% DABCO in PBS and immobilised in 1% Low gelling temperature agarose before viewing under the fluorescent microscope using DAPI and DsRed filters. Images were merged using the free software, GIMP. Bar = 10  $\mu\text{m}$ ; K = Kinetoplast; N = Nucleus.

None of the clones showed any apparent difference in mitochondrial internal morphology when compared to the wild-type bloodstream forms of *T. brucei* 427 as determined by Mito-Tracker Red CMXRos staining (Figure 5.7). Therefore, the loss of the mitochondrial membrane potential by the isometamidium resistant clones was not due to changes in the internal morphology of the mitochondria but in line with the suggested need to maintain a low mitochondrial membrane potential to reduce the accumulation of the drug by the resistant cells as earlier reported (Wilkes *et al.*, 1997).

### 5.2.3 Metabolic changes in isometamidium resistant BSF *T. brucei*

The reduction of the mitochondrial membrane potential by the isometamidium resistant cells to reduce the accumulation of the drug is likely to have implications on the metabolism of the parasites. The mitochondrial membrane potential is generated during the energy metabolism of trypanosomes. In the case of bloodstream forms of *T. brucei* this is done by the break-down of ATP through the reverse function of ATPase (Brown *et al.*, 2006; Schnauffer *et al.*, 2005). Further, the mitochondrial membrane potential is used for the importation of nuclearly encoded proteins into the mitochondrion (Schnauffer *et al.*, 2002). Therefore, a reduction of the mitochondrial potential would affect the metabolism of the parasites. It is for this reason that we used untargeted metabolomics to determine the effect of reduced mitochondrial membrane potential on the metabolism of the parasites. We used untargeted metabolomics to assess alterations in global metabolite profiles that may have resulted from the effect of induced isometamidium by comparing derived isometamidium resistant clones with the parental wild-type.

Metabolomes of resistant clones growing in the presence of 40 nM and 1  $\mu$ M were compared to the parental wild-type bloodstream form *T. brucei* strain 427. We attempted to establish the anticipated energy metabolic differences with the view that the altered  $\Delta\Psi_m$  could be achieved through adjustments to the energy metabolism which is linked to generation of  $\Delta\Psi_m$  by the isometamidium resistant clones.

There were no apparent metabolite differences between the wild-type and the derived isometamidium resistant clones with regard to the energy metabolism. Changes in the glycolytic pathway would have been good indicators of alterations in the energy metabolism of the bloodstream forms of *T. brucei*, but none were noted. Classically it was believed glucose catabolism by BSF *T. brucei* proceeded only to pyruvate. However, recent data (Creek *et al.*, Unpublished) indicates that numerous other pathways exist, e.g. succinate, fumarate and malate are all produced and some succinate is secreted. These metabolites were detected in the various isometamidium resistant clones, but there were no

apparent differences as compared to the detected levels in the parental wild-type cells. However, a metabolomics analysis of the clone of the highest resistance (1  $\mu\text{M}$ ) showed differences in some of the metabolites that were identified (Figure 5.8; Attached CD).

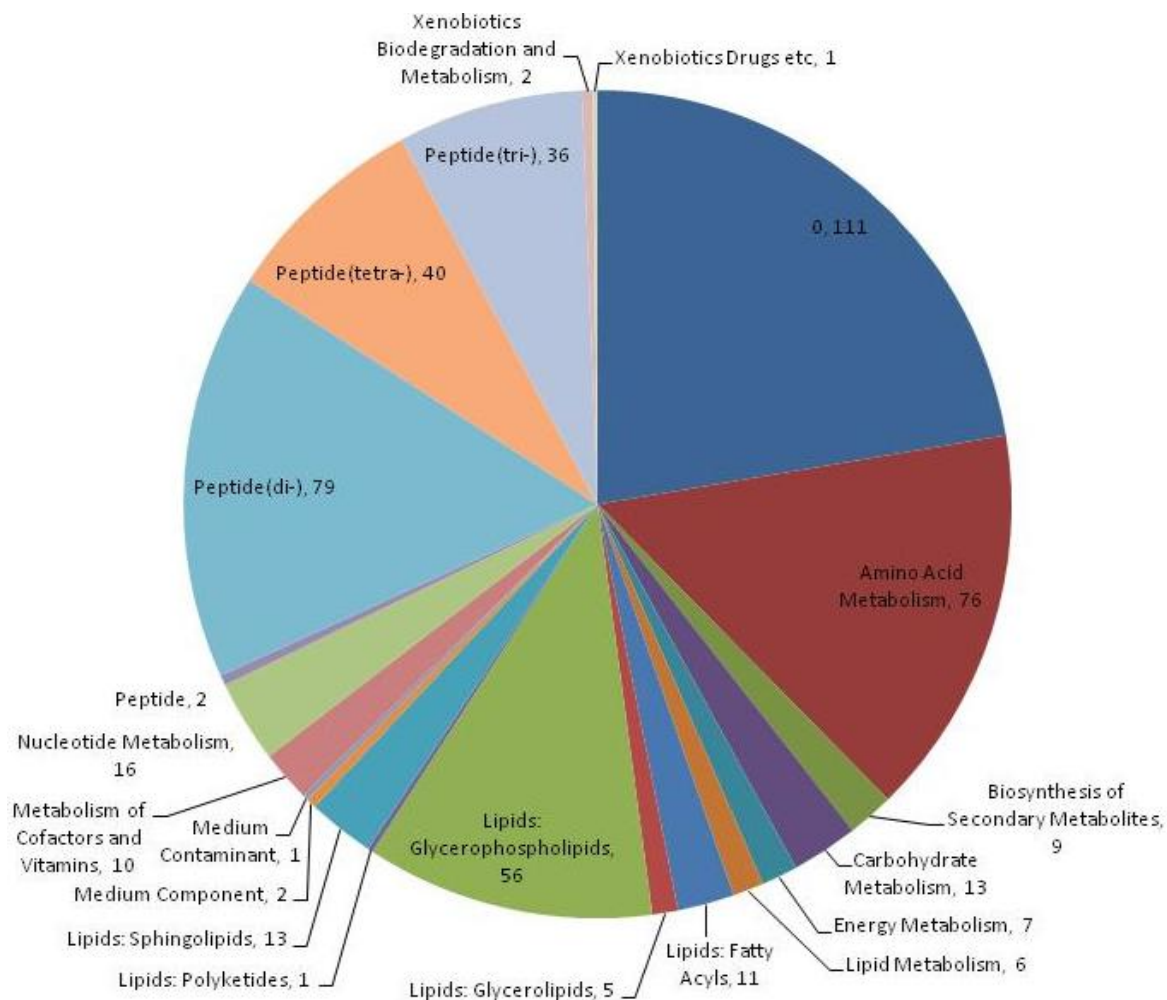


**Figure 5.8** Pie chart representation of all identified metabolites analysed using IDEOM. The summary represents all the metabolites identified in the wild-type and the isometamidium resistant clone growing in the presence of 1  $\mu\text{M}$  isometamidium. The samples were extracted with methanol:chloroform:water mixture and separated and detected using LC/MS. The pie chart was generated using IDEOM.

Using the built-in statistical analysis of IDEOM we generated the Principal Components Analysis (PCA) of all the identified metabolites to check for metabolite clustering according to sample source. We observed a clear separation of the clustered samples from wild-type and the derived-isometamidium resistant clone, indicative of differences between the two cell lines or groups (Figure 5.9). It is worth noting that the quality control samples (QC) clearly clustered together and the medium related samples also clustered

together. The PCA separated the samples into clusters composed of experimental replicates for the wild-type and the isometamidium resistant clone.

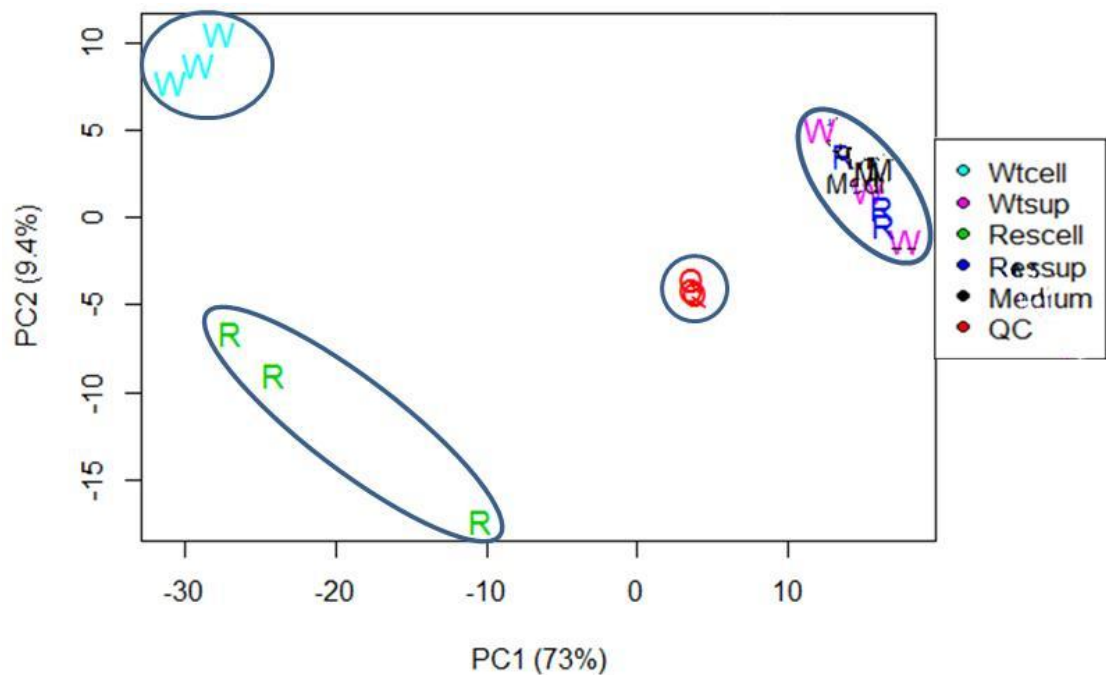


**Figure 5.9** Differentiation of the wild-type from the isometamidium resistant clone by PCA. The wild-type *T. brucei* 427 differentiated from the derived isometamidium resistant clone growing in the presence of 1  $\mu$ M isometamidium by clustering them into experimental replicates, three for each. The first principal exhibits the most changing variables while the second component depicts other possible variabilities in the data. The PCA was generated using IDEOM.

Spingolipids have been linked to roles in growth, cytokinesis and segregation of the kinetoplast during cell division of *T. brucei* (Fridberg *et al.*, 2008).

Sphingolipids consisting of sphingomyelin (SM), ethanolamine phosphorylceramide (EPC) and inositol phosphorylceramide (IPC), make up about 10 to 15% of the total phospholipids in *T. brucei* (Richmond *et al.*, 2010). *T. brucei* bloodstream forms synthesize SM and EPC while the procyclic forms synthesize SM as well as IPC (Sutterwala *et al.*, 2008). A total of 13 sphingolipids were identified (Figure 5.8). We observed both increased and reduced levels of different sphingolipids in the resistant samples as compared to the wild-type samples (Table 5.3). Relative abundance graphs of the detected sphingolipid metabolites (Figure 5.10) are superimposed on the *T. brucei* sphingolipid biosynthetic pathway (Smith and Butikofer, 2010).

Similar profiles of sphingolipid metabolite changes were observed in the clones growing in the presence of 4 nM and 40 nM ISMM. The two lower level resistant clones showed a similar pattern of depleted relative abundance level of sphingomyelin when compared to the wild-type. The change in relative abundance of sphingomyelin in the resistant clone growing in the presence of 1  $\mu$ M ISMM was more pronounced as compared to the two lower resistant clones.

Mass (m/z)	RT	Formula	Putative metabolite identified	Fold change
555.52	3.695	C <sub>34</sub> H <sub>69</sub> NO <sub>4</sub>	[SP hydroxy(16:0)] N-(hexadecanoyl)-4S-hydroxysphinganine	5.91
<b>537.51</b>	<b>3.673</b>	<b>C<sub>34</sub>H<sub>67</sub>NO<sub>3</sub></b>	<b>Ceramide</b>	<b>2.65</b>
565.54	3.664	C <sub>36</sub> H <sub>71</sub> NO <sub>3</sub>	[SP (18:0)] N-(octadecanoyl)-sphing-4-enine	2.04
285.3	8.981	C <sub>18</sub> H <sub>39</sub> NO	[SP] 1-deoxy-sphinganine	1.61
688.55	4.07	C <sub>38</sub> H <sub>77</sub> N <sub>2</sub> O <sub>6</sub> P	[SP (18:0/14:0)] N-(octadecanoyl)-tetradecasphing-4-enine-1-phosphoethanolamine	1.30
727.6	3.742	C <sub>42</sub> H <sub>81</sub> NO <sub>8</sub>	Glucosylceramide (d18:1/18:0)	1.23
509.48	3.692	C <sub>32</sub> H <sub>63</sub> NO <sub>3</sub>	Dihydroceramide	1.18
<b>511.5</b>	<b>3.686</b>	<b>C<sub>32</sub>H<sub>65</sub>NO<sub>3</sub></b>	<b>Dihydroceramide</b>	<b>1</b>
861.62	3.778	C <sub>46</sub> H <sub>87</sub> NO <sub>13</sub>	Lactosylceramide	0.84
<b>301.3</b>	<b>7.21</b>	<b>C<sub>18</sub>H<sub>39</sub>NO<sub>2</sub></b>	<b>Sphinganine</b>	<b>0.72</b>
273.27	7.232	C <sub>16</sub> H <sub>35</sub> NO <sub>2</sub>	Hexadecasphinganine	0.30
<b>676.55</b>	<b>4.17</b>	<b>C<sub>37</sub>H<sub>77</sub>N<sub>2</sub>O<sub>6</sub>P</b>	<b>Sphingomyelin</b>	<b>0.12</b>

**Table 5.3 Sphingolipids identified in isometamidium resistant clone and the wild-type cells. Sphingolipids in bold font are superimposed in the pathway in figure 5.10. The metabolites were separated, detected and identified using LC/MS and IDEOM. RT = Retention time, fold change is the comparison of the metabolite level in isometamidium resistant derived samples to that from the wild-type.**

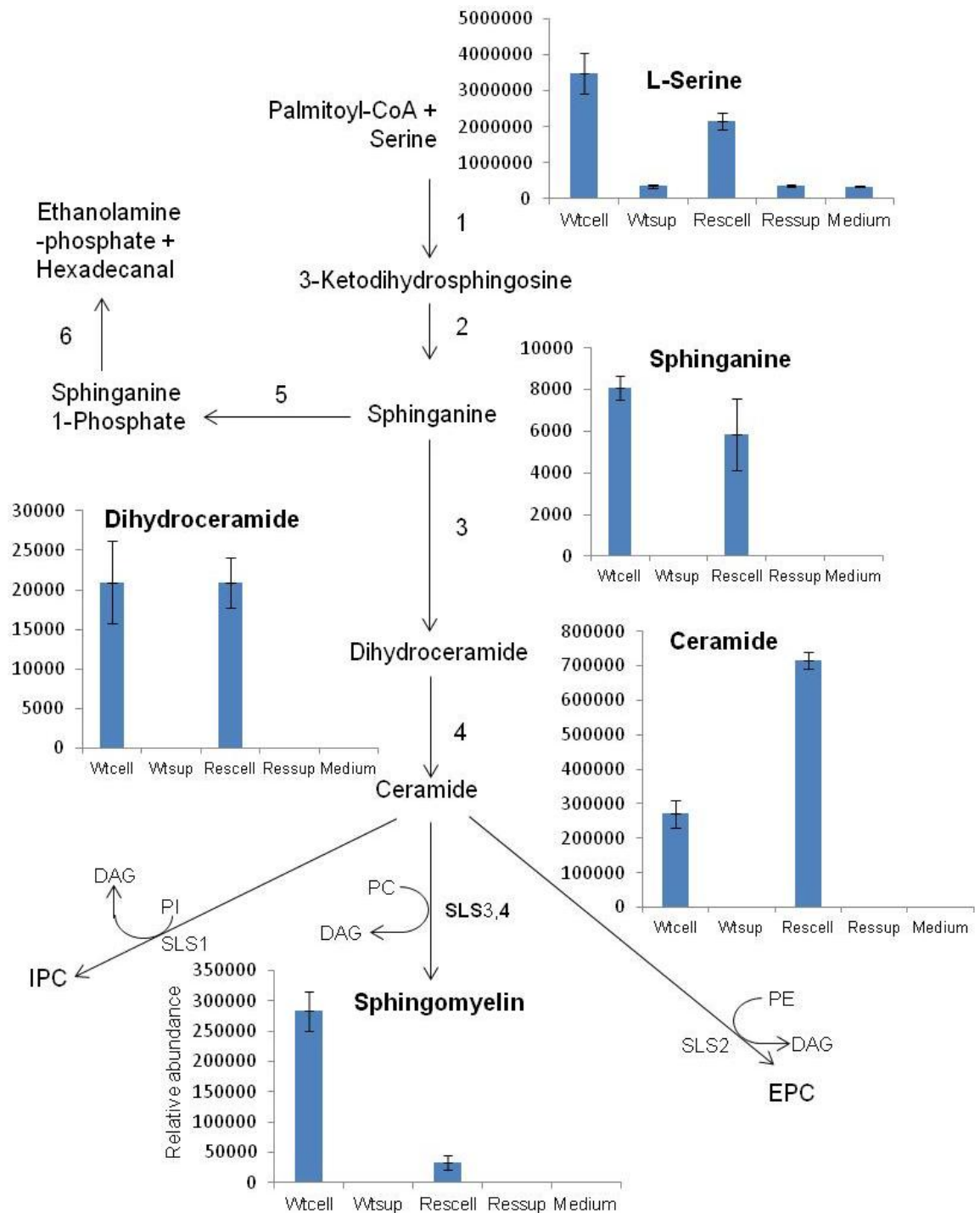


**Figure 5.10** Most changing *T. brucei* metabolites of the sphingolipid biosynthetic pathway. Comparison of the sphingolipid metabolite relative abundances between the wild-type *T. brucei* and the derived isometamidium resistant clone growing in the presence of 1  $\mu$ M isometamidium and inserted in the sphingolipid biosynthetic pathway. The samples were extracted at 4°C using methanol:chloroform:water mixture and analysed by LC/MS and IDEOM. The results are for at least three replicates. 1 = Serine palmitoyltransferase; 2 = 3-Ketosphingosine reductase; 3 = Dihydroceramide synthase; 4 = Dihydroceramide desaturase; 5 = Sphingosine kinase; 6 = Sphingosine-1-phosphate lyase; SLS1 = Sphingosine synthase 1; SLS2 = Sphingosine synthase 2; SLS3 = Sphingosine synthase 3; SLS4 = Sphingosine synthase 4. IPC = Inositol phosphorylceramide; EPC = Ethanolamine phosphorylceramide; DAG = Diacylglycerol. (Sphingolipid biosynthetic pathway adapted from Smith and Butikofer, 2010).

The first part of the sphingolipid biosynthetic pathway (Figure 5.10) leading to ceramide in eukaryotic cells occurs in the endoplasmic reticulum while the

second part that starts from ceramide to the various sphingolipids occurs in the Golgi complex (Futerman and Riezman, 2005). Although the genes for all the enzymes of the sphingolipid pathway of *T. brucei* have been identified, only the first enzyme of the pathway, serine palmitoyltransferase, and the four sphingolipid synthases, TbSLS1-4, have been characterized. SLS1 and SLS2 catalyze the synthesis of IPC and EPC, respectively while SLS3 and SLS4 are bifunctional and lead to synthesis of either SM or EPC from ceramide (Fridberg *et al.*, 2008; Mina *et al.*, 2009; Sevova *et al.*, 2010; Sutterwala *et al.*, 2008).

#### 5.2.4 Genetic status of sphingolipid pathway enzymes

Following the alterations in the sphingolipid metabolites we determined whether the enzymes of the pathway were altered at the gene level from our whole genome sequencing by NGS of the wild-type and the resistant clones. The observed depletion in relative abundance levels of some of the sphingolipid metabolites (Figure 5.10) from metabolomics analysis led us to focus on the genetic status of the sphingolipid pathway's enzymes. With the use of the metabolomics analysis results, a comparison of the sphingolipid pathway enzyme gene sequences of the parental wild-type with those of the isometamidium resistant clones, revealed 8 SNPs in choline phosphorylceramide synthase (SLS4) (Table 5.4).

SLS4 on chromosome 9, whose substrate ceramide accumulated in the resistant cells (Figure 5.10), had 8 SNPs involving 4 synonymous mutations and 4 non-synonymous mutations (Table 5.4). Two of the 4 non-synonymous mutations affected the same codon resulting in three non-conservative substitutions of residues in the enzyme. The wild-type and ISMM resistant sequencing reads aligned showed presence of the mutations in 50% of the reads from ISMM resistant lines implying that the mutations were heterozygous. The mutations were found to be outside the predicted catalytic site and they were also outside the four highly conserved sphingolipid synthases signature residues, D1-4, and outside the six trans-membrane domains, TM1-6 (Figure 5.11) (Sevova *et al.*, 2010; Sutterwala *et al.*, 2008). There were no SNPs detected in the other enzymes of the pathway.

SNP Position	Mutation		Amino acid substitution
	Non-synonymous	Synonymous	
Tb427_09_v4			
1450214 2850	Gac to Aac		D177N
1450218 2854		tgT to tgC	C175
1450222 2858	cTg to cAg		L174K
1450223 2859	Ctg to Atg		
1450233 2869		gcG to gcT	A170
1450236 2872		ccG to ccT	P169
1450239 2875	ttG to ttT		L168F
1450245 2881		acG to acA	T166

**Table 5.4** Choline phosphorylceramide synthase point mutations of ISMM resistant clones. Genomic DNA of the wild-type *T. brucei* 427 bloodstream and the derived isometamidium resistant cells was extracted using the Phenol: chloroform: isoamyl alcohol (25:24:1). The genomic DNA was sequenced using NGS. The isometamidium resistant cells gDNA sequences were aligned to the parental wild-type gDNA and both to the reference genome sequence of *T. brucei* Lister strain 427.

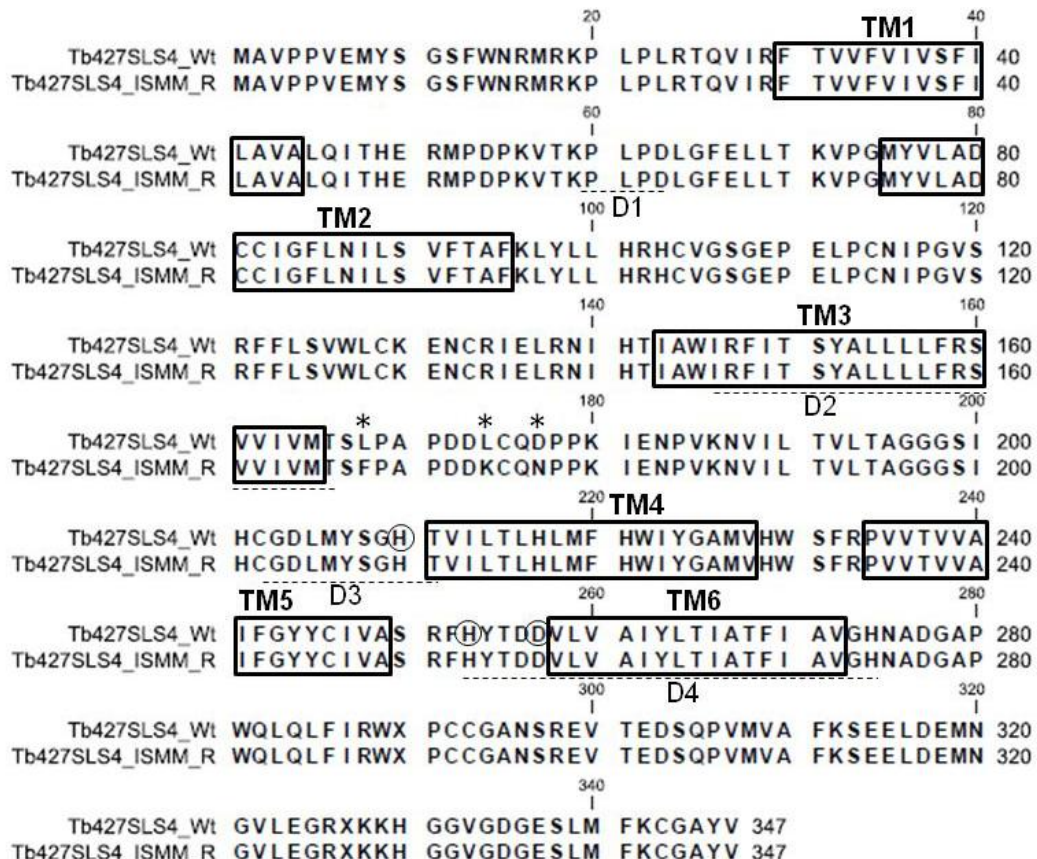


**Figure 5.11** Non-synonymous mutations detected in choline phosphorylceramide synthase. The non-synonymous mutations are indicated by asterisks while the six trans-membrane domains (TM1-6) are boxed and the four highly conserved signature residues (D1-4) of SLSs are underlined with a dashed line. The predicted triad residues found in the catalytic site of the enzyme are circled. Alignment of the wild-type (Wt) and the mutated protein sequences of choline phosphorylceramide synthase (SLS4) downloaded from Trityp websites was done using CLC Genomics Workbench 6.0.4. Enzyme features adapted from Sutterwala et al., 2008.

### 5.2.5 Comparison of endocytosis between the wild-type and ISMM resistant *T. brucei* through uptake of Lucifer yellow CH dye

Perturbation of the sphingolipid from the committed step catalysed by serine palmitoyltransferase has been linked with reduced endocytosis in *T. brucei* (Sutterwala *et al.*, 2007). Depletion of dihyrosphingosine or sphinganine in *S. cerevisiae* has been shown to reduce the internalisation step of endocytosis (Zanolari *et al.*, 2000). Following the noted perturbation of the sphingolipid biosynthetic pathway in our isometamidium resistant cells we investigated whether there were differences in endocytosis by the resistant cells in comparison to the parental wild-type cells through monitoring the uptake of Lucifer yellow CH fluorescent dye (Zanolari *et al.*, 2000). Dr. Federica Giordani showed that there was no appreciable difference in the fluorescence given off by Lucifer yellow CH in the endosomes located between the kinetoplast and the nucleus of the two cell lines with both cell lines showing similar fluorescence (Figure 5.12).

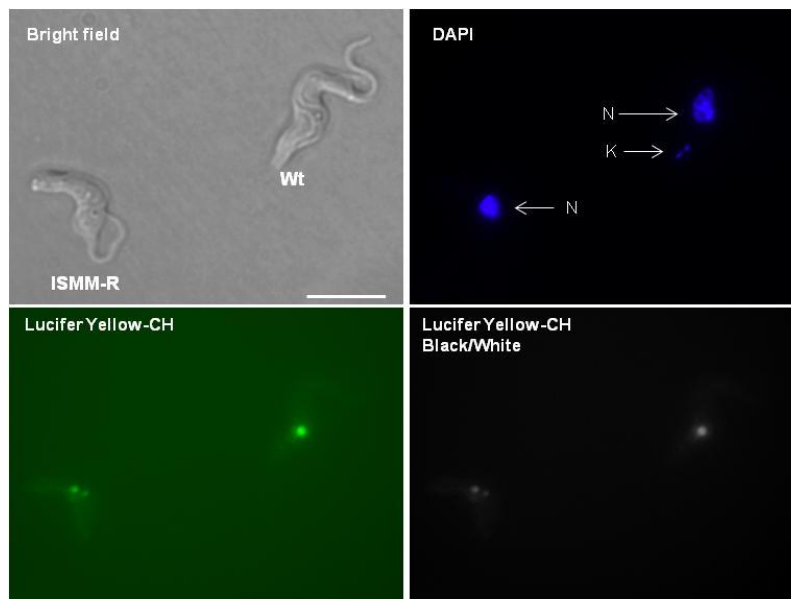


**Figure 5.12 Comparison of the internalisation of lucifer yellow CH fluorescent dye.** The stained endosomes located between the nucleus and the kinetoplast in the posterior region of the cells are clearly seen in both the wild-type and ISMM resistant (ISMM-R) cells. The two cell lines were mixed and stained with 4.4 mM Lucifer yellow CH (LY-CH) in growth medium for 1 hour at 37°C and washed in PBS before addition of 20 µM DAPI. The cells were immobilised in 1% low melting temperature agarose before application to glass slides. The cells were viewed under oil immersion on a ZEISS Axioplan 2 Imaging fluorescent microscope after applying the cover slips using the GFP filters. K = kinetoplast; N = nucleus; Bar = 10 µm. The top row images are for the wild-type while the bottom row images are for the ISMM resistant cell line. (Data generated by Federica Giordani). Images were merged using GIMP free software.

Our untargeted metabolomics comparison of the wild-type and the ISMM resistant cell lines showed peptides which represented the largest number of identifications as a group compared to the other groupings of the identified metabolites (Figure 5.8). The peptides, dipeptides, tripeptides and tetrapeptides were found to show marked differences in abundance level between the wild-type and the resistant cells. However, we were unable to identify any of the most changing peptides.

## 5.3 Discussion

Resistance to trypanocidal drugs is of major concern in veterinary productivity in Africa. Understanding modes of action and resistance mechanism can help delay selection and spread of resistance. Here we have initiated a characterization of isometamidium resistance.

### 5.3.1 Isometamidium resistance selection

It took 9 months involving 115 passages to generate clones of the higher level (1  $\mu\text{M}$ ) isometamidium resistance in *T. brucei* 427 bloodstream forms *in vitro* and about 4.5 months to move from the lower level resistance (4 nM) to reach the higher level of resistance (1  $\mu\text{M}$ ). This is comparable to 11 months it took to induce higher isometamidium resistance in *T. congolense* *in vivo* (Peregrine *et al.*, 1997). Isometamidium seems to have a cumulative effect on *T. brucei* bloodstream forms as at low concentrations of the drug the wild-type cells died at about the third or fourth passage. It was noticed that past the fifth passage the cells would continue to survive and grow at a given concentration indicating that the cells were able to tolerate the drug at that given concentration in the growth medium.

It took 19, 23 and 28 weeks to attain 3.0 -, 10.6 -, and 94.2 - fold increases in the isometamidium  $\text{EC}_{50}$  values for the clones growing in the presence of 4 nM, 40 nM and 1  $\mu\text{M}$  isometamidium. The associated cross-resistance to diminazene aceturate was 1.6 -, 2.7 -, and 9.9 - fold increase, and 1.20 -, 1.42 -, and 2.72 - fold increase for ethidium bromide, respectively. The modest cross-resistance to diminazene aceturate by the clone growing in the presence of 40 nM is consistent with the results of Peregrine *et al.* (1997) and therefore diminazene

could be used as a sanative drug for these isometamidium resistant clones. At this stage ethidium bromide could also be used for the same purpose for this particular clone. However, our results indicate a loss of sanative use of isometamidium and diminazene aceturate at higher isometamidium resistance, due to increased isometamidium cross-resistance to diminazene aceturate.

### **5.3.2 Isometamidium cross-resistance to diminazene aceturate and ethidium bromide**

Diminazene and ethidium are two compounds that contribute to the overall structure of isometamidium (Kinabo, 1993) and therefore all three drugs share similarities of certain parts of their structures (Figure 1.10 and Figure 1.11).

Ethidium bromide appears to target the free minicircles of the kinetoplast and prevents the initiation of their replication. It also inhibits nuclear DNA replication in cells that have no kinetoplast (Chowdhury *et al.*, 2010).

Diminazene is not an intercalating agent like ethidium but it binds specifically to the adenine - thymine pairs of the minor groove of DNA (Peregrine and Mamman, 1993). However, resistance to diminazene has been linked to loss of the drug's transporters in trypanosomes (de Koning *et al.*, 2004; Witola *et al.*, 2004). The susceptibility of the derived resistant clones, especially the clone growing in the presence of less than 40 nM isometamidium, to these two drugs then could be attributed to ethidium's ability to kill cells that have no kinetoplast through inhibition of the nuclear DNA and probably the presence of the diminazene transporters in these cells. The presence of these transporters could lead to the accumulation of the drug in the cells and hence their killing. The fact that the kinetoplast is lost by the ISMM resistant clone of lower resistance and yet they showed a modest cross resistance to diminazene aceturate and ethidium bromide indicates a modest participation of the kinetoplast in ISMM cross-resistance to these drugs although they are known to interact with the kinetoplast.

It was long reported that cross-resistance between drugs that belong to different groups of chemical compounds can result from sharing the route of uptake or drug efflux mechanism or indeed having the same target or a combination of these themes (Barrett and Fairlamb, 1999). Cross resistance between arsenicals and diamidines in *T. brucei* has been a perplexing problem for a long time

because these two drugs belong to two different chemical compound groupings (Barrett and Fairlamb, 1999). However, it has now been shown as earlier reported that cross-resistance between the two drugs was possible in the cells whose both alleles of aquaglyceroporin 2 gene were knocked out (Baker *et al.*, 2012; Munday *et al.*, 2014). This confirmed the earlier reported notion of drugs belonging to different chemical groupings sharing the mode of entry into the cell would have cross-resistance between them in the absence of their shared transporter. However, we observed isometamidium cross-resistance to pentamidine with a 21.9 fold-increase in  $EC_{50}$  although there was no cross resistance to melarsoprol in all our isometamidium resistant clones as would be expected. This would indicate non-participation of aquaglyceroporin 2 transporter's participation in isometamidium cross-resistance to pentamidine. Pentamidine is known to induce loss of the kinetoplast in *Trypanosoma* species (Shapiro and Englund, 1995) and it is also known to interact with the minicircles of *L. donovani* and *L. amazonensis* (Basselin *et al.*, 1998). This implies that the kinetoplast contributes to the accumulation of the drug in the cells. The loss of the kinetoplast by our ISMM resistant cells means the cells retain less pentamidine than the progenitor wild-type cells. Indeed, the loss of the kinetoplast was observed in low resistant cell lines growing in the presence of the 4 nM ISMM. This may explain the 2-fold increase in ISMM cross-resistance to pentamidine by these cells as they had lost the means to retain the drug. The continued increase in cross-resistance to pentamidine by the clones of higher ISMM resistance could then have been due to other contributing factors.

### **5.3.3 Susceptibility of ISMM resistant BSF *T. brucei* to eflornithine**

Eflornithine is used for treatment of HAT and is more effective against *T. b. gambiense* than against *T. b. rhodesiense* (Brun *et al.*, 2011). It is an amino acid analogue of ornithine, a non-proteinogenic amino acid. Eflornithine is an irreversible inhibitor of ornithine decarboxylase of the polyamine pathway and thus exerts its inhibitory effect on the growth of *T. brucei* by blockage of this pathway (Bacchi *et al.*, 1980). Resistance to eflornithine is due to the deletion of the amino acid transporter TbAAT6 gene which leads to reduced accumulation of the drug in the resistant cells (Vincent *et al.*, 2010). Our isometamidium resistant clones showed progressive increase in susceptibility to eflornithine as

the level of isometamidium resistance increased. This happened despite there being no difference in levels of arginine, ornithine, putrescine, spermidine, N1-acetylspermidine and N-acetylputrescine of the polyamine pathway determined by metabolomics analysis of the resistant cells as compared to the wild-type cells. The increased sensitivity of the resistance cells to eflornithine when compared to the wild-type cells must be therefore attributed to other factors other than changes in the polyamine pathway. These remain elusive.

### 5.3.4 Maintenance of a low $\Delta\Psi_m$ by ISMM resistant BSF *T. brucei*

Use of a diminished  $\Delta\Psi_m$  to reduce the accumulation of the drug in the mitochondria, thereby reducing the concentration of the drug reaching its target, has been reported to be a strategy utilised by isometamidium and ethidium bromide resistant *Trypanosoma* parasites (Chowdhury *et al.*, 2010; Wilkes *et al.*, 1997). Thus the accumulation of ethidium and isometamidium into the mitochondrion has been reported to be decreased by the reduction in the  $\Delta\Psi_m$  expressed by *T. brucei* and *T. congolense*, respectively (Chowdhury *et al.*, 2010; Wilkes *et al.*, 1997). However, the  $\Delta\Psi_m$  is required for the importation of proteins encoded by the nuclear DNA into the mitochondrial matrix where they perform various functions (Schnauffer *et al.*, 2005). In this study, the derived resistant clones showed a much reduced  $\Delta\Psi_m$  as monitored by the actively accumulating mitochondrial dependent dye, TMRE, compared to the wild type cells. The reduction in the  $\Delta\Psi_m$  would have implications on the transport processes between the cytosol and mitochondrial matrix (Schnauffer *et al.*, 2005). This may have been responsible for the reduced growth phenotype of the derived resistant cells, especially clones of higher isometamidium resistance as they exhibited a much reduced  $\Delta\Psi_m$ . The fact that kDNA encodes many proteins that contribute to  $\Delta\Psi_m$  could underlie this loss. Specific point mutations in the  $\gamma$  subunit, which is encoded in the nucleus, of ATPase have been shown to compensate for the loss of the kDNA, hence rendering essential kDNA encoded proteins dispensable, in acriflavine resistant bloodstream forms of *T. brucei*. The mutations have been suggested to lead to uncoupling of the  $F_0$  and  $F_1$  components of the ATPase complex (Dean *et al.*, 2013). The uncoupling of  $F_0$  and  $F_1$  components result in the shift of generation of  $\Delta\Psi_m$  from the hydrolysis of ATP by ATPase complex to the use of the proposed ADP/ATP carrier (AAC) which

works in conjunction with only the F<sub>1</sub> component of ATPase complex (Dean *et al.*, 2013; Schnauffer *et al.*, 2005). Our isometamidium resistant cell lines showed none of the reported compensatory mutation or any mutations unique to them as compared to the parental wild-type cells.

Our failure to select PCF trypanosomes resistant to ISMM might relate to the essentiality of the kinetoplast and dependence on the electron transport chain for the generation of the  $\Delta\Psi_m$  in these cells (Schnauffer *et al.*, 2002). Further, loss of the kinetoplast has been suggested to lock the trypanosomes in the bloodstream form and their transmission becomes mechanical because they cannot survive in the insect host (Schnauffer *et al.*, 2002).

Kinetoplastids including *T. brucei*, *Leishmania* species and *T. cruzi* have had most of the genes for putative enzymes involved in *de novo* metabolism of the major phospholipids identified and some of these have already been characterised (Serricchio and Buetikofer, 2011; Smith and Butikofer, 2010). Bloodstream forms of *T. brucei* require *de novo* biosynthesis of sphingolipids for their viability (Sutterwala *et al.*, 2007). Probably the essentiality of this pathway in bloodstream forms of *T. brucei* resulted in failure to generate serine palmitoyltransferase RNAi cell lines (Fridberg *et al.*, 2008).

The roles of sphingolipids in most eukaryotic cells are known to range from cell signalling, mediation in heat stress to protein targeting (Cowart and Obeid, 2007). Little is known about the role of sphingolipids in protozoan cells apart from being components of the cell membranes as in other eukaryotic cells (Futerman and Riezman, 2005; Zhang *et al.*, 2010). However, functions of sphingolipids in trypanosomatids have started to emerge and are essential for *T. brucei* cell viability (Fridberg *et al.*, 2008; Sutterwala *et al.*, 2007).

### **5.3.5 Perturbation of the sphingolipid biosynthetic pathway**

The reduction in *de novo* synthesis of sphingolipids was reported during RNAi and myriocin inhibition of the first enzyme, serine palmitoyltransferase, of the sphingolipid biosynthetic pathway (Figure 5.10) in procyclic and bloodstream forms of *T. brucei* (Fridberg *et al.*, 2008; Sutterwala *et al.*, 2007). The cells exhibited a reduced growth phenotype, abnormal cytokinesis and failure to

segregate the kinetoplast during cell division. This led to the suggestion that sphingolipids could be essential in cell proliferation signalling, although these characteristics could not be attributed to changes in levels of either a particular end product or an intermediate of the sphingolipid biosynthetic pathway but the perturbation of the pathway in its entirety (Fridberg *et al.*, 2008). Therefore, our akinetoplastic isometamidium resistant cells' perturbed sphingolipid synthesis may have been a response to reduced requirement of these metabolites for kinetoplast segregation. Our akinetoplastic isometamidium resistant clones of higher resistance exhibited a reduced growth phenotype which may have been due to the perturbations in the sphingolipid biosynthetic pathway that were detected in metabolomics analysis of these cells. In particular they showed an accumulation of ceramide and depleted levels of sphingomyelin, a metabolite that has been shown to be more abundant in bloodstream forms than the procyclic forms of *T. brucei* (Richmond *et al.*, 2010). The depleted sphingomyelin in the isometamidium resistant cells may be attributed to the four heterozygous non-synonymous mutations that were found in the resistant line's SLS4, although none of these mutations form part of the predicted catalytic site of the enzyme. But all the mutations were outside the various predicted trans-membrane domains of the enzyme and conserved signatures of the SLSs. *T. brucei* SLS4 has six trans-membrane domains and has been shown to localise to the Golgi (Sutterwala *et al.*, 2008). The accumulated levels of ceramide (2.65 fold difference with the wild-type) in our resistant cells is consistent with the 3.5 fold increase in accumulated ceramide in *T. brucei* whose SLSs were silenced by RNAi (Sutterwala *et al.*, 2008). In our case the elevated levels of ceramide in the resistant cells could be attributed to point mutations in SLS4. Amino acid residues in the catalytic site of the SLSs have been indicated to specify the products of the enzymes and an alteration of these residues lead to altered enzyme product specificity (Sutterwala *et al.*, 2008). This would suggest that mutations in the active site are rare as these enzymes are developmentally regulated to maintain synthesis of particular sphingolipids at particular stages of life cycle of trypanosomes (Sutterwala *et al.*, 2008).

Prolonged blockage of the sphingolipid biosynthetic pathway from the rate determining step catalyzed by serine palmitoyltransferase has a mild effect of reduced endocytosis processes of bloodstream *T. brucei* (Sutterwala *et al.*,

2007). Participation of sphingolipids in endocytosis has been reported in *S. cerevisiae*. The internalisation step of endocytosis in *S. cerevisiae* was shown to be facilitated by dihyrosphingosine (DHS) or sphinganine (Figure 5.10) (Zanolari *et al.*, 2000). It was later shown that sphingolipids with fatty acyl groups consisting of 26 carbon atoms were required for synthesis of a functional  $V_1$  unit of the  $V_1V_0$ -ATPase assembly in yeast (Chung *et al.*, 2003). Blockage of DHS synthesis and lack of availability of C26 acyl groups in sphingolipids of yeast resulted in fragmented vacuoles (Chung *et al.*, 2003; Zanolari *et al.*, 2000). Yeast V-ATPases are located in the vacuole membranes where the  $V_1$  component hydrolyzes ATP to power the pumping of proton by the  $V_0$  component into the vacuoles to create a proton gradient. The proton gradient is used for transportation of ions, small molecules including drugs, metabolites and amino acids into the vacuole (Graham *et al.*, 2000). Exposure of *T. brucei* to isometamidium and use of RIT-seq approach (Alsford *et al.*, 2012) to seek genes whose loss of function can underlie resistance has revealed the up-regulation of various components of the acidic compartments like vacuolar ATPase system and the adaptins (Appendix C)(Baker *et al.*, 2014). A corroboration of these data and perturbation of the sphingolipid biosynthetic pathway resulting in depleted levels of sphingoid bases (i.e. sphinganine and hexadecasphinganine) and sphingomyelin in our isometamidium resistant cell lines suggest a likelihood of involvement of endocytosis in the uptake of isometamidium. However, we have been unable to show an appreciable difference in internalisation of Lucifer yellow dye between the parental wild-type and the ISMM resistant cells. This result is consistent with the unaltered uptake of isometamidium in cells whose V-ATPase subunits were knocked-out (Baker *et al.*, 2014). However, It has already been demonstrated that isometamidium resistant *T. congolense* take up and accumulate less isometamidium than the wild-type cells (Sutherland *et al.*, 1992; Sutherland *et al.*, 1991).

## Chapter Six

### 6 General Discussion

#### 6.1 Amphotericin B resistance

The importance of AmB in leishmaniasis treatment cannot be overemphasised especially that no documented resistance to the drug has been reported. There have been views that resistance to the drug is possible due to the fact that resistance can be induced *in vitro* (Croft *et al.*, 2006). The absence of resistance to the drug in the field and the capability of the parasites to develop resistance *in vitro* offers a timely opportunity to study AmB resistance as this will offer ways and means of countering resistance to the drug and prolong the use of the drug should resistance develop in future.

The effect of AmB on perturbation of the parasites ergosterol biosynthetic pathway is well known. However, most of the studies have highlighted the metabolite changes in the resistant cells with no indication of how this perturbation comes about in *Leishmania*. Absence of the active S-adenosyl-L-methionine: C-24- $\Delta$ -sterol methyltransferase A (SCMT-A) and over expression of copies of SCMT-B has been reported in *L. donovani* resistant to AmB with a corresponding absence of ergosterol in these cells (Pourshafie *et al.*, 2004; Purkait *et al.*, 2012). These results suggested that the absence of ergosterol was due to absence of SCMT-A in the AmB resistant cells. Although ergosterol was not detected in these cells it was thought to be replaced by Cholesta-5,7,24-trien-3 $\beta$ -ol, a metabolite that was detected in the resistant cells due to loss of C24 transmethylation (Purkait *et al.*, 2012). We did not observe any results that could be connected with SCMT. In our study we have identified a non-synonymous mutation (N176I) in lanosterol 14 $\alpha$ -demethylase which was outside the catalytic site. We observed a modest but statistically significant cross resistance to ketoconazole with a 1.7 fold increase in EC<sub>50</sub> value. Ketoconazole is a specific inhibitor of lanosterol 14 $\alpha$ -demethylase. Associated with this mutation was the accumulation of the product of lanosterol 14 $\alpha$ -demethylase, 4, 4-dimethylcholesta-8, 14, 24-trien-3 $\beta$ -ol and depleted levels of ergosterol. We have speculated the accumulation of the reaction product of the mutated

lanosterol 14 $\alpha$ -demethylase to be due to a probable loss of lanosterol 14 $\alpha$ -demethylase's interaction to a different protein.

Extra-chromosomal expression of the wild-type lanosterol 14 $\alpha$ -demethylase in AmB resistant cells restored the levels of ergosterol in the re-expresser cells. Restoration of ergosterol was accompanied by reversal of the AmB resistance and cross resistance to ketoconazole. This indicated a difference between the wild-type and the mutated lanosterol 14 $\alpha$ -demethylase. It is for this reason that we hope to test for differences in activity of the two enzymes following our successful over-expression of the two enzymes in *E. coli*. We also observed loss of susceptibility to pentamidine by AmB resistant cells following expression of the wild-type lanosterol 14 $\alpha$ -demethylase in these cells. AmB resistant cells were found to be highly sensitive to pentamidine (Chapter 4). These results taken together indicate that ergosterol is an important determining factor in AmB resistance as has already been reported. Further, our expression of the wild-type lanosterol 14 $\alpha$ -demethylase in AmB resistant cells and the accompanying reversal of characteristics of AmB resistant cells suggest that N176I mutation underlies AmB resistance in *L. mexicana*. Thus for the first time, to our knowledge, we have identified the role of lanosterol 14 $\alpha$ -demethylase in AmB resistance. It would be interesting to check for the presence of N176I in AmB resistant species of *Leishmania* in other studies (Al-Mohammed *et al.*, 2005; Mbongo *et al.*, 1998; Purkait *et al.*, 2012) to confirm that this mutation underlies AmB resistance in other species of *Leishmania*. The relevance of this mutation is further supported by the fact that lanosterol 14 $\alpha$ -demethylase is essential to these parasites as double knock of the gene was not possible (Verma *et al.*, 2011). Therefore, a homozygous mutation in this gene has resulted in depleted levels of ergosterol, reducing the drug's target, while a heterozygous mutation we speculate would render the parasites susceptible to AmB due to continued synthesis of ergosterol albeit at reduced level. This would not make parasites with a heterozygous mutation in lanosterol 14 $\alpha$ -demethylase resistant but of reduced susceptibility to AmB, since AmB has been reported to kill cells by a mere binding to ergosterol in yeast (Gray *et al.*, 2012).

Susceptibility to oxidative stress is enhanced with inhibition of the sterol biosynthetic pathway from episterol (Figure 1.8) as the metabolites after this

point contain a conjugated double bond in ring B that is important in protection against ROS attack through their proximity to the hydroxyl group in ring A (Figure 3.14) (Dupont *et al.*, 2012). Therefore perturbation of the pathway at an even earlier point such as from lanosterol 14 $\alpha$ -demethylase would render the parasites susceptible to oxidative stress. Indeed our AmB resistant parasites were more susceptible to oxidative stress than the parental wild-type. Exposure of yeast to AmB has been reported to either up-regulate or down-regulated the expression of membrane transporter proteins to counter the loss of ions and nutrients through membrane pores formed by AmB in yeast. Among the induced transport proteins were the drug resistance protein, MDR protein and ABC transporter protein (Zhang *et al.*, 2002). In line with the up-regulation of membrane transport proteins, the multidrug resistance protein 1 (MDR1) was found to be up-regulated in AmB resistant *L. donovani* and this was linked to increased drug efflux than in the wild-type cells (Purkait *et al.*, 2012). Natamycin, a related polyene antibiotic has been shown to inhibit membrane proteins in a general way as different types of transporters were affected by the exposure of yeast and fungi to the drug. It was suggested that the inhibition of these proteins is brought about by the drug's ability to bind to ergosterol in the membranes (te Welscher *et al.*, 2012). Indeed we found that the AmB resistant cells showed cross resistance to miltefosine which was reversed in re-expressor cells. Chemical withdrawal of sterols from membranes was shown to reduce sensitivity to miltefosine by both wild-type and miltefosine resistant cells (Saint-Pierre-Chazalet *et al.*, 2009). Against the background of susceptibility to oxidative stress and anticipated disturbances in membrane transport proteins and increased uptake of pentamidine by the AmB resistant cells, we observed a very significant sensitisation of the AmB resistant parasites to pentamidine. It is worth noting that AmB resistant *Leishmania* highly sensitized towards pentamidine was not reported in studies by Mbongo *et al.*, (1998) and Garcia-Hernandez *et al.*, (2012). Pentamidine is able to induce ROS production and has been suggested to kill leishmania by oxidative stress (Mehta and Shaha, 2004; Moreira *et al.*, 2011). In view of all this, our results taken together suggest a possible use of this drug to counter AmB resistance. The reversal of sensitivity to pentamidine by the re-expressor cells following restoration of ergosterol synthesis suggested a key role of ergosterol levels in sensitivity to pentamidine by the AmB resistant cells. Pentamidine and paromomycin may hold promise to

counter AmB resistant leishmania due to their increased toxicity towards AmB resistant cells we observed, therefore part of the future work will aim at determining how pentamidine enters the AmB resistant cells as this may suggest other ways that can be utilised to tackle the resistant cells.

*Leishmania* amastigotes are clinically relevant but we used the promastigotes that are found in insect vectors. AmB resistant promastigotes were shown to infect mice and the isolated amastigotes from such mice were found to maintain the AmB resistance trait albeit with altered morphology of promastigotes, i.e., promastigotes without flagella (Al-Mohammed *et al.*, 2005). Our AmB resistant promastigotes were able to infect macrophages. To further explore the relevance of AmB resistant parasites carrying the N176I mutation, it would be interesting to pass these parasites in insects to find out whether the mutation compromises their fitness of survival in insects. This would also provide information on the possible transmission of these parasites to humans especially where the disease is anthroponotic.

The identification of mutated lanosterol 14 $\alpha$ -demethylase could not have happened without other compensatory mutations that would have occurred in response to the altered ergosterol levels in the parasites and the general process of resistance induction. Indeed there were a lot of SNPs that were observed in our resistant cells. It is important to appreciate that our analysis of the gDNA analysis was guided by the metabolomics and partly proteomics results. Therefore there could have been other genetic changes that could be relevant to AmB resistance that may have been missed by our analysis possibly because they operate in the background.

## 6.2 Isometamidium resistance

African animal trypanosomiasis is a major impediment to the realisation of the potential contribution of livestock to economic development in rural Africa where livestock is a source of livelihood through provision of draught power, transportation, food, etc., (Welburn *et al.*, 2006). The situation is further exacerbated by the presence of parasites resistant to the few commonly used drugs. ISMM is mostly used for prophylactic purposes but also for treatment of animals against trypanosomiasis caused by *T. congolense* (Delespaux *et al.*,

2008; Geerts *et al.*, 2001). However, little is known about the mode of action and mechanism of resistance to ISMM. Various possible targets of ISMM were reported earlier (Kinabo, 1993) although lately reports have reiterated the involvement of processes in the mitochondrion of the parasites. Thus, reduction of the mitochondrial membrane potential and accumulation of the drug in the mitochondrion, with a specific association with the kinetoplast, have been linked with ISMM resistance (Wilkes *et al.*, 1997). Characterisation of the ISMM resistant parasites will offer an opportunity to prolong the use of the current drugs in the absence of a vaccine as this would open up ways and means of handling the resistant parasites and hence informed drug policy formulation regarding drug treatment regimens.

ISMM resistant *T. congolense* has been shown to take up and accumulate less ISMM than the wild-type (Sutherland *et al.*, 1992; Sutherland *et al.*, 1991). It was shown by fluorescence properties of ISMM that it associates with the kinetoplast in the mitochondrion (Wilkes *et al.*, 1997). Isometamidium is said to promote kDNA - protein complex formation which can be easily cleaved by topoisomerase II leading to linearization of the minicircles and generation of free minicircles in *T. equiperdum* (Shapiro and Englund, 1990). Loss of isometamidium fluorescence by resistant parasites in the region of the kinetoplast was reported (Wilkes *et al.*, 1997). We have shown loss of the kinetoplast by ISMM resistant *T. brucei* BSF. We showed the loss of the kinetoplast by use of the DNA specific stain DAPI and confirmed by absence of NADH dehydrogenase subunit genes that are found in the maxicircles that form part of the kDNA using PCR. The loss of the kinetoplast was possible even at very low isometamidium resistance level as exhibited by resistant clones growing in the presence of 0.01 nM ISMM. Although ISMM resistance is accompanied by loss of the kinetoplast, it does not easily happen as was deduced from the length of time it took us to generate the resistant parasites. It took us 9 months to generate parasites of the highest ISMM resistance, 1  $\mu\text{M}$  with a 94-fold increase in  $\text{EC}_{50}$ . A result consistent with that done *in vivo* and took 11 months to achieve a 94-fold increase in resistance involving a  $\text{CD}_{50}$  ( $\text{CD}_{50}$  is the concentration of the drug required to eliminate the symptoms in 50% of the animals tested) change from 0.018 mg/kg body weight to 1.7 mg/kg bodyweight in *T. congolense* (Peregrine *et al.*, 1997). Indeed it has been reported that it is not easy to generate dyskinetoplastic parasites either *in*

*vivo* or *in vitro* (Timms *et al.*, 2002). Perhaps the difficulty associated with generation of isometamidium resistant parasites involving loss of the kinetoplast could be the determining factor in resistance to this drug as it involves the loss of the maxicircles that harbour the genes that are required for the transmission of the parasites in the insect without which they are incapable of surviving in the insect due to failure to switch their energy metabolism involving the electron transport chain and hence failure to transform into procyclic forms (Schnauffer *et al.*, 2002; Timms *et al.*, 2002). Acriflavine induced loss of the kinetoplast hence the maxicircle genes has been reported to be compensated by mutations in  $\gamma$  subunit of the ATPase that allows the resistant parasite to shift the generation of the mitochondrial membrane potential from breakdown of the ATP by  $F_1$  which allows translocation of protons through the  $F_0$  during the reverse function of the ATPase to use of ADP/ATP carrier (AAC) which works in conjunction with only the  $F_1$  component of ATPase complex to generate the mitochondrial membrane potential (Dean *et al.*, 2013; Schnauffer *et al.*, 2005). Our isometamidium resistant cells did not show presence of mutations in the  $\gamma$  subunit of the ATPase that were unique to these cells. Therefore, kinetoplast loss is most likely the key to isometamidium resistance and therefore this would suggest a possible use of the loss of the kinetoplast as a marker of ISMM resistance.

The loss of the kinetoplast which has been suggested to be the target of the drug would seem to reduce the accumulation of the drug in the mitochondrion. Another strategy used by the parasites to reduce the accumulation of the drug in mitochondria is the maintenance of a reduced mitochondrial membrane potential. The mitochondrial membrane potential has been suggested to lead to accumulation of isometamidium and ethidium bromide in the mitochondrion (Chowdhury *et al.*, 2010; Wilkes *et al.*, 1997), while a reduced mitochondrial membrane potential was thought to lead to reduced accumulation of the drugs. We have showed a much reduced mitochondrial membrane potential by our ISMM resistant cells as compared to the parental wild-type cells. Because the mitochondrial membrane potential is generated during the energy metabolism of trypanosomes, we hypothesised that the reduced mitochondrial membrane potential would have pronounced changes in energy metabolite profile of the parasites. However we observed no apparent changes in metabolite profiles

connected with energy metabolism in resistant parasites as compared to the parental wild-type. However, we observed changes in the sphingolipid metabolites.

The differences in uptake and accumulation of isometamidium by the wild-type and the resistant parasites did not provide information on how the drug enters the parasites. The perturbation of the sphingolipid biosynthesis has been shown to induce reduced growth phenotype, abnormal cytokinesis and failure to segregate the kinetoplast (Fridberg *et al.*, 2008). Sphingolipid depletion has also been reported to reduce endocytosis processes of bloodstream *T. brucei* (Sutterwala *et al.*, 2008). A similar effect has also been shown to affect the internalisation step of endocytosis in yeast (Zanolari *et al.*, 2000) where sphingolipids with fatty acyls made up of specific number of carbon atoms are required for the synthesis of functional  $V_1$  components of  $V_1V_0$ -ATPase are required (Chung *et al.*, 2003). Exposure of *T. brucei* to ISMM induces overexpression of the various elements of the acidic vacuole system including V-ATPases and adaptins (see appendix C) (Baker *et al.*, 2014). Our ISMM resistant parasites have shown alterations in the sphingolipid biosynthetic pathway although there was no appreciable difference in internalisation of Lucifer yellow and hence endocytosis.

The fact that we found an association between the appearance of heterozygous mutations in SLS4 and isometamidium resistance suggests an important experiment that time constraints have not allowed in this thesis. Specifically the mutant allele should be expressed in wild-type parasites, to determine whether this expression can yield isometamidium resistance; either immediately or at an increased rate should it be a predisposition to kinetoplast loss that underlies the effect.

With very few drugs available for treatment of AAT, occurrence of ISMM cross resistance to other AAT drugs poses the challenge of limited alternative treatment drugs should resistance develop to one of the drugs. We have shown increasing ISMM cross resistance to DA with increasing level of resistance to ISMM. *T. brucei* of lower ISMM resistance, i.e. those growing in the presence of 400 nM or less, show modest ISMM cross resistance to diminazene aceturate and

ethidium bromide. This is in agreement with earlier reports in *T. congolense* (Peregrine *et al.*, 1997), although our ISMM resistant clones achieved this in about 8 months compared to 11 months by Peregrine and co-workers (1997). ISMM cross resistance to ethidium bromide in our resistant clones was 2.7 fold in contrast with that reported earlier for *T. congolense* standing at 34-fold increase in 50% inhibitory concentration of the drug. ISMM is normally used as a prophylactic drug while diminazene aceturate is recommended for treatment of AAT cases. Therefore treatment with diminazene aceturate where higher ISMM resistance exists would result in more treatment failures.

Several methods are employed to elucidate drug resistance mechanisms (Berg *et al.*, 2013a; Horn and Duraisingh, 2014), here we show that polyomics can be used to decipher drug resistance mechanisms. Complementary use of untargeted metabolomics and gDNA sequencing is a worthwhile combination of techniques that can be used, especially that the cost of sequencing has continued to go down and the technique has continued to be developed (Liu *et al.*, 2012). On the other hand metabolomics has also continued to evolve resulting in improved LC/MS methods and improved data analysis platforms that are applicable to study of mode of action and mechanisms of resistance to anti-protozoal drugs (Creek and Barrett, 2014). Metabolomics involves minimal sample handling thereby ruling out degradation of samples during sample extraction. While proteomics has also continued to evolve perhaps it has one disadvantage of multistep sample handling which predisposes protein samples to degradation.

## Appendices

### Appendix A: Reagent recipes

#### A1 NTE buffer

10 mM Tris-HCl pH 8.0

100 mM NaCl

5 mM EDTA

#### A2 Tb BSF buffer

90 mM Na-PO<sub>4</sub> pH7.3      1.8 mL

5 mM KCl                      166.6  $\mu$ L

50 mM HEPES pH7.3              1 mL

0.15 mM CaCl<sub>2</sub>              30  $\mu$ L

dd H<sub>2</sub>O                      7 mL

Store at 4 °C

#### A3 TAE (1 $\times$ )

40 mM Tris acetate (pH 8.5)

1 mM EDTA

#### A4 Assay Buffer

33 mM      HEPES

98 mM NaCl

4.6 mM KCl

0.55 mM CaCl<sub>2</sub>

0.07 mM MgSO<sub>4</sub>

5.8 mM NaH<sub>2</sub>PO<sub>4</sub> · 2H<sub>2</sub>O

0.3 mM MgCl<sub>2</sub>

23 mM NaHCO<sub>3</sub>

14 mM Glucose

Adjust pH to 7.3

#### A5 Lysis buffer:

6 M urea

2 M thiourea

4% CHAPS  
25 mM tris base

**A6 DiGE Rehydration buffer**

6 M Urea  
4% CHAPS  
2 M Thiourea  
65 mM DTT  
0.5% IPG buffer  
Trace bromophenol blue

**A7 DiGE Equilibration Buffer I**

2 % SDS  
50 mM Tris-HCl pH 8.8  
6 M urea  
30 % (v/v) glycerol  
0.002% bromophenol blue  
1% DTT

**A8 DiGE Equilibration Buffer II**

2 % SDS  
50 mM Tris-HCl pH 8.8  
6 M urea  
30 % (v/v) glycerol  
0.002% bromophenol blue  
2.5 Idoacetamide

**A9 Coomassie blue stain solution**

10 ml Acetic acid  
45 ml water  
0.1 g Coomassie blue stain

**A10 Destaining solution**

40% methanol  
10% acetic acid

**A11 SDS Running buffer (5X)**

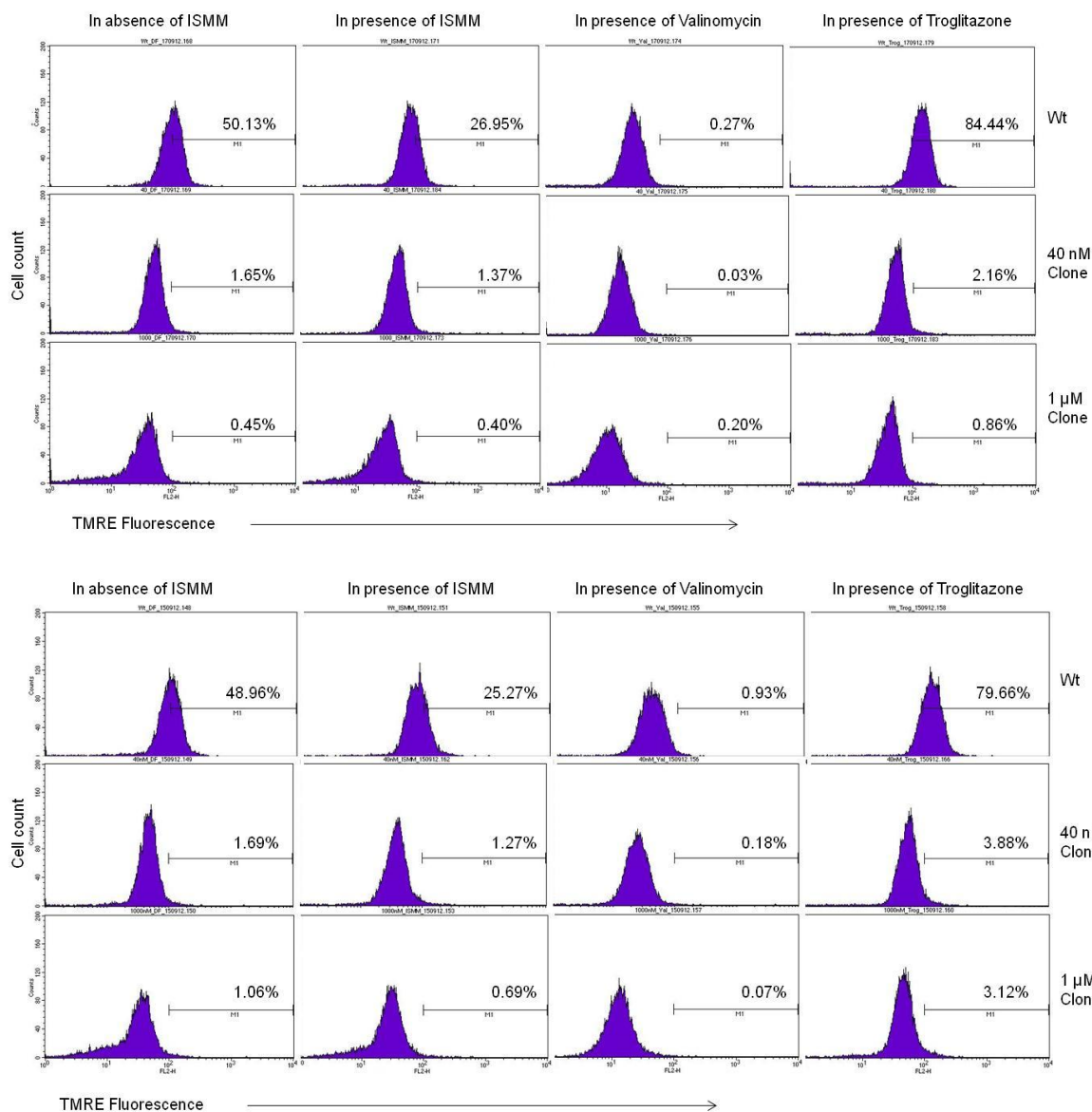
Tris 30.3 g

Glycine 144.0g

SDS 10.0 g

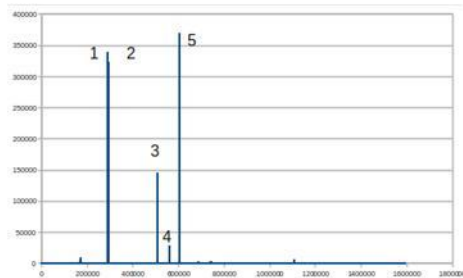
Made up to 2000 ml with dH<sub>2</sub>O

## Appendix B: Monitoring mitochondrial membrane potential

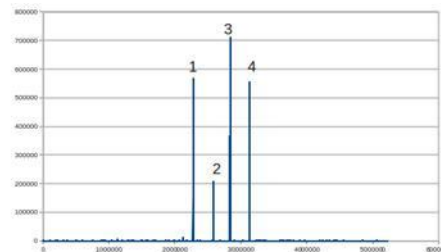


Monitoring of the mitochondrial membrane potential by accumulation of TMRE by the parental wild-type and derived isometamidium resistant clones

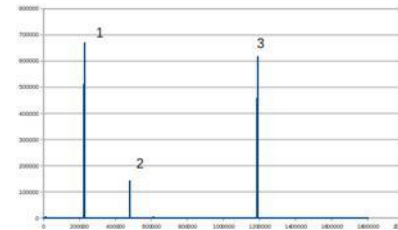
## Appendix C: Ritseq result of the *T. b. brucei* 927 exposed to isometamidium



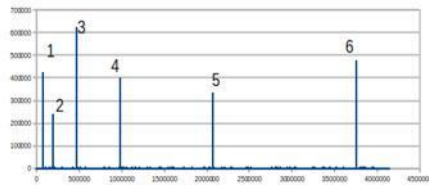
1. V-type ATPase, A subunit, putative 288, 35 to 290,176 (Chromosome: 4) Tb927.4.1080
2. Endosomal integral membrane protein, putative 290,368 to 292,772 (Chromosome: 4) Tb927.4.1090
3. Mu-adaptin 3, putative, adaptor complex AP-3 medium unit, putative 507,952 to 509,511 (Chromosome: 4) Tb927.4.202
4. Tb927.4.2170 559,014 to 560,459 (Chromosome: 4)
5. Tb927.4.2170 604,337 to 605,700 (Chromosome: 4)



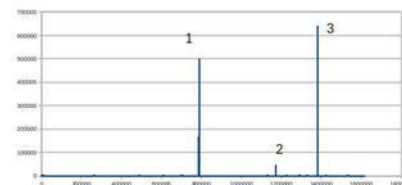
1. Tb927.11.8310 2,275,607 to 2,276,675 (Chromosome: 11)
2. ATP synthase, putative 2,581,173 to 2,582,770 (Chromosome: 11) Tb927.11.9420
3. Beta adaptin 3, putative, adaptptin complex 3 subunit, putative 2,836,046 to 2,839,364 (Chromosome: 11) Tb927.11.10650
4. Vacuolar ATP synthase subunit b, putative, v-ATPase B subunit. Vacuolar proton pump B subunit 3,135,788 to 3,138,260 (Chromosome: 11) Tb927.11.11690



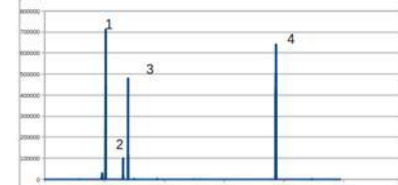
1. Vacuolar ATP synthase, putative 228, 316 to 229,739 (Chromosome: 5) Tb927.5.550
2. Vacuolar proton translocating ATPase subunit A, putative 481,546 to 484,682 (Chromosome: 5) Tb927.10.1300
3. Vacuolar ATP synthase subunit d, putative 976, 594 to 977,949 (Chromosome: 10) Tb927.10.3760
4. Adaptor complex protein (AP) 3 delta subunit 1, putative 1,185,580 to 1,189,703 (Chromosome: 5) Tb927.10.8370



1. Vacuolar ATP synthase, putative 74, 489 to 75,381 (Chromosome: 10) Tb927.10.200
2. ATP synthase, putative 187,319 to 190,277 (Chromosome: 10) Tb927.10.730
3. Tb927.10.1740 462,978 to 464,366 (Chromosome: 10)
4. Vacuolar ATP synthase subunit d, putative 976, 594 to 977,949 (Chromosome: 10) Tb927.10.3760
5. Tb927.10.8370 2,066,935 to 2,068,238 (Chromosome: 10)
6. Tb927.10.15320 3,752,175 to 3,753,239 (Chromosome: 10)



1. Tb927.6.2590 787,440 to 788,675 (Chromosome: 6)
2. Small glutamine-rich tetratricopeptide repeat protein (SGT), putative 290,368 to 292,772 (Chromosome: 4) Tb927.6.4000
3. V-type ATPase, C subunit, putative 1,381,779 to 1,382,930 (Chromosome: 4) Tb927.4.1080



1. Tb927.8.1,570,510,700 to 512,565 (Chromosome: 8)
2. Cyclophilin type peptidyl-prolyl cis-trans isomerase, putative (PPIase) 657,734 to 658,456 (Chromosome: 8) Tb927.8.2090
3. Beta adaptin 3, putative, adaptptin complex 3 subunit, putative 2,836,046 to 2,839,364 (Chromosome: 11) Tb927.11.10650
4. (H)-ATPase G subunit, putative, 1,933,277 to 1,933,910 (Chromosome: 8) Tb927.8.6680

Alterations in the various components of the acidic compartments following exposure of wild-type *T. brucei* to isometamidium

## Appendix D: *S. cerevisiae* sterol biosynthetic pathway enzymes and *L. mexicana* orthologs

<i>S. cerevisiae</i> gene and enzyme sequence Blasted	Sequences producing High-scoring Segment Pairs	L. Mexicana Enzyme ID	High score	Smallest sum probability		EC #
				P(N)	N	
ERG1(squalene monooxygenase)	LmxM.13.1620.1..pep	squalene monooxygenase-like protein	471	2.0e-46	1	1.14.13.132
ERG2 (C-5 sterol desaturase)	LmxM.08_29.2140.1..pep	C-8 sterol isomerase-like protein	442	2.4e-43	1	
ERG3 (C-5 sterol desaturase)	LmxM.23.1300.1..pep	lathosterol oxidase-like protein	480	2.2e-47	1	1.14.21.6
	LmxM.30.0590.1..pep	C-5 sterol desaturase, putative	127	3.3e-07	1	
ERG4 (C-24 sterol reductase)	LmxM.32.0680.1..pep	sterol C-24 reductase, putative	704	4.1e-71	1	1.3.1.71
	LmxM.31.2320.1..pep	C-14 sterol reductase, putative	232	1.9e-18	1	
ERG5 (C-22 sterol desaturase)	LmxM.29.3550.1..pep	cytochrome p450-like protein	442	2.4e-43	1	1.14.14.1
	LmxM.33.3330.1..pep	cytochrome p450-like protein	169	6.0e-11	1	
	LmxM.11.1100.1..pep	lanosterol 14-alpha-demethylase, putative	147	1.2e-08	1	1.14.13.70
ERG 6 (SAM:C-24 sterol methyltransferase)	LmxM.36.2390.1..pep	sterol 24-c-methyltransferase, putative	673	7.9e-68	1	
	LmxM.36.2380.1..pep	sterol 24-c-methyltransferase, putative	672	1.0e-67	1	
ERG 7 (2,3-oxidosqualene-lanosterol cyclase)	LmxM.06.0650.1..pep	lanosterol synthase, putative	1017	3.7e-111	2	5.4.99.8
	LmxM.33.4030.1..pep	geranylgeranyltransferase, putative	74	0.63	1	2.5.1-
ERG 8 (phosphomevalonate kinase)	LmxM.15.1460.1..pep	phosphomevalonate kinase-like protein	373	4.9e-36	1	2.7.4.2
	LmxM.30.0560.1..pep	mevalonate kinase, putative	69	0.64	2	
ERG9 (squalene synthetase)	LmxM.30.2940.1..pep	farnesyltransferase, putative	673	7.9e-68	1	2.5.1.21
ERG10 (acetoacetyl CoA thiolase)	LmxM.30.1640.1..pep	thiolase protein-like protein	365	3.4e-35	1	2.3.1.16
	LmxM.30.1640.1..pep	3-ketoacyl-CoA thiolase-like protein, putative	306	6.1e-29	1	2.3.1.16
	LmxM.23.0690.1..pep	3-ketoacyl-CoA thiolase-like protein	92	4.1e-07	3	2.3.1.16
ERG 11 (cytochrome P450)	LmxM.11.1100.1..pep	lanosterol 14-alpha-demethylase,	475	6.5e-54	2	1.14.13.70

lanosterol 14a-demethylase)		putative				
	LmxM.29.3550.1..pep	cytochrome p450-like protein	165	1.1e-14	2	1.14.14.-
	LmxM.33.3330.1..pep	cytochrome p450-like protein	178	6.0e-12	1	
ERG12 (mevalonate kinase)*	LmxM.30.0560.1..pep	mevalonate kinase, putative	120	1.7e-09	3	
ERG13 (3-hydroxy-3-methylglutaryl coenzyme A synthase) *	LmxM.24.2110.1..pep	hypothetical protein, conserved	190	7.8e-17	2	
ERG 20 (farnesyl diphosphate synthetase)	LmxM.22.1360.1..pep	farnesyl pyrophosphate synthase, putative	545	2.9e-54	1	2.5.1.10
	LmxM.15.1020.1..pep	farnesyl synthetase, putative	107	9.9e-05	1	
ERG24 (C-14 sterol reductase)	LmxM.31.2320.1..pep	C-14 sterol reductase, putative	674	6.2e-68	1	
	LmxM.32.0680.1..pep	sterol C-24 reductase, putative	231	2.9e-35	2	1.3.1.71
ERG25 (C-4 sterol methyl oxidase)*	LmxM.36.2540.1..pep	hypothetical protein, unknown function	143	7.0e-09	2	
	LmxM.23.1300.1..pep	lanosterol oxidase-like protein	136	2.8e-08	1	1.3.3.2
	LmxM.30.0590.1..pep	C-5 sterol desaturase, putative	120	1.5e-06	1	
ERG26 (C-3 sterol dehydrogenase)*	LmxM.06.0350.1..pep	NAD(p)-dependent steroid dehydrogenase-like protein	263	2.2e-24	1	
ERG27 (3-keto sterol reductase)*	LmxM.34.1230.1..pep	short chain dehydrogenase, putative	82	0.028	2	
	LmxM.34.2150.1..pep	hypothetical protein, conserved	63	0.69	2	
ERG28(Polypeptide: subunit of C-4 demethylation complex)* (Subunit composition of C-4 demethylation - ERG25;ERG26;ERG27ERG28)	LmxM.08_29.1970.1..pep	hypothetical protein, unknown function	51	0.14	1	
	LmxM.29.1625.1..pep	hypothetical protein, conserved	60	0.62	1	

## Appendix E: Ergosterol pathway enzyme wise SNP and CNV annotations for Wt and AmB-R cell lines

Ergosterol Pathway Enzyme wise SNP and CNV annotations for WT and AmpB-R																	
1. Thiolase protein-like (most likely trifunctional protein Beta subunit)											LmxM.30.1640						
No SNPs in WT																	
No SNPs in AmpB-R																	
OrthomclID	Chromosome	Chromosome Ploidy	# Genes in Ref	Region Start	Region End	CN total	mean coverage	mean fpkm	Haploid number	Gene Dose	Gene List	Description	total coverage	total fpkm	coverage per kb	Rounded Haploid	Rounded Gene Dose
<b>WT</b>																	
OG5_131200	GeneDB LmxM.30	4	2	765531	768619	7.145	170.712	507793	1.79	7.1	LmxM.30.1630, LmxM.30.1640	Thiolase protein-like protein, 3-ketoacyl-CoA thiolase-like protein, putative	341.423	1015586	110.56	2	8
<b>AmpB-R</b>																	
OG5_131200	GeneDB LmxM.30	4	2	765531	768619	6.5	155.922	510457	1.62	6.5	LmxM.30.1630, LmxM.30.1640	Thiolase protein-like protein, 3-ketoacyl-CoA thiolase-like protein, putative	311.843	1020914	100.99	2	8
2. Hydroxy-3-methylglutaryl coenzyme a reductase											LmxM.29.3190						
No SNPs in WT																	
No SNPs in AmpB-R																	

OrthomclID	Chromosome	Chromosome Ploidy	# Genes in Ref	Region Start	Region End	CN total	mean coverage	mean fpkm	Haploid Number	Gene Dose	Gene List	Description	total coverage	total fpkm	coverage per kb	Rounded Haploid	Rounded Gene Dose
<b>WT</b>																	
OG5_127955	GeneDB Lm xM.29	2	1	1144534	1145839	1.984	44.626	138831	0.99	2	LmxM.29.3190	3-hydroxy-3-methylglutaryl-CoA reductase, putative	44.6258	138831	34.2	1	2
<b>AmpB-R</b>																	
OG5_127955	GeneDB Lm xM.29	2	1	1144534	1145839	2.123	45.709	157109	1.06	2.1	LmxM.29.3190	3-hydroxy-3-methylglutaryl-CoA reductase, putative	45.7086	157109	35.03	1	2
<b>3. Mevalonate kinase</b>										<b>LmxM.30.0560</b>							
No SNPs in WT																	
No SNPs in AmpB-R																	
OrthomclID	Chromosome	Chromosome Ploidy	# Genes in Ref	Region Start	Region End	CN total	mean coverage	mean fpkm	Haploid Number	Gene Dose	Gene List	Description	total coverage	total fpkm	coverage per kb	Rounded Haploid	Rounded Gene Dose
<b>WT</b>																	
OG5_128331	GeneDB Lm xM.30	4	1	214235	215294	2.902	138.565	412434	0.73	2.9	LmxM.30.0560	Mevalonate kinase, putative	138.565	412434	130.85	1	4
<b>AmpB-R</b>																	
OG5_128331	GeneDB Lm xM.30	4	1	214235	215294	2.64	127.166	414612	0.66	2.6	LmxM.30.0560	Mevalonate kinase, putative	127.166	414612	120.08	1	4
<b>4. Phosphomevalonate kinase</b>										<b>LmxM.15.1460</b>							
No SNPs in WT																	

No SNPs in AmpB-R																	
OrthomclID	Chromosome	Chromosome Ploidy	# Genes in Ref	Region Start	Region End	CN total	mean coverage	mean fpkm	Haploid Number	Gene Dose	Gene List	Description	total coverage	total fpkm	coverage per kb	Rounded Haploid	Rounded Gene Dose
<b>WT</b>																	
OG5_131773	GeneDB LmxM.15	2	1	532092	533469	1.834	31.345	104123	0.92	1.8	LmxM.15.1460	Phosphomevalonate kinase-like protein	31.3452	104123	22.76	1	2
<b>AmpB-R</b>																	
OG5_131773	GeneDB LmxM.15	2	1	532092	533469	1.932	34.099	123345	0.97	1.9	LmxM.15.1460	Phosphomevalonate kinase-like protein	34.0989	123345	24.76	1	2
<b>5. Diphosphomevalonate decarboxylase</b>																	
<b>LmxM.18.0020</b>																	
Chromosome Number	SNP Position	Within CDS	Region	Distance to the nearest CDS	Start of current CDS	End of current CDS	Gene ID containing current CDS	Strand sense	Estimated Reading Frame	Estimated Number of Stop Codons	Codon	Amino Acid	synonymous				
<b>WT</b>																	
GENEDB LMXM.18	5569	N	Intro nic	783	6352	7503	LmxM.18.0020	-	NA	NA	NA	NA	NA				
GENEDB LMXM.18	5691	N	Intro nic	661	6352	7503	LmxM.18.0020	-	NA	NA	NA	NA	NA				
GENEDB LMXM.18	6333	N	Intro nic	19	6352	7503	LmxM.18.0020	-	NA	NA	NA	NA	NA				
GENEDB LMXM.18	6466	Y	Exon ic	NA	6352	7503	LmxM.18.0020	-	-1	^0	TT[T/C]	[F/F]	Y				
GENEDB LMXM.18	7025	Y	Exon ic	NA	6352	7503	LmxM.18.0020	-	-1	^0	A[A/G]C	[N/S]	N				
GENEDB LMXM.18	7072	Y	Exon ic	NA	6352	7503	LmxM.18.0020	-	-1	^0	GG[C/T]	[G/G]	γ***				
<b>AmpB-R</b>																	
GENEDB LMXM	5445	N	Intro	907	6352	7503	LmxM.18	-	NA	NA	NA	NA	NA				

.18			nic				.0020										
GENEDB LMXM .18	5569	N	Intro nic	783	6352	7503	LmxM.18 .0020	-	NA	NA	NA	NA	NA				
GENEDB LMXM .18	5691	N	Intro nic	661	6352	7503	LmxM.18 .0020	-	NA	NA	NA	NA	NA				
GENEDB LMXM .18	6197	N	Intro nic	155	6352	7503	LmxM.18 .0020	-	NA	NA	NA	NA	NA				
GENEDB LMXM .18	6333	N	Intro nic	19	6352	7503	LmxM.18 .0020	-	NA	NA	NA	NA	NA				
GENEDB LMXM .18	6466	Y	Exon ic	NA	6352	7503	LmxM.18 .0020	-	-1	^0	TT[T/C]	[F/F]	Y				
GENEDB LMXM .18	7025	Y	Exon ic	NA	6352	7503	LmxM.18 .0020	-	-1	^0	A[A/G]C	[N/S]	N				
GENEDB LMXM .18	7072	Y	Exon ic	NA	6352	7503	LmxM.18 .0020	-	-1	^0	GG[C/T]	[G/G]	Y***				
GENEDB LMXM .18	7330	Y	Exon ic	NA	6352	7503	LmxM.18 .0020	-	-1	^0	GT[C/T]	[V/V]	Y***				
GENEDB LMXM .18	7627	N	Intro nic	124	6352	7503	LmxM.18 .0020	-	NA	NA	NA	NA	NA				
OrthomclID	Chromosome	Chromosome Ploidy	# Genes in Ref	Region Start	Region End	CN total	mean coverage	mean fpkm	Haploid Number	Gene Dose	Gene List	Description	total coverage	total fpkm	coverage per kb	Rounded Haploid	Rounded Gene Dose
<b>WT</b>																	
OG5_128252	GeneDB Lm xM.18	2	1	6351	7503	2.573	53.331	166002	1.29	2.6	LmxM.18. 0020	Diphosphomeval onate decarboxylase, putative	53.3315	1660 02	46.29	1	2
<b>AmpB-R</b>																	
OG5_128252	GeneDB Lm xM.18	2	1	6351	7503	2.163	44.266	152238	1.08	2.2	LmxM.18. 0020	Diphosphomeval onate decarboxylase, putative	44.2661	1522 38	38.43	1	2
6. Isopentenyl-diphosphate delta-isomerase										LmxM.34.5330							

Chromosome Number	SNP Position	Within CDS	Region	Distance to the nearest CDS	Start of current CDS	End of current CDS	Gene ID containing current CDS	Strand sense	Estimated Reading Frame	Estimated Number of Stop Codons	Codon	Amino Acid	synonymous				
<b>WT</b>																	
GENEDB LMXM .34	1930162	N	Intro nic	298	1930 460	1931 530	LmxM.34 .5330	+	NA	NA	NA	NA	NA				
GENEDB LMXM .34	1931192	Y	Exon ic	NA	1930 460	1931 530	LmxM.34 .5330	+	2	1	[G/C]CT	[A/P]	N				
GENEDB LMXM .34	1931194	Y	Exon ic	NA	1930 460	1931 530	LmxM.34 .5330	+	2	1	GC[T/G]	[A/A]	γ***				
GENEDB LMXM .34	1931272	Y	Exon ic	NA	1930 460	1931 530	LmxM.34 .5330	+	2	1	CT[G/A]	[L/L]	γ***				
GENEDB LMXM .34	1931368	Y	Exon ic	NA	1930 460	1931 530	LmxM.34 .5330	+	2	1	AC[A/G]	[T/T]	γ***				
GENEDB LMXM .34	1931437	Y	Exon ic	NA	1930 460	1931 530	LmxM.34 .5330	+	2	1	AT[C/G]	[I/M]	N				
GENEDB LMXM .34	1931567	N	Intro nic	37	1930 460	1931 530	LmxM.34 .5330	+	NA	NA	NA	NA	NA				
GENEDB LMXM .34	1931605	N	Intro nic	75	1930 460	1931 530	LmxM.34 .5330	+	NA	NA	NA	NA	NA				
GENEDB LMXM .34	1931615	N	Intro nic	85	1930 460	1931 530	LmxM.34 .5330	+	NA	NA	NA	NA	NA				
GENEDB LMXM .34	1931818	N	Intro nic	288	1930 460	1931 530	LmxM.34 .5330	+	NA	NA	NA	NA	NA				
GENEDB LMXM .34	1931908	N	Intro nic	378	1930 460	1931 530	LmxM.34 .5330	+	NA	NA	NA	NA	NA				
GENEDB LMXM .34	1931974	N	Intro nic	444	1930 460	1931 530	LmxM.34 .5330	+	NA	NA	NA	NA	NA				
<b>AmpB-R</b>																	
GENEDB LMXM .34	1930162	N	Intro nic	298	1930 460	1931 530	LmxM.34 .5330	+	NA	NA	NA	NA	NA				
GENEDB LMXM .34	1930424	N	Intro nic	36	1930 460	1931 530	LmxM.34 .5330	+	NA	NA	NA	NA	NA				
GENEDB LMXM .34	1931192	Y	Exon ic	NA	1930 460	1931 530	LmxM.34 .5330	+	2	1	[G/C]CT	[A/P]	N				
GENEDB LMXM .34	1931194	Y	Exon ic	NA	1930 460	1931 530	LmxM.34 .5330	+	2	1	GC[T/G]	[A/A]	γ***				
GENEDB LMXM .34	1931272	Y	Exon ic	NA	1930 460	1931 530	LmxM.34 .5330	+	2	1	CT[G/A]	[L/L]	γ***				

GENEDB LMXM.34	1931368	Y	Exonic	NA	1930460	1931530	LmxM.34.5330	+	2	1	AC[A/G]	[T/T]	γ***					
GENEDB LMXM.34	1931437	Y	Exonic	NA	1930460	1931530	LmxM.34.5330	+	2	1	AT[C/G]	[I/M]	N					
GENEDB LMXM.34	1931567	N	Intronic	37	1930460	1931530	LmxM.34.5330	+	NA	NA	NA	NA	NA					
GENEDB LMXM.34	1931605	N	Intronic	75	1930460	1931530	LmxM.34.5330	+	NA	NA	NA	NA	NA					
GENEDB LMXM.34	1931615	N	Intronic	85	1930460	1931530	LmxM.34.5330	+	NA	NA	NA	NA	NA					
GENEDB LMXM.34	1931818	N	Intronic	288	1930460	1931530	LmxM.34.5330	+	NA	NA	NA	NA	NA					
GENEDB LMXM.34	1931908	N	Intronic	378	1930460	1931530	LmxM.34.5330	+	NA	NA	NA	NA	NA					
GENEDB LMXM.34	1931974	N	Intronic	444	1930460	1931530	LmxM.34.5330	+	NA	NA	NA	NA	NA					
OrthomclID	Chromosome	Chromosome Ploidy	# Genes in Ref	Region Start	Region End	CN total	mean coverage	mean fpkm	Haploid Number	Gene Dose	Gene List	Description	total coverage	total fpkm	coverage per kb	Rounded Haploid	Rounded Gene Dose	
<b>WT</b>																		
OG5_131452	GeneDB LmxM.34	2	1	1930459	1931530	1.937	45.672	141239	0.97	1.9	LmxM.34.5330	Isomerase, putative, isopentenyl-diphosphate delta-isomerase, putative	45.6724	141239	42.64	1	2	
<b>AmpB-R</b>																		
OG5_131452	GeneDB LmxM.34	2	1	1930459	1931530	2.225	49.84	170316	1.11	2.2	LmxM.34.5330	Isomerase, putative, isopentenyl-diphosphate delta-isomerase, putative	49.8402	170316	46.54	1	2	
<b>7. Farnesyl pyrophosphate synthase FPPS</b>																		
<b>LmxM.22.1360</b>																		

Chromosome Number	SNP Position	Within CDS	Region	Distance to the nearest CDS	Start of current CDS	End of current CDS	Gene ID containing current CDS	Strand sense	Estimated Reading Frame	Estimated Number of Stop Codons	Codon	Amino Acid	synonymous					
<b>WT</b>																		
GENEDB LMXM.22	563569	N	Intro nic	1342	564911	565999	LmxM.22.1360	-	NA	NA	NA	NA	NA					
GENEDB LMXM.22	566244	N	Intro nic	245	564911	565999	LmxM.22.1360	-	NA	NA	NA	NA	NA					
<b>AmpB-R</b>																		
GENEDB LMXM.22	566244	N	Intro nic	245	564911	565999	LmxM.22.1360	-	NA	NA	NA	NA	NA					
OrthomclID	Chromosome	Chromosome Ploidy	# Genes in Ref	Region Start	Region End	CN total	mean coverage	mean fpkm	Haploid Number	Gene Dose	Gene List	Description	total coverage	total fpkm	coverage per kb	Rounded Haploid	Rounded Gene Dose	
<b>WT</b>																		
OG5_127590	GeneDB LmxM.22	2	1	564910	565999	2.497	49.995	157763	1.25	2.5	LmxM.22.1360	Farnesyl pyrophosphate synthase, putative	49.9953	157763	45.91	1	2	
<b>AmpB-R</b>																		
OG5_127590	GeneDB LmxM.22	3	1	564910	565999	2.604	77.471	267691	0.87	2.6	LmxM.22.1360	Farnesyl pyrophosphate synthase, putative	77.4711	267691	71.14	1	3	
<b>8. Prenyltransferase, putative</b>										<b>LmxM.28.1320</b>								
No SNPs in WT																		
No SNPs in AmpB-R																		

OrthomclID	Chromosome	Chromosome Ploidy	# Genes in Ref	Region Start	Region End	CN total	mean coverage	mean fpkm	Haploid Number	Gene Dose	Gene List	Description	total coverage	total fpkm	coverage per kb	Rounded Haploid	Rounded Gene Dose
<b>WT</b>																	
OG5_127332	GeneDB LmxM.28	2	1	481248	482718	2.319	52.357	161148	1.16	2.3	LmxM.28.1320	Prenyltransferase, putative	52.357	161148	35.62	1	2
<b>AmpB-R</b>																	
OG5_127332	GeneDB LmxM.28	2	1	481248	482718	2.399	52.484	178820	1.2	2.4	LmxM.28.1320	Prenyltransferase, putative	52.484	178820	35.7	1	2
<b>9. Farnesyl pyrophosphate synthetase   solanesyl diphosphate synthase</b>											<b>LmxM.15.1020</b>						
No SNPs in WT																	
No SNPs in AmpB-R																	
OrthomclID	Chromosome	Chromosome Ploidy	# Genes in Ref	Region Start	Region End	CN total	mean coverage	mean fpkm	Haploid Number	Gene Dose	Gene List	Description	total coverage	total fpkm	coverage per kb	Rounded Haploid	Rounded Gene Dose
<b>WT</b>																	
OG5_126937	GeneDB LmxM.15	2	1	402341	403421	1.864	32.516	105814	0.93	1.9	LmxM.15.1020	Farnesyl synthetase, putative	32.5158	105814	30.11	1	2
<b>AmpB-R</b>																	
OG5_126937	GeneDB LmxM.15	2	1	402341	403421	1.791	31.791	114328	0.9	1.8	LmxM.15.1020	Farnesyl synthetase, putative	31.791	114328	29.44	1	2
<b>10. Geranylgeranyl transferase type II beta subunit, putative</b>											<b>LmxM.33.4030</b>						
No SNPs in WT																	
No SNPs in AmpB-R																	

OrthomclID	Chromosome	Chromosome Ploidy	# Genes in Ref	Region Start	Region End	CN total	mean coverage	mean fpkm	Haploid Number	Gene Dose	Gene List	Description	total coverage	total fpkm	coverage per kb	Rounded Haploid	Rounded Gene Dose
<b>WT</b>																	
OG5_127744	GeneDB Lm xM.33	2	1	1526900	1527893	1.674	39.131	124080	0.84	1.7	LmxM.33.4030	Geranylgeranyltransferase, putative	39.1313	124080	39.41	1	2
<b>AmpB-R</b>																	
OG5_127744	GeneDB Lm xM.33	2	1	1526900	1527893	1.768	38.364	135228	0.88	1.8	LmxM.33.4030	Geranylgeranyltransferase, putative	38.3642	135228	38.63	1	2
<b>11. Squalene synthase   farnesyl transferase</b>										<b>LmxM.30.2940</b>							
No SNPs in WT																	
No SNPs in AmpB-R																	
OrthomclID	Chromosome	Chromosome Ploidy	# Genes in Ref	Region Start	Region End	CN total	mean coverage	mean fpkm	Haploid Number	Gene Dose	Gene List	Description	total coverage	total fpkm	coverage per kb	Rounded Haploid	Rounded Gene Dose
<b>WT</b>																	
OG5_129470	GeneDB Lm xM.30	4	1	1342726	1343971	2.669	125.114	379380	0.67	2.7	LmxM.30.2940	Farnesyltransferase, putative	125.114	379380	100.49	1	4
<b>AmpB-R</b>																	
OG5_129470	GeneDB Lm xM.30	4	1	1342726	1343971	2.859	134.369	449052	0.71	2.9	LmxM.30.2940	Farnesyltransferase, putative	134.369	449052	107.93	1	4
<b>12. Squalene monooxygenase</b>										<b>LmxM.13.1620</b>							
No SNPs in WT																	
No SNPs in AmpB-R																	

OrthomclID	Chromosome	Chromosome Ploidy	# Genes in Ref	Region Start	Region End	CN total	mean coverage	mean fpkm	Haploid Number	Gene Dose	Gene List	Description	total coverage	total fpkm	coverage per kb	Rounded Haploid	Rounded Gene Dose
<b>WT</b>																	
OG5_129832	GeneDB Lm xM.13	3	1	571618	573328	2.806	96.015	297034	0.94	2.8	LmxM.13.1620	Squalene monooxygenase-like protein	96.0149	297034	56.15	1	3
<b>AmpB-R</b>																	
OG5_129832	GeneDB Lm xM.13	3	1	571618	573328	2.715	78.298	268588	0.91	2.7	LmxM.13.1620	Squalene monooxygenase-like protein	78.298	268588	45.79	1	3
<b>13. Lanosterol synthase</b>																	
										<b>LmxM.06.0650</b>							
No SNPs in WT																	
No SNPs in AmpB-R																	
OrthomclID	Chromosome	Chromosome Ploidy	# Genes in Ref	Region Start	Region End	CN total	mean coverage	mean fpkm	Haploid Number	Gene Dose	Gene List	Description	total coverage	total fpkm	coverage per kb	Rounded Haploid	Rounded Gene Dose
<b>WT</b>																	
OG5_127966	GeneDB Lm xM.06	2	1	230609	233618	1.806	40.944	136592	0.9	1.8	LmxM.06.0650	Lanosterol synthase, putative	40.9442	136592	13.61	1	2
<b>AmpB-R</b>																	
OG5_127966	GeneDB Lm xM.06	2	1	230609	233618	1.787	28.007	103714	0.89	1.8	LmxM.06.0650	Lanosterol synthase, putative	28.0074	103714	9.31	1	2
<b>14. Sterol 14-alpha (lanosterol) demethylase (CP51)</b>										<b>LmxM.11.1100</b>							

Chromosome Number	SNP Position	Within CDS	Region	Distance to the nearest CDS	Start of current CDS	End of current CDS	Gene ID containing current CDS	Strand sense	Estimated Reading Frame	Estimated Number of Stop Codons	Codon	Amino Acid	synonymous				
<b>WT</b>																	
GENEDB LMXM.11	441733	N	Intro nic	1040	442773	444212	LmxM.11.1100	+	NA	NA	NA	NA	NA				
GENEDB LMXM.11	441733	N	Intro nic	1040	442773	444212	LmxM.11.1100	+	NA	NA	NA	NA	NA				
<b>AmpB-R</b>																	
GENEDB LMXM.11	441733	N	Intro nic	1040	442773	444212	LmxM.11.1100	+	NA	NA	NA	NA	NA				
GENEDB LMXM.11	443299	Y	Exon ic	NA	442773	444212	LmxM.11.1100	+	2	0	A[A/T]C	[N/I]	N				
OrthomclID	Chromosome	Chromosome Ploidy	# Genes in Ref	Region Start	Region End	CN total	mean coverage	mean fpkm	Haploid Number	Gene Dose	Gene List	Description	total coverage	total fpkm	coverage per kb	Rounded Haploid	Rounded Gene Dose
<b>WT</b>																	
OG5_129288	GeneDB LmxM.11	2	1	442772	444212	2.468	53.446	168137	1.23	2.5	LmxM.11.1100	Lanosterol 14-alpha-demethylase, putative	53.4463	168137	37.12	1	2
<b>AmpB-R</b>																	
OG5_129288	GeneDB LmxM.11	2	1	442772	444212	2.006	44.519	152519	1	2	LmxM.11.1100	Lanosterol 14-alpha-demethylase, putative	44.5185	152519	30.92	1	2
<b>15. C-14 sterol reductase, putative</b>										<b>LmxM.31.2320</b>							

Chromosome Number	SNP Position	Within CDS	Region	Distance to the nearest CDS	Start of current CDS	End of current CDS	Gene ID containing current CDS	Strand sense	Estimated Reading Frame	Estimated Number of Stop Codons	Codon	Amino Acid	synonymous				
<b>WT</b>																	
GENEDB LMXM.31	906599	N	Intronic	39	906638	907951	LmxM.31.2320	-	NA	NA	NA	NA	NA				
<b>AmpB-R</b>																	
GENEDB LMXM.31	906599	N	Intronic	39	906638	907951	LmxM.31.2320	-	NA	NA	NA	NA	NA				
OrthomclID	Chromosome	Chromosome Ploidy	# Genes in Ref	Region Start	Region End	CN total	mean coverage	mean fpkm	Haploid Number	Gene Dose	Gene List	Description	total coverage	total fpkm	coverage per kb	Rounded Haploid	Rounded Gene Dose
<b>WT</b>																	
OG5_128488	GeneDB LmxM.31	2	1	906637	907951	2.12	47.956	150211	1.06	2.1	LmxM.31.2320	C-14 sterol reductase, putative	47.9563	150211	36.5	1	2
<b>AmpB-R</b>																	
OG5_128488	GeneDB LmxM.31	2	1	906637	907951	1.927	42.383	146660	0.96	1.9	LmxM.31.2320	C-14 sterol reductase, putative	42.383	146660	32.25	1	2
<b>16. NAD(p)-dependent steroid dehydrogenase-like protein</b>											<b>LmxM.06.0350</b>						
No SNPs in WT																	
No SNPs in AmpB-R																	
OrthomclID	Chromosome	Chromosome Ploidy	# Genes in Ref	Region Start	Region End	CN total	mean coverage	mean fpkm	Haploid Number	Gene Dose	Gene List	Description	total coverage	total fpkm	coverage per kb	Rounded Haploid	Rounded Gene Dose

<b>WT</b>																	
OG5_128811	GeneDB LmxM.06	2	1	118081	119173	5.48	139.392	414527	2.74	5.5	LmxM.06.0350	NAD(p)-dependent steroid dehydrogenase-like protein	139.392	414527	127.65	3	6
<b>AmpB-R</b>																	
OG5_128811	GeneDB LmxM.06	2	1	118081	119173	3.909	69.779	226937	1.95	3.9	LmxM.06.0350	NAD(p)-dependent steroid dehydrogenase-like protein	69.7792	226937	63.9	2	4
<b>17. Sterol 24-c-methyltransferase</b>										<b>LmxM.36.2380   LmxM.36.2390</b>							
Chromosome Number	SNP Position	Within CDS	Region	Distance to the nearest CDS	Start of current CDS	End of current CDS	Gene ID containing current CDS	Strand sense	Estimated Reading Frame	Estimated Number of Stop Codons	Codon	Amino Acid	synonymous				
<b>WT</b>																	
GENEDB LMXM.20	951390	Y	Exonic	NA	950430	951491	LmxM.36.2380	+	3	1	[G/A]TT	[V/I]	N				
GENEDB LMXM.20	951814	N	Intronic	323	950430	951491	LmxM.36.2380	+	NA	NA	NA	NA	NA				
GENEDB LMXM.20	955152	Y	Exonic	NA	954192	955253	LmxM.36.2390	+	3	1	[G/A]TT	[V/I]	N				
<b>AmpB-R</b>																	
GENEDB LMXM.20	950820	Y	Exonic	NA	950430	951491	LmxM.36.2380	+	3	1	[G/A]TC	[V/I]	N				
GENEDB LMXM.20	951390	Y	Exonic	NA	950430	951491	LmxM.36.2380	+	3	1	[G/A]TT	[V/I]	N				
GENEDB LMXM.20	951793	N	Intronic	302	950430	951491	LmxM.36.2380	+	NA	NA	NA	NA	NA				
GENEDB LMXM.20	951814	N	Intronic	323	950430	951491	LmxM.36.2380	+	NA	NA	NA	NA	NA				
GENEDB LMXM.20	955152	Y	Exonic	NA	954192	955253	LmxM.36.2390	+	3	1	[G/A]TT	[V/I]	N				

OrthomclID	Chromosome	Chromosome	# Genes in Ref	Region Start	Region End	CN total	mean coverage	mean fpkm	Haploid Number	Gene Dose	Gene List	Description	total coverage	total fpkm	coverage per kb	Rounded Haploid	Rounded Gene Dose
<b>WT</b>																	
OG5_129172	GeneDB LmxM.20	2	2	950429	955253	3.133	36.467	114546	1.57	3.1	LmxM.36.2380, LmxM.36.2390	Sterol 24-c-methyltransferase, putative	72.934	229092	15.12	2	4
<b>AmpB-R</b>																	
OG5_129172	GeneDB LmxM.20	2	2	950429	955253	3.541	39.295	135564.5	1.77	3.5	LmxM.36.2380, LmxM.36.2390	Sterol 24-c-methyltransferase, putative	78.5893	271129	16.29	2	4
<b>18. C8-sterol isomerase</b>																	
<b>LmxM.08_29.2140</b>																	
Chromosome Number	SNP Position	Within CDS	Region	Distance to the nearest CDS	Start of current CDS	End of current CDS	Gene ID containing current CDS	Strand sense	Estimated Reading Frame	Estimated Number of Stop Codons	Codon	Amino Acid	synonymous				
<b>WT</b>																	
GENEDB LMXM.08	256270	N	Intronic	2872	259142	259813	LmxM.08_29.2140	+	NA	NA	NA	NA	NA				
GENEDB LMXM.08	260427	N	Intronic	614	259142	259813	LmxM.08_29.2140	+	NA	NA	NA	NA	NA				
<b>AmpB-R</b>																	
GENEDB LMXM.08	256270	N	Intronic	2872	259142	259813	LmxM.08_29.2140	+	NA	NA	NA	NA	NA				

OrthomclID	Chromosome	Chromosome Ploidy	# Genes in Ref	Region Start	Region End	CN total	mean coverage	mean fpkm	Haploid Number	Gene Dose	Gene List	Description	total coverage	total fpkm	coverage per kb	Rounded Haploid	Rounded Gene Dose
<b>WT</b>																	
OG5_131051	GeneDB Lm xM.08	2	1	259141	259813	1.931	43.822	132965	0.97	1.9	LmxM.08_29.2140	C-8 sterol isomerase-like protein	43.8216	132965	65.21	1	2
<b>AmpB-R</b>																	
OG5_131051	GeneDB Lm xM.08	2	1	259141	259813	2.276	51.72	171371	1.14	2.3	LmxM.08_29.2140	C-8 sterol isomerase-like protein	51.7203	171371	76.96	1	2
<b>19. Lathosterol oxidase-like protein   C5 sterol desaturase</b>																	
										<b>LmxM.23.1300</b>							
Chromosome Number	SNP Position	Within CDS	Region	Distance to the nearest CDS	Start of current CDS	End of current CDS	Gene ID containing current CDS	Strand sense	Estimated Reading Frame	Estimated Number of Stop Codons	Codon	Amino Acid	synonymous				
<b>WT</b>																	
GENEDB LMXM .23	598377	N	Intronic	1175	596294	597202	LmxM.23 .1300	+	NA	NA	NA	NA	NA				
<b>AmpB-R</b>																	
GENEDB LMXM .23	598377	N	Intronic	1175	596294	597202	LmxM.23 .1300	+	NA	NA	NA	NA	NA				
<b>WT</b>																	
OG5_129040	GeneDB Lm xM.23	2	1	596293	597202	3.324	75.912	226314	1.66	3.3	LmxM.23.1300	Lathosterol oxidase-like	75.9121	226314	83.51	2	4

												protein					
<b>AmpB-R</b>																	
OG5_129040	GeneDB Lm xM.23	2	1	596293	5972 02	3.22	71.364	234356	1.61	3.2	LmxM.23. 1300	Lathosterol oxidase-like protein	71.3637	2343 56	78.51	2	4
<b>20. C-22 sterol desaturase   cytochrome p450-like protein</b>											<b>LmxM.29.3550</b>						
No SNPs in WT																	
No SNPs in AmpB-R																	
OrthomclID	Chromosome	Chromosome Ploidy	# Genes in Ref	Region Start	Region End	CN total	mean coverage	mean fpkm	Haploid Number	Gene Dose	Gene List	Description	total coverage	total fpkm	coverage per kb	Rounded Haploid	Rounded Gene Dose
<b>WT</b>																	
OG5_131167	GeneDB Lm xM.29	2	1	1268313	1269 843	2.401	54.542	168044	1.2	2.4	LmxM.29.35 50	Cytochrome p450-like protein	54.5424	1680 44	35.65	1	2
<b>AmpB-R</b>																	
OG5_131167	GeneDB Lm xM.29	2	1	1268313	1269 843	2.528	55.445	187039	1.26	2.5	LmxM.29.35 50	Cytochrome p450-like protein	55.4446	1870 39	36.24	1	2
<b>21. C-24 sterol desaturase</b>											<b>LmxM.32.0680</b>						
No SNPs in WT																	
No SNPs in AmpB-R																	
<b>WT</b>																	
OG5_132400	GeneDB Lm xM.32	2	1	228539	2300 30	3.303	80.178	240526	1.65	3.3	LmxM.32.06 80	Sterol C-24 reductase, putative	80.1776	2405 26	53.77	2	4

<b>AmpB-R</b>																	
OG5_132400	GeneDB Lm xM.32	2	1	228539	2300 30	3.106	71.831	236890	1.55	3.1	LmxM.32.06 80	Sterol C-24 reductase, putative	71.8314	2368 90	48.18	2	4

Data analysis by Dr. Manikhandan Mudaliar - Glasgow Polyomics.

## Appendix F: *L. mexicana* lanosterol 14 $\alpha$ -demethylase gene and enzyme sequences

LmxM.11.1100, A to T non-synonymous mutation, Forward strand.

ATGATCGGCGAGCTTCTCCTTCTCCTGACCGCCGGTCTGGCGCTGTACGGCTGGTACTTC  
 TGCAAGTCCTTCAACACAACCCGTCCGACCGATCCGCCGGTCATTCACCTGCACGACGCCT  
 TTTGTGGGTACATCATCCAGTTCGGCAAGGATCCCCTGGGCTTTATGTTGAGTGCGAAG  
 AAGAAGTACGGCGGCATATTCACCATGAACATCTGCGGCAACCGCATCACTATTGTTGGT  
 GACGTTACCCAGCACAGCAAGTTCACCCCGCGTAACGAGATTCTCTCCCCGCGTGAG  
 GTCTACAGCTTCATGGTGCCCGTCTTTGGCGAGGGCGTCGCCTACGCCGCGCCGTACCCG  
 CGCATGCGCGAGCAGCTCAACTTCCTGGCCGAGGAGCTGACTGTGGCCAAGTTCAGAAC  
 TTCGCTCCATCGATCCAGCACGAGGTGCGCAAGTTTATGAAGGCGAACTGGGACAAGGAC  
 GAAGGCGAGATCAACATCCTCGACGACTGCAGCGCCATGATCATCA**AC**ACCGCTTGCCAG  
 TGCCTCTTCGGCGAGGACCTGCGCAGGCGCCTGGACGCGCGCCAGTTCGCACAGCTGCTG  
 GCCAAGATGGAGACCTGCCTCATCCCCGCCGCTGTCTTCCTGCCGTGGATCCTGAAACTG  
 CCGCTGCCTCAGTTCCTACCGCTGCCGCGACGCCCGCGCTGAGCTGCAGGAAATCCTCAGC  
 GAGATTATCATCGCTCGCGAGAAGGAGGAAGCTCAGAAGGACAGCAACACGTCCGGACCTG  
 CTCGCCGGTCTGCTGGGCGCCGTGTACCGCGATGGCACCCGCATGTCTCAGCACGAGGTG  
 TGCGGAATGATCGTTGCCGCCATGTTTGTGGCCAGCACACCTCCACTATTACCACCACC  
 TGGTCCCTCCTGCATCTGATGGATCCTCGCAACAAGAGGCACCTCGCGAAACTGCATCAG  
 GAGATCGACGAGTTCCTGGCGCAGCTGAACTACGACAACGTCATGGAGGAGATGCCGTTT  
 GCGGAGCAGTGCGCGCGCAGTTCGATTCGCCGCGACCCGCCGCTCGTTATGCTCATGCGA  
 AAGGTGCTGAAGCCGGTCCAGGTGGGCAAGTACGTCGTGCCAGAGGGCGACATCATCGCC  
 TGCTCGCCGCTCCTCTCGCACCCAGGATGAGGAGGCATTTCCGAATCCGCGTGAGTGGAAC  
 CCAGAGCGCAACATGAAGCTCGTCGACGGTGCCTTCTGCGGCTTTGGTGGCCGGCGTCCAC  
 AAGTGCATCGGTGAGAAGTTCGGCCTCCTCAGGTCAAGACGGTGTGGCGACGGTCTTG  
 CGCGACTACGACTTTGAGCTCCTCGGCCACTGCCGGAACCGAACTACCACACCATGGTG  
 GTGGGCCCGACGGCCAGCCAGTGCCGCGTGAAGTACATCAAGAAGAAGGCGGCGGCTTAG

Affected codon by the non-synonymous mutation is underlined and the affected nucleotide is shown in bold.

Lanosterol 14 $\alpha$ -demethylase amino acid residue sequence, N176I point mutation  
 MIGELLLLLTAGLALYGWYFCKSFNTTRPTDPPVIHCTTPFVGHIIQFGKDPLGFMLS  
 KKYGGIFTMNICGNRITIVGDVHQHSKFFTPRNEILSPREVYSFMVPVFGEGVAYAAPYP  
 RMREQLNFLAEELTVAKFQNFAPSIQHEVRKFMKANWDKDEGEINILDDCSAMI **INT**ACQ  
 CLFGEDLRRRLDARQFAQLLAKMETCLIPAAVFLPWILKLPLPQSYRCRDARAELQEILS  
 EIIIIAREKEEAQKDSNTSDLLAGLLGAVYRDGTRMSQHEVCGMIVAAMFAGQHTSTITTT  
 WSLHLMDPRNKRHLAKLHQEIDEFFAQLNYDNVMEEMPFAEQCARESIRRDPPLVMLMR  
 KVLKPVQVGKYVVEGDIIACSPLLSHQDEEAFPNPREWNPENMKLVDGAFCGFGAGVH  
 KCIGEKFGLLQVKTVLATVLRDYDFELGPLEPNYHTMVVGPTASQCRVKYIKKAAA

The residue affected by the point mutation is shown in bold font and underlined

## Appendix G: Comparison of lanosterol 14 $\alpha$ -demethylase sequences of trypanosomatids, *S. cerevisiae* and *H. sapiens*

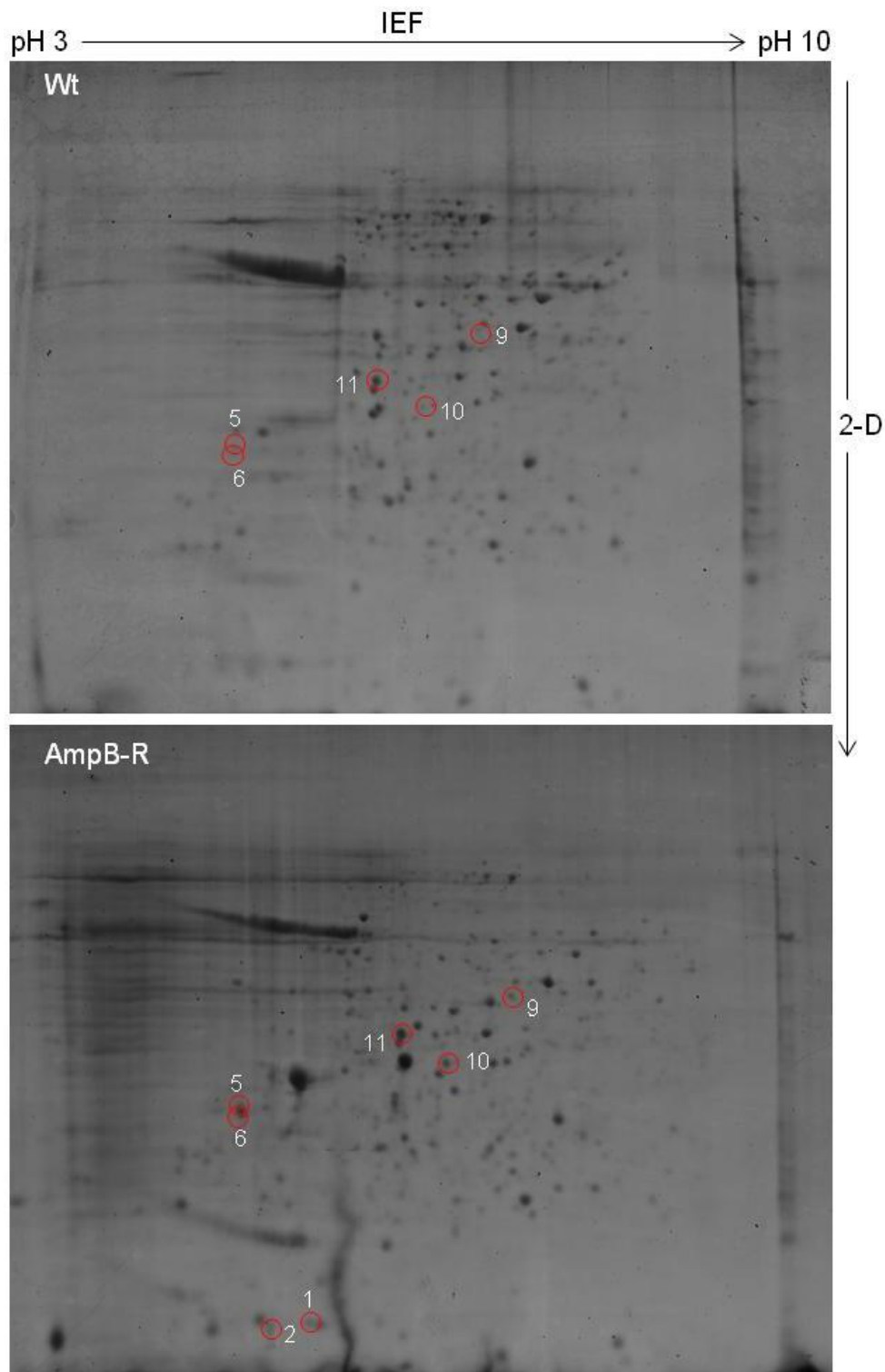
L donovani	M-----	---IGELLLL	LTAGLALYGW	YFCKSFNTT	27
L infantum	M-----	---IGELLLL	LAAGLALYGW	YFCKSFNTT	27
L mexicana	M-----	---IGELLLL	LTAGLALYGW	YFCKSFNTT	27
L major	M-----	---IGEFFLL	LTAGLALYGW	YFCKSFNTT	27
L braziliensis	M-----	---IGELLLL	LAAGLALYGW	YFCQSFNTT	27
L. tarentolae	M-----	---IGEILFF	LSAGLVLYGW	YFCRSFNTT	27
T. brucei LS427	M-----	---LLEVAIF	LLTALALYSF	YFVKSFNVT	27
T. brucei TREU927	M-----	---LLEVAIF	LLTALALYSF	YFVKSFNVT	27
Tb gambiense DAL972	M-----	---LLEVAIF	LLTALALYSF	YFVKSFNVT	27
T vivax	M-----	---LLEVITF	LLTVLVLYSV	YFVVSFNVT	27
T. cruzi CL BE-like	M-----	---FIEAIVL	ALTALILYSV	YSVKSFNTT	27
T. cruzi CL B Non-E-like	M-----	---FIEAIVL	GLTALILYSV	YSVKSFNTT	27
<i>S. cerevisiae</i>	M-----SAT	KSIVGEALEY	VNIGLSHFL	ALPLAQRISL	33
<i>H. sapiens</i>	MLLLGLLQAG	GSVLLGQAMEK	VTGGNLLSML	LIACAFLLS	40
Consensus	M-----	---IGE*LLL	LL*GLALY*W	YF*KSFNTT-	
L donovani	-----	-----RP	TDPPVHGT	PFVGHIIQFG	49
L infantum	-----	-----RP	TDPPVHGT	PFVGHIIQFG	49
L mexicana	-----	-----RP	TDPPVIHCT	PFVGHIIQFG	49
L major	-----	-----RP	TDPPVHGT	PFVGHIIQFG	49
L braziliensis	-----	-----RA	TDPPVRCCT	PFVGHIIQFG	49
L. tarentolae	-----	-----RP	TDPPVPCCT	PFVGHIIQFG	49
T. brucei LS427	-----	-----RP	TDPPVYPVT	PILGHIQFG	49
T. brucei TREU927	-----	-----RP	TDPPVYPVT	PILGHIQFG	49
Tb gambiense DAL972	-----	-----RP	TDPPVYPVT	PILGHIQFG	49
T vivax	-----	-----RP	TDPPVRHVA	PFLGHIQFG	49
T. cruzi CL BE-like	-----	-----RP	TDPPVYPVT	PFLGHIQFG	49
T. cruzi CL B Non-E-like	-----	-----RP	TDPPVYPVT	PFLGHIQFG	49
<i>S. cerevisiae</i>	IIIIIPFIYNI	VWOLLYSLRK	DRPPLVFYWI	PWVGSAVYFG	73
<i>H. sapiens</i>	VYLIRLAAGH	LVQLPAGVKS	--PPYIFSPI	PFLGHAIAFG	78
Consensus	-----	-----RP	TDPPVYPVT*	PF*GHIQFG	
L donovani	KDPLGFMLKA	KKKY-GGIFT	MNICGNRITV	VGDVHQHSKF	88
L infantum	KDPLGFMLKA	KKKY-GGIFT	MNICGNRITV	VGDVHQHSKF	88
L mexicana	KDPLGFMLSA	KKKY-GGIFT	MNICGNRITI	VGDVHQHSKF	88
L major	KDPLDFMLNA	KKKY-GGVFT	MNICGNRVTI	VGDVHQHSKF	88
L braziliensis	KDPLGFMLNA	KRKY-GGIFT	MNVCGNRITI	VGDVHQHSKF	88
L. tarentolae	KDPLGFMLKA	KKQY-GGFT	MNICGNRITV	VGDVHQHSKF	88
T. brucei LS427	KSPLGFMQEC	KRQLKSGIFT	INIVGKRVTI	VGDPHEHSRF	89
T. brucei TREU927	KSPLGFMQEC	KRQLKSGIFT	INIVGKRVTI	VGDPHEHSRF	89
Tb gambiense DAL972	KSPLGFMQEC	KRQLKSGIFT	INIVGKRVTI	VGDPHEHSRF	89
T vivax	KDPLGFMLEC	KRKLRSQVFT	INIMGKRVTI	VGDPHEHSRF	89
T. cruzi CL BE-like	KNPLEFMQRC	KRELKSGVFT	ISIGGQRVTI	VGDPHEHSRF	89
T. cruzi CL B Non-E-like	KNPLEFMQRC	KRDLKSGVFT	ISIGGQRVTI	VGDPHEHSRF	89
<i>S. cerevisiae</i>	MKPYEFFEFC	QKKY-GDIFS	FVLLGRVMTV	YLGPKGHEFV	112
<i>H. sapiens</i>	KSPIEFLENA	YEKY-GPVFS	FTMVGKTFTY	LLGSDAAALL	117
Consensus	KDPLGFMLE*	KRKY-GGIFT	*NICGNRVTI	VGDPH*HS*F	
L donovani	FTPRNEILSP	REVYSFMV-P	VFGEVAYAA	PYPRMREQLN	127
L infantum	FTPRNEILSP	REVYSFMV-P	VFGEVAYAA	PYPRMREQLN	127
L mexicana	FTPRNEILSP	REVYSFMV-P	VFGEVAYAA	PYPRMREQLN	127
L major	FTPRNEILSP	REVYSFMV-P	VFGEVAYAA	PYPRMREQLN	127
L braziliensis	FTPRNEILSP	REVYSFMV-P	VFGEVAYAA	PYPRMREQLN	127
L. tarentolae	FTPRNEILSP	REYKFMV-P	VFGEVAYAA	PYARMREQLN	127
T. brucei LS427	FLPRNEVLS	REVYSFMV-P	VFGEVAYAA	PYPRMREQLN	128
T. brucei TREU927	FLPRNEVLS	REVYSFMV-P	VFGEVAYAA	PYPRMREQLN	128
Tb gambiense DAL972	FLPRNEVLS	REVYSFMV-P	VFGEVAYAA	PYPRMREQLN	128
T vivax	FLPRNEVLS	REYAFMV-P	VFGEVAYAA	PYPRMREQLN	128
T. cruzi CL BE-like	FSPRNEILSP	REYTIMT-P	VFGEVAYSA	PYPRMREQLN	128
T. cruzi CL B Non-E-like	FSPRNEILSP	REYTIMT-P	VFGEVAYAA	PYPRMREQLN	128
<i>S. cerevisiae</i>	FNAKLADVSA	EAAVAHLTTP	VFGKGVYDC	PNSRLMEQKK	152
<i>H. sapiens</i>	FNSKNEVLNA	EDVYSRLTTP	VFGKGVAYDV	PNPVFLQKK	157
Consensus	FTPRNEILSP	REVYSFMV-P	VFGEVAYAA	PYPRMREQLN	
L donovani	FLAEELTVAK	FQNFAPSIQH	EVRKFMKANW	N-----KDEG	162
L infantum	FLAEELTVAK	FQNFAPSIQH	EVRKFMKANW	N-----KDEG	162
L mexicana	FLAEELTVAK	FQNFAPSIQH	EVRKFMKANW	D-----KDEG	162
L major	FLAEELTVAK	FQNFAPSIQH	EVRKFMKANW	N-----KDEG	162
L braziliensis	FLAEELTVAK	FQNFAPSIQH	EVRKFMKANW	D-----KDEG	162
L. tarentolae	FLAEELTVAK	FQNFAPSIQH	EVRKFMKANW	D-----KDEG	162
T. brucei LS427	FLAEELTVAK	FQNFVPAIQH	EVRKFMKANW	D-----KDEG	163
T. brucei TREU927	FLAEELTVAK	FQNFVPAIQH	EVRKFMKANW	D-----KDEG	163
Tb gambiense DAL972	FLAEELTVAK	FQNFVPAIQH	EVRKFMKANW	D-----KDEG	163
T vivax	FLAEELTVAK	FQNFVPAIQH	EARKFLENW	N-----KDEG	163
T. cruzi CL BE-like	FLAEELTVAK	FQNFVPAIQH	EVRKFMKANW	K-----KDEG	163
T. cruzi CL B Non-E-like	FLAEELTVAK	FQNFVPAIQH	EVRKFMKANW	K-----KDEG	163
<i>S. cerevisiae</i>	FVKGALTKEA	FKSYVPLIAE	EYKYFRDSK	NFRLNERTTG	192
<i>H. sapiens</i>	MLKSGLNIAH	FKQHSIIEK	ETKEYFESWG	E-----SG	190
Consensus	FLAEELTVAK	FQNFVPAIQH	EVRKFMKANW	D-----KDEG	

L donovani	EINILDDCSA	MIINTACQCL	FGEDLRKRLD	ARQFAQLLAK	202
L infantum	EINILDDCSA	MIINTACQCL	FGEDLRKRLD	ARQFAQLLAK	202
L mexicana	EINILDDCSA	MIINTACQCL	FGEDLRKRLD	ARQFAQLLAK	202
L major	EINILDDCSA	MIINTACQCL	FGEDLRKRLD	ARQFAQLLAK	202
L braziliensis	EINILEDCSA	MIINTACQCL	FGEDLRKRLD	ARQFAQLLAK	202
L. tarentolae	EINILEDCSA	MIINTACQCL	FGEDLRKRLD	ARQFAQLLAK	202
T. brucei LS427	EINLLED CST	MIINTACQCL	FGEDLRKRLD	ARRFAQLLAK	203
T. brucei TREU927	EINLLED CST	MIINTACQCL	FGEDLRKRLD	ARRFAQLLAK	203
Tb gambiense DAL972	EINLLED CST	MIINTACQCL	FGEDLRKRLD	ARRFAQLLAK	203
T vivax	QVNLED CSA	MIINTACQCL	FGEDLRKRLD	ARRFAQLLAK	203
T. cruzi CL BE-like	VINLED CGA	MIINTACQCL	FGEDLRKRLN	ARHFAQLLSK	203
T. cruzi CL B Non-E-like	VINLED CGA	MIINTACQCL	FGEDLRKRLN	ARHFAQLLSK	203
S. cerevisiae	TIDVMVTQPE	MTIFTASRSL	LKEMRAKLD	T-DFAYLYSD	231
H. sapiens	EKNVFEALSE	LIIILTASHCL	HGKEIRSQLN	E-KVAQLYAD	229
Consensus	EIN*LEDCSA	MIINTACQCL	FGEDLRKRLD	ARQFAQLLAK	
L donovani	MESCLIPAAV	FLPWILKLP	PQSYRCRDAR	AELQDILSEI	242
L infantum	MESCLIPAAV	FLPWILKLP	PQSYRCRDAR	AELQDILSEI	242
L mexicana	MESCLIPAAV	FLPWILKLP	PQSYRCRDAR	AELQDILSEI	242
L major	MESCLIPAAV	FLPWILKLP	PQSYRCRDAR	AELQDILSEI	242
L braziliensis	MESCLIPAAV	FLPWILKLP	PQSYRCRDAR	AELQDILSEI	242
L. tarentolae	MESSLIPAAV	FMPWILKLP	PQSYRCRDAR	AELQDILSEI	242
T. brucei LS427	MESSLIPAAV	FLPILLKLP	PQSARCHEAR	TELQKILSEI	243
T. brucei TREU927	MESSLIPAAV	FLPILLKLP	PQSARCHEAR	TELQKILSEI	243
Tb gambiense DAL972	MESSLIPAAV	ALPILLTLP	PQSARCHEAR	TELQKILSEI	243
T vivax	MESSLIPAAV	FMPSLLLLP	PQSACCRDAR	EELQLILSEI	243
T. cruzi CL BE-like	MESSLIPAAV	FMPWLLRPL	PQSARCREAR	AELQKILGEI	243
T. cruzi CL B Non-E-like	MESSLIPAAV	FMPWLLRPL	PQSARCREAR	AELQKILGEI	243
S. cerevisiae	LDKGFTPIEF	VFPN-L--PL	EHYRKRDRHQ	KALSGTYMSL	268
H. sapiens	LDGGFSHAAW	LLPGWL--PL	PSFRRRDRAH	REIKDIFYKA	267
Consensus	MESSLIPAAV	FLPW*LKLP	PQS*RCRDAR	AELQ*ILSEI	
L donovani	IIAREKEEAQ	KDNTSDLLA	GLL-GAVYRD	GTRMSQHEVC	281
L infantum	IIAREKEEAQ	KDNTSDLLA	GLL-GAVYRD	GTRMSQHEVC	281
L mexicana	IIAREKEEAQ	KDNTSDLLA	GLL-GAVYRD	GTRMSQHEVC	281
L major	IIAREKEEAQ	KDNTSDLLA	GLL-GAVYRD	GTRMSQHEVC	281
L braziliensis	IIAREKEEAQ	KDNTSDLLA	GLL-GAVYRD	GTRMSQHEVC	281
L. tarentolae	IIAREKEESQ	KDNTSDLLT	GLL-NAVYRD	GTRMSQHEVC	281
T. brucei LS427	IIARKEEEVS	KDSSTSDLLS	GLL-SAVYRD	GTPMSLHEVC	282
T. brucei TREU927	IIARKEEEVN	KDSSTSDLLS	GLL-SAVYRD	GTPMSLHEVC	282
Tb gambiense DAL972	IIARKEEEVN	KDSSTSDLLS	GLL-SAVYRD	GTPMSLHEVC	282
T vivax	ILARKREEVN	KDSSTSDLLS	GLL-SAVYRD	GTPMSLHEVC	282
T. cruzi CL BE-like	IVAREKEEAS	KDNNTSDLLG	GLL-KAVYRD	GTRMSLHEVC	282
T. cruzi CL B Non-E-like	IVAREKEEAS	KDNNTSDLLG	GLL-KAVYRD	GTRMSLHEVC	282
S. cerevisiae	IKERRKNDI	QDR---DLID	SLMKNSTYKD	GVKMTDQEIA	305
H. sapiens	IQKRRSQEK	ID---DILQ	TLL-DATYKD	GRPLTDDEVA	302
Consensus	IIAREKEEAQ	KDNTSDLLA	GLL-GAVYRD	GTRMS*HEVC	
L donovani	GMIVAAMFAG	QHTSTITTTW	SLLHLM DPRN	KRHAKLHQE	321
L infantum	GMIVAAMFAG	QHTSTITTTW	SLLHLM DPRN	KRHAKLHQE	321
L mexicana	GMIVAAMFAG	QHTSTITTTW	SLLHLM DPRN	KRHAKLHQE	321
L major	GMIVAAMFAG	QHTSTITTTW	SLLHLM DPRN	KRHAKLHQE	321
L braziliensis	GMIVAAMFAG	QHTSTITTTW	SLLHLM DPRN	KKHLMKLHEE	321
L. tarentolae	GMIVAAMFAG	QHTSSITTTW	SLLHLM DPRN	KKHLEKLHQE	321
T. brucei LS427	GMIVAAMFAG	QHTSSITTTW	SMLHLMHPAN	VKHLEALRKE	322
T. brucei TREU927	GMIVAAMFAG	QHTSSITTTW	SMLHLMHPAN	VKHLEALRKE	322
Tb gambiense DAL972	GMIVAAMFAG	QHTSSITTTW	SMLHLMHPAN	VKHLEALRKE	322
T vivax	GMIVAAMFAG	QHTSTITTTW	SLLHLMHPAN	KKHLET LRKE	322
T. cruzi CL BE-like	GMIVAAMFAG	QHTSTITTSW	SMLHLMHPKN	KKWLDKLHKE	322
T. cruzi CL B Non-E-like	GMIVAAMFAG	QHTSTITTSW	SMLHLMHPKN	KKWLDKLHKE	322
S. cerevisiae	NLLIGVLMGG	QHTSAATSAW	ILLHLAERP	VQ--QELYEE	343
H. sapiens	GMLIGLLLAG	QHTSSTTSAW	MGFFLARDKT	LQ--KKCYLE	340
Consensus	GMIVAAMFAG	QHTSTITTTW	SLLHLM*PRN	KKHLEKLHKE	
L donovani	----IDEFPA	QLNYDNVME	MPFAEQCARE	SIRRDPLVM	357
L infantum	----IDEFPA	QLNYDNVME	MPFAEQCARE	SIRRDPLVM	357
L mexicana	----IDEFPA	QLNYDNVME	MPFAEQCARE	SIRRDPLVM	357
L major	----IDEFPA	QLNYDNVME	MPFAEQCARE	SIRRDPLIM	357
L braziliensis	----IDEFPA	QLNYDNVME	MPFAEQCARE	SIRRDPLVM	357
L. tarentolae	----IDEFPA	QLNYDNVME	MPFAEQCARE	SIRRDPLVM	357
T. brucei LS427	----IEEFPA	QLNYNNVME	MPFAERCARE	SIRRDPLLM	358
T. brucei TREU927	----IEEFPA	QLNYNNVME	MPFAERCARE	SIRRDPLLM	358
Tb gambiense DAL972	----IEEFPA	QLNYNNVME	MPFAERCARE	SIRRDPLLM	358
T vivax	----IEEFPA	QLNYSNVME	MPFAERCARE	SIRRDPLIM	358
T. cruzi CL BE-like	----IDEFPA	QLNYDNVME	MPFAERCARE	SIRRDPLLM	358
T. cruzi CL B Non-E-like	----IDEFPA	QLNYDNVME	MPFAERCARE	SIRRDPLLM	358
S. cerevisiae	QMRVLDGGKK	ELTYD-LLQE	MPLLNQTIKE	TLRMHHP LHS	382
H. sapiens	QKTVCGENLP	PLTYD-QLKD	LNLLDRCIKE	TLRLRPPIMI	379
Consensus	----IDEFPA	QLNYDNVME	MPFAERCARE	SIRRDPL*M	

L donovani	LMRKVLKPVQ	VGK--YVVP	GDIIACSPLL	SHQDEEAFPN	395
L infantum	LMRKVLKPVQ	VGK--YVVP	GDIIACSPLL	SHQDEEAFPN	395
L mexicana	LMRKVLKPVQ	VGK--YVVP	GDIIACSPLL	SHQDEEAFPN	395
L major	LMRKVLKPVQ	VGK--YVVP	GDIIACSPLL	SHQDEEAFPN	395
L braziliensis	LMRKVLKPVQ	VGK--YVVP	GDIIACSPLL	SHQDEEAFPN	395
L. tarentolae	LMRKVLKPVQ	VGK--YVVP	GDIIACSPVL	SHQDEEAFPN	395
T. brucei LS427	LMRKVMADVQ	VGS--YVVPK	GDIIACSPLL	SHHDEEAFPE	396
T. brucei TREU927	LMRKVMADVQ	VGS--YVVPK	GDIIACSPLL	SHHDEEAFPE	396
Tb gambiense DAL972	LMRKVMADVQ	VGS--YVVPK	GDIIACSPLL	SHHDEEAFPE	396
T vivax	LMRKVLADVQ	VGS--YVVPK	GDIIACSPLL	SHHDEEAFPD	396
T. cruzi CL BE-like	VMRMVKAQVK	VGS--YVVPK	GDIIACSPLL	SHHDEEAFPN	396
T. cruzi CL B Non-E-like	VMRMVKAQVK	VGS--YVVPK	GDIIACSPLL	SHHDEEAFPN	396
S. cerevisiae	LFRKVMKDMH	VPNTSYVIPA	G YHVLVSPGY	THLRDEYFNP	422
H. sapiens	MMRMA---R	TPQTV-----	-----AGY	T-----IPP	397
Consensus	LMRKVLKPV*	VG*--YVVP*	GDIIACSPLL	SH*DEEAFPN	
L donovani	PRE-----	-----	-----WN	PER-----NM	405
L infantum	PRE-----	-----	-----WN	PER-----NM	405
L mexicana	PRE-----	-----	-----WN	PER-----NM	405
L major	PRE-----	-----	-----WN	PER-----NM	405
L braziliensis	PRE-----	-----	-----WN	PER-----NM	405
L. tarentolae	PRE-----	-----	-----WN	PER-----NM	405
T. brucei LS427	PRR-----	-----	-----WD	PER-----DE	406
T. brucei TREU927	PRR-----	-----	-----WD	PER-----DE	406
Tb gambiense DAL972	PRR-----	-----	-----WD	PER-----DE	406
T vivax	PRR-----	-----	-----WD	PER-----DE	406
T. cruzi CL BE-like	PRL-----	-----	-----WD	PER-----DE	406
T. cruzi CL B Non-E-like	PRL-----	-----	-----WD	PER-----DE	406
S. cerevisiae	AHQF---NI	HRWNKDSASS	YSVGEEVDYG	FGAI-----S	453
H. sapiens	GHQVCVSPTV	NQRLKDSWV-	-----ERLDFN	PDRYLQDNPA	432
Consensus	PRE-----	-----	-----WN	PER-----N*	
L donovani	KLVDGAF*CGF	GAGVHKCIGE	KFGLLQVKTV	LATVLRDYDF	445
L infantum	KLVDGAF*CGF	GAGVHKCIGE	KFGLLQVKTV	LATVLRDYDF	445
L mexicana	KLVDGAF*CGF	GAGVHKCIGE	KFGLLQVKTV	LATVLRDYDF	445
L major	KLVDGAF*CGF	GAGVHKCIGE	KFGLLQVKTV	LATVLRDYDF	445
L braziliensis	KLVDGAF*CGF	GAGVHKCIGE	KFGLLQVKTV	LATVLRDYDF	445
L. tarentolae	KLVDGAF*CGF	GAGVHKCIGE	KFGLLQVKTV	LATVLRDYDF	445
T. brucei LS427	K-VEGAF*IGF	GAGVHKCIGQ	KFGLLQVKTI	LATAFRSYDF	445
T. brucei TREU927	K-VEGAF*IGF	GAGVHKCIGQ	KFGLLQVKTI	LATAFRSYDF	445
Tb gambiense DAL972	K-VEGAF*IGF	GAGVHKCIGQ	KFGLLQVKTI	LATAFRSYDF	445
T vivax	V-IEGAF*IGF	GAGVHKCIGQ	KFGLLQVKTI	LATVLRDYDF	445
T. cruzi CL BE-like	K-V*DGAF*IGF	GAGVHKCIGQ	KFALLQVKTI	LATAFREYDF	445
T. cruzi CL B Non-E-like	K-V*DGAF*IGF	GAGVHKCIGQ	KFALLQVKTI	LATAFREYDF	445
S. cerevisiae	KGVSSPYLPF	GGGRHRCIGE	HFAYCQLGLV	MSIFIRTLKW	493
H. sapiens	SGEKFAVYVF	GAGRHRRCIGE	NFAYVQIKTI	WSTMLRLYEF	472
Consensus	KLVDGAF*GF	GAGVHKCIGE	KFGLLQVKTI	LATVLRDYDF	
L donovani	ELL-GP-LPE	PNYHTMVVGP	TASQCRVKYI	KKKKAAA	480
L infantum	ELL-GP-LPE	PNYHTMVVGP	TASQCRVKYI	KKKKAAA	480
L mexicana	ELL-GP-LPE	PNYHTMVVGP	TASQCRVKYI	KKK-AAA	479
L major	ELL-GP-LPE	PNYHTMVVGP	TASQCRVKYI	RKK-AAA	479
L braziliensis	ELL-GS-LPE	PNYHTMVVGP	TASQCRVKYI	KKK-ATA	479
L. tarentolae	ELL-GP-LPE	PNYHTMVVGP	TASQCRVKYI	RKRKAAA	480
T. brucei LS427	QLLRDE-VPD	PDYHTMVVGP	TASQCRVKYI	RRKAAA	481
T. brucei TREU927	QLLRDE-VPD	PDYHTMVVGP	TASQCRVKYI	RRKAAA	481
Tb gambiense DAL972	QLLRDE-VPD	PDYHTMVVGP	TASQCRVKYI	RRKAAA	481
T vivax	ELPRDE-VPE	PDYHTMVVGP	TSSQCRVRYI	RRKKPAS	481
T. cruzi CL BE-like	QLLRDE-VPD	PDYHTMVVGP	TLNQCLVKYT	RKKKLPS	481
T. cruzi CL B Non-E-like	QLLRDE-VPD	PDYHTMVVGP	TLNQCLVKYT	RKKKLPS	481
S. cerevisiae	HYPEGKTVPP	PDFTSMVTL	TGPAKIWEK	RNPEQKI	530
H. sapiens	DLIDGY-FPT	VNYTTMHTP	ENP--VIRYK	RRSK---	503
Consensus	ELLRGE-VPE	P*YHTMVVGP	TASQCRVKYI	RKKKAAA	

The conflicts in sequences are indicated by an asterisk.

## Appendix H: Two-Dimensional electrophoresis gels showing differences in proteins from *L. mexicana* wild-type and AmB resistant cell lines.



Some of the analysed gel spots are shown by a red circle and number of the spot corresponding to gel spot numbers in the possible identifications table in appendix I.

## Appendix I: Possible identifications of the gel 2-DE spots from *L. mexicana* wild-type and the derived AmB resistant cell lines.

Gel spot #	Possible protein IDs	Gene accession number	Mascot score	% Coverage/ Match	Nominal mass	Calc pl	Vol. Ratio
R1	hypothetical protein, conserved	LmxM.34.4470	67	17	21880	4.20	-2.66
	hypothetical protein, conserved	LmxM.30.1000	30	0	121698	4.92	
	mitochondrial carrier protein-like protein	LmxM.29.1050	22	3	37338	9.63	
R3	unspecified product	LmxM.08.1171	307	22	50319	4.71	2.50
	alpha tubulin	LmxM.13.0280	119	13	61058	5.45	
	RNA helicase, putative	LmxM.21.1552	85	14	49723	5.95	
	thiol-dependent reductase 1	LmxM.32.0240	49	13	45700	5.65	
	hypothetical protein, conserved	LmxM.31.0950	31	8	102299	5.95	
	S-adenosylhomocysteine hydrolase	LmxM.36.3910	29	5	48525	5.66	
	udp-glc 4'-epimerase, putative	LmxM.32.2300	25	3	43972	5.68	
	hypothetical protein, conserved	LmxM.09.0520	22	2	87324	6.82	
	peptidase t, putative,peptidase T, putative, metallo-peptidase, ClanMH, family M20B	LmxM.17.0140	22	2	47457	5.87	
R4	N-acyl-L-amino acid amidohydrolase	LmxM.20.1550	190	12	43957	5.73	2.55
	S-adenosylhomocysteine hydrolase	LmxM.36.3910	141	14	48525	5.66	
	udp-glc 4'-epimerase	LmxM.32.2300	51	8	43972	5.68	
	RNA helicase	LmxM.21.1552	30	4	49723	5.95	
	HSP70-like protein	LmxM.01.0640	28	1	1302	6.94	
R7	hypothetical protein, conserved	LmxM.33.2030	28	2	131098	9.87	3.62
	3-oxo-5-alpha-steroid 4-dehydrogenase, putative	LmxM.25.1770	27	3	34286	9.62	
	kinesin K39, putative	LmxM.14.1120	20	1	298624	4.52	
	hypothetical protein, conserved	LmxM.23.1240	17	0	79509	7.70	
	hypothetical protein, conserved	LmxM.36.4790	16	1	103151	9.56	
R8	peptidyl-prolyl cis-trans isomerase, putative	LmxM.34.4770	316	42	39005	5.57	4.18
	glutamine synthetase, putative	LmxM.06.0370	86	9	42893	5.71	
	hypothetical protein, conserved	LmxM.29.3090	57	5	35504	5.72	
	fructose-1,6-bisphosphate aldolase	LmxM.36.1260	40	4	41150	8.97	
	hypothetical protein, conserved	LmxM.25.1220	27	1	884	8.27	
	alpha tubulin	LmxM.13.0280	21	1	61058	5.45	

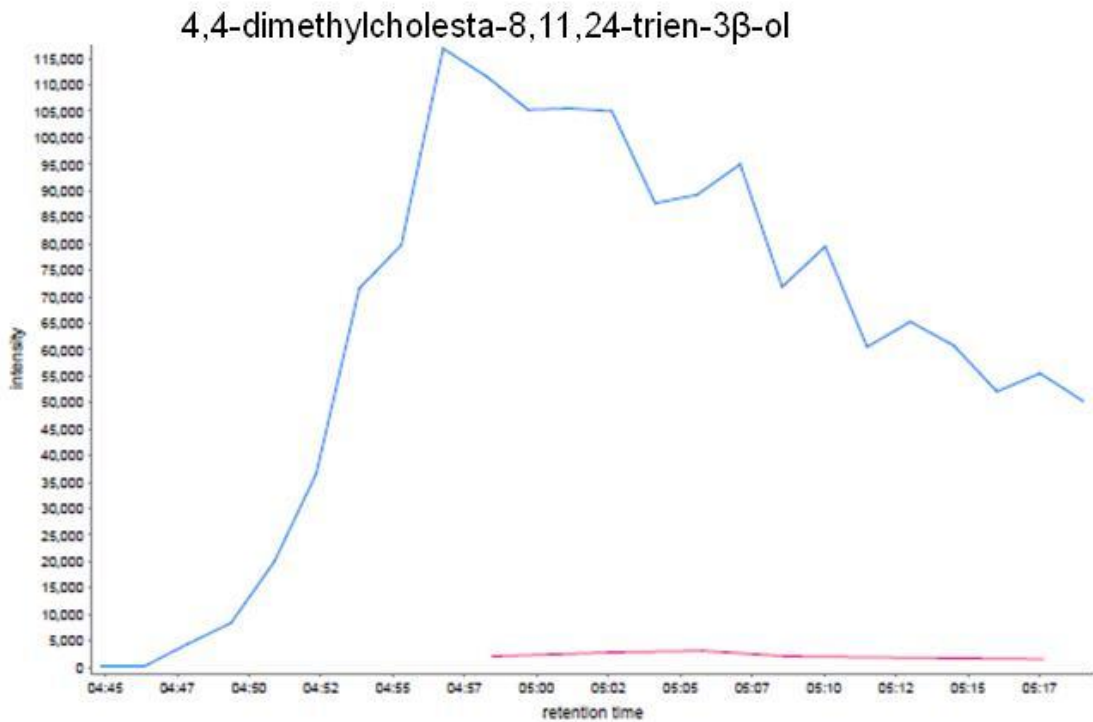
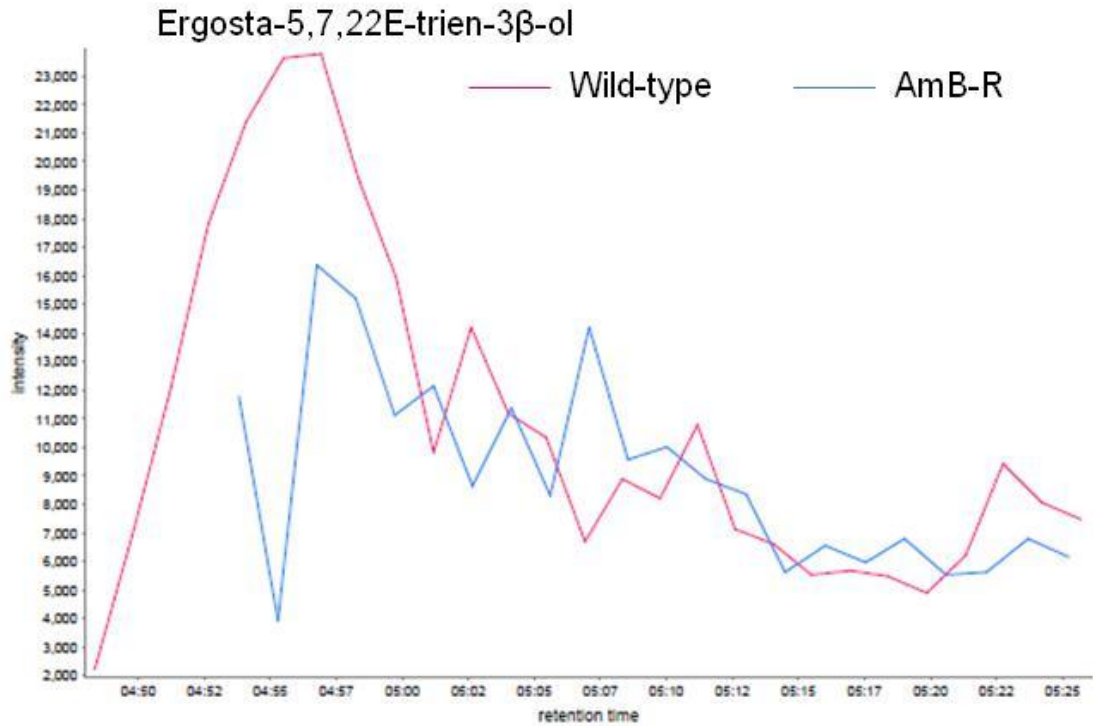
R9	actin	LmxM.04.1230	105	36	40685	5.83	2.36
	axoneme central apparatus protein	LmxM.20.1400	146	8	55699	5.49	
	hypothetical protein, conserved	LmxM.07.0640	128	17	55699	5.42	
	hypothetical protein, conserved	LmxM.29.0560	46	2	38162	5.58	
	farnesyl pyrophosphate synthase, putative	LmxM.22.1360	32	4	41460	5.42	
	alpha tubulin	LmxM.13.0280	29	1	61058	5.45	
	fructose-1,6-bisphosphate aldolase	LmxM.36.1260	28	11	41150	8.97	
	hypothetical protein, conserved	LmxM.20.0970	17	2	39482	5.46	
R10	hypothetical protein, conserved	LmxM.10.1280	388	46	35957	5.31	2.32
	adenosine kinase, putative	LmxM.29.0880	149	20	37766	5.21	
	heat shock protein 83-1	LmxM.32.0312	33	1	81035	5.04	
	alanyl-tRNA synthetase, putative	LmxM.22.1540	33	1	106668	5.52	
	3'-nucleotidase/nuclease, putative	LmxM.12.0400	32	9	41121	5.24	
	hypothetical protein, conserved	LmxM.25.2290	27	4	33755	8.68	
	unspecified product	LmxM.08.1171	26	8	50319	4.71	
	helicase-like protein	LmxM.28.1600	25	0	123221	8.94	
cis-prenyltransferase-like protein	LmxM.13.0020	25	2	44180	8.47		
hypothetical protein, conserved	LmxM.30.1000	23	0	121698	4.92		
R11	pyruvate dehydrogenase E1 beta subunit, putative	LmxM.25.1710	216	37	38476	5.42	4.08
	glyceraldehyde 3-phosphate dehydrogenase, glycosomal	LmxM.29.2980	123	27	39326	9.1	
	eukaryotic translation initiation factor 3 subunit, putative	LmxM.36.3880	56	2	38805	5.21	
	hypothetical protein, conserved	LmxM.24.0960	30	0	108178	9.27	
	hypothetical protein, conserved	LmxM.30.1000	26	2	121698	4.92	
R16	hypothetical protein, conserved	LmxM.30.2990	40	0	214988	6.25	2.34
	glutamate dehydrogenase	LmxM.15.1010	36	2	115208	7.88	
R19	hypothetical protein, conserved	LmxM.22.0800	61	10	24068	5.57	2.39
	hypothetical protein, conserved	LmxM.30.1000	24	0	121698	4.92	
	hypothetical protein, unknown function	LmxM.11.0940	18	0	154771	9.58	
R21	heat shock protein, putative	LmxM.18.1370	246	18	92808	5.09	-3.02
	elongation factor 2	LmxM.36.0180	160	15	94852	5.77	
	hypothetical protein, unknown function	LmxM.08_29.12	93	3	80327	5.32	
		40					
	hypothetical protein, conserved	LmxM.07.0310	60	3	90007	5.54	
aconitase, putative	LmxM.18.0510	62	3	98265	6.75		
Wt2	protein kinase, putative	LmxM.08.0930	22	0	122349	7.80	3.59
	aldo/keto reductase, putative,aldo/keto reductase family-like protein	LmxM.26.1210	16	3	45466	7.28	

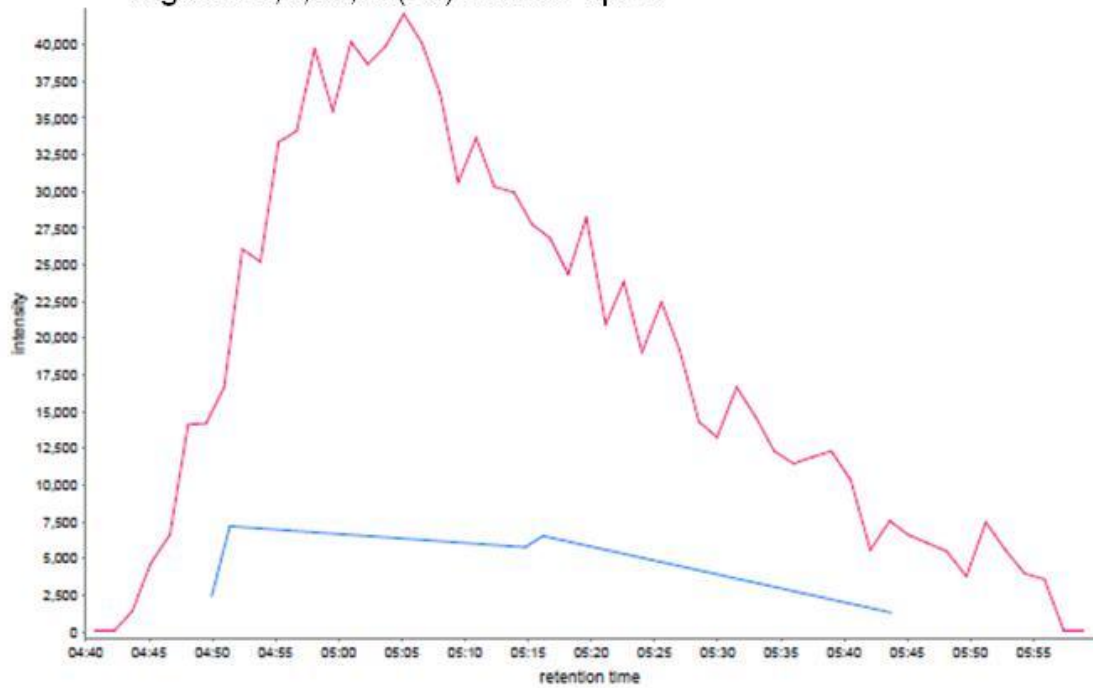
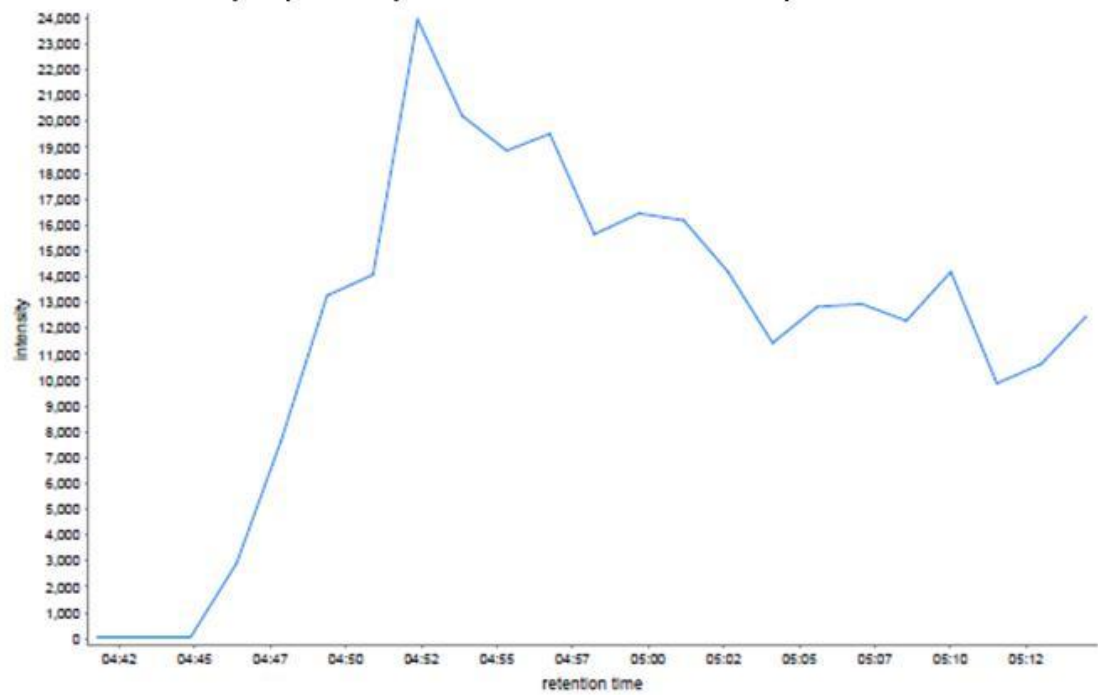
Wt3	alpha tubulin	LmxM.13.0280	473	35	61058	5.45	2.50
	aconitase, putativehypothetical protein, conserved	LmxM.18.0510	240	1	98265	6.75	
	hypothetical protein, conserved	LmxM.31.0950	34	4	102299	5.95	
	hypothetical protein, conserved	LmxM.24.0960	27	0	108178	9.27	
	calpain-like cysteine peptidase, putative,cysteine peptidase, Clan CA, family C2, putative	LmxM.31.0970	22	0	202700	6.24	
Wt4	alpha tubulin	LmxM.13.0280	268	28	61058	5.45	2.55
	unspecified product	LmxM.08.1171	182	15	50319	4.71	
	thiol-dependent reductase 1	LmxM.32.0240	61	4	45700	5.65	
	3'-nucleotidase/nuclease RNA helicase, putative	LmxM.36.3910	60	2	48525	5.66	
	hypothetical protein, unknown function	LmxM.26.2680	26	2	41239	5.26	
	hypothetical protein, conserved	LmxM.25.2290	25	4	33755	8.68	
Wt5	hypothetical protein, conserved	LmxM.09.0520	21	5	87324	6.82	2.55
	unspecified product	LmxM.08.1171	597	38	50319	4.71	
	beta tubulin	LmxM.21.1860	467	32	50394	4.74	
	alpha tubulin	LmxM.13.0280	271	21	61058	5.45	
	40S ribosomal protein S4, putative	LmxM.13.1220	161	21	48291	9.97	
	14-3-3 protein, putative	LmxM.11.0350	73	10	29414	5.19	
	hypothetical protein, conserved	LmxM.36.4230	55	1	119323	4.91	
60S ribosomal protein L2, putative	LmxM.31.3900	35	12	28597	10.7		
Wt6	unspecified product	LmxM.08.1171	244	23	50319	4.71	2.27
	alpha tubulin	LmxM.13.0280	97	7	61058	5.45	
	40S ribosomal protein S4, putative	LmxM.13.1220	55	5	48291	9.97	
	40S ribosomal protein S6, putative	LmxM.21.1780	30	6	28302	11.4	
Wt9	Actin	LmxM.04.1230	220	38	40685	5.83	2.36
	axoneme central apparatus protein, putative	LmxM.20.1400	91	5	55699	5.49	
	40S ribosomal protein S4, putative	LmxM.13.1220	53	4	48291	9.97	
	elongation factor 1-alpha	LmxM.17.0080	52	1	49575	9.03	
	cysteinyl-tRNA synthetase, putative	LmxM.12.0250	38	11	88814	5.55	
	cysteine conjugate beta-lyase, aminotransferase- like protein	LmxM.32.1330	33	8	46836	5.70	
	minchromosome maintenance (MCM) complex subunit, putative	LmxM.24.0910	27	0	87400	8.93	
Wt10	alpha tubulin	LmxM.13.0280	337	16	61058	5.45	2.32
	dihydroorotate dehydrogenase, putative	LmxM.16.0530	71	6	34287	5.48	
	succinyl-CoA ligase [GDP-forming] beta-chain, putative	LmxM.36.2950	49	10	44526	6.77	
	elongation factor 2	LmxM.36.0180	41	5	94852	5.77	

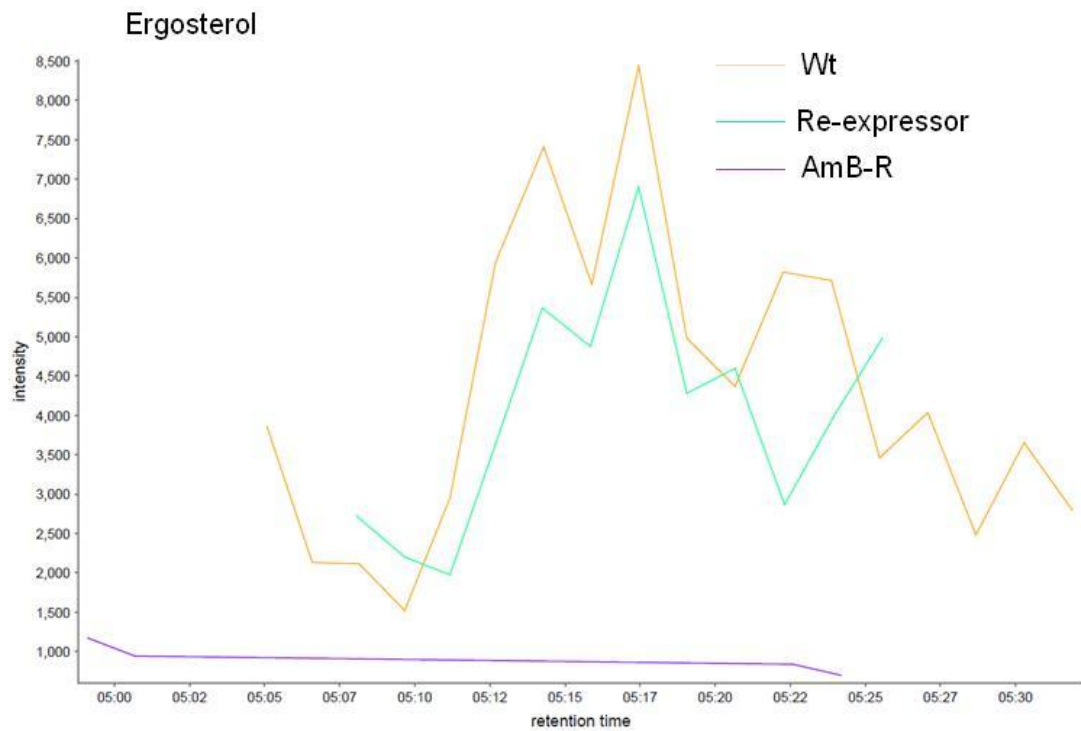
	hypothetical protein, conserved	LmxM.34.5340	39	6	39265	5.31	
	protein phosphatase 2C-like protein	LmxM.36.0530	37	4	33468	5.30	
	pyruvate dehydrogenase E1 beta subunit, putative	LmxM.25.1710	29	3	38476	5.42	
	hypothetical protein, conserved	LmxM.31.1700	18	0	90069	9.08	
Wt11	mannose-1-phosphate guanyltransferase	LmxM.23.0110	984	53	41849	5.29	4.8
	unspecified product	LmxM.08.1171	234	14	50319	4.71	
	elongation factor 2	LmxM.36.0180	68	5	94852	5.77	
	S-adenosylmethionine synthetase	LmxM.29.3500	38	7	43558	5.42	
	heat-shock protein hsp70, putative	LmxM.28.2770	35	2	71482	5.34	
	alpha tubulin	LmxM.13.0280	32	6	61058	5.45	
	hypothetical protein, conserved	LmxM.24.0960	31	0	108178	9.27	
	glyceraldehyde 3-phosphate dehydrogenase, glycosomal	LmxM.29.2980	31	1	39326	9.18	
	pyruvate dehydrogenase E1 beta subunit, putative	LmxM.25.1710	28	8	38476	5.42	
	glutamine synthetase, putative	LmxM.06.0370	25	6	42893	5.71	
	hypothetical protein, conserved	LmxM.33.2920	15	8	10474	9.71	
Wt12	mannose-1-phosphate guanyltransferase	LmxM.23.0110	134	10	41849	5.29	2.06
	heat shock 70-related protein 1, mitochondrial precursor, putative	LmxM.29.2490	69	7	72990	5.68	
	40S ribosomal protein S3A, putative	LmxM.34.0400	46	6	30245	10.3	
	unspecified product						
	isocitrate dehydrogenase, putative	LmxM.32.2550	39	6	46754	5.51	
	elongation factor 1-beta	LmxM.33.0820	30	15	26061	5.00	
	hypothetical protein, conserved	LmxM.24.0960	30	0	108178	9.27	
	ATP synthase F1 subunit gamma protein, putative	LmxM.21.1770	30	10	34671	9.29	
	alpha tubulin	LmxM.13.0280	27	6	61058	5.45	
	hypothetical protein, conserved	LmxM.02.0460	24	3	32685	8.87	
Wt13	alpha tubulin	LmxM.13.0280	308	16	61058	5.45	4.64
	heat-shock protein hsp70, putative	LmxM.28.2770	120	12	71482	5.34	
	hs1vu complex proteolytic subunit-like,hs1vu complex proteolytic subunit-like, threonine peptidase, Clan T(1), family T1B	LmxM.36.3990	70	9	24793	6.09	
	Malic enzyme	LmxM.24.0761	67	8	62922	5.79	
	40S ribosomal protein S8, putative	LmxM.24.2070	33	5	24729	11.4	
	hypothetical protein, conserved	LmxM.33.2580	32	5	22615	9.90	
Wt14	alpha tubulin	LmxM.13.0280	102	12	61058	5.45	4.23
	hypothetical protein, conserved	LmxM.34.5340	64	9	39265	5.31	
	hypothetical protein, conserved	LmxM.24.0960	27	0	108178	9.27	

	calpain-like protein, putative,cysteine peptidase, Clan CA, family C2, putative cytochrome c oxidase assembly factor, putative hypothetical protein, conserved	LmxM.30.0400 LmxM.04.1130 LmxM.34.3720	25 24 23	0 3 3	104139 33701 50938	7.07 5.61 5.93	
Wt15	eukaryotic translation initiation factor 6 (eIF-6), putative hypothetical protein, conserved unspecified product acyl-coenzyme a dehydrogenase, putative	LmxM.36.0890 LmxM.36.6760 LmxM.08.1171 LmxM.06.0880	281 80 70 44	57 29 8 3	27454 29148 50319 45641	5.05 5.37 4.71 7.97	4.27
Wt16	cystathione gamma lyase, putative vacuolar ATP synthase subunit b, putative seryl-tRNA synthetase, putative hypothetical protein, conserved hypothetical protein, conserved eukaryotic translation initiation factor 6 (eIF-6), putative	LmxM.34.3230 LmxM.28.2430 LmxM.11.0100 LmxM.30.1000 LmxM.31.1700 LmxM.36.0890	158 52 49 27 21 18	12 4 4 2 0 6	45102 55837 53671 121698 90069 27454	6.05 5.72 5.29 4.92 9.08 5.05	2.34
Wt17	coatomer epsilon subunit, putative alpha tubulin unspecified product elongation factor 1-alpha	LmxM.31.1730 LmxM.13.0280 LmxM.08.1171 LmxM.17.0080	578 298 185 91	56 22 18 13	35083 61058 50319 49575	5.11 5.45 4.71 9.03	2.68
Wt18	unspecified product alpha tubulin peptidase m20/m25/m40 family-like protein mannose-1-phosphate guanyltransferase hypothetical protein, conserved phosphodiesterase, putative	LmxM.08.1171 LmxM.13.0280 LmxM.30.1890 LmxM.23.0110 LmxM.30.1000 LmxM.18.1090	217 97 34 22 20 18	17 14 15 8 0 1	50319 61058 37608 41849 121698 71449	4.71 5.45 5.10 5.29 4.92 5.48	4.33
Wt20	alpha tubulin hypothetical protein, conserved dihydroorotate dehydrogenase, putative hypothetical protein, conserved 40S ribosomal protein S3A, putative unspecified product	LmxM.13.0280 LmxM.33.0230 LmxM.16.0530 LmxM.26.0870 LmxM.34.0400 LmxM.08.1171	446 74 38 28 20 19	20 2 3 1 5 4	61058 81890 34287 80727 30245 50319	5.45 5.42 5.48 9.48 10.3 4.71	3.30

## Appendix J: Chromatograms of the sterol metabolites detected in wild-type AmB resistant and re-expressor *L. mexicana* cell lines.



Ergosta-5,7,22,24(28)-tetraen-3 $\beta$ -ol4 $\alpha$ -formyl-4 $\beta$ -methyl-5 $\alpha$ -cholesta-8-24-dien-3 $\beta$ -ol



The chromatographic resolution using hydrophilic interaction liquid chromatography (HILIC) and is poor. However, the changes in abundance remain clear. Chromatography using a C-18 reverse-phase column should now be performed to obtain more quantitative information. Absence of a 4 $\alpha$ -formyl-4 $\beta$ -methyl-5 $\alpha$ -cholesta-8-24-dien-3 $\beta$ -ol chromatogram for the wild-type means it was not detected in the samples derived from the wild-type cells. Chromatograms of intensity against retention time of the most changing metabolites were constructed using PeakML Viewer 1.0.0 (Scheltema *et al.*, 2011).

## References

- Aebersold, R., and Mann, M. (2003). Mass spectrometry-based proteomics. *Nature*, 422(6928), 198-207.
- Al-Mohammed, H.I., Chance, M.L., and Bates, P.A. (2005). Production and characterization of stable amphotericin-resistant amastigotes and promastigotes of *Leishmania mexicana*. *Antimicrobial Agents and Chemotherapy*, 49(8), 3274-3280.
- Allsopp, R. (2001). Options for vector control against trypanosomiasis in Africa. *Trends in Parasitology*, 17(1), 15-19.
- Allwood, J.W., and Goodacre, R. (2010). An Introduction to Liquid Chromatography-Mass Spectrometry Instrumentation Applied in Plant Metabolomic Analyses. *Phytochemical Analysis*, 21(1), 33-47.
- Alsford, S., Eckert, S., Baker, N., Glover, L., Sanchez-Flores, A., Leung, K. F., Turner, D. J., Field, M. C., Berriman, M., and Horn, D. (2012). High-throughput decoding of antitrypanosomal drug efficacy and resistance. *Nature*, 482(7384), 232-236.
- Alvar, J., Croft, S., and Olliaro, P. (2006). Chemotherapy in the treatment and control of leishmaniasis. *Adv Parasitol*, 61, 223-274.
- Andrade-Neto, V. V., de Matos-Guedes, H. L., de Oliveira Gomes, D. C., do Canto-Cavalheiro, M. M., Rossi-Bergmann, B., and Torres-Santos, E. C. (2012). The stepwise selection for ketoconazole resistance induces upregulation of C14-demethylase (CYP51) in *Leishmania amazonensis*. *Memorias Do Instituto Oswaldo Cruz*, 107(3), 416-419.
- Ansorge, W. J. (2009). Next-generation DNA sequencing techniques. *New Biotechnology*, 25(4), 195-203.
- Aphasizhev, R., and Aphasizheva, I. (2011). Uridine insertion/deletion editing in trypanosomes: a playground for RNA-guided information transfer. *Wiley Interdisciplinary Reviews-Rna*, 2(5), 669-685.
- Aronow, B., Kaur, K., McCartan, K., and Ullman, B. (1987). 2 High-affinity nucleoside transporters in *Leishmania donovani*. *Molecular and Biochemical Parasitology*, 22(1), 29-37.
- Ashutosh, Sundar, S., and Goyal, N. (2007). Molecular mechanisms of antimony resistance in Leishmania. *Journal of medical microbiology*, 56(Pt 2), 143-153.

- Atamna, H., Pascarmona, G., and Ginsburg, H. (1994). Hexose-monophosphate shunt activity in intact *Plasmodium falciparum*-infected erythrocytes and in free parasites. *Molecular and Biochemical Parasitology*, 67(1), 79-89.
- Bacchi, C. J. (1981). Content, synthesis, and function of polyamines in trypanosomatids - relationship to chemotherapy. *Journal of Protozoology*, 28(1), 20-27.
- Bacchi, C. J., Nathan, H. C., and Hutner, S. H. (1980). Polyamine metabolism - a potential therapeutic target in trypanosomes. *Science*, 210(4467), 332-334.
- Baker, N, Glover, L., Munday, J.C., Andres, D.A., Barrett, M.P., de Koning, H.P., and Horn, D. (2012). Aquaglyceroporin 2 controls susceptibility to melarsoprol and pentamidine in African trypanosomes. *Proceedings of the National Academy of Sciences of the United States of America*, 109(27), 10996-11001.
- Baker, N., Barrett, M. P., Wilkes, J., Hamilton, G., and Horn, D. (2014). An RNAi screen for drug resistance in African trypanosomes reveal a link between acidic compartment function and mitochondrial F<sub>0</sub>F<sub>1</sub>-ATPase function. *British Society for Parasitology 2014 Scientific program and abstracts, 52nd Annual Spring meeting and Trypanosomiasis and Leishmaniasis symposium*, pp-184; Cambridge.
- Baloch, R. I., Mercer, E. I., Wiggins, T. E., and Baldwin, B. C. (1984). Inhibition of ergosterol biosynthesis in *saccharomyces-cerevisiae* and *ustilago-maydis* by tridemorph, fenpropimorph and fenpropidin. *Phytochemistry*, 23(10), 2219-2226.
- Banuls, A. L., Hide, M., and Prugnolle, F. (2007). Leishmania and the leishmaniasis: A parasite genetic update and advances in taxonomy, epidemiology and pathogenicity in humans. In J. R. Baker, R. Mller & D. Rollinson (Eds.), *Advances in Parasitology, Vol 64* (Vol. 64, pp. 1-109). San Diego: Elsevier Academic Press Inc.
- Baquer, N. Z., Hothersall, J. S., McLean, P., and Greenbaum, A. L. (1977). Aspects of carbohydrate-metabolism in developing brain. *Developmental Medicine and Child Neurology*, 19(1), 81-104.
- Bard, M., Bruner, D. A., Pierson, C. A., Lees, N. D., Biermann, B., Frye, L., Koegel, C., and Barbuch, R. (1996). Cloning and characterization of ERG25, the *Saccharomyces cerevisiae* gene encoding C-4 sterol methyl oxidase. *Proceedings of the National Academy of Sciences of the United States of America*, 93(1), 186-190.
- Barrett, M. P., and Fairlamb, A. H. (1999). The biochemical basis of arsenical-diamidine crossresistance in African trypanosomes. *Parasitology Today*, 15(4), 136-140.

- Barrett, M. P., and Gilbert, I. H. (2006). Targeting of toxic compounds to the trypanosome's interior. In J. R. Baker, R. Muller & D. Rollinson (Eds.), *Advances in Parasitology*, Vol 63 (Vol. 63, pp. 125-183).
- Barrett, M.P., Burchmore, R.J.S., Stich, A., Lazzari, J.O., Frasch, A.C., Cazzulo, J.J., and Krishna, S. (2003). The trypanosomiasis. *Lancet*, 362(9394), 1469-1480.
- Basselin, M., Badet-Denisot, M. A., and Robert-Gero, M. (1998). Modification of kinetoplast DNA minicircle composition in pentamidine-resistant *Leishmania*. *Acta Tropica*, 70(1), 43-61.
- Basselin, M., Coombs, G. H., and Barrett, M. P. (2000). Putrescine and spermidine transport in *Leishmania*. *Molecular and Biochemical Parasitology*, 109(1), 37-46.
- Basselin, M., Denise, H., Coombs, G. H., and Barrett, M. P. (2002). Resistance to pentamidine in *Leishmania mexicana* involves exclusion of the drug from the mitochondrion. *Antimicrobial Agents and Chemotherapy*, 46(12), 3731-3738.
- Bates, P. A. (1994). Complete developmental cycle of *Leishmania mexicana* in axenic culture. *Parasitology*, 108, 1-9.
- Bates, P. A., Robertson, C. D., Tetley, L., and Coombs, G. H. (1992). Axenic cultivation and characterization of *Leishmania mexicana* amastigote-like forms. *Parasitology*, 105, 193-202.
- Beach, D. H., Goad, L. J., and Holz, G. G. (1988). Effects of antimycotic azoles on growth and sterol biosynthesis of leishmania promastigotes. *Molecular and Biochemical Parasitology*, 31(2), 149-162.
- Bello, A.R., Nare, B., Freedman, D., Hardy, L., and Beverley, S.M. (1994). Ptr1 - A Reductase Mediating Salvage of Oxidized Pteridines and Methotrexate Resistance in the Protozoan Parasite *Leishmania major*. *Proceedings of the National Academy of Sciences of the United States of America*, 91(24), 11442-11446.
- Berens, R. L., Brun, R., and Krassner, S. M. (1976). Simple monophasic medium for axenic culture of hemoflagellates. *Journal of Parasitology*, 62(3), 360-365.
- Berg, M., Mannaert, A., Vanaerschot, M., Van der Auwera, G., and Dujardin, J. C. (2013a). (Post-) Genomic approaches to tackle drug resistance in *Leishmania*. *Parasitology*, 140(12), 1492-1505.
- Berg, M., Vanaerschot, M., Jankevics, A., Cuypers, B., Maes, I., Mukherjee, S. B., Khanal, B., Rijal, S., Roy, S., Opperdoes, F.R., Breitling, R., and Dujardin, J. C. (2013b). Metabolic adaptations of *Leishmania donovani* in

relation to differentiation, drug resistance, and drug pressure. *Molecular Microbiology*, 90(2), 428-442.

- Berger, B. J., and Fairlamb, A. H. (1994). Properties of melarsamine hydrochloride (cymelarsan) in aqueous-solution. *Antimicrobial Agents and Chemotherapy*, 38(6), 1298-1302.
- Berman, J. D. (1988). Chemotherapy for leishmaniasis - biochemical-mechanisms, clinical efficacy, and future strategies. *Reviews of Infectious Diseases*, 10(3), 560-586.
- Besteiro, S., Barrett, M.P., Riviere, L., and Bringaud, F. (2005). Energy generation in insect stages of *Trypanosoma brucei*: metabolism in flux. *Trends in Parasitology*, 21(4), 185-191.
- Bhargava, P., Kumar, K., Chaudhaery, S. S., Saxena, A. K., and Roy, U. (2010). Cloning, overexpression and characterization of *Leishmania donovani* squalene synthase. *FEMS Microbiol Lett*, 311(1), 82-92.
- Bocedi, A., Dawood, K. F., Fabrini, R., Federici, G., Gradoni, L., Pedersen, J. Z., and Ricci, G. (2010). Trypanothione efficiently intercepts nitric oxide as a harmless iron complex in trypanosomatid parasites. *Faseb Journal*, 24(4), 1035-1042.
- Boutte, Y., Men, S., and Grebe, M. (2011). Fluorescent in situ visualization of sterols in Arabidopsis roots. *Nature Protocols*, 6(4), 446-456.
- Breitling, R., Pitt, A. R., and Barrett, M. P. (2006). Precision mapping of the metabolome. *Trends in Biotechnology*, 24(12), 543-548.
- Bringaud, F., Ebikeme, C., and Boshart, M. (2010). Acetate and succinate production in amoebae, helminths, diplomonads, trichomonads and trypanosomatids : common and diverse metabolic strategies used by parasitic lower eukaryotes. *Parasitology*, 137(9), 1315-1331.
- Bringaud, F., Riviere, L., and Coustou, V. (2006). Energy metabolism of trypanosomatids: Adaptation to available carbon sources. *Molecular and Biochemical Parasitology*, 149(1), 1-9.
- Brown, S. V., Hosking, P., Li, J. L., and Williams, N. (2006). ATP synthase is responsible for maintaining mitochondrial membrane potential in bloodstream form *Trypanosoma brucei*. *Eukaryotic Cell*, 5(1), 45-53.
- Brun, R., Blum, J., Chappuis, F., and Burri, C. (2010). Human African trypanosomiasis. *Lancet*, 375(9709), 148-159.
- Brun, R., Don, R., Jacobs, R. T., Wang, M. Z., and Barrett, M. P. (2011). Development of novel drugs for human African trypanosomiasis. *Future Microbiology*, 6(6), 677-691.

- Brun, R., and Schonenberger, M. (1979). Cultivation and invitro cloning of procyclic culture forms of *Trypanosoma brucei* in a semi-defined medium. *Acta Tropica*, 36(3), 289-292.
- Burchmore, R. J. S., and Barrett, M. P. (2001). Life in vacuoles - nutrient acquisition by *Leishmania amastigotes*. *International Journal for Parasitology*, 31(12), 1311-1320.
- Carrero-Lerida, J., Perez-Moreno, G., Castillo-Acosta, V. M., Ruiz-Perez, L. M., and Gonzalez-Pacanowska, D. (2009). Intracellular location of the early steps of the isoprenoid biosynthetic pathway in the trypanosomatids *Leishmania major* and *Trypanosoma brucei*. *International Journal for Parasitology*, 39(3), 307-314.
- Carter, N. S., Yates, P., Arendt, C. S., Boitz, J. M., and Ullman, B. (2008). Purine and pyrimidine metabolism in *Leishmania*. *Drug Targets in Kinetoplastid Parasites*, 625, 141-154.
- Cazzulo, J.J. (1992). Aerobic Fermentation of Glucose by Trypanosomatids. *Faseb Journal*, 6(13), 3153-3161.
- Chaudhuri, M., Ott, R.D., and Hill, G.C. (2006). Trypanosome alternative oxidase: from molecule to function. *Trends in Parasitology*, 22(10), 484-491.
- Chawla, B., Jhingran, A., Panigrahi, A. K., Stuart, K. D., and Madhubala, R. (2011). Paromomycin Affects Translation and Vesicle-Mediated Trafficking as Revealed by Proteomics of Paromomycin -Susceptible -Resistant *Leishmania donovani*. *Plos One*, 6(10).
- Chawla, B., and Madhubala, R. (2010). Drug targets in *Leishmania*. *Journal of parasitic diseases : official organ of the Indian Society for Parasitology*, 34(1), 1-13.
- Chowdhury, A.R., Bakshi, R., Wang, J.Y., Yildirim, G., Liu, B.Y., Pappas-Brown, V., Tolun, G., Griffith, J.D., Shapiro, T.A., Jensen, R.E., and Englund, P.T. (2010). The Killing of African Trypanosomes by Ethidium Bromide. *Plos Pathogens*, 6(12).
- Chung, J. H., Lester, R. L., and Dickson, R. C. (2003). Sphingolipid requirement for generation of a functional V-1 component of the vacuolar ATPase. *Journal of Biological Chemistry*, 278(31), 28872-28881.
- Claborn, D. M. (2010). The biology and control of leishmaniasis vectors. *Journal of global infectious diseases*, 2(2), 127-134.
- Coelho, A. C., Boisvert, S., Mukherjee, A., Leprohon, P., Corbeil, J., and Ouellette, M. (2012). Multiple Mutations in Heterogeneous Miltefosine-

Resistant *Leishmania major* Population as Determined by Whole Genome Sequencing. *Plos Neglected Tropical Diseases*, 6(2).

- Cojean, S., Houze, S., Haouchine, D., Huteau, F., Lariven, S., Hubert, V., Michard, F., Bories, C., Pratlong, F., Le Bras, J., Loiseau, P. M., and Matheron, S. (2012). Leishmania Resistance to Miltefosine Associated with Genetic Marker. *Emerging Infectious Diseases*, 18(4), 704-706.
- Colotti, G., and Ilari, A. (2011). Polyamine metabolism in Leishmania: from arginine to trypanothione. *Amino Acids*, 40(2), 269-285.
- Coppens, I., Baudhuin, P., Opperdoes, F. R., and Courtoy, P. J. (1988). Receptors for the host low-density lipoproteins on the hemoflagellate *Trypanosoma brucei* - Purification and involvement in the growth of the parasite. *Proceedings of the National Academy of Sciences of the United States of America*, 85(18), 6753-6757.
- Coustou, V., Besteiro, S., Biran, M., Diolez, P., Bouchaud, V., Voisin, P., Michels, P.A.M., Canioni, P., Baltz, T., and Bringaud, F. (2003). ATP generation in the *Trypanosoma brucei* procyclic form - Cytosolic substrate level phosphorylation is essential, but not oxidative phosphorylation. *Journal of Biological Chemistry*, 278(49), 49625-49635.
- Cowart, L. Ashley, and Obeid, Lina M. (2007). Yeast sphingolipids: Recent developments in understanding biosynthesis, regulation, and function. *Biochimica Et Biophysica Acta-Molecular and Cell Biology of Lipids*, 1771(3), 421-431.
- Creek, D. J., Anderson, J., McConville, M. J., and Barrett, M. P. (2012a). Metabolomic analysis of trypanosomatid protozoa. *Molecular and Biochemical Parasitology*, 181(2), 73-84.
- Creek, D. J., and Barrett, M. P. (2014). Determination of antiprotozoal drug mechanisms by metabolomics approaches. *Parasitology*, 141(1), 83-92.
- Creek, D. J., Jankevics, A., Breitling, R., Watson, D. G., Barrett, M. P., and Burgess, K. E., V. (2011). Toward Global Metabolomics Analysis with Hydrophilic Interaction Liquid Chromatography-Mass Spectrometry: Improved Metabolite Identification by Retention Time Prediction. *Analytical Chemistry*, 83(22), 8703-8710.
- Creek, D. J., Jankevics, A., Burgess, K. E., V, Breitling, R., and Barrett, M. P. (2012b). IDEOM: an Excel interface for analysis of LC-MS-based metabolomics data. *Bioinformatics*, 28(7), 1048-1049.
- Creek, D. J., Nijagal, B., Kim, D. H., Rojas, F., Matthews, K. R., and Barrett, M. P. (2013). Metabolomics Guides Rational Development of a Simplified Cell Culture Medium for Drug Screening against *Trypanosoma brucei*. *Antimicrobial Agents and Chemotherapy*, 57(6), 2768-2779.

- Croft, S. L., and Olliaro, P. (2011). Leishmaniasis chemotherapy-challenges and opportunities. *Clinical Microbiology and Infection*, 17(10), 1478-1483.
- Croft, S.L., Sundar, S., and Fairlamb, A.H. (2006). Drug resistance in leishmaniasis. *Clinical Microbiology Reviews*, 19(1), 111-126.
- Darling, T.N., Balber, A.E., and Blum, J.J. (1988). A Comparative-Study of D-Lactate, L-Lactate and Glycerol Formation by 4 Species of Leishmania and by *Trypanosoma lewisi* and *Trypanosoma brucei gambiense*. *Molecular and Biochemical Parasitology*, 30(3), 253-257.
- Das, M., Mukherjee, S. B., and Shaha, C. (2001). Hydrogen peroxide induces apoptosis-like death in *Leishmania donovani* promastigotes. *Journal of Cell Science*, 114(13), 2461-2469.
- Das, M., Saudagar, P., Sundar, S., and Dubey, V. K. (2013). Miltefosine-unresponsive *Leishmania donovani* has a greater ability than miltefosine-responsive *L. donovani* to resist reactive oxygen species. *Febs Journal*, 280(19), 4807-4815.
- Davidson, R.N., den Boer, M., and Ritmeijer, K. (2009). Paromomycin. *Transactions of the Royal Society of Tropical Medicine and Hygiene*, 103(7), 653-660.
- Davies, C.R., Kaye, P., Croft, S.L., and Sundar, S. (2003). Leishmaniasis: new approaches to disease control. *British Medical Journal*, 326(7385), 377-382.
- de Koning, H. P., Anderson, L. F., Stewart, M., Burchmore, R. J. S., Wallace, L. J. M., and Barrett, M. P. (2004). The trypanocide diminazene aceturate is accumulated predominantly through the TbAT1 purine transporter: additional insights on diamidine resistance in African trypanosomes. *Antimicrobial Agents and Chemotherapy*, 48(5), 1515-1519.
- de Macedo-Silva, S. T., Urbina, J. A., de Souza, W., and Fernandes Rodrigues, J. C. (2013). In Vitro Activity of the Antifungal Azoles Itraconazole and Posaconazole against *Leishmania amazonensis*. *Plos One*, 8(12).
- de Souza, W., and Rodrigues, J. C. F. (2009). Sterol Biosynthesis Pathway as Target for Anti-trypanosomatid Drugs. *Interdisciplinary perspectives on infectious diseases, 2009*, 642502.
- Dean, S., Gould, M. K., Dewar, C. E., and Schnauffer, A. C. (2013). Single point mutations in ATP synthase compensate for mitochondrial genome loss in trypanosomes. *Proceedings of the National Academy of Sciences of the United States of America*, 110(36), 14741-14746.
- Debieu, D., Bach, J., Arnold, A., Brousset, S., Gredt, M., Taton, M., Rahier, A., Malosse, C., and Leroux, P. (2000). Inhibition of ergosterol biosynthesis by morpholine, piperidine, and spiroketalamine fungicides in *Microdochium*

- nivale: Effect on sterol composition and sterol Delta(8) -> Delta(7)-isomerase activity. *Pesticide Biochemistry and Physiology*, 67(2), 85-94.
- Debieu, D., Bach, J., Hugon, M., Malosse, C., and Leroux, P. (2001). The hydroxylanilide fenhexamid, a new sterol biosynthesis inhibitor fungicide efficient against the plant pathogenic fungus *Botryotinia fuckeliana* (*Botrytis cinerea*). *Pest Management Science*, 57(11), 1060-1067.
- DeKoning, H.P., and Jarvis, S.M. (1997). Hypoxanthine uptake through a purine-selective nucleobase transporter in *Trypanosoma brucei brucei* procyclic cells is driven by protonmotive force. *European Journal of Biochemistry*, 247(3), 1102-1110.
- Delespaux, V., Geysen, D., van den Bossche, P., and Geerts, S. (2008). Molecular tools for the rapid detection of drug resistance in animal trypanosomes. *Trends in Parasitology*, 24(5), 236-242.
- den Boer, M., Argaw, D., Jannin, J., and Alvar, J. (2011). Leishmaniasis impact and treatment access. *Clinical Microbiology and Infection*, 17(10), 1471-1477.
- Denninger, V., Figarella, K., Schoenfeld, C., Brems, S., Busold, C., Lang, F., Hoheisel, J., and Duszenko, M. (2007). Troglitazone induces differentiation in *Trypanosoma brucei*. *Experimental Cell Research*, 313(9), 1805-1819.
- Desjeux, P. (2004). Leishmaniasis: current situation and new perspectives. *Comparative Immunology Microbiology and Infectious Diseases*, 27(5), 305-318.
- Desquesnes, M., Dargantes, A., Lai, D. H., Lun, Z. R., Holzmuller, P., and Jittapalapong, S. (2013). *Trypanosoma evansi* and Surra: A Review and Perspectives on Transmission, Epidemiology and Control, Impact, and Zoonotic Aspects. *Biomed Research International*.
- Dettmer, K., Aronov, P.A., and Hammock, B.D. (2007). Mass spectrometry-based metabolomics. *Mass Spectrometry Reviews*, 26(1), 51-78.
- Domingo, G.J., Palazzo, S.S., Wang, B.B., Pannicucci, B., Salavati, R., and Stuart, K.D. (2003). Dyskinetoplastic *Trypanosoma brucei* contains functional editing complexes. *Eukaryotic Cell*, 2(3), 569-577.
- Dorlo, T.P.C., Balasegaram, M., Beijnen, J.H., and de Vries, P.J. (2012). Miltefosine: a review of its pharmacology and therapeutic efficacy in the treatment of leishmaniasis. *Journal of Antimicrobial Chemotherapy*, 67(11), 2576-2597.
- Downing, T., Imamura, H., Decuypere, S., Clark, T. G., Coombs, G. H., Cotton, J. A., Hilley, J. D., de Doncker, S., Maes, I., Mottram, J. C., Quail, M. A., Rijal, S., Sanders, M., Schoenian, G., Stark, O., Sundar, S., Vanaerschot, M,

- Hertz-Fowler, C., Dujardin, J. C., and Berriman, M. (2011). Whole genome sequencing of multiple *Leishmania donovani* clinical isolates provides insights into population structure and mechanisms of drug resistance. *Genome Research*, 21(12), 2143-2156.
- Drummelsmith, J., Girard, I., Trudel, N., and Ouellette, M. (2004). Differential protein expression analysis of *Leishmania major* reveals novel roles for methionine adenosyltransferase and S-adenosylmethionine in methotrexate resistance. *Journal of Biological Chemistry*, 279(32), 33273-33280.
- Dufourc, E. J. (2008). Sterols and membrane dynamics. *Journal of chemical biology*, 1(1-4), 63-77.
- Dupont, S., Lemetais, G., Ferreira, T., Cayot, P., Gervais, P., and Beney, L. (2012). Ergosterol biosynthesis: A fungal pathway for life on land? *Evolution*, 66(9), 2961-2968.
- Ebikeme, C., Hubert, J., Biran, M., Gouspillou, G., Morand, P., Plazolles, N., Guegan, F., Diolez, P., Franconi, J.M., Portais, J.C., and Bringaud, F. (2010). Ablation of Succinate Production from Glucose Metabolism in the Procyclic Trypanosomes Induces Metabolic Switches to the Glycerol 3-Phosphate/Dihydroxyacetone Phosphate Shuttle and to Proline Metabolism. *Journal of Biological Chemistry*, 285(42), 32312-32324.
- Eisler, M. C., Maruta, J., Nqindi, J., Connor, R. J., UshewokunzeObatolu, U., Holmes, P. H., and Peregrine, A. S. (1996). Isometamidium concentrations in the sera of cattle maintained under a chemoprophylactic regime in a tsetse-infested area of Zimbabwe. *Tropical Medicine & International Health*, 1(4), 535-541.
- Fairlamb, A. H., Blackburn, P., Ulrich, P., Chait, B. T., and Cerami, A. (1985). Trypanothione - a novel bis(glutathionyl)spermidine cofactor for glutathione-reductase in trypanosomatids. *Science*, 227(4693), 1485-1487.
- Fairlamb, A. H., and Cerami, A. (1992). Metabolism and functions of trypanothione in the kinetoplastida. *Annual Review of Microbiology*, 46, 695-729.
- Fairlamb, A.H. (2003). Chemotherapy of human African trypanosomiasis: current and future prospects. *Trends in Parasitology*, 19(11), 488-494.
- Figarella, K., Rawer, M., Uzcategui, N. L., Kubata, B. K., Lauber, K., Madeo, F., Wesselborg, S., and Duszenko, M. (2005). Prostaglandin D-2 induces programmed cell death in *Trypanosoma brucei* bloodstream form. *Cell Death and Differentiation*, 12(4), 335-346.
- Fridberg, A., Olson, C.L., Nakayasu, E.S., Tyler, K.M., Almeida, I.C., and Engman, D.M. (2008). Sphingolipid synthesis is necessary for kinetoplast segregation and cytokinesis in *Trypanosoma brucei*. *Journal of Cell Science*, 121(4), 522-535.

- Futerman, A. H., and Riezman, H. (2005). The ins and outs of sphingolipid synthesis. *Trends in Cell Biology*, 15(6), 312-318.
- Gachotte, D., Eckstein, J., Barbuch, R., Hughes, T., Roberts, C., and Bard, M. (2001). A novel gene conserved from yeast to humans is involved in sterol biosynthesis. *Journal of Lipid Research*, 42(1), 150-154.
- Garcia-Hernandez, R., J., Ignacio M., Castanys, S., and Gamarro, F. (2012). *Leishmania donovani* Develops Resistance to Drug Combinations. *Plos Neglected Tropical Diseases*, 6(12).
- Geerts, S., Holmes, P.H., Diall, O., and Eisler, M.C. (2001). African bovine trypanosomiasis: the problem of drug resistance. *Trends in Parasitology*, 17(1), 25-28.
- Ginger, M. L., Chance, M. L., and Goad, L. J. (1996). Carbon sources for fatty acid and sterol biosynthesis in *Leishmania* species. *Biochemical Society Transactions*, 24(3), S434-S434.
- Ginger, M. L., Chance, M. L., and Goad, L. J. (1999). Elucidation of carbon sources used for the biosynthesis of fatty acids and sterols in the trypanosomatid *Leishmania mexicana*. *Biochemical Journal*, 342, 397-405.
- Ginger, M. L., Chance, M. L., Sadler, I. H., and Goad, L. J. (2001). The biosynthetic incorporation of the intact leucine skeleton into sterol by the trypanosomatid *Leishmania mexicana*. *Journal of Biological Chemistry*, 276(15), 11674-11682.
- Ginger, M. L., Prescott, M. C., Reynolds, D. G., Chance, M. L., and Goad, L. J. (2000). Utilization of leucine and acetate as carbon sources for sterol and fatty acid biosynthesis by Old and New World *Leishmania* species, *Endotrypanum monterogeii* and *Trypanosoma cruzi*. *European Journal of Biochemistry*, 267(9), 2555-2566.
- Goad, L. J., Holz, G. G., and Beach, D. H. (1984). Sterols of *Leishmania* species - implications for biosynthesis. *Molecular and Biochemical Parasitology*, 10(2), 161-170.
- Graham, L. A., Powell, B., and Stevens, T. H. (2000). Composition and assembly of the yeast vacuolar H<sup>+</sup>-ATPase complex. *Journal of Experimental Biology*, 203(1), 61-70.
- Gray, K. C., Palacios, D. S., Dailey, I., Endo, M. M., Uno, B. E., Wilcock, B. C., and Burke, M. D. (2012). Amphotericin primarily kills yeast by simply binding ergosterol. *Proceedings of the National Academy of Sciences of the United States of America*, 109(7), 2234-2239.

- Green, H. P., Portela, M. D. M., St Jean, E. N., Lugli, E. B., and Raper, J. (2003). Evidence for a *Trypanosoma brucei* lipoprotein scavenger receptor. *Journal of Biological Chemistry*, 278(1), 422-427.
- Grevelink, S.A., and Lerner, E.A. (1996). Leishmaniasis. *Journal of the American Academy of Dermatology*, 34(2), 257-272.
- Gutierrez, C., Corbera, J. A., Bayou, K., and van Gool, F. (2008). Use of Cymelarsan in Goats Chronically Infected with *Trypanosoma evansi*. In O. A. E. Sparagano, J. C. Maillard & J. V. Figueroa (Eds.), *Animal Biodiversity and Emerging Diseases: Prediction and Prevention* (Vol. 1149, pp. 331-333).
- Haanstra, J.R., van Tuijl, A., Kessler, P., Reijnders, W., Michels, P.A.M., Westerhoff, H.V., Parsons, M., and Bakker, B.M. (2008). Compartmentation prevents a lethal turbo-explosion of glycolysis in trypanosomes. *Proceedings of the National Academy of Sciences of the United States of America*, 105(46), 17718-17723.
- Hagos, A., Goddeeris, B. M., Yilkal, K., Alemu, T., Fikru, R., Yacob, H. T., Feseha, G., and Claes, F. (2010). Efficacy of Cymelarsan (R) and Diminasan (R) against *Trypanosoma equiperdum* infections in mice and horses. *Veterinary Parasitology*, 171(3-4), 200-206.
- Haldar, A. K., Sen, P., and Roy, S. (2011). Use of antimony in the treatment of leishmaniasis: current status and future directions. *Molecular biology international*, 2011, 571242-571242.
- Handman, E. (2001). Leishmaniasis: Current status of vaccine development. *Clinical Microbiology Reviews*, 14(2), 229-243.
- Hargrove, J. W., Omolo, S., Msalilwa, J. S. I., and Fox, B. (2000). Insecticide-treated cattle for tsetse control: the power and the problems. *Medical and Veterinary Entomology*, 14(2), 123-130.
- Hargrove, T. Y., Wawrzak, Z., Liu, J., Nes, W. D., Waterman, M. R., and Lepesheva, G. I. (2011). Substrate Preferences and Catalytic Parameters Determined by Structural Characteristics of Sterol 14 alpha-Demethylase (CYP51) from *Leishmania infantum*. *Journal of Biological Chemistry*, 286(30), 26838-26848.
- Hasne, M. P., and Ullman, B. (2005). Identification and characterization of a polyamine permease from the protozoan parasite *Leishmania major*. *Journal of Biological Chemistry*, 280(15), 15188-15194.
- Hirumi, H., and Hirumi, K. (1994). Axenic culture of african trypanosome blood-stream forms. *Parasitology Today*, 10(2), 80-84.

- Horn, D., and Duraisingh, M. T. (2014). Antiparasitic Chemotherapy: From Genomes to Mechanisms. In P. A. Insel (Ed.), *Annual Review of Pharmacology and Toxicology*, (Vol. 54, pp. 71-94).
- Hui, P. (2014). Next Generation Sequencing: Chemistry, Technology and Applications. In N. L. S. Tang & T. Poon (Eds.), *Chemical Diagnostics: From Bench to Bedside* (Vol. 336, pp. 1-18).
- Ignacio, M. J., Carvalho, L., Garcia-Hernandez, R., J., Antonio P., J., Antonio F., Castanys, S., and Gamarro, F. (2011). Uptake of the antileishmania drug tafenoquine follows a sterol-dependent diffusion process in *Leishmania*. *Journal of Antimicrobial Chemotherapy*, 66(11), 2562-2565.
- Jensen, R.E., Simpson, L., and Englund, P.T. (2008). What happens when *Trypanosoma brucei* leaves Africa. *Trends in Parasitology*, 24(10), 428-431.
- Jimenez-Jimenez, C., Carrero-Lerida, J., Sealey-Cardona, M., Ruiz Perez, L. M., Urbina, J. A., and Gonzalez Pacanowska, D. (2008). Delta(24(25))-sterol methenyltransferase: Intracellular localization and azasterol sensitivity in *Leishmania major* promastigotes over expressing the enzyme. *Molecular and Biochemical Parasitology*, 160(1), 52-59.
- Kapuscinski, J. (1995). DAPI - A DNA-specific fluorescent-probe. *Biotechnic & Histochemistry*, 70(5), 220-233.
- Katz, A. S. (2000). Topical antifungal agents. *Current Problems in Dermatology-Ur*, 12(5), 226-229.
- Keiser, J., Ericsson, O., and Burri, C. (2000). Investigations of the metabolites of the trypanocidal drug melarsoprol. *Clinical Pharmacology & Therapeutics*, 67(5), 478-488.
- Kinabo, L.D.B. (1993). Pharmacology of Existing Drugs for Animal Trypanosomiasis. *Acta Tropica*, 54(3-4), 169-183.
- Kinabo, L.D.B., and Bogan, J.A. (1988). The Pharmacology of Isometamidium. *Journal of Veterinary Pharmacology and Therapeutics*, 11(3), 233-245.
- Krauth-Siegel, R. L., Meiering, S. K., and Schmidt, H. (2003). The parasite-specific trypanothione metabolism of trypanosoma and leishmania. *Biological Chemistry*, 384(4), 539-549.
- Kristjanson, P.M., Swallow, B.M., Rowlands, G.J., Kruska, R.L., and de Leeuw, P.N. (1999). Measuring the costs of African animal trypanosomosis, the potential benefits of control and returns to research. *Agricultural Systems*, 59(1), 79-98.
- Lai, D.H., Hashimi, H., Lun, Z.R., Ayala, F.J., and Lukes, J. (2008). Adaptations of *Trypanosoma brucei* to gradual loss of kinetoplast DNA: *Trypanosoma*

*equiperdum* and *Trypanosoma evansi* are petite mutants of *T-brucei*. *Proceedings of the National Academy of Sciences of the United States of America*, 105(6), 1999-2004.

- Lamour, N., Riviere, L., Coustou, V., Coombs, G.H., Barrett, M.P., and Bringaud, F. (2005). Proline metabolism in procyclic *Trypanosoma brucei* is down-regulated in the presence of glucose. *Journal of Biological Chemistry*, 280(12), 11902-11910.
- Landfear, S. M. (2000). Genetics and biochemistry of Leishmania membrane transporters. *Current Opinion in Microbiology*, 3(4), 417-421.
- Landfear, S. M., Ullman, B., Carter, N. S., and Sanchez, M. A. (2004). Nucleoside and nucleobase transporters in parasitic protozoa. *Eukaryotic Cell*, 3(2), 245-254.
- Landolfo, S., Zara, G., Zara, S., Budroni, M., Ciani, M., and Mannazzu, I. (2010). Oleic acid and ergosterol supplementation mitigates oxidative stress in wine strains of *Saccharomyces cerevisiae*. *International Journal of Food Microbiology*, 141(3), 229-235.
- Lanteri, C. A., Tidwell, R. R., and Meshnick, S. R. (2008). The mitochondrion is a site of trypanocidal action of the aromatic diamidine DB75 in bloodstream forms of *Trypanosoma brucei*. *Antimicrobial Agents and Chemotherapy*, 52(3), 875-882.
- Lemke, A., Kiderlen, A., and Kayser, O. (2005). Amphotericin B. *Applied Microbiology and Biotechnology*, 68(2), 151-162.
- Lepesheva, G. I., and Waterman, M. R. (2007). Sterol 14 alpha-demethylase cytochrome P450 (CYP51), a P450 in all biological kingdoms. *Biochimica Et Biophysica Acta-General Subjects*, 1770(3), 467-477.
- Lepesheva, G. I., and Waterman, M. R. (2011a). Sterol 14alpha-Demethylase (CYP51) as a Therapeutic Target for Human Trypanosomiasis and Leishmaniasis. *Current Topics in Medicinal Chemistry*, 11(16), 2060-2071.
- Lepesheva, G. I., and Waterman, M. R. (2011b). Structural basis for conservation in the CYP51 family. *Biochimica Et Biophysica Acta-Proteins and Proteomics*, 1814(1), 88-93.
- Lepesheva, G. I., Zaitseva, N. G., Nes, W. D., Zhou, W. X., Arase, M., Liu, J., Hill, G. C., and Waterman, M. R. (2006). Cyp51 from *Trypanosoma cruzi* - A phyla-specific residue in the B' helix defines substrate preferences of sterol 14 alpha-demethylase. *Journal of Biological Chemistry*, 281(6), 3577-3585.
- Leprohon, P., Legare, D., Raymond, F., Madore, E., Hardiman, G., Corbeil, J., and Ouellette, M. (2009). Gene expression modulation is associated with

- gene amplification, supernumerary chromosomes and chromosome loss in antimony-resistant *Leishmania infantum*. *Nucleic Acids Research*, 37(5), 1387-1399.
- Leventhal, A. R., Chen, W. G., Tall, A. R., and Tabas, I. (2001). Acid sphingomyelinase-deficient macrophages have defective cholesterol trafficking and efflux. *Journal of Biological Chemistry*, 276(48), 44976-44983.
- Liu, L., Li, Y. H., Li, S. L., Hu, N., He, Y. M., Pong, R., Lin, D. N., Lu, L. H., and Law, M. (2012). Comparison of Next-Generation Sequencing Systems. *Journal of Biomedicine and Biotechnology*, 2012, 251364.
- Lokhov, P., and Archakov, A., I. (2008). Mass Spectrometry Methods in Metabolomics. *Biomeditsinskaya Khimiya*, 54(5), 497-511.
- Lorenz, R. T., and Parks, L. W. (1991). Involvement of heme components in sterol-metabolism of *Saccharomyces-cerevisiae*. *Lipids*, 26(8), 598-603.
- Mallick, P., and Kuster, B. (2010). Proteomics: a pragmatic perspective. *Nature Biotechnology*, 28(7), 695-709.
- Marcireau, C., Guyonnet, D., and Karst, F. (1992). Construction and growth-properties of a yeast-strain defective in sterol 14-reductase. *Current Genetics*, 22(4), 267-272.
- Mardis, E. R. (2008). Next-generation DNA sequencing methods. *Annu Rev Genomics Hum Genet*, 9, 387-402.
- Marouga, R., David, S., and Hawkins, E. (2005). The development of the DIGE system: 2D fluorescence difference gel analysis technology. *Analytical and Bioanalytical Chemistry*, 382(3), 669-678.
- Matovu, E., Seebeck, T., Enyaru, J.C.K., and Kaminsky, R. (2001). Drug resistance in *Trypanosoma brucei* spp., the causative agents of sleeping sickness in man and nagana in cattle. *Microbes and Infection*, 3(9), 763-770.
- Matrangolo, F. S., V, Liarte, D. B., Andrade, L. C., de Melo, M. F., Andrade, J. M., Ferreira, R. F., Santiago, A. S., Pirovani, C. P., Silva-Pereira, R. A., and Murta, S. M. (2013). Comparative proteomic analysis of antimony-resistant and -susceptible *Leishmania braziliensis* and *Leishmania infantum chagasi* lines. *Molecular and Biochemical Parasitology*, 190(2), 63-75.
- Maugeri, D. A., Cazzulo, J. J., Burchmore, R. J. S., Barrett, M. P., and Ogbunude, P. O. J. (2003). Pentose phosphate metabolism in *Leishmania mexicana*. *Molecular and Biochemical Parasitology*, 130(2), 117-125.

- Mazet, M., Morand, P., Biran, M., Bouyssou, G., Courtois, P., Daulouede, S., Millerioux, Y., Franconi, J. M., Vincendeau, P., Moreau, P., and Bringaud, F. (2013). Revisiting the Central Metabolism of the Bloodstream Forms of *Trypanosoma brucei*: Production of Acetate in the Mitochondrion Is Essential for Parasite Viability. *Plos Neglected Tropical Diseases*, 7(12).
- Mbongo, N., Loiseau, P.M., Billion, M.A., and Robert-Gero, M. (1998). Mechanism of amphotericin B resistance in *Leishmania donovani* promastigotes. *Antimicrobial Agents and Chemotherapy*, 42(2), 352-357.
- Mehta, A., and Shaha, C. (2004). Apoptotic death in *Leishmania donovani* promastigotes in response to respiratory chain inhibition - Complex II inhibition results in increased pentamidine cytotoxicity. *Journal of Biological Chemistry*, 279(12), 11798-11813.
- Messana, I., Cabras, T., Iavarone, F., Vincenzoni, F., Urbani, A., and Castagnola, M. (2013). Unraveling the different proteomic platforms. *Journal of Separation Science*, 36(1), 128-139.
- Milhaud, J., Lancelin, J. M., Michels, B., and Blume, A. (1996). Association of polyene antibiotics with sterol-free lipid membranes .1. Hydrophobic binding of filipin to dimyristoylphosphatidylcholine bilayers. *Biochimica Et Biophysica Acta-Biomembranes*, 1278(2), 223-232.
- Millerioux, Y., Ebikeme, C., Biran, M., Morand, P., Bouyssou, G., Vincent, I. M., Mazet, M., Riviere, L., Franconi, J. M., Burchmore, R. J., Moreau, P., Barrett, M. P., and Bringaud, F. (2013). The threonine degradation pathway of the *Trypanosoma brucei* procyclic form: the main carbon source for lipid biosynthesis is under metabolic control. *Molecular Microbiology*, 90(1), 114-129.
- Mina, J. G., Pan, S. Y., Wansadhipathi, N. K., Bruce, C. R., Shams-Eldin, H., Schwarz, R. T., Steel, P. G., and Denny, P. W. (2009). The *Trypanosoma brucei* sphingolipid synthase, an essential enzyme and drug target. *Molecular and Biochemical Parasitology*, 168(1), 16-23.
- Mo, C. Q., and Bard, M. (2005). A systematic study of yeast sterol biosynthetic protein-protein interactions using the split-ubiquitin system. *Biochimica Et Biophysica Acta-Molecular and Cell Biology of Lipids*, 1737(2-3), 152-160.
- Moco, S., Bino, R. J., De Vos, R. C., and Vervoort, J. (2007). Metabolomics technologies and metabolite identification. *Trac-Trends in Analytical Chemistry*, 26(9), 855-866.
- Moll, H., Fuchs, H., Blank, C., and Rollinghoff, M. (1993). Langerhans Cells Transport *Leishmania major* from the Infected Skin to the Draining Lymph-Node for Presentation to Antigen-Specific T-Cells. *European Journal of Immunology*, 23(7), 1595-1601.

- Mondal, D., Alvar, J., Hasnain, M. G., Hossain, M. S., Ghosh, D., Huda, M. M., Nabi, S. G., Sundar, S., Matlashewski, G., and Arana, B. (2014). Efficacy and safety of single-dose liposomal amphotericin B for visceral leishmaniasis in a rural public hospital in Bangladesh: a feasibility study. *The Lancet Global Health*, 2(1), e51-e57.
- Monera, O. D., Sereda, T. J., Zhou, N. E., Kay, C. M., and Hodges, R. S. (1995). Relationship of sidechain hydrophobicity and alpha-helical propensity on the stability of the single-stranded amphipathic alpha-helix. *J Pept Sci*, 1(5), 319-329.
- Moreira, W., Leprohon, P., and Ouellette, M. (2011). Tolerance to drug-induced cell death favours the acquisition of multidrug resistance in *Leishmania*. *Cell Death & Disease*, 2, e201.
- Mubamba, C., Sitali, J., and Gurnmow, B. (2011). Trends of selected cattle diseases in eastern Zambia between 1988 and 2008. *Preventive Veterinary Medicine*, 101(3-4), 163-172.
- Mukherjee, A., Boisvert, S., do Monte-Neto, R. L., Coelho, A. C., Raymond, F., Mukhopadhyay, R., Corbeil, J., and Ouellette, M. (2013). Telomeric gene deletion and intrachromosomal amplification in antimony-resistant *Leishmania*. *Molecular Microbiology*, 88(1), 189-202.
- Munang'andu, H., Siamudaala, V., Munyeme, M., and Nalubamba, K. (2012). A review of ecological factors associated with the epidemiology of wildlife trypanosomiasis in the Luangwa and Zambezi valley ecosystems of Zambia. *Interdisciplinary Perspectives on Infectious Diseases*, 2012, 372523-Article.
- Munday, J. C., Eze, A. A., Baker, N., Glover, L., Clucas, C., Aguinaga Andres, D., Natto, M. J., Teka, I. A., McDonald, J., Lee, R. S., Graf, F. E., Ludin, P., Burchmore, R. J., Turner, C. M., Tait, A., Macleod, A., Maser, P., Barrett, M. P., Horn, D., and De Koning, H. P. (2014). *Trypanosoma brucei* aquaglyceroporin 2 is a high-affinity transporter for pentamidine and melaminophenyl arsenic drugs and the main genetic determinant of resistance to these drugs. *J Antimicrob Chemother*, 69(3), 651-663.
- Mwanakasale, V., and Songolo, P. (2011). Disappearance of some human African trypanosomiasis transmission foci in Zambia in the absence of a tsetse fly and trypanosomiasis control program over a period of forty years. *Transactions of the Royal Society of Tropical Medicine and Hygiene*, 105(3), 167-172.
- Naewbanij, M., Seib, P. A., Burroughs, R., Seitz, L. M., and Chung, D. S. (1984). Determination of ergosterol using thin-layer chromatography and ultraviolet spectroscopy. *Cereal Chemistry*, 61(5), 385-388.
- Natter, K., Leitner, P., Faschinger, A., Wolinski, H., McCraith, S., Fields, S., and Kohlwein, S. D. (2005). The spatial organization of lipid synthesis in the yeast *Saccharomyces cerevisiae* derived from large scale green fluorescent

protein tagging and high resolution microscopy. *Molecular & Cellular Proteomics*, 4(5), 662-672.

- Naula, C. M., Logan, F. M., Wong, P. E., Barrett, M. P., and Burchmore, R. J. (2010). A Glucose Transporter Can Mediate Ribose Uptake Definition of residues that confer substrate specificity in a sugar transporter. *Journal of Biological Chemistry*, 285(39), 29721-29728.
- Ndoutamia, G., Moloo, S. K., Murphy, N. B., and Peregrine, A. S. (1993). Derivation and characterization of a quinapyramine-resistant clone of *Trypanosoma congolense*. *Antimicrobial Agents and Chemotherapy*, 37(5), 1163-1166.
- Nyren, P., and Lundin, A. (1985). Enzymatic Method for Continuous Monitoring of Inorganic Pyrophosphate Synthesis. *Analytical Biochemistry*, 151(2), 504-509.
- Ofarrell, P.H. (1975). High-Resolution 2-Dimensional Electrophoresis of Proteins. *Journal of Biological Chemistry*, 250(10), 4007-4021.
- Olliaro, P. L. (2010). Drug combinations for visceral leishmaniasis. *Current Opinion in Infectious Diseases*, 23(6), 595-602.
- Opperdoes, F. R. (1987). Compartmentation of carbohydrate metabolism in trypanosomes. *Annu Rev Microbiol*, 41, 127-151.
- Opperdoes, F. R., Baudhuin, P., Coppens, I., Deroe, C., Edwards, S. W., Weijers, P. J., and Misset, O. (1984). Purification, morphometric analysis, and characterization of the glycosomes (microbodies) of the protozoan hemoflagellate *trypanosoma-brucei*. *Journal of Cell Biology*, 98(4), 1178-1184.
- Opperdoes, F. R., and Coombs, G. H. (2007). Metabolism of Leishmania: proven and predicted. *Trends in Parasitology*, 23(4), 149-158.
- Opperdoes, F.R., and Borst, P. (1977). Localization of 9 Glycolytic Enzymes in A Microbody-Like Organelle in *Trypanosoma-Bruce* - Glycosome. *Febs Letters*, 80(2), 360-364.
- Ortiz-Gomez, A., Jimenez, C., Estevez, A. M., Carrero-Lerida, J., Ruiz-Perez, L. M., and Gonzalez-Pacanowska, D. (2006). Farnesyl diphosphate synthase is a cytosolic enzyme in *Leishmania major* promastigotes and its overexpression confers resistance to risedronate. *Eukaryotic Cell*, 5(7), 1057-1064.
- Ortiz, D., Sanchez, M. A., Koch, H. P., Larsson, H. P., and Landfear, S. M. (2009). An Acid-activated Nucleobase Transporter from *Leishmania major*. *Journal of Biological Chemistry*, 284(24), 16164-16169.

- Ortiz, D., Sanchez, M. A., Pierce, S., Herrmann, T., Kimblin, N., Bouwer, H. G. A., and Landfear, S. M. (2007). Molecular genetic analysis of purine nucleobase transport in *Leishmania major*. *Molecular Microbiology*, 64(5), 1228-1243.
- Ouellette, M., Drummelsmith, J., and Papadopoulou, B. (2004). Leishmaniasis: drugs in the clinic, resistance and new developments. *Drug Resistance Updates*, 7(4-5), 257-266.
- Papadopoulou, B., Roy, G., and Ouellette, M. (1992). A Novel Antifolate Resistance Gene on the Amplified H-Circle of *Leishmania*. *Embo Journal*, 11(10), 3601-3608.
- Patti, G. J., Yanes, O., and Siuzdak, G. (2012). Metabolomics: the apogee of the omics trilogy. *Nature Reviews Molecular Cell Biology*, 13(4), 263-269.
- Pena-Diaz, J., Montalvetti, A., Flores, C. L., Constan, A., Hurtado-Guerrero, R., De Souza, W., Gancedo, C., Ruiz-Perez, L. M., and Gonzalez-Pacanowska, D. (2004). Mitochondrial localization of the mevalonate pathway enzyme 3-hydroxy-3-methyl-glutaryl-CoA reductase in the trypanosomatidae. *Molecular Biology of the Cell*, 15(3), 1356-1363.
- Peregrine, A., Gray, M. A., and Moloo, S. K. (1997). Cross-resistance associated with development of resistance to isometamidium in a clone of *Trypanosoma congolense*. *Antimicrobial Agents and Chemotherapy*, 41(7), 1604-1606.
- Peregrine, A.S., and Mamman, M. (1993). Pharmacology of Diminazene - A Review. *Acta Tropica*, 54(3-4), 185-203.
- Perez-Victoria, F. J., Castanys, S., and Gamarro, F. (2003a). *Leishmania donovani* resistance to miltefosine involves a defective inward translocation of the drug. *Antimicrobial Agents and Chemotherapy*, 47(8), 2397-2403.
- Perez-Victoria, F. J., Gamarro, F., Ouellette, M., and Castanys, S. (2003b). Functional cloning of the miltefosine transporter - A novel P-type phospholipid translocase from *Leishmania* involved in drug resistance. *Journal of Biological Chemistry*, 278(50), 49965-49971.
- Perry, S.W., Norman, J.P., Barbieri, J., Brown, E.B., and Gelbard, H.A. (2011). Mitochondrial membrane potential probes and the proton gradient: a practical usage guide. *Biotechniques*, 50(2), 98-115.
- Pimenta, P. F. P., and Desouza, W. (1987). *Leishmania mexicana* - Distribution of intramembranous particles and filipin sterol complexes in amastigotes and promastigotes. *Experimental Parasitology*, 63(2), 117-135.

- Polak-Wyss, A. (1995). Mechanism of action of antifungals and combination therapy. *Journal of the European Academy of Dermatology and Venereology*, 4(0), S11-S16.
- Pourshafie, M., Morand, S., Virion, A., Rakotomanga, M., Dupuy, C., and Loiseau, P. M. (2004). Cloning of S-adenosyl-L-Methionine: C-24-Delta-sterol-methyltransferase (ERG6) from *Leishmania donovani* and characterization of mRNAs in wild-type and amphotericin B-resistant promastigotes. *Antimicrobial Agents and Chemotherapy*, 48(7), 2409-2414.
- Prenni, J. E., Avery, A. C., and Olver, C. S. (2007). Proteomics: a review and an example using the reticulocyte membrane proteome. *Veterinary Clinical Pathology*, 36(1), 13-24.
- Priotto, G., Kasparion, S., Mutombo, W., Ngouama, D., Ghorashian, S., Arnold, U., Ghabri, S., Baudin, E., Buard, V., Kazadi-Kyanza, S., Ilunga, M., Mutangala, W., Pohlig, G., Schmid, C., Karunakara, U., Torreele, E., and Kande, V. (2009). Nifurtimox-eflornithine combination therapy for second-stage African *Trypanosoma brucei gambiense* trypanosomiasis: a multicentre, randomised, phase III, non-inferiority trial. *Lancet*, 374(9683), 56-64.
- Purkait, B., Kumar, A., Nandi, N., Sardar, A. H., Das, S., Kumar, S., Pandey, K., Ravidas, V., Kumar, M., De, T., Singh, D., and Das, P. (2012). Mechanism of Amphotericin B Resistance in Clinical Isolates of *Leishmania donovani*. *Antimicrobial Agents and Chemotherapy*, 56(2), 1031-1041.
- Rabhi, I., Rabhi, S., Ben-Othman, R., Rasche, A., Daskalaki, A., Trentin, B., Piquemal, D., Regnault, B., Descoteaux, A., Guizani-Tabbane, L., and Sysco, Consortium. (2012). Transcriptomic Signature of Leishmania Infected Mice Macrophages: A Metabolic Point of View. *Plos Neglected Tropical Diseases*, 6(8).
- Rai, S., Bhaskar, Goel, S. K., Dwivedi, U. N., Sundar, S., and Goyal, N. (2013). Role of Efflux Pumps and Intracellular Thiols in Natural Antimony Resistant Isolates of *Leishmania donovani*. *Plos One*, 8(9).
- Ralston, K. S., and Hill, K. L. (2008). The flagellum of *Trypanosoma brucei*: New tricks from an old dog. *International Journal for Parasitology*, 38(8-9), 869-884.
- Ramos, H., Valdivieso, E., Gamargo, M., Dagger, F., and Cohen, B.E. (1996). Amphotericin B kills unicellular leishmanias by forming aqueous pores permeable to small cations and anions. *Journal of Membrane Biology*, 152(1), 65-75.
- Raymond, F., Boisvert, S., Roy, G., Ritt, J. F., Legare, D., Isnard, A., Stanke, M., Olivier, M., Tremblay, M. J., Papadopoulou, B., Ouellette, M., and Corbeil, J. (2012). Genome sequencing of the lizard parasite *Leishmania tarentolae*

reveals loss of genes associated to the intracellular stage of human pathogenic species. *Nucleic Acids Research*, 40(3), 1131-1147.

- Raz, B., Iten, M., GretherBuhler, Y., Kaminsky, R., and Brun, R. (1997). The Alamar Blue<sup>(R)</sup> assay to determine drug sensitivity of African trypanosomes (*T. b. rhodesiense* and *T. b. gambiense*) *in vitro*. *Acta Tropica*, 68(2), 139-147.
- Richmond, G.S., Gibellini, F., Young, S.A., Major, L., Denton, H., Lilley, A., and Smith, T.K. (2010). Lipidomic analysis of bloodstream and procyclic form *Trypanosoma brucei*. *Parasitology*, 137(9), 1357-1392.
- Riou, M., Grasseau, I., Blesbois, E., and Kerboeuf, D. (2007). Relationships between sterol/phospholipid composition and xenobiotic transport in nematodes. *Parasitology Research*, 100(5), 1125-1134.
- Riviere, L., Moreau, P., Allmann, S., Hahn, M., Biran, M., Plazolles, N., Franconi, J. M., Boshart, M., and Bringaud, F. (2009). Acetate produced in the mitochondrion is the essential precursor for lipid biosynthesis in procyclic trypanosomes. *Proceedings of the National Academy of Sciences of the United States of America*, 106(31), 12694-12699.
- Roberts, C. W., McLeod, R., Rice, D. W., Ginger, M., Chance, M. L., and Goad, L. J. (2003). Fatty acid and sterol metabolism: potential antimicrobial targets in apicomplexan and trypanosomatid parasitic protozoa. *Molecular and Biochemical Parasitology*, 126(2), 129-142.
- Roberts, S. C. (2011). The genetic toolbox for Leishmania parasites. *Bioengineered bugs*, 2(6), 320-326.
- Rodriguez-Contreras, D., Feng, X., Keeney, K. M., Bouwer, H. G. A., and Landfear, S. M. (2007). Phenotypic characterization of a glucose transporter null mutant in *Leishmania mexicana*. *Molecular and Biochemical Parasitology*, 153(1), 9-18.
- Rogers, M. B., Hilley, J. D., Dickens, N. J., Wilkes, J., Bates, P. A., Depledge, D. P., Harris, D., Her, Y., Herzyk, P., Imamura, H., Otto, T. D., Sanders, M., Seeger, K., Dujardin, J. C., Berriman, M., Smith, D. F., Hertz-Fowler, C., and Mottram, J. C. (2011). Chromosome and gene copy number variation allow major structural change between species and strains of Leishmania. *Genome Research*, 21(12), 2129-2142.
- Rothberg, J. M., Hinz, W., Rearick, T. M., Schultz, J., Mileski, W., Davey, M., Leamon, J. H., Johnson, K., Milgrew, M. J., Edwards, M., Hoon, J., Simons, J. F., Marran, D., Myers, J. W., Davidson, J. F., Branting, A., Nobile, J. R., Puc, B. P., Light, D., Clark, T. A., Huber, M., Branciforte, J. T., Stoner, I. B., Cawley, S. E., Lyons, M., Fu, Y., Homer, N., Sedova, M., Miao, X., Reed, B., Sabina, J., Feierstein, E., Schorn, M., Alanjary, M., Dimalanta, E., Dressman, D., Kasinskas, R., Sokolsky, T., Fidanza, J. A., Namsaraev, E., McKernan, K. J., Williams, A., Roth, G. T., and Bustillo, J. (2011). An

integrated semiconductor device enabling non-optical genome sequencing. *Nature*, 475(7356), 348-352.

- Saint-Pierre-Chazalet, M., Ben Brahim, M., Le Moyec, L., Bories, C., Rakotomanga, M., and Loiseau, P. M. (2009). Membrane sterol depletion impairs miltefosine action in wild-type and miltefosine-resistant *Leishmania donovani* promastigotes. *The Journal of antimicrobial chemotherapy*, 64(5), 993-1001.
- Sanchez, M. A., Tryon, R., Pierce, S., Vasudevan, G., and Landfear, S. M. (2004). Functional expression and characterization of a purine nucleobase transporter gene from *Leishmania major*. *Molecular Membrane Biology*, 21(1), 11-18.
- Saunders, E. C., de Souza, D. P., Naderer, T., Sernee, M. F., Ralton, J. E., Doyle, M. A., MacRae, J. I., Chambers, J. L., Heng, J., Nahid, A., Likic, V. A., and McConville, M. J. (2010). Central carbon metabolism of *Leishmania* parasites. *Parasitology*, 137(9), 1303-1313.
- Scheltema, R. A., Decuypere, S., T'Kindt, R., Dujardin, J. C., Coombs, G. H., and Breitling, R. (2010). The potential of metabolomics for *Leishmania* research in the post-genomics era. *Parasitology*, 137(9), 1291-1302.
- Scheltema, R. A., Jankevics, A., Jansen, R. C., Swertz, M. A., and Breitling, R. (2011). PeakML/mzMatch: A File Format, Java Library, R Library, and Tool-Chain for Mass Spectrometry Data Analysis. *Analytical Chemistry*, 83(7), 2786-2793.
- Schnauffer, A., Clark-Walker, G. D., Steinberg, A. G., and Stuart, K. (2005). The F-1-ATP synthase complex in bloodstream stage trypanosomes has an unusual and essential function. *Embo Journal*, 24(23), 4029-4040.
- Schnauffer, A., Domingo, G.J., and Stuart, K. (2002). Natural and induced dyskinetoplastic trypanosomatids: how to live without mitochondrial DNA. *International Journal for Parasitology*, 32(9), 1071-1084.
- Schofield, C.J., and Maudlin, I. (2001). Trypanosomiasis control. *International Journal for Parasitology*, 31(5-6), 615-620.
- Seifert, K., Perez-Victoria, F. J., Stettler, M., Sanchez-Canete, M. P., Castanys, S., Gamarro, F., and Croft, S. L. (2007). Inactivation of the miltefosine transporter, LdMT, causes miltefosine resistance that is conferred to the amastigote stage of *Leishmania donovani* and persists in vivo. *International Journal of Antimicrobial Agents*, 30(3), 229-235.
- Serricchio, M., and Buetikofer, P. (2011). *Trypanosoma brucei*: a model micro-organism to study eukaryotic phospholipid biosynthesis. *Febs Journal*, 278(7), 1035-1046.

- Sevova, E. S., Goren, M. A., Schwartz, K. J., Hsu, F. F., Turk, J., Fox, B. G., and Bangs, J. D. (2010). Cell-free Synthesis and Functional Characterization of Sphingolipid Synthases from Parasitic Trypanosomatid Protozoa. *Journal of Biological Chemistry*, 285(27), 20580-20587.
- Shapiro, T. A., and Englund, P. T. (1990). Selective cleavage of kinetoplast DNA minicircles promoted by antitrypanosomal drugs. *Proceedings of the National Academy of Sciences of the United States of America*, 87(3), 950-954.
- Shapiro, T. A., and Englund, P. T. (1995). The structure and replication of kinetoplast DNA. *Annual Review of Microbiology*, 49, 117-143.
- Simarro, P. P., Diarra, A., Postigo, J. A., Franco, J. R., and Jannin, J. G. (2011). The Human African Trypanosomiasis Control and Surveillance Programme of the World Health Organization 2000-2009: The Way Forward. *Plos Neglected Tropical Diseases*, 5(2).
- Simarro, P. P., Jannin, J., and Cattand, P. (2008). Eliminating human African trypanosomiasis: Where do we stand and what comes next? *Plos Medicine*, 5(2), 174-180.
- Simpson, L. (1987). The Mitochondrial Genome of Kinetoplastid Protozoa - Genomic Organization, Transcription, Replication, and Evolution. *Annual Review of Microbiology*, 41, 363-382.
- Simukoko, H., Marcotty, T., Phiri, I., Geysen, D., Vercruyse, J., and van den Bossche, P. (2007). The comparative role of cattle, goats and pigs in the epidemiology of livestock trypanosomiasis on the plateau of eastern Zambia. *Veterinary Parasitology*, 147(3-4), 231-238.
- Simukoko, H., Marcotty, T., Vercruyse, J., and van den Bossche, P. (2011). Bovine trypanosomiasis risk in an endemic area on the eastern plateau of Zambia. *Research in Veterinary Science*, 90(1), 51-54.
- Sinha, P. K., and Bhattacharya, S. (2014). Single-dose liposomal amphotericin B: an effective treatment for visceral leishmaniasis. *The Lancet Global Health*, 2(1), e7-e8.
- Sinyangwe, L., Delespaux, V., Brandt, J., Geerts, S., Mubanga, J., Machila, N., Holmes, P.H., and Eisler, M.C. (2004). Trypanocidal drug resistance in eastern province of Zambia. *Veterinary Parasitology*, 119(2-3), 125-135.
- Smith, T. K., and Butikofer, P. (2010). Lipid metabolism in *Trypanosoma brucei*. *Molecular and Biochemical Parasitology*, 172(2), 66-79.
- Sokol-Anderson, M., Sligh, J. E., Elberg, S., Brajtburg, J., Kobayashi, G. S., and Medoff, G. (1988). Role of cell defense against oxidative damage in the

resistance of *Candida albicans* to the killing effect of amphotericin B. *Antimicrobial Agents and Chemotherapy*, 32(5), 702-705.

- Stephens, J.W.W., and Fantham, H.B. (1910). On the peculiar morphology of a trypanosome from a case of Sleeping Sickness and the possibility of its being a new species (*T. rhodesiense*). *Proceedings of the Royal Society of London Series B-Containing Papers of A Biological Character*, 83(561), 28-33.
- Sundar, S. (2001). Drug resistance in Indian visceral leishmaniasis. *Tropical Medicine and International Health*, 6(11), 849-854.
- Sundar, S., Chakravarty, J., Agarwal, D., Rai, M., and Murray, H. W. (2010). Single-Dose Liposomal Amphotericin B for Visceral Leishmaniasis in India. *New England Journal of Medicine*, 362(6), 504-512.
- Sundar, S., More, D. K., Singh, M. K., Singh, V. P., Sharma, S., Makharia, A., Kumar, P. C. K., and Murray, H. W. (2000). Failure of pentavalent antimony in visceral leishmaniasis in India: Report from the center of the Indian epidemic. *Clinical Infectious Diseases*, 31(4), 1104-1107.
- Surve, S., Heestand, M., Panicucci, B., Schnauffer, A., and Parsons, M. (2012). Enigmatic Presence of Mitochondrial Complex I in *Trypanosoma brucei* Bloodstream Forms. *Eukaryotic Cell*, 11(2), 183-193.
- Sutherland, I. A., Mounsey, A., and Holmes, P. H. (1992). Transport of isometamidium (samorin) by drug-resistant and drug-sensitive *Trypanosoma congolense*. *Parasitology*, 104, 461-467.
- Sutherland, I. A., Peregrine, A. S., Lonsdaleeccles, J. D., and Holmes, P. H. (1991). Reduced accumulation of isometamidium by drug-resistant *Trypanosoma congolense*. *Parasitology*, 103, 245-251.
- Sutterwala, S. S., Creswell, C. H., Sanyal, S., Menon, A. K., and Bangs, J. D. (2007). De novo sphingolipid synthesis is essential for viability, but not for transport of glycosylphosphatidylinositol-anchored proteins, in African trypanosomes. *Eukaryotic Cell*, 6(3), 454-464.
- Sutterwala, S. S., Hsu, F. F., Sevova, E. S., Schwartz, K. J., Zhang, K., Key, P., Turk, J., Beverley, S. M., and Bangs, J. D. (2008). Developmentally regulated sphingolipid synthesis in African trypanosomes. *Molecular Microbiology*, 70(2), 281-296.
- t'Kindt, R., Scheltema, R.A., Jankevics, A., Brunker, K., Rijal, S., Dujardin, J.C., Breitling, R., Watson, D.G., Coombs, G.H., and Decuypere, S. (2010). Metabolomics to Unveil and Understand Phenotypic Diversity between Pathogen Populations. *Plos Neglected Tropical Diseases*, 4(11).

- Takahashi, S., and Koyama, T. (2006). Structure and function of cis-prenyl chain elongating enzymes. *Chemical Record*, 6(4), 194-205.
- Takamura, A., Sakai, N., Shinpoo, M., Noguchi, A., Takahashi, T., Matsuda, S., Yamamoto, M., Narita, A., Ohno, K., Ohashi, T., Ida, H., and Eto, Y. (2013). The useful preliminary diagnosis of Niemann-Pick disease type C by filipin test in blood smear. *Molecular Genetics and Metabolism*, 110(3), 401-404.
- te Welscher, Y. M., van Leeuwen, M. R., de Kruijff, B., Dijksterhuis, J., and Breukink, E. (2012). Polyene antibiotic that inhibits membrane transport proteins. *Proceedings of the National Academy of Sciences of the United States of America*, 109(28), 11156-11159.
- Tetaud, E., Lecuix, I., Sheldrake, T., Baltz, T., and Fairlamb, A.H. (2002). A new expression vector for *Crithidia fasciculata* and *Leishmania*. *Molecular and Biochemical Parasitology*, 120(2), 195-204.
- Tielens, A.G.M., and van Hellemond, J.J. (2009). Surprising variety in energy metabolism within Trypanosomatidae. *Trends in Parasitology*, 25(10), 482-490.
- Timms, M. W., van Deursen, F. J., Hendriks, E. F., and Matthews, K. R. (2002). Mitochondrial development during life cycle differentiation of African trypanosomes: Evidence for a kinetoplast-dependent differentiation control point. *Molecular Biology of the Cell*, 13(10), 3747-3759.
- Unlu, M., Morgan, M.E., and Minden, J.S. (1997). Difference gel electrophoresis: A single gel method for detecting changes in protein extracts. *Electrophoresis*, 18(11), 2071-2077.
- Urbina, J. A., Concepcion, J. L., Rangel, S., Visbal, G., and Lira, R. (2002). Squalene synthase as a chemotherapeutic target in *Trypanosoma cruzi* and *Leishmania mexicana*. *Molecular and Biochemical Parasitology*, 125(1-2), 35-45.
- van Grinsven, K.W.A., Van Den Abbeele, J., van den Bossche, P., van Hellemond, J.J., and Tielens, A.G.M. (2009). Adaptations in the Glucose Metabolism of Procyclic *Trypanosoma brucei* Isolates from Tsetse Flies and during Differentiation of Bloodstream Forms. *Eukaryotic Cell*, 8(8), 1307-1311.
- van Hellemond, J. J., Bakker, B. M., and Tielens, A. G. M. (2005a). Energy metabolism and its compartmentation in *Trypanosoma brucei*. In R. K. Poole (Ed.), *Advances in Microbial Physiology*, Vol 50 (Vol. 50, pp. 199-226). San Diego: Elsevier Academic Press Inc.
- van Hellemond, J.J., Opperdoes, F.R., and Tielens, A.G.M. (2005b). The extraordinary mitochondrion and unusual citric acid cycle in *Trypanosoma brucei*. *Biochemical Society Transactions*, 33, 967-971.

- Van Leeuwen, M. R., Smant, W., de Boer, W., and Dijksterhuis, J. (2008). Filipin is a reliable in situ marker of ergosterol in the plasma membrane of germinating conidia (spores) of *Penicillium discolor* and stains intensively at the site of germ tube formation. *Journal of Microbiological Methods*, 74(2-3), 64-73.
- van Weelden, S.W.H., Fast, B., Vogt, A., van der Meer, P., Saas, J., van Hellemond, J.J., Tielens, A.G.M., and Boshart, M. (2003). Procyclic *Trypanosoma brucei* do not use Krebs cycle activity for energy generation. *Journal of Biological Chemistry*, 278(15), 12854-12863.
- van Weelden, S.W.H., van Hellemond, J.J., Opperdoes, F.R., and Tielens, A.G.M. (2005). New functions for parts of the Krebs cycle in procyclic *Trypanosoma brucei*, a cycle not operating as a cycle. *Journal of Biological Chemistry*, 280(13), 12451-12460.
- Ventura, S., and Villaverde, A. (2006). Protein quality in bacterial inclusion bodies. *Trends in Biotechnology*, 24(4), 179-185.
- Verma, S., Mehta, A., and Shaha, C. (2011). CYP5122A1, a Novel Cytochrome P450 Is Essential for Survival of *Leishmania donovani*. *Plos One*, 6(9).
- Vickerman, K. (1985). Developmental Cycles and Biology of Pathogenic Trypanosomes. *British Medical Bulletin*, 41(2), 105-114.
- Villalta, F., Dobish, M. C., Nde, P. N., Kleshchenko, Y. Y., Hargrove, T. Y., Johnson, C. A., Waterman, M. R., Johnston, J. N., and Lepesheva, G. I. (2013). VNI Cures Acute and Chronic Experimental Chagas Disease. *Journal of Infectious Diseases*, 208(3), 504-511.
- Vincent, I. M., Creek, D. J., Burgess, K., Woods, D. J., Burchmore, R. J., and Barrett, M. P. (2012). Untargeted Metabolomics Reveals a Lack Of Synergy between Nifurtimox and Eflornithine against *Trypanosoma brucei*. *Plos Neglected Tropical Diseases*, 6(5).
- Vincent, I. M., Creek, D., Watson, D. G., Kamleh, M. A., Woods, D. J., Wong, P. E., Burchmore, R. J. S., and Barrett, M. P. (2010). A Molecular Mechanism for Eflornithine Resistance in African Trypanosomes. *Plos Pathogens*, 6(11).
- Vreysen, M.J.B., Saleh, K.M., Ali, M.Y., Abdulla, A.M., Zhu, Z.R., Juma, K.G., Dyck, V.A., Msangi, A.R., Mkonyi, P.A., and Feldmann, H.U. (2000). *Glossina austeni* (Diptera : *Glossinidae*) eradicated on the Island of Unguja, Zanzibar, using the sterile insect technique. *Journal of Economic Entomology*, 93(1), 123-135.
- Wainwright, M. (2010). Dyes, trypanosomiasis and DNA: a historical and critical review. *Biotechnic and Histochemistry*, 85(6), 341-354.

- Wang, L. (2009). Towards revealing the structure of bacterial inclusion bodies. *Prion*, 3(3), 139-145.
- Waterman, M. R., and Lepesheva, G. I. (2005). Sterol 14 alpha-demethylase, an abundant and essential mixed-function oxidase. *Biochemical and Biophysical Research Communications*, 338(1), 418-422.
- Welburn, S.C., Coleman, P.G., Maudlin, I., Fevre, E.M., Odiit, M., and Eisler, M.C. (2006). Crisis, what crisis? Control of Rhodesian sleeping sickness. *Trends in Parasitology*, 22(3), 123-128.
- Wheeler, R. J. (2010). The trypanolytic factor-mechanism, impacts and applications. *Trends in Parasitology*, 26(9), 457-464.
- Wheeler, R. J., Gluenz, E., and Gull, K. (2011). The cell cycle of Leishmania: morphogenetic events and their implications for parasite biology. *Molecular Microbiology*, 79(3), 647-662.
- Whitfield, G. B., Brock, T. D., Ammann, A., Gottlieb, D., and Carter, H. E. (1955). Filipin, an antifungal antibiotic - isolation and properties. *Journal of the American Chemical Society*, 77(18), 4799-4801.
- WHO. (2010). Control of the Leishmaniases *Control of the Leishmaniases: Report of a Meeting of the Who Expert Committee on the Control of Leishmaniases, Geneva, 22-26 March 2010* (Vol. 949, pp. 1-186).
- Wilkes, J.M., Mulugeta, W., Wells, C., and Peregrine, A.S. (1997). Modulation of mitochondrial electrical potential: A candidate mechanism for drug resistance in African trypanosomes. *Biochemical Journal*, 326, 755-761.
- Wilkinson, S.R., and Kelly, J.M. (2009). Trypanocidal drugs: mechanisms, resistance and new targets. *Expert Reviews in Molecular Medicine*, 11, e31.
- Williams, N. (1994). The mitochondrial ATP synthase of *Trypanosoma brucei* - structure and regulation. *Journal of Bioenergetics and Biomembranes*, 26(2), 173-178.
- Wilson, Z. N., Gilroy, C. A., Boitz, J. M., Ullman, B., and Yates, P. A. (2012). Genetic Dissection of Pyrimidine Biosynthesis and Salvage in *Leishmania donovani*. *Journal of Biological Chemistry*, 287(16), 12759-12770.
- Witola, W. H., Inoue, N., Ohashi, K., and Onuma, M. (2004). RNA-interference silencing of the adenosine transporter-1 gene in *Trypanosoma evansi* confers resistance to diminazene aceturate. *Experimental Parasitology*, 107(1-2), 47-57.
- Yates, J. R., Ruse, C. I., and Nakorchevsky, A. (2009). Proteomics by Mass Spectrometry: Approaches, Advances, and Applications *Annual Review of Biomedical Engineering* (Vol. 11, pp. 49-79). Palo Alto: Annual Review.

- Zanolari, B., Friant, S., Funato, K., Sutterlin, C., Stevenson, B. J., and Riezman, H. (2000). Sphingoid base synthesis requirement for endocytosis in *Saccharomyces cerevisiae*. *Embo Journal*, 19(12), 2824-2833.
- Zhang, K., Bangs, J. D., and Beverley, S. M. (2010). Sphingolipids in Parasitic Protozoa. In C. Chalfant & M. DelPoeta (Eds.), *Sphingolipids as Signaling and Regulatory Molecules* (Vol. 688, pp. 238-248).
- Zhang, L., Zhang, Y., Zhou, Y. M., An, S., Zhou, Y. X., and Cheng, J. (2002). Response of gene expression in *Saccharomyces cerevisiae* to amphotericin B and nystatin measured by microarrays. *Journal of Antimicrobial Chemotherapy*, 49(6), 905-915.